

UMTRI-85-51

MVMA TWO-DIMENSIONAL CRASH VICTIM SIMULATION:

AUDIO-VISUAL PROGRAM

Bruce M. Bowman, Associate Research Scientist  
D. Hurley Robbins, Research Scientist  
Robert O. Bennett, Senior Research Associate

Transportation Research Institute  
The University of Michigan  
Huron Parkway and Baxter Road  
Ann Arbor, Michigan 48109

December 6, 1985



Technical Report Documentation Page

1. Report No. UMTRI-85-51		2. Government Accession No.		3. Recipient's Catalog No.	
4. Title and Subtitle MVMA Two-Dimensional Crash Victim Simulation Tutorial System: Audio Visual Program				5. Report Date December 6, 1985	
				6. Performing Organization Code 389077	
7. Author(s) Bowman, Bruce M., Robbins, D. Hurley, and Bennett, Robert O.				8. Performing Organization Report No. UMTRI-85-51	
9. Performing Organization Name and Address Transportation Research Institute The University of Michigan Huron Parkway & Baxter Road Ann Arbor, Michigan 48109				10. Work Unit No. (TRAIS)	
				11. Contract or Grant No. 86-0327-P1	
12. Sponsoring Agency Name and Address Motor Vehicle Manufacturers Association 320 New Center Building Detroit, Michigan 48202 CO-SPONSOR Isuzu Motors Limited 8 Tsuchidana, Fujisawa-shi Kanagawa-ken 252, Japan				13. Type of Report and Period Covered Final Report	
				14. Sponsoring Agency Code	
16. Abstract <p>The MVMA Two-Dimensional Crash Victim Simulator is a mathematical model used for predicting occupant dynamics in a crash environment. The computer model is large and complex. Its many options and features provide the automotive safety engineer considerable flexibility in defining a crash event but at the same time impose considerable demands for specification of input data. As a means of facilitating learning to use the model, the Tutorial System combines a Self-Study Guide and an Audio-Visual Program. Both are divided into thirteen segments, called "modules," each of which deals with the data requirements of a set of related model features. Each audio-visual module consists of 35 mm slides and approximately twenty minutes of narration on a tape cassette.</p> <p>Tutorial System documentation is in two volumes. The Self-Study Guide consists of text, illustrations, and example problems. The Audio-Visual Program includes the narration text and figures used for the 35 mm slides. All documentation is loose-leaf.</p>					
17. Key Words Audio-Visual Program Automotive Safety Design Crash Victim Simulation Whole-Body Occupant Dynamics Response				18. Distribution Statement UNLIMITED	
19. Security Classif. (of this report) Unclassified		20. Security Classif. (of this page) Unclassified		21. No. of Pages 440	22. Price

Form DOT F 1700.7 (8-72)

Reproduction of completed page authorized

12/6/85



## TABLE OF CONTENTS

		Page
NARRATION FOR AUDIO-VISUAL MODULES		
MODULE		
1	Introduction to the MVMA 2-D Crash Victim Simulation	1
12	Model Operation	67
2	The Body Linkage	97
3	Neck and Shoulder Models	141
4	Contact Surfaces Attached to the Occupant	173
5	Contact Surfaces Attached to the Vehicle	201
6	Generation of Contact Forces on the Occupant: Parts 1 and 2	223, 255
7	Occupant Positioning with Respect to the Vehicle	285
8	Crash Deceleration Profiles and Head Applied Forces	315
9	Belt Restraint Systems	335
10	Airbag Restraint System	365
11	(Module 11 is reserved for an energy-absorbing steering column.)	
13	Example Crash Simulations	385

### AUDIO-VISUAL SLIDES AND CASSETTES

MODULE	NUMBER OF SLIDES	NARRATION TIME
1	32	30' 10"
2	21	22' 30"
3	15	24' 30"
4	11	22' 20"
5	10	16' 15"
6	Part 1, 14; Part 2, 13	21' 50"; 24' 30"
7	13	19' 20"
8	9	13' 45"
9	12	23' 40"
10	7	16' 50"
11	-	-
12	14	16' 05"
13	27	36' 10"



**MVMA 2-D  
CRASH VICTIM SIMULATION**

**\* \* \***

**MODULE 1**

**GENERAL INTRODUCTION TO THE  
MVMA 2-D MAN MODEL**

**UNIVERSITY OF MICHIGAN  
HIGHWAY SAFETY RESEARCH INSTITUTE**

**MVMA 2-D  
CRASH VICTIM SIMULATION**



**MODULE 1**

**GENERAL INTRODUCTION TO THE  
MVMA 2-D MAN MODEL**

**UNIVERSITY OF MICHIGAN  
HIGHWAY SAFETY RESEARCH INSTITUTE**

**SLIDE 1-1**



MODULE 1 -- INTRODUCTION TO THE MVMA 2-D CRASH VICTIM SIMULATION

SLIDE 1

Since 1966, sophisticated analyses have been developed which can be used for estimating the dynamic response of a human or an anthropomorphic dummy in a crash environment. The use of such mathematical models as tools in automotive safety design has been made possible by modern large-storage, high-speed computers.

**COMPUTER SIMULATION  
OF OCCUPANT DYNAMICS  
IN A CRASH ENVIRONMENT**

**GIVEN (Input):**

- 1) Description of a biomechanical system representing the occupant
- 2) Description of a mechanical system representing the occupant compartment
- 3) Time-history of occupant compartment motion
- 4) Occupant position at onset of crash

**DETERMINED (Output):**

- 1) Occupant motion
- 2) Forces on Occupant
- 3) Derived descriptions and measures of the crash dynamics

FIGURE 1-1 Computer Simulation of Occupant Dynamics

## SLIDE 2

The problem of determining occupant dynamics in a crash environment can be simply stated. A description of a mechanical or biomechanical system, the occupant, is given. A description of a potentially interacting mechanical system, the occupant compartment, is given. The occupant's position and orientation and their rates of change are specified for some single instant of time. And finally, the motion in space of the occupant compartment as a function of time is specified. It is required to determine the subsequent motion of the occupant and the forces which describe his interaction with the vehicle interior.

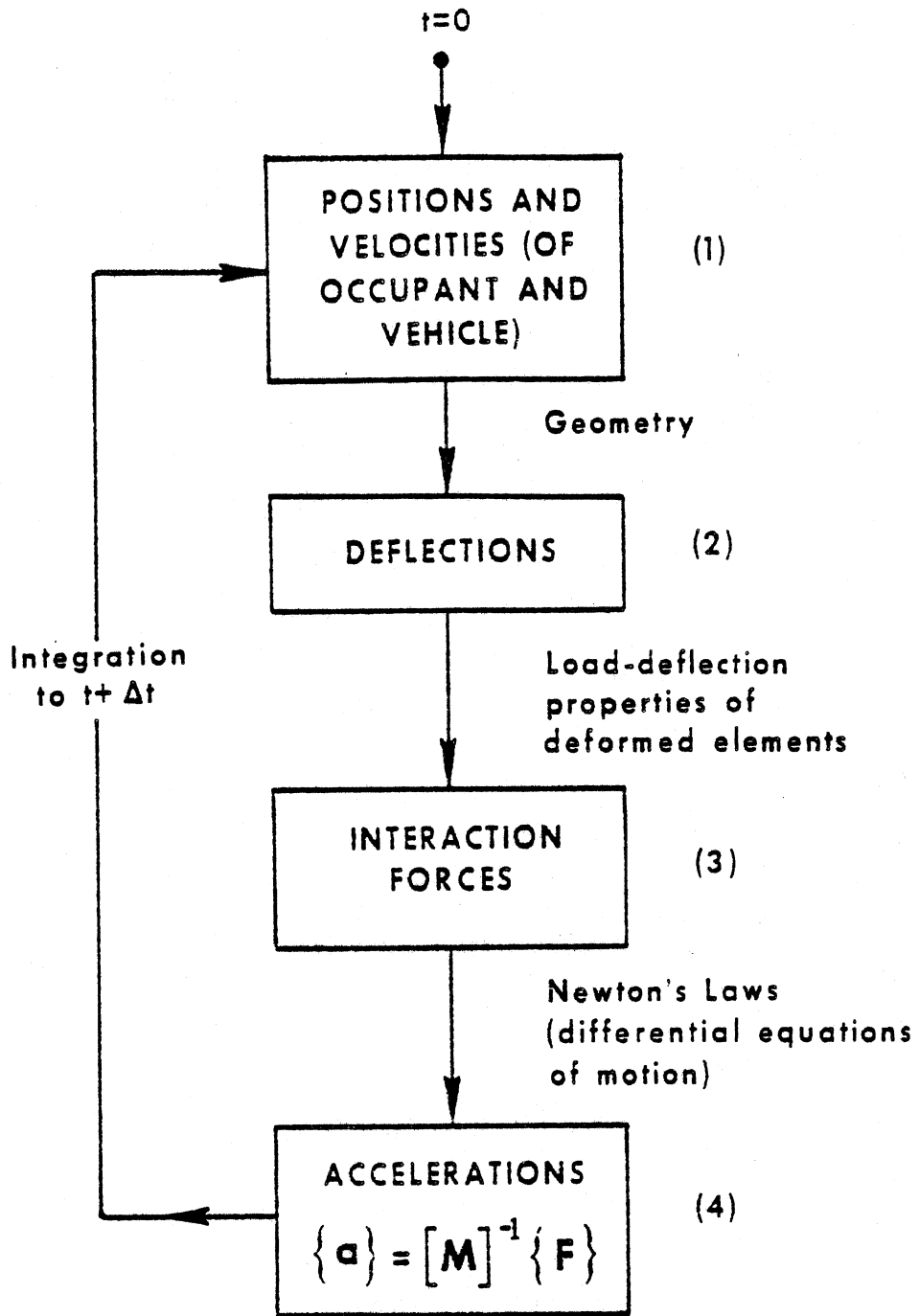


FIGURE 1-2 Relationship of Position Conditions and Interaction Forces Within the Framework of an Initial Value Problem

SLIDE 1-3

### SLIDE 3

This figure illustrates the relationship between the motion and the forces. From the initial position and velocity conditions of the occupant relative to a vehicle-fixed reference frame, the instantaneous state of displacements between body and vehicle elements, and hence the interaction forces, may be determined. The instantaneous interaction forces thus found, together with the motion equations of classical mechanics, namely Newton's Laws, determine the instantaneous accelerations essentially as force divided by mass. Integration of the accelerations then yields the occupant velocities and positions at a new time, different from the time at which forces were determined by an arbitrarily small amount,  $\Delta t$ . New position and velocity conditions having been determined, new deflections can be determined and so forth so that the entire time histories for motion and forces are established.

This flow sequence is an appropriate description for all mathematical models which could be used for determining occupant dynamics.

The embodiment of a mathematical model within a computer program is called a "computer model." Computer models which have been used to simulate occupant crash dynamics include both two-dimensional and three-dimensional motion simulators. The two-dimensional models are appropriately used for simulating crash events in which primary occupant motions may be expected to lie within a plane. Thus, two-dimensional models are most useful for simulating front-end and rear-end impacts. With care, however, they may be used for some oblique and side impacts as well. One such planar motion model, the "MVMA Two-Dimensional Crash Victim Simulator," is the subject of this Tutorial System.

# MODULES OF THE MVMA 2-D CRASH VICTIM SIMULATION TUTORIAL SYSTEM

## MODULE

- 1 Introduction to the MVMA 2-D Crash Victim Simulation
- 2 The Body Linkage
- 3 Neck and Shoulder Models
- 4 Contact Surfaces Attached to the Occupant
- 5 Contact Surfaces Attached to the Vehicle
- 6 Generation of Contact Forces on the Occupant (Parts 1 and 2)
- 7 Occupant Positioning with Respect to the Vehicle
- 8 Crash Deceleration Profiles and Head Applied Forces
- 9 Belt Restraint Systems
- 10 Airbag Restraint System
- 11 (Module 11 is reserved for an energy absorbing steering column)
- 12 Model Operation
- 13 Example Crash Simulations

FIGURE 1-3 Modules of the MVMA 2-D Crash Victim Simulation Tutorial System

SLIDE 1-4

#### SLIDE 4

The MVMA 2-D model is a large and complex computer program. Its many options and features provide the user considerable flexibility in defining a crash event but at the same time impose considerable demands for specification of input data. As a means of facilitating learning to use the model, the Tutorial System combines a self-study guide with an audio-visual program. Both the self-study manual and the audio-visual program are divided into thirteen segments called "modules." Each of the Modules 2 through 12 deals with the data requirements of a set of related model features. Data decks for two example simulations are described and assembled in Module 13. The titles of the modules are descriptive of their content and are listed here. It should be noted that Module 6 is in two parts and that there is no Module 11.

## PREREQUISITES

- User familiarity with basic engineering terms is required.
- Knowledge of algebra and analytical geometry is required.
- Good engineering judgment and an understanding of the fundamentals of Newtonian mechanics are important.

SLIDE 1-5



## SLIDE 5

The Tutorial System is intended for use by engineers. It is assumed that the user is familiar with basic engineering terms such as "acceleration," "force-deflection loading curve," and "moment of inertia." No mathematical skills are required for understanding most of the material presented in the Tutorial System modules, but any user of the computer model is expected to understand the basics of algebra and analytic geometry. These are required for some aspects of the task of input data preparation. Knowledge of calculus, differential equations, and Lagrangian mechanics is not a necessity for any user, but it is normally the case that a user with skills in these areas is better able to use the model effectively. But most important, and independent from a user's mathematical background, are good engineering judgment and an understanding of the fundamentals of Newtonian mechanics.

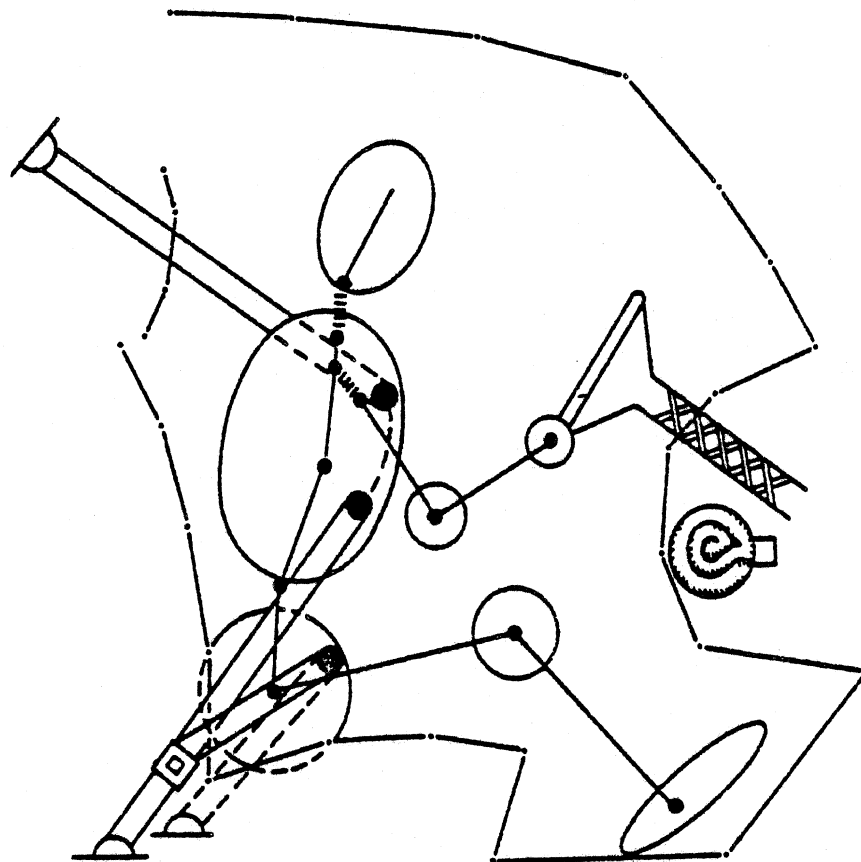
# MATHEMATICAL SIMULATION

- Focus of the Tutorial System: preparation of input data
  - Design data
  - The mathematical model
  - Engineering judgment
- Good experimental data for model input parameters is of critical importance.

SLIDE 1-6

## SLIDE 6

The focus of the Tutorial System is preparation of input data. It is here that design data, the mathematical model, and engineering judgment must be brought together. The mathematical model, like all mathematical models, will allow only imperfect representations of reality. In order to simulate physical phenomena as accurately as possible with the model, it is necessary for the user to understand the manner by which features of the occupant/vehicle system have been approximated analytically. Therefore, most of the material in the Tutorial System is explanation of the features of the mathematical model and the associated parameters for which the user must supply values. Engineering judgment is brought to bear in deciding, for simulation of a specific crash event, which features of the model are best used, how they are used, and what parameters are critical and therefore require special attention. For example, special attention might be given to an important parameter by experimentally measuring its value as accurately as possible. It has been demonstrated time and again that for satisfactory performance of mathematical models, there is no substitute for good experimental data. Reality can be simulated only if reality is represented.



## MVMA 2-D MODEL

1. Nine-Mass Occupant Model
2. Contact-Sensing Ellipses
3. Collapsing Vehicle Interior
4. Vehicle Exterior for Pedestrian Studies
5. Extensible Two-Joint Neck
6. Flexible Shoulder
7. Time-Dependent Muscle Contraction
8. Deployable Airbag
9. Energy-Absorbing Steering Column
10. Two Belt Restraint-System Submodels
11. Horizontal, Vertical, and Pitching Vehicle Motions

FIGURE 1-4 The MVMA 2-D Model

SLIDE 1-7

SLIDE 7

This is a schematic of the occupant, vehicle interior, and restraint systems of the MVMA 2-D model. Listed with the schematic are some of the basic features of the model. Much of the remainder of this module is summary of these features. Modules 2 through 12 treat these subjects in detail.

## THE OCCUPANT MODEL

- A nine-mass, ten-segment body linkage
- An extensible, two-joint neck and a realistically-flexible shoulder complex
- Energy-absorbing joints
- Time-dependent muscle activity level
- Contact-sensing ellipses of arbitrary size, position, and number which define the body profile
- General and arbitrarily-definable nonlinear materials with energy-absorbing capability for all parts of the body

SLIDE 1-8

SLIDE 8

The MVMA 2-D model includes the following features in its representation of the crash victim, which may be either a human or an anthropomorphic dummy:

1. A nine-mass, ten-segment body linkage;
2. An extensible, two-joint neck and a realistically-flexible shoulder complex;
3. Energy-absorbing joints;
4. Time-dependent muscle activity level;
5. Contact-sensing ellipses of arbitrary size, position, and number which define the body profile; and,
6. General and arbitrarily-definable nonlinear materials with energy-absorbing capability for all parts of the body.

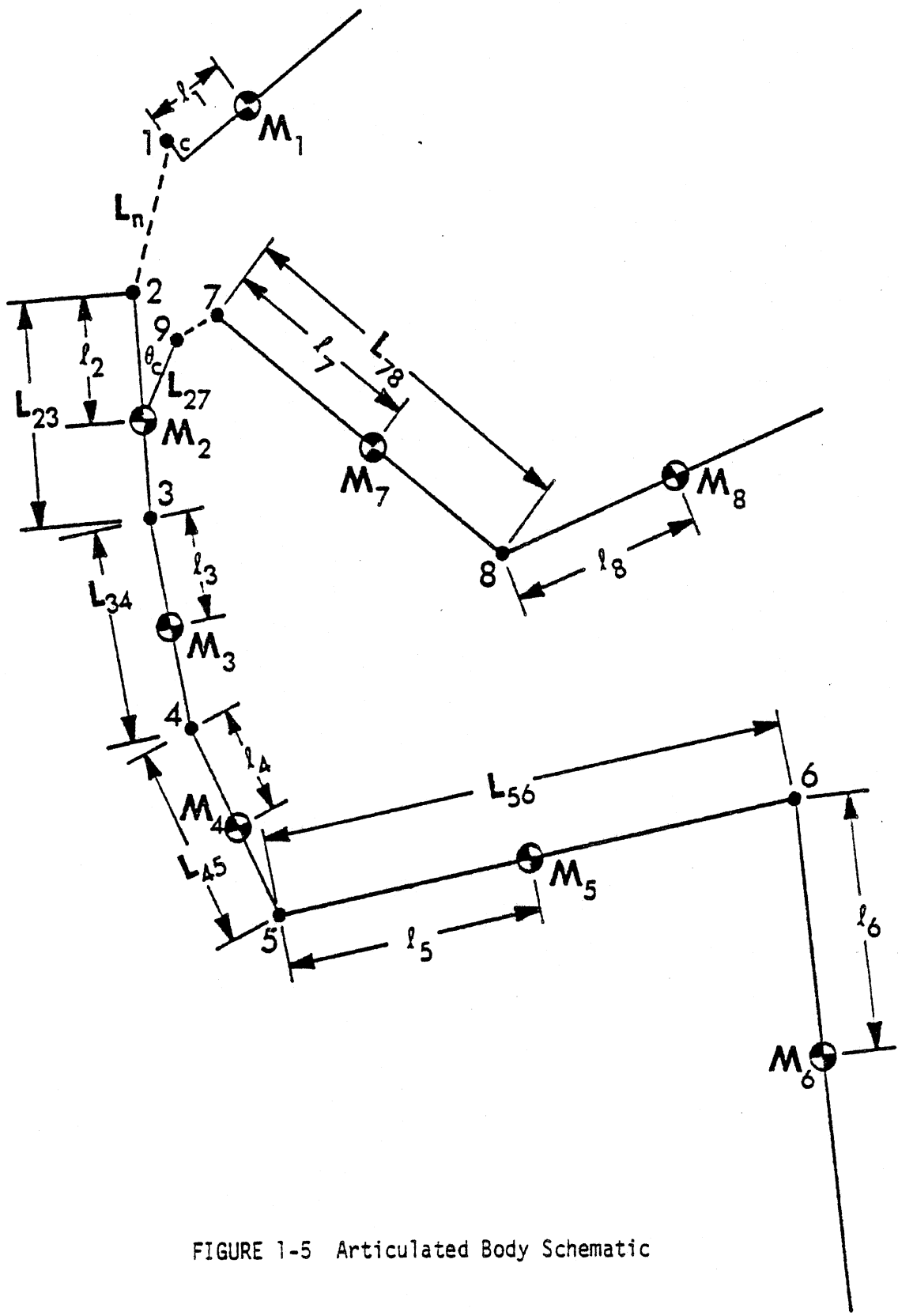


FIGURE 1-5 Articulated Body Schematic

SLIDE 1-9



## SLIDE 9

Some of these features are illustrated in this schematic of the body linkage. Note that since this is a planar model, a single two-link leg represents right and left legs combined. Similarly, there are only two arm links. Angulations at joints are restricted by user specification of range-of-motion limits and viscoelastic parameters for hard-tissue resistance.

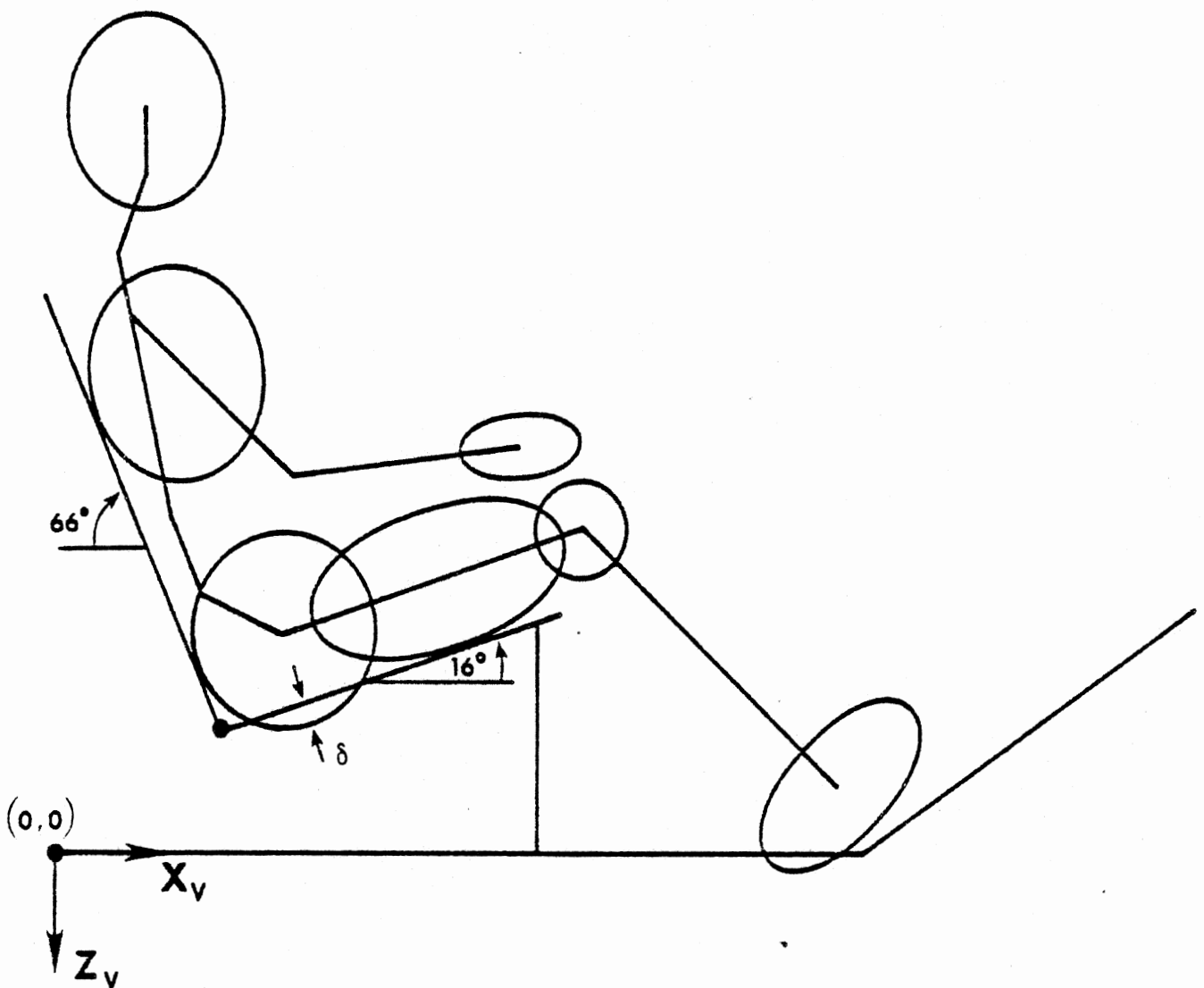
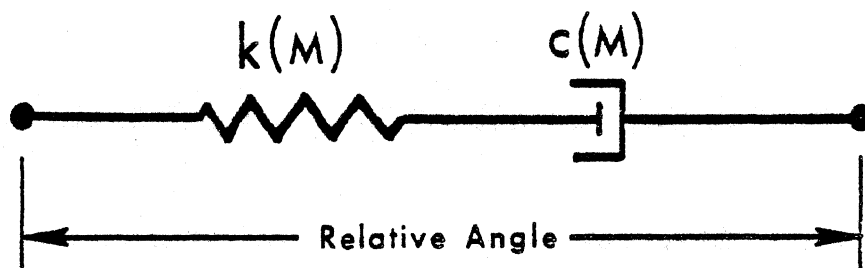


FIGURE 1-6 Seated Occupant in Position of Approximate Equilibrium

SLIDE 1-10

SLIDE 10

This figure illustrates a typical occupant profile defined by user-specified contact-sensing ellipses.



$$k = a_1 + a_2 |M|$$

$$c = a_3 |M|$$

$M = M(t)$ , muscle activity level

FIGURE 1-7 Muscle element

SLIDE 1-11

## SLIDE 11

A feature that is unique to the MVMA 2-D Crash Victim Simulator is its muscle model. Moderate levels of muscle contraction generally have a significant effect on the crash dynamics, especially for low-g impacts, so analytical representation of the effect is of obvious value. Provision is made for calculation of muscle torques at the eight joints of the body linkage. The muscle model is shown here. It does not include a contractile element, but the passive viscoelastic parameters  $k$  and  $c$  are functions of a user-prescribed, time-dependent muscle activity level.

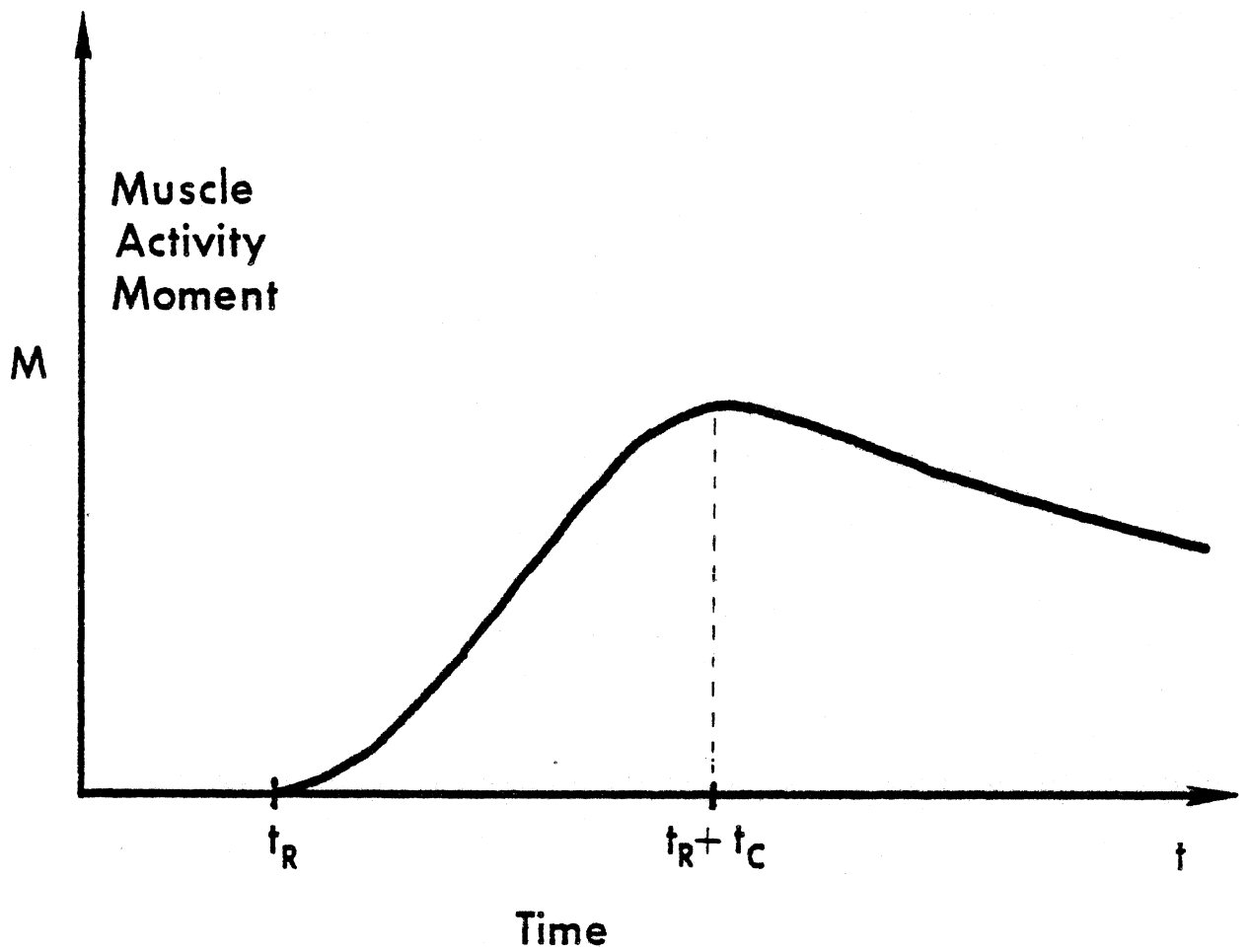


FIGURE 1-8 Muscle activity moment as a function of time

SLIDE 1-12

SLIDE 12

The typical dependence on time of the muscle activity level is illustrated here.  $t_R$  and  $t_C$  are reflex and contraction times for the muscle.

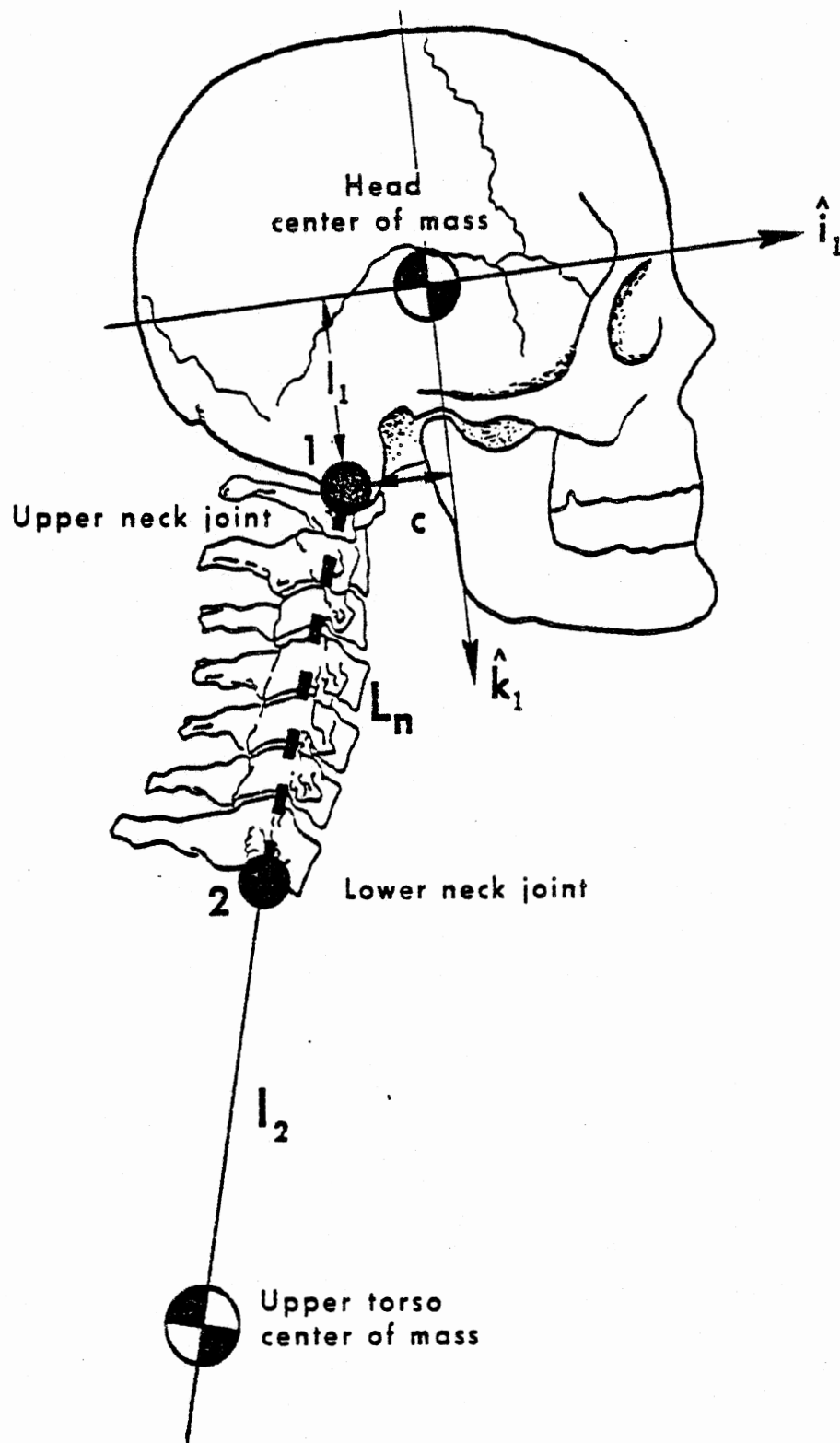


FIGURE 1-9 MVMA-2D extensible neck geometry

SLIDE 1-13



SLIDE 13

The extensible two-joint neck is illustrated in this figure. Viscoelastic elements are not shown. The joints are at either end of the cervical spine. The upper neck joint may be positioned arbitrarily with respect to the head center of mass.

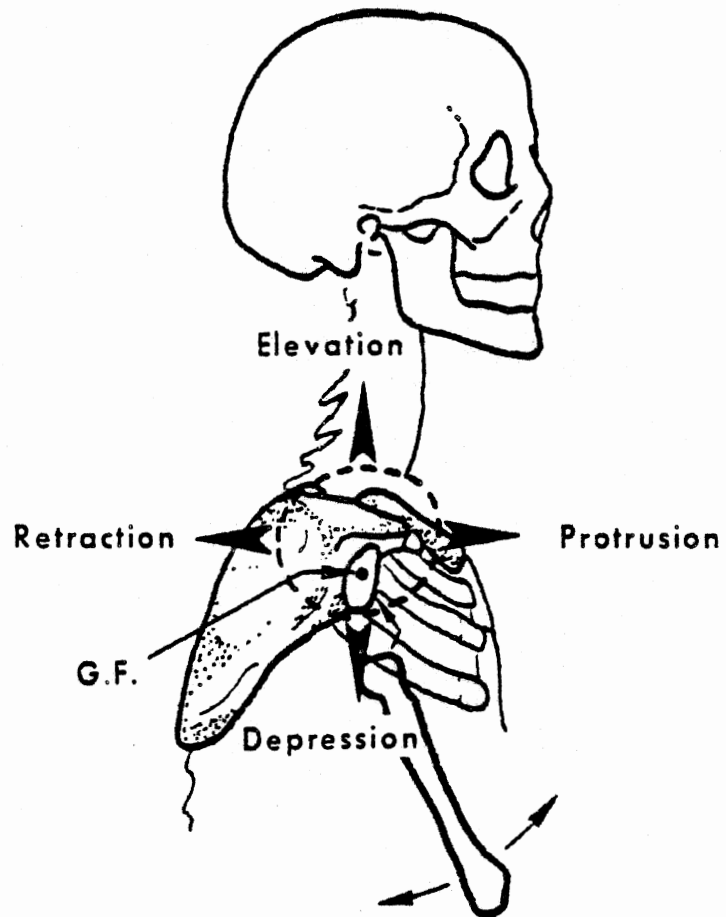


FIGURE 1-10 Maximum range of motion of the glenoid fossa (shoulder socket) in shrugging movements

SLIDE 1-14

SLIDE 14

Shoulder "shrugging" motions may be represented in simulations with the MVMA 2-D model. Angular articulations of the upper arm link are independent from the translatory motions of its proximal end.

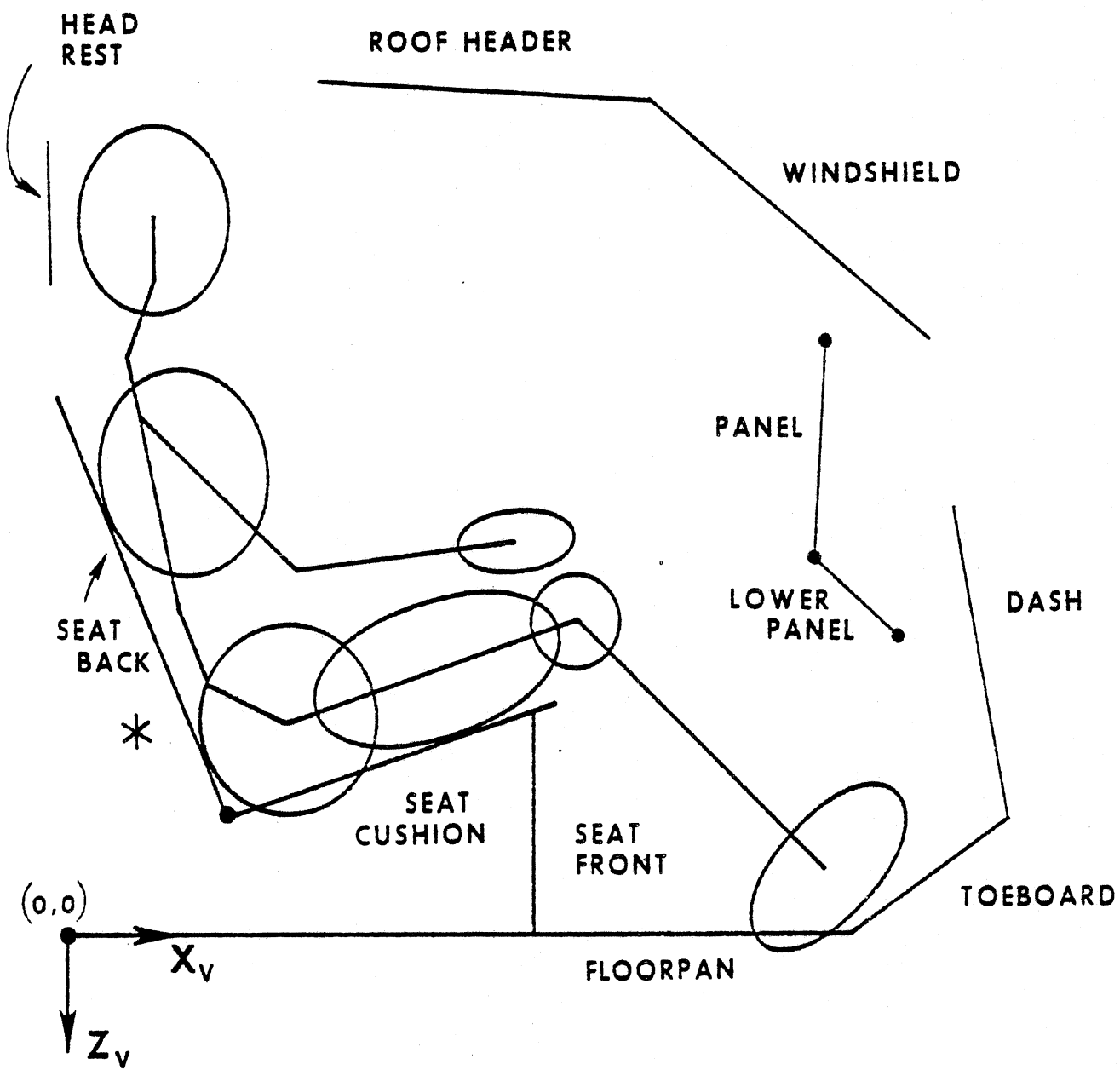


FIGURE 1-11 Example Profile of Vehicle-Interior Surfaces

SLIDE 1-15

## SLIDE 15

Forces between the occupant and the vehicle interior are generated by the model as a result of interaction of a profile of occupant ellipses with a user-defined vehicle-interior profile. This profile is a set of connected or disconnected straight-line segments. The example profile illustrated has eleven segments. However, any number of segments may be prescribed and their lengths and locations are arbitrary. Time-dependent positioning of the segments makes possible simulation of direct intrusions into the occupant compartment or secondary frontal interior displacements resulting from gross deformation of the engine compartment.

## MATERIAL PROPERTIES

- Tabular or polynomial loading curves
- Material yield point deflection
- Force saturation level for plastic loading
- Hysteretic unloading characteristics that depend on maximum deformation
- Surface friction characteristics

SLIDE 1-16

## SLIDE 16

The line segments may be assigned material properties or they may be specified as rigid. Material properties for elements of the vehicle interior (and also for occupant ellipses) include the following:

1. Tabular or polynomial loading curves;
2. Material yield point deflection;
3. Force saturation level for plastic loading;
4. Hysteretic unloading characteristics that depend on maximum deformation;
5. Surface friction characteristics.

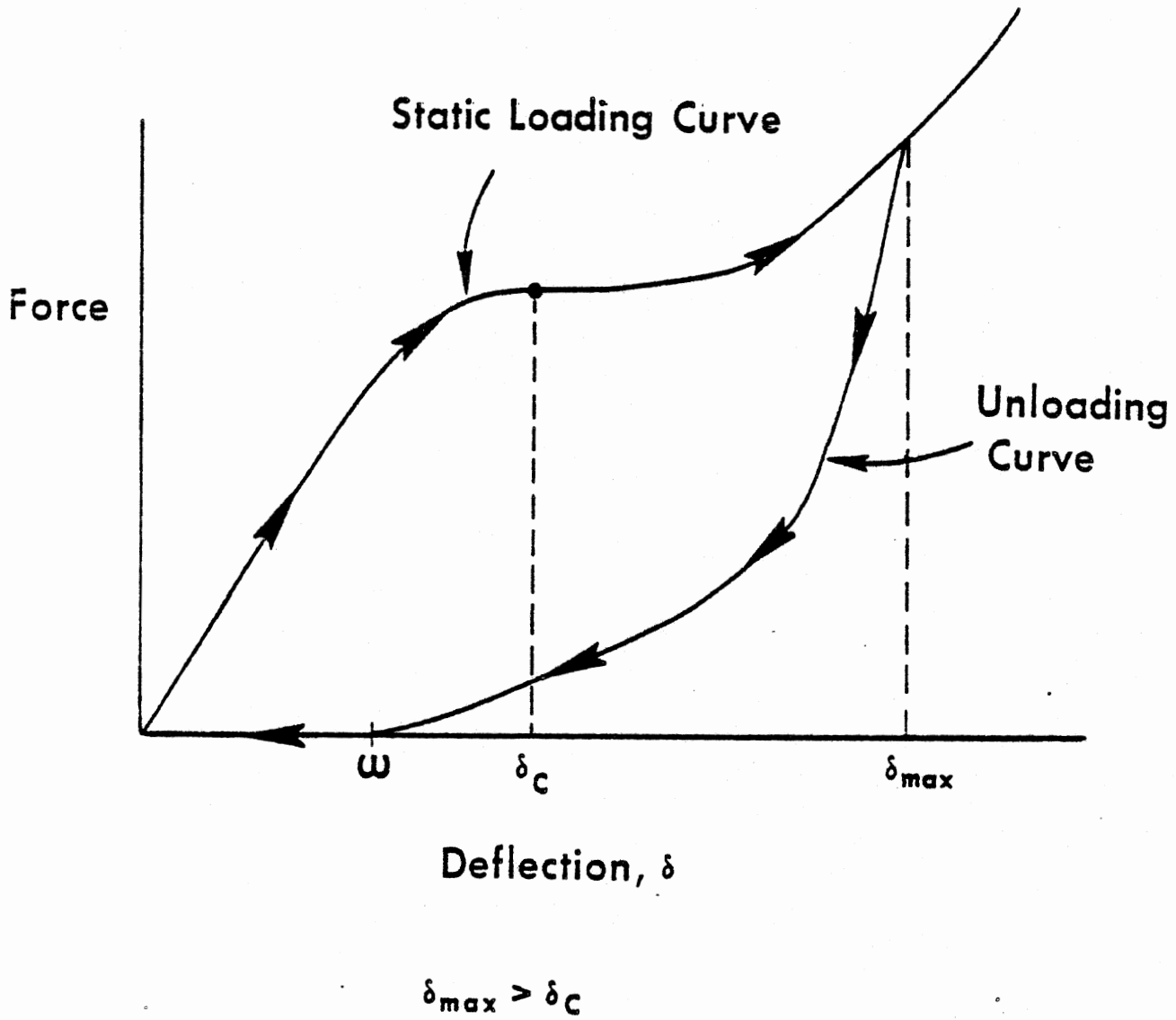


FIGURE 1-12 Unloading With Permanent Deformation from Deflections Greater Than  $\delta_c$



SLIDE 17

Example loading and unloading curves are shown on this slide.

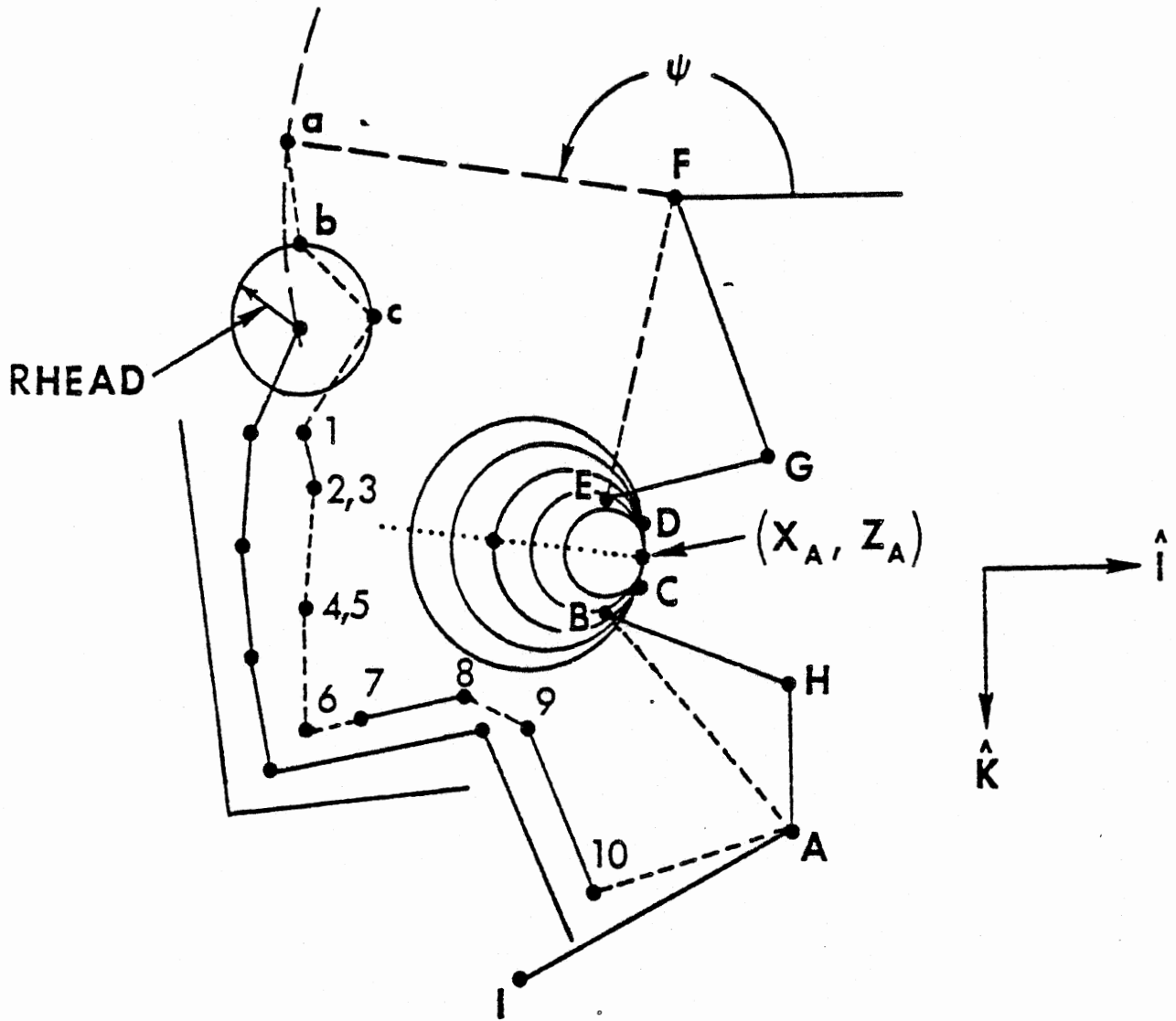


FIGURE 1-13 MVMA 2-D Airbag Model

SLIDE 1-18

## SLIDE 18

Three optional occupant restraint systems may be used in MVMA 2-D simulations. Two are belt systems and the third is an airbag model, which is illustrated.

The figure shows the bag expanding from its source toward the occupant, for which an airbag contact profile is defined with straight-line segments. Estimation of bag forces is based on solution of the differential equations of gas thermodynamics. The airbag is inflated at a time-dependent rate specified by the user; inlet mass flow rate is a tabular input to the simulation. When the bag is fully inflated, restraining forces due to internal pressure and skin tension are generated if the bag is in contact with the occupant. The shape of the bag is allowed to conform to that of the occupant and the vehicle interior with free sections of the perimeter defined as circular segments. When the pressure in the bag reaches a specified level, gas is allowed to flow out of the bag through defined orifices or through porous bag fabric.

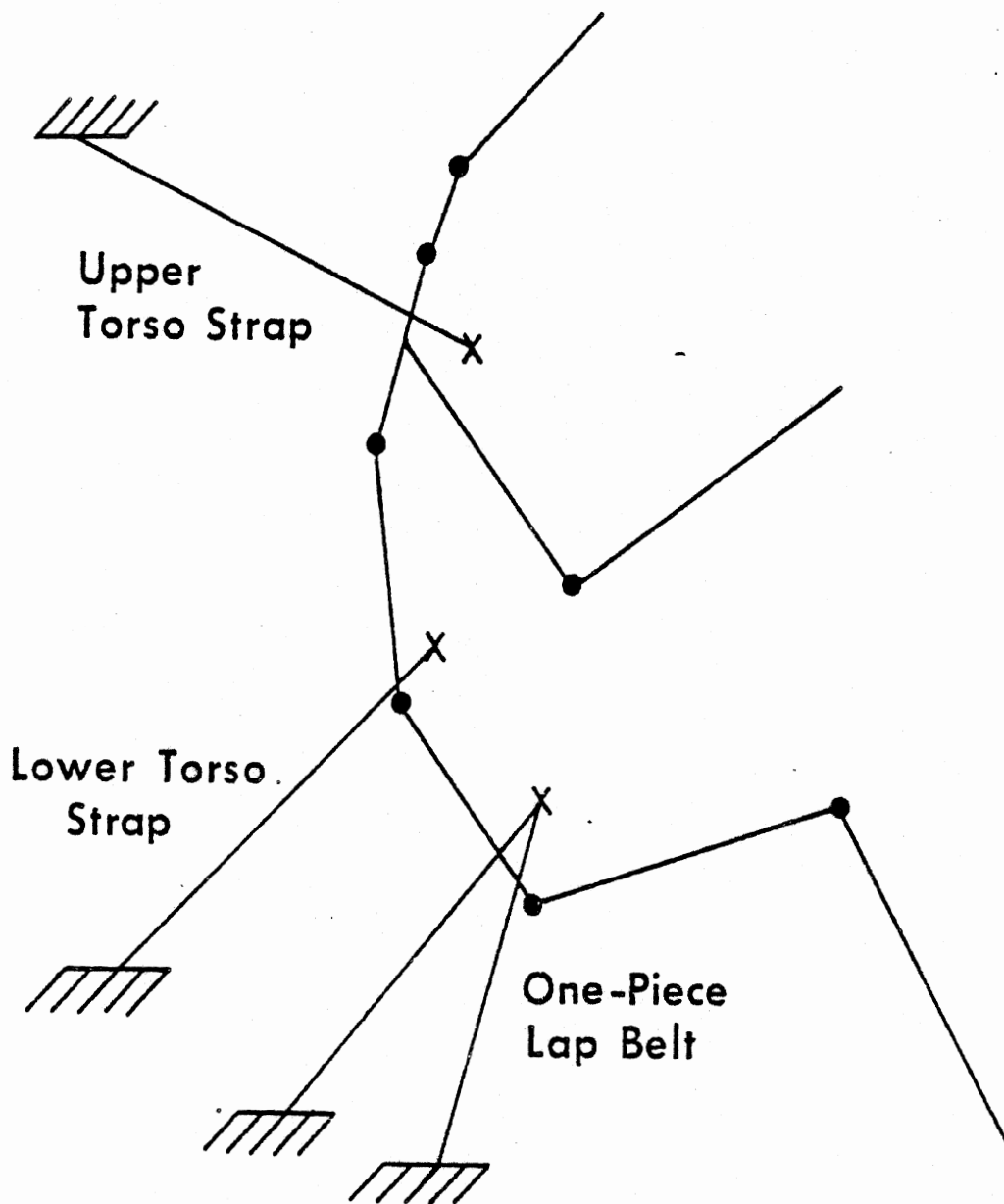


FIGURE 1-14 Simple Belt System

SLIDE 1-19.

## SLIDE 19

The first optional belt system consists of: 1) a one-piece lap belt attached to the lower torso element and anchored at each end to the vehicle; 2) an upper torso harness strap attached to the upper torso element and anchored to the vehicle; 3) a lower torso harness strap attached arbitrarily to any torso element and anchored to the vehicle. This belt-restraint submodel is effectively a three-belt system. The two-segment lap belt shown in the figure is treated by the computer model as a single piece of webbing that slides freely over the pelvis through a user-specified point on the lower-torso element. Thus, a lap-belt tension is determined from the elongation or strain of the total belt length, with no adjustment for possible friction effects, and the established tension is applied at the attachment point on the body through both the inboard and outboard segments. The lap belt anchor positions in the vehicle, as well as the attachment point on the lower-torso segment, can be specified arbitrarily by the user.

The torso harness restraint consists of two individual straps: an upper strap attached to a fixed point on the upper torso segment and a lower strap attached to a fixed point on the upper- middle-, or lower-torso segment.

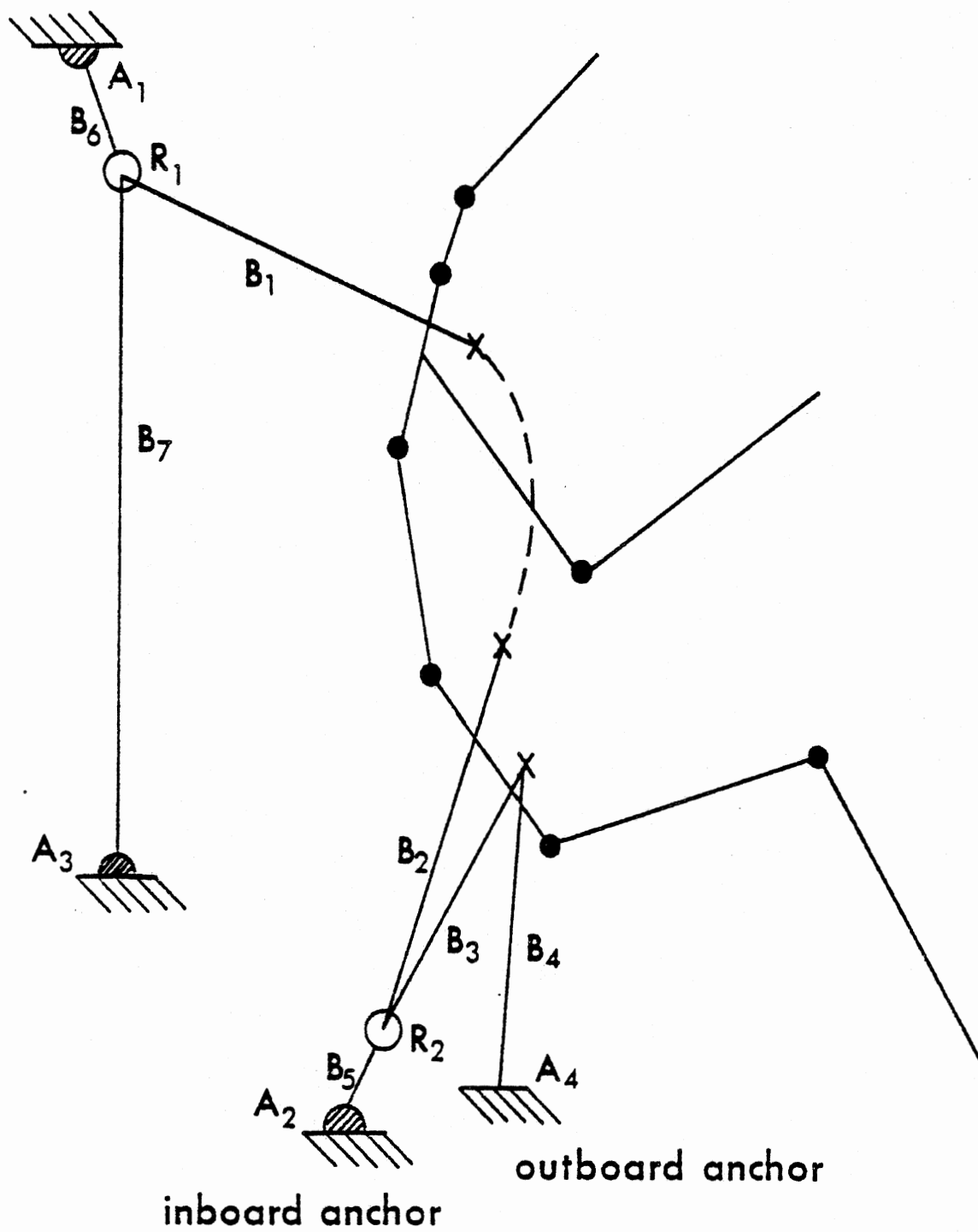


FIGURE 1-15 Advanced Belt System

SLIDE 1- 20

## SLIDE 20

This is a schematic of the second optional belt-restraint system. It includes the following features: 1) seven belt segments which may be independent or, at option, may be paired in certain combinations to act as a lesser number of separate lengths of webbing by use of various free-slipping and friction elections at the torso and lap and at slip points; 2) a slip point in the three-belt upper harness system; 3) a slip point between the lower torso and lap sections; 4) optionally, inertia reels, either vehicle-sensitive or webbing-sensitive, at three of the four anchor locations.

The slip points are shown as open circles, rings  $R_1$  and  $R_2$ . The rings may be fastened to ring straps, which lead to anchors  $A_1$  and  $A_2$ , or they may be fixed to the vehicle frame at anchor locations  $A_1$  and  $A_2$ , in which case the corresponding ring straps,  $B_6$  and  $B_5$ , are absent. The belt pairs  $B_1$ - $B_7$  and  $B_2$ - $B_3$ , may be considered common straps that may slip freely through their respective rings or with an amount of frictional resistance which depends on the resultant normal force at the ring. Also, three optional methods are available for simulating the effects of torso belt slippage and friction against the torso.

As for the simpler belt system, webbing properties for this system may be prescribed either in terms of force-deflection or force-strain characteristics.

Inertial reference frame

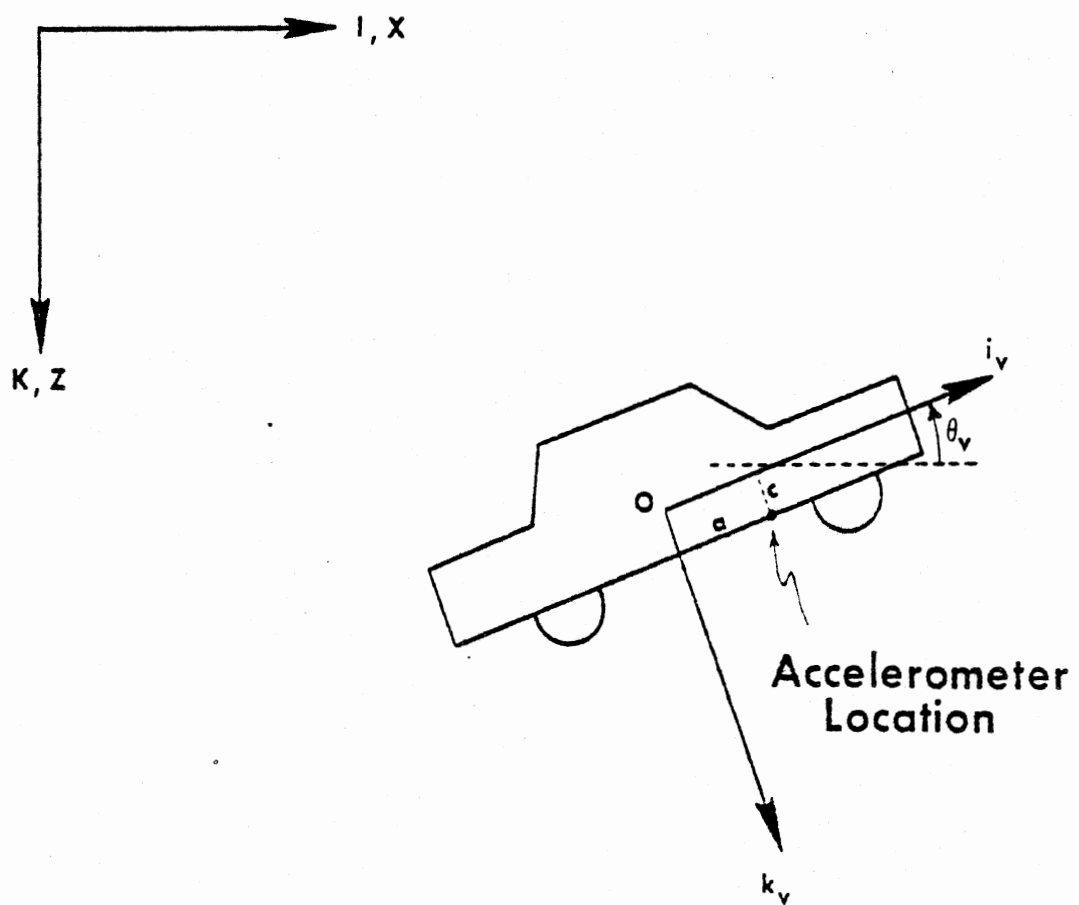


FIGURE 1-16 Vehicle Coordinates

SLIDE 1-21



## SLIDE 21

The crash victim's environment is made to be dynamic by specifying vehicle motion. Three independent motions are prescribed in tabular form as functions of time: 1) a horizontal acceleration; 2) a vertical acceleration; and 3) an angular "pitching" acceleration. The three degrees of freedom for vehicle motion are shown here. Example piecewise-linear approximations of hypothetical crash profiles are shown on the next slide.

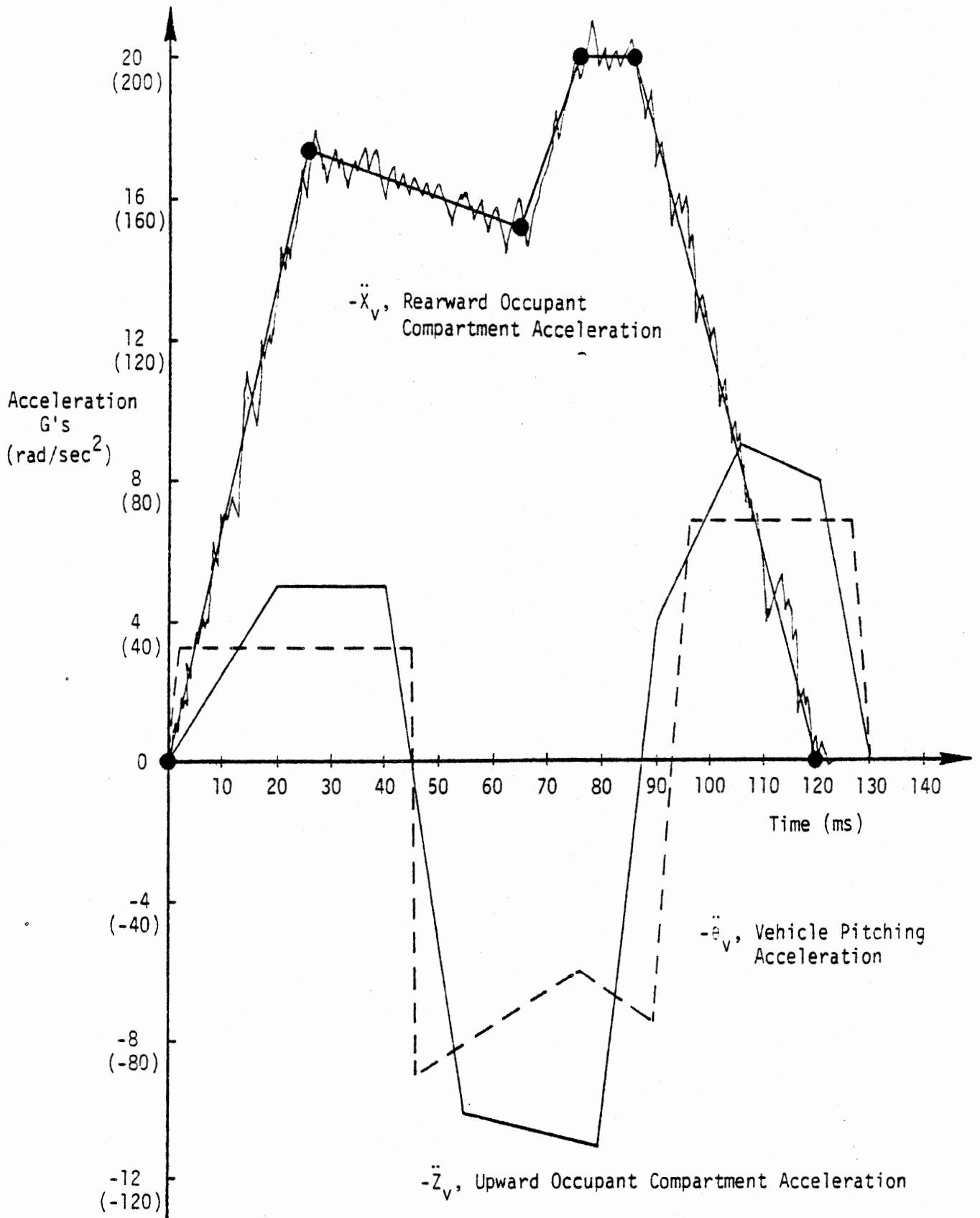


FIGURE 1-17 Vehicle Acceleration Profiles

SLIDE 1-22

## SLIDE 22

For user convenience several options are available with regard to specification of vehicle accelerations. Horizontal and vertical components may be defined as the responses of a biaxial accelerometer mounted on a part of the frame that is fixed with respect to the occupant compartment. Alternatively, the accelerations may be prescribed as motion components within an inertial frame of reference. The accelerations may be entered in g's or in physical units. Pitching accelerations may be in either  $\text{rad/sec}^2$  or  $\text{deg/sec}^2$ .

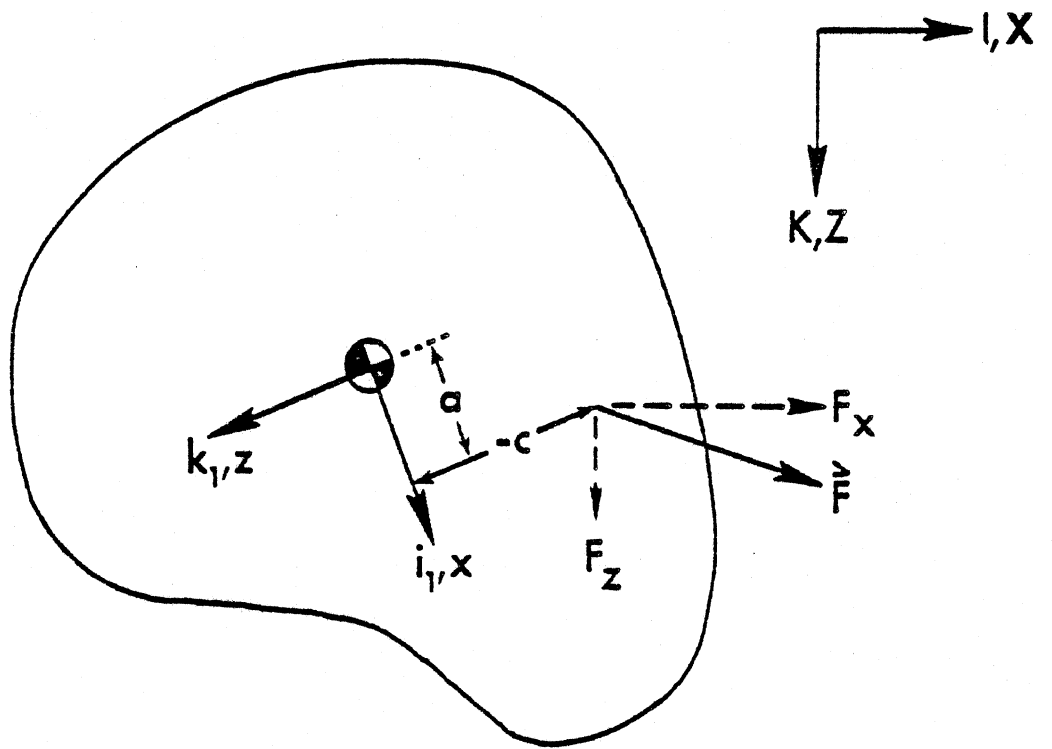


FIGURE 1-18 Schematic of Force Applied to Head

SLIDE 1-23

6/28/79

SLIDE 23

In special applications of the MVMA 2-D model, it can be useful to be able to specify time-dependent forces for direct application to the occupant. Provision is made for applying such a force to any desired point on the head, as shown.

## THE MULTIPROCESSOR MVMA 2-D MODEL

- IN = Input Processor
- GO = Dynamics Solution Processor, or Execution Processor
- OUTP = Output Pre-Processor
- OUT = Output Processor

FIGURE 1-19 The Multiprocessor MVMA 2-D Model

SLIDE 1-24

## SLIDE 24

The MVMA 2-D computer model is organized as a multiprocessor in that it is divided into five parts which operate in turn. The first processor is called the Input Pre-Processor, or INP.\* It reads data cards and writes the main program for the second processor. The second processor is called the Input Processor, or IN. It packs input data into binary tables and records those tables for use by subsequent processors. It also writes two programs needed by the third processor, including the main program. The third processor is called the Dynamics Solution Processor, or GO. It reads the binary tables, solves the equations of motion, and incorporates the computed results into the binary tables. The fourth processor is the Output Pre-Processor, or OUTP. It reads data cards and writes three programs needed by the fifth processor, including the main program. The fifth processor is called the Output Processor, or OUT. It reads the binary tables produced by the other processors and prints a comprehensive summary of all recorded information as the user specifies.

Discussion of the MVMA 2-D model in preceding sections of this module is pertinent only to the functions of the first three processors, that is: 1) reading and interpreting the input data; 2) solving the equations of motion for the simulated crash; and 3) storing results. The following discussion is pertinent to the output processor.

---

\* INP is not now used. It was used in an earlier version of the model. 12/4/85

## **FUNCTIONS OF THE OUTPUT PROCESSOR**

- **Digital filtering of accelerations**
- **Calculation and testing of potential injury indicators**
- **Printout of forty categories of computed results**
- **Formatted printout of input quantities**
- **Stick-figure printer plots**

**SLIDE 1-25**



## SLIDE 25

The Output Processor has two primary functions: 1) to process and analyze computed results with various so-called "post-processor" subroutines, and 2) to produce printed output.

Post-processor subroutines make possible digital filtering of occupant accelerations. Either filtered or unfiltered accelerations may be used in determinations of the Head Injury Criterion, HIC, and head and chest Severity Indices. Also, axial and shear components of femur and tibia loads can be calculated. Up to eighteen standard potential injury indicators including accelerations, loads, HIC, and severity indices can be compared against user-specified test values. Joint relative angles can be similarly tested. In addition, it is possible to compare any recorded response variable against any other or against high and low test values.

In its second function, printing time histories of response variables, the output processor deals with fifty different categories of computed results. They include information about vehicle motion, occupant motion, joint torques, and forces resulting from occupant interaction with elements of the vehicle interior and restraint systems. Any or all of these categories can be requested by the user for printout. In addition, it is possible to obtain formatted printout of input quantities. Finally, the output processor can produce printer-plot stick-figure representations of the occupant, the vehicle interior, and the restraint configuration. One stick figure from a time sequence of plots is shown on the next slide.

STICK FIGURE PRINTER PLOT FRAME FOR TIME= 60.00 MSEC.



Coordinate ranges for plot are X = 0.0 (at left) to 64.00 (at right) and Z = 2.24 (at bottom) to -41.24 (at top). Scale factor is (in) = 4.923 (in), X and Z point resolution errors equal respectively 0.246 and 0.410 (in) in scale.

FIGURE 1-20 Example of Printer Plot Output

SLIDE 1-26

SLIDE 26

One printer plot from a time sequence of plots is shown in this slide.

# DATA DECKS

## Card Number

100	Cards read by IN 100, 200, ..., 900 content used for automatic titling of pages
101	
102	
⋮	
1000	1000 (blank) marks end of data deck
1001	Cards read by OUTP.
1002	
1003	
⋮	
1600	1600 (blank) marks end of data deck

FIGURE 1-22 Data Decks

SLIDE 1-27

## SLIDE 27

Two data decks are required for computer simulations made with the MVMA 2-D model. Each data deck consists of a series of eighty-character lines which will be called "cards" in this discussion. The first data deck is read by the Input Processor, and the cards are identified by numbers 100 through 1000 in columns 78-80 or 77-80. Primarily, these cards contain data which describe the crash event, the occupant, the vehicle interior, and the restraint systems. The second data deck is read by the Output Pre-Processor. Each card is identified by a number 1001 through 1600 in columns 77-80. These cards contain data which control printout and the use of post-processors discussed previously. In general, data cards can be in any order within a data deck. Cards which control model options not used for a particular simulation need not be present. Also, various quantities can be defaulted to constants stored within the program by omitting their cards from the data deck.

1	2	3	4	5	6	7	8	9	ID NO.
00000000	00000000	00000000	00000000	00000000	00000000	00000000	00000000	00000000	00000000
11111111	11111111	11111111	11111111	11111111	11111111	11111111	11111111	11111111	11111111
22222222	22222222	22222222	22222222	22222222	22222222	22222222	22222222	22222222	22222222
33333333	33333333	33333333	33333333	33333333	33333333	33333333	33333333	33333333	33333333
44444444	44444444	44444444	44444444	44444444	44444444	44444444	44444444	44444444	44444444
55555555	55555555	55555555	55555555	55555555	55555555	55555555	55555555	55555555	55555555
66666666	66666666	66666666	66666666	66666666	66666666	66666666	66666666	66666666	66666666
77777777	77777777	77777777	77777777	77777777	77777777	77777777	77777777	77777777	77777777
88888888	88888888	88888888	88888888	88888888	88888888	88888888	88888888	88888888	88888888
99999999	99999999	99999999	99999999	99999999	99999999	99999999	99999999	99999999	99999999

HIGHWAY SAFETY  
RESEARCH INSTITUTE  
**HSri**  
The University of Michigan  
Ann Arbor

Acceptable data formats

F	E	D
123.4	1.234E2	1.234D2

FIGURE 1-23 A Data Card

## SLIDE 28

Each card consists of ten fields. The tenth field is reserved for the previously mentioned card identification number. The first nine fields, consisting of eight columns each, are data fields. Thus, up to nine numbers may be required per card although most cards make use of a smaller number of fields. Numerical data must be specified in either F, E, or D format, examples of which are given with the figure.

TABLE 7. INPUT DATA

FRICTION COEFFICIENTS  
(9 Fields of 8)

Fields	Name of Quantity	Units	Description	Defaults
1			Ellipse friction class (1. to 5.)	
2			Region friction class (1. to 10.)	
3	CMU (·,·,1), $\mu_k^0$		Constant friction coefficient.	0.
4	CMU (·,·,2), $\mu_k^1$	1/in (1/cm)	Linear friction coefficient.	0.
5	CMU (·,·,3), $\mu_k^2$	1/in <sup>2</sup> (1/cm <sup>2</sup> )	Second order friction coefficient	0.

NOTES: 1. A non-linear friction coefficient is computed to simulate "plowing."

$$\mu = \mu_k^0 + \mu_k^1 \delta + \mu_k^2 \delta^2$$

2. There must be one 412 card for each combination of ellipse and region friction class indicated on Cards 215 and Cards 402.

3. See Section 2.6.6.

MVMA 2-D Model  
Card 412

FIGURE 1-24 Example Card Layout from Volume 2 of MVMA 2-D Report Manuals



## SLIDE 29

The Tutorial System self-study guide and audio-visual program are intended to facilitate learning to use the MVMA Two-Dimensional Crash Victim Simulator. The point must be made, however, that the model user must have the MVMA 2-D report manuals, specifically Volume 2, in order to prepare data for a simulation. The Tutorial System self-study guide is not intended to be a replacement for the report manuals, but rather, a detailed supplement.

Volume 2 of the MVMA 2-D report manuals include a description of all data cards and their content, card by card and field by field. The slide shows a typical card layout from Volume 2. The table from which this example page is taken includes over 100 such card layouts. They must be referenced in the preparation of a data set, but they are not included with the Tutorial System. The table, in addition to collecting in one place a description of all required input data, includes information regarding default values for fields of cards omitted from the data deck and also information regarding required units for data, field by field. The units required for running the model with metric-system or English-system data are indicated separately.

DATA CARDS REFERENCED BY MODULES

Module	Data Cards Referenced
2	201-217, 303, 227-238
3	201-203, 205-217, 227, 228, 233, 235-242, 303
4	102, 103, 106, 219-226, 402, 412, 903, 907-909
5	102, 103, 106, 219, 401-412
6-1	103, 219, 221-226, 401, 403-408, 702-716
6-2	102, 103, 219, 222, 401, 402, 404, 409, 410, 412, 605, 606, 705
7	205, 206, 215, 216, 301-304, 409, 1501, 1502
8	601-606
9	102, 218, 501, 701-723
10	102, 411, 901-909
11	-
12	101, 102, 104, 105, 107-111, 218, 1000-1004, 1100-1107, 1200-1202, 1300, 1400, 1401, 1500-1502, 1600

FIGURE 1-25 Data Cards Referenced By Modules

SLIDE 1-30

## SLIDE 30

As previously mentioned, Tutorial System Modules 2 through 12 deal with different groups of related model features. However, it is not possible to make the treatment of all subject matter in each module completely self-contained. For example, Module 9 describes the two optional belt restraint systems in detail. But the description of general material property specifications, which are relevant to belt webbing, body parts, and elements of the vehicle interior, is in Module 6. Thus, reference to belt webbing material properties is made in more than one module. Two tables are included in Module 1 to aid the Tutorial System user in locating information within the self-study guide relevant to any input data parameter. The first shows all data cards referenced by each module.

DATA CARD FIELDS  
AND REFERENCING MODULES

Card	Field								
	1	2	3	4	5	6	7	8	9
101	12	12	12	12	12	12	12	12	12
102	9,12	10,12	12	4	4,5	4	6-2	12	12
103	6-2	6-2	6-1	6-1	6-2	5	5	4	4
104	12	12	12	12	12	12	12	12	12
105	12	12	12	12	12	12	12	12	12
106	4,5	4,5	4,5	4,5					
107	12	12	12	12	12	12	12	12	12
108	12	12	12	12	12	12	12	12	12
109	12	12	12	12	12	12	12	12	12
110	12	12	12	12	12	12	12	12	12
111	12	12	12	12					
201	2,3	2	2	2	2		2	3	3
202	2,3	2,3	2	2	2	2	2	2	3
203	2	2	2	2	2	2	2	2	2,3
204	2	2	2	2	2	2	2	2	
205	2,3	2,3	2,3	2,3	2,3	2,3	2,3	2,3,7	2,3
206	2,3	2,3	2,3	2,3	2,3	2,3	2,3	2,3,7	2,3
207	2	2	2	2	2	2	2	2	2
208	2	2	2	2	2	2	2	2	2
209	2	2	2	2	2	2	2	2	2
210	2	2	2	2	2	2	2	2	2
211	2,3	2,3	2,3	2,3	2,3	2,3	2,3	2,3	2,3
212	2	2	2	2	2	2	2	2	2

FIGURE 1-26 Data Card Fields Referencing Modules (Page 1 of 6)

SLIDE 1-31

SLIDE 31

The second table, one page of which is shown here, indicates all modules which reference each field of each card.

## USING THE TUTORIAL SYSTEM

- Sequential viewing of the audio-visual modules, followed by use of the self-study guide

or

- Alternate use of the audio-visual program and the self-study guide

SLIDE 1-32

## SLIDE 32

Module 1 has served as an introduction to the MVMA Two-Dimensional Crash Victim Simulator and the Tutorial System. The Tutorial System should be used in either of two ways.

First, the thirteen audio-visual modules may all be run, sequentially, before the self-study manual is used. The audio-visual modules, each consisting of 35 mm slides and narration on a tape cassette, treat model features in much greater detail than they have been discussed in this introductory module. However, they cover their material in much less depth than the self-study manual; each includes only 15-25 minutes of narration. Therefore, they can be used together as a detailed, four and one-half hour, audio-visual introduction to the model. They need not be viewed in one session, of course. In this method of using the Tutorial System, use of the self-study guide would follow viewing of all modules.

Alternatively, viewing of audio-visual modules and use of the self-study guide can alternate. In this method, the user of the Tutorial System would study the subject matter of a module in detail before proceeding to the next module.

Either method should be effective in preparing the user for applying the MVMA Two-Dimensional Crash Victim Simulator to problems of automotive safety design. After study of Module 13, the user should be ready to exercise the model. The MVMA 2-D model can be applied in various ways for the modeling of dynamical systems. A broad range of front, rear, and even side impacts for driver and passenger have been simulated. Applications have included simulating anthropomorphic dummy drops onto a hard surface and human fall victims striking yielding and unyielding surfaces. Uses have included simulating pedestrians struck by a vehicle. Simulations have been done of laboratory tests in which lateral neck response of human subjects was measured when the head was jerked to the side by a falling weight. But use of the MVMA 2-D model need not be restricted to simulating human or human-analog systems. Diverse applications are possible if the user is clever in utilizing the many features of the model.





**MVMA 2-D**  
**CRASH VICTIM SIMULATION**

**\* \* \***

**MODULE 12**

**MODEL OPERATION**

The next module is MODULE 12 -- "MODEL OPERATION."

Module 12 has been moved to this location, following Module 1, since it helps in giving an overall view of the MVMA 2-D model. (12/4/85)

**MVMA 2-D**  
**CRASH VICTIM SIMULATION**

**\* \* \***

**MODULE 12**

**MODEL OPERATION**

**SLIDE 12-1**

## MODULE 12 -- MODEL OPERATION

### SLIDE 1

The MVMA Two-Dimensional Crash Victim Simulator is a large and complex computer program. Some of the input quantities to the MVMA 2-D Model deal with the alternatives in operation of the computer program as opposed to the description of the event being simulated. Understanding some of the program controls entails some knowledge of the architecture of the model program.

## THE MULTIPROCESSOR MVMA 2-D MODEL

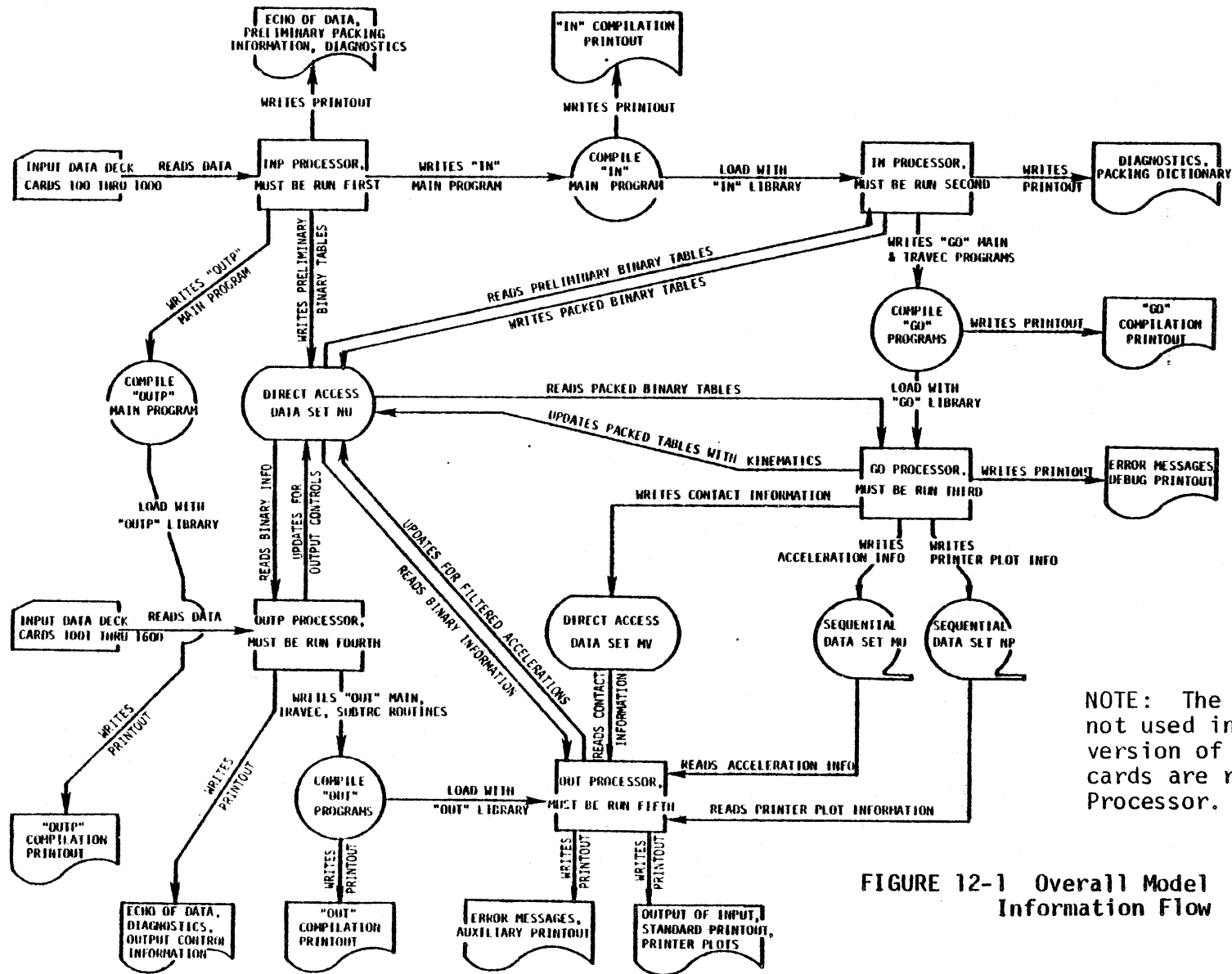
- IN = Input Processor
- GO = Dynamics Solution Processor, or Execution Processor
- OUTP = Output Pre-Processor
- OUT = Output Processor

SLIDE 12-2

6/28/79

## SLIDE 2

The MVMA 2-D computer model is organized as a multiprocessor in that it is divided into five parts which operate in turn. The first processor is called the Input Pre-Processor, or INP. It reads data cards and writes the main program for the second processor. The second processor is called the Input Processor, or IN. It packs input data into binary tables and records those tables for use by subsequent processors. It also writes two programs needed by the third processor, including the main program. The third processor is called the Dynamics Solution Processor, or GO. It reads the binary tables, solves the equations of motion, and incorporates the computed results into the binary tables. The fourth processor is the Output Pre-Processor, or OUP. It reads data cards and writes three programs needed by the fifth processor, including the main program. The fifth processor is called the Output Processor, or OUT. It reads the binary tables produced by the other processors and prints a comprehensive summary of all recorded information as the user specifies.



NOTE: The INP Processor is not used in the current version of the model. Data cards are read by the IN Processor.

FIGURE 12-1 Overall Model Information Flow

### SLIDE 3

The flow diagram summarizes the communication between the five processors by means of four external files which store the binary tables. All data generated by a computer run are contained in these files, and they may be used for input into post-processors such as the Validation Command Language or a graphics package.

## EXTERNAL COMMUNICATION FILES

FILE	TYPE	CONTENT
NU	Direct access	All input and all fixed-length computed results
MU	Sequential	Head, chest, and hip acceleration results
MV	Direct Access	Variable-length computed results
NP	Sequential	Information for printer-plot output

SLIDE 12-4



#### SLIDE 4

The four files are called NU, MU, MV, and NP, respectively for the four variables used to reference the logical device numbers to which they are attached. NU is a direct access data set which contains all input quantities and all fixed-length computed results. MU is a sequential data set which contains head, chest, and hip acceleration information for every integration time step. MV is a direct access data set which contains the variable-length computed results, which include contact interactions, region movement, and region summary quantities. NP is a sequential data set which contains the special information needed for production of stick-figure printer-plot output.

Category Number	Description
0	Formatted Printout of Input Quantities
1	Vehicle Response
2	Real Line Region Parameters
3	Real Line Region Individual Line Segment Movement
4	Contact Forces Including Occupant-Vehicle, Occupant-Belt, Occupant-Occupant
5	Neck Reaction Forces
6	Unfiltered Body Accelerations (Head, Chest, Pelvis)
7	Filtered Body Accelerations (Head, Chest, Pelvis)
8	Unfiltered Severity Indices
9	Filtered Severity Indices
10	Body Link Angles
11	Body Link Angular Velocities
12	Body Link Angular Accelerations
13	Body Joint Coordinates
14	Body Joint Velocities
15	Body Joint Torques
16	Body Joint Absorbed Energies
17	Body Kinetic Energies
18	Airbag Variables
19	Airbag Contact Forces
20	Airbag Center of Mass Forces and Moments
21	Neck Joint Coordinates
22	Shoulder Joint Coordinates
23	Joint Torque Elastic Components
24	Joint Torque Joint-Stop Components
25	Joint Torque Friction Components
26	Joint Torque Viscosity Components
27	Joint Absorbed Energy Joint Stop Components
28	Joint Absorbed Energy Friction Components
29	Joint Absorbed Energy Viscosity Components
30	Center of Mass X-Component Forces
31	Center of Mass Z-Component Forces

FIGURE 12-2a List of Output Categories

SLIDE 12-5

## SLIDE 5

The computed results are broken into subjects, or categories, which correspond to output pages for the fixed-length output and to "typical output pages" for the variable-length output. There are forty-five such categories and these are numbered 1-40 and 46-50. In addition to these, there are six special types of output for which it was convenient to use the same numbering scheme even though they are not recorded in the same manner. These categories are numbered 0 and 41 through 45. This slide and the following one list all forty-six categories. Categories 1-40 and 46-50 may be optionally recorded on binary files under control of the recording switches. These switches may be set by the user to inhibit the recording of the information for the respective categories.

The input to the output pre-processor allows specification of which categories are to be printed during the execution of OUT and the order in which the categories are to appear. The ordering of the categories is entirely general except that category number zero, for output of the input values, must occur first if it occurs at all.

Category Number	Description
32	Center of Mass Resultant Moments
33	Steering Column Coordinates
34	Steering Column Generalized Coordinates
35	Steering Column Forces and Moments
36	Forces and Moments on Body Due to Steering Column
37	Neck and Shoulder Forces
38	Muscle Tension Forces
39	Muscle Tension Energy Absorption
40	Femur and Tibia Accelerations and Loads
41	Joint Relative Angle Comparisons Against Upper and Lower Test Values
42	Standard List of Quantities to be Compared Against Test Values
43	Individual Type A Comparisons
44	Individual Type B Comparisons
45	Printer-Plots of Stick Figures
46	Head Center-of-Gravity Motion
47	Chest Center-of-Gravity Motion
48	Hip Motion
49	Joint Relative Angles
50	Joint Relative Angle Velocities

FIGURE 12-2b List of Output Categories

SLIDE 12-6

## SLIDE 6

The output processors may be re-run with specification of different categories for printout as many times as desired as long as the binary tables remain undisturbed. A particular category will be printed if the category was recorded by GO and was specified as desired for printout in the input to OUP.

## GENERAL MODEL CONTROLS

- Model operation in metric or English units
- Acceleration due to gravity,  $g$  (standard values are  $32.174 \text{ ft/sec}^2$  and  $9.80665 \text{ m/sec}^2$ )
- Editing of accelerations for minimum non-zero magnitude
- Relative error bound for matrix inversion
- Switches for use of optional submodels
- Integration controls

SLIDE 12-7

## SLIDE 7

General model controls will be discussed next.

The MVMA 2-D CVS Model is capable of accepting input and producing output in either metric units or in American standard units. Interpretation of input data with respect to system of units is controlled by a user-set switch.

The acceleration due to gravity is specifiable by the user. The values shown on the slide are used within the program for determining accelerations that are to be printed out in G-units.

It is sometimes useful to edit acceleration values. Accelerations smaller in magnitude than a user-specified value will be set to zero. The editing facility can improve the appearance of the tabulated results and rarely will affect the accuracy of a computation.

A parameter which must be specified for each simulation is a relative error bound used for identifying the occurrence of a singular matrix for the equations of motion. 0.000001 is the recommended value.

Four optional subsystems are available within the MVMA 2-D CVS Model for two belt models, an airbag model and an energy-absorbing steering column model. These four options are controlled by three switches. The first switch is used to indicate the general belt system to be used or to indicate that no belt system is to be considered. The belt-restraint options are the three-belt submodel using either the lap belt only or both lap belt and shoulder harness and the advanced belt-system submodel. The other two switches deal with airbag and steering column respectively and are set non-zero to indicate use of the respective subsystem.

Finally, values are required for the simulation beginning time, ending time, integration time step, tabular output time step, time step for plot recording, and an execution time limit.

## DEBUGGING PRINTOUT

- Sixteen debug switches
- Switches are four-level
  - 0 = off
  - 1 = primary debugging printout
  - 2 = secondary debugging printout
  - 3 = tertiary debugging printout
- Switch levels are functions of simulated time

SLIDE 12-8



## SLIDE 8

A large amount of optional auxiliary, or "debugging," printout can be obtained from the execution processor, GO. Printouts are organized under sixteen four-level switches. Each switch corresponds to a particular section of the program. The level for a particular switch controls the depth of detail of the debugging printout from the section of the program which the switch covers. The four levels are: off, primary, secondary, and tertiary. Setting a switch for tertiary printout will automatically produce secondary and primary level printout. Similarly, a setting for secondary printout will produce primary printout as well. To avoid needless volume of printout, the level for each of the switches may be varied with simulated time.

The standard use of the auxiliary output is for debugging abnormal runs. For particularly elusive "bugs" it can be useful to examine the contents of the computer core at some value of simulated time. A dump of core is possible through use of switch 16. A complete description of debug switches and the printout they control may be found in Volume 3 of the MVMA 2-D manuals.

## DATA DECKS

### Card Number

100

101

102

⋮

1000

Cards read by IN

100, 200, ..., 900 content used for  
automatic titling of pages

1000 (blank) marks end of data deck

1001

1002

1003

⋮

1600

Cards read by OUTP.

1600 (blank) marks end of data deck

SLIDE 12-9

## SLIDE 9

Input data described in preceding modules and to this point in Module 12 have been for the input pre-processor, IN. These data are sufficient for IN to produce a data set which can be read by the GO processor. Additional data are needed, however, by the output processor. These are discussed in the remainder of this module. Cards read by IN have identification numbers 100 through 1000. Cards read by OUTP are numbered 1001 and greater.

Much of the data used by the output processor relate to calculation and monitoring of response parameters that are potential injury indicators. For example, femur and tibia loads will be printed if the user requests Category Number 40 both for the recording and printing of results, as previously explained. Associated input data read by OUTP are the position of a simulated femur load sensor and the upper leg mass between the sensor and the knee.

### Characteristics of a Martin-Graham Digital Filter

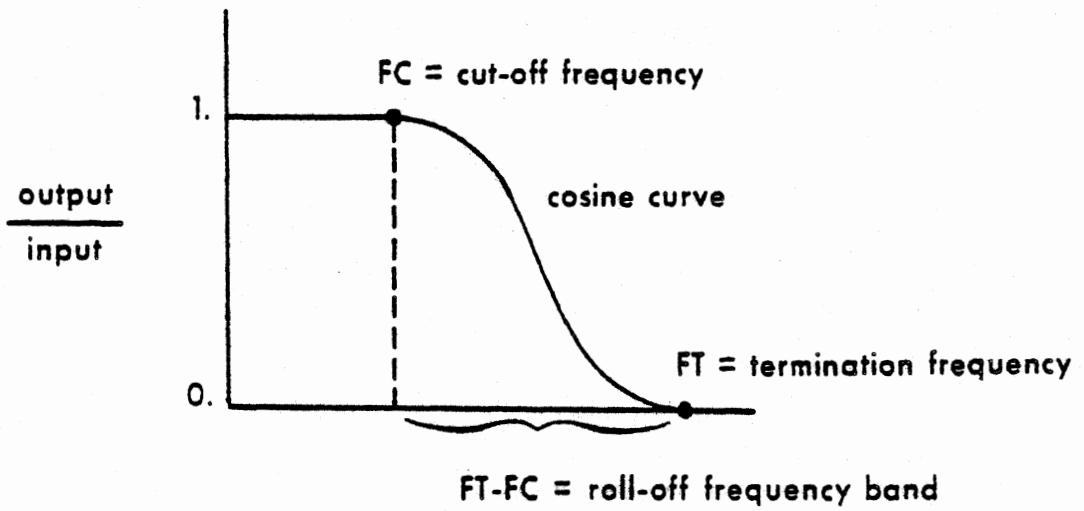


FIGURE 12-6 Characteristics of a Martin-Graham Digital Filter

SLIDE 12-10

## SLIDE 10

Other potential injury indicators are accelerations and acceleration-functionals such as the Head Injury Criterion, or HIC, and the Severity Index. By requesting appropriate category numbers, the user can obtain printout of values determined from filtered or unfiltered accelerations, or both. A Martin-Graham low-pass digital filter is used in the MVMA 2-D model. This figure illustrates the attenuation ratio, or gain, for this filter. Filter controls required from the user include cut-off frequency, termination frequency, and the number of filter weights. Also, the user can specify that either a polar image or a mirror image be used for analytical extensions of the unfiltered signal.

Number	Quantity Description
1	Head frontal acceleration at the center of gravity (Anterior-posterior, A-P)
2	Head vertical acceleration at the center of gravity (Superior-inferior, S-I)
3	Head resultant acceleration at the center of gravity
4	Head angular acceleration
5	Head injury criterion (HIC)
6	Face loads as measured on a deformable head contact ellipse
7	Chest deflection as measured on a deforming chest contact ellipse
8	Chest load as measured on a deforming chest contact ellipse
9	Chest frontal acceleration at the center of gravity (A-P)
10	Chest vertical acceleration at the center of gravity (S-I)
11	Chest resultant acceleration at the center of gravity (3 msec average)
12	Chest frontal severity index (A-P)
13	Chest vertical severity index (S-I)
14	Chest resultant severity index
15	Pelvic horizontal acceleration at the hip joint
16	Pelvic vertical acceleration at the hip joint
17	Pelvic resultant acceleration at the hip joint
18	Femur load at a specified point along the length representing the location of a sensor

FIGURE 12-9 List of Injury Related Test Quantities

SLIDE 12-11

## SLIDE 11

Eighteen potential injury indicators are listed here. The user may optionally monitor any of these by specifying that the magnitudes of the quantities be checked to see if they exceed prescribed test values. For each time range during which a test value is exceeded, output is produced. The output includes the quantity name, the peak value, the time at which the peak occurs, and the time duration during which the quantity exceeds the specified test value together with the points in time at which the quantity exceeds and then returns below the test value.

## COMPARISON TESTS FOR POTENTIAL INJURY INDICATORS

INDICATORS	COMPARED AGAINST
● Eighteen in standard list	Magnitude limits
● Joint relative angles	High and low test values
● Any variable recorded for printing	High and low test values (Type A Comparison)
● Any variable recorded for printing	Any other variable recorded for printing (Type B Comparison)

SLIDE 12-12

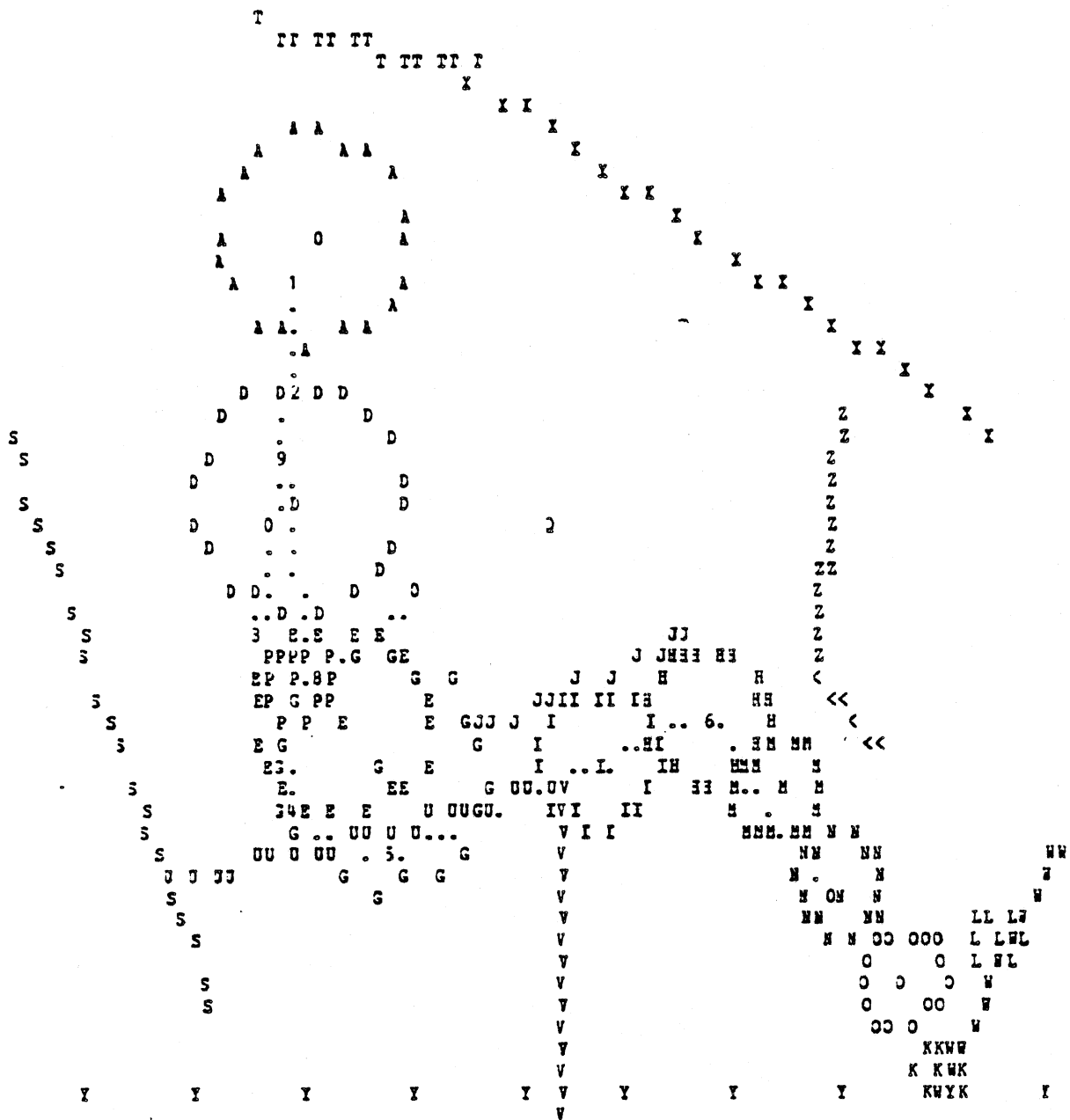


## SLIDE 12

In addition, relative angles at all eight joints can be compared with high and low test values. If the joint relative angle exceeds the high test value or goes below the low test value, printout will include the quantity name, peak value, time of peak, violation duration, beginning time of violation, and ending time of violation.

Two other types of tests can be made of response variables. The class of variables that can be examined by these tests consists of all quantities that are recorded for printing. The first test is called a Type A comparison. It involves the comparison in time of any response variable against high and low test values. The printout is similar to that produced for the joint relative angle test. The second test is called a Type B Comparison. It allows comparison of any recorded response variable against any other. The produced output lists each of the variables, their difference, and an indication of which is larger.

STICK FIGURE PRINTER PLOT FRAME FOR TIME= 60.00 MSEC.



Coordinate ranges for plot are X = 0.0 (at left) to 64.00 (at right) and Z = 2.24 (at bottom) to -41.24 (at top). Scale factor is (in) = 4.923 (in), X and Z point resolution errors equal respectively 0.246 and 0.410 (in) in scale.

FIGURE 12-12 Example of Printer Plot Output

SLIDE 12-13

## SLIDE 13

The MVMA Two-Dimensional CVS Model optionally produces a printer-plot stick-figure representation of the occupant, the vehicle interior, and the restraint configuration. The model can produce a stick-figure plot based on input data alone or a time sequence of plots based on computed results from the Dynamic Solution Processor, or both. The plot based on input data can be obtained even if the output processors are run after the input processors without the intermediate execution of the Dynamics Solution Processor.

The slide shows an example of a stick-figure plot. The location of each of the body joints is represented by an integer. The link lines between joints are represented with dots or decimal points. Zeroes represent the positions of the centers of gravity of the head, upper torso, lower arm, and lower leg. Ellipses and contact regions are represented by letters. The positions of the vehicle coordinate axes are shown with asterisks.

The primary specifications required of the user for the generation of stick-figure printout are minimum and maximum x- and z-coordinates for framing the occupant compartment and simulation times at which plots are desired. Desired plot times may be individually specified, or equally-spaced plot times can be generated by the program on the basis of a user-prescribed plot-time increment. In either case a maximum of 27 plots is allowed.

## SUMMARY OF MODEL OPERATION OPTIONS AND DATA REQUIREMENTS

- Simulation time parameters
- Metric or English system units
- Digital filter specifications
- 45 optional standard output categories
- 6 optional special output categories
  - Printout of input data
  - Printer-plot stick-figure sequences
  - Tests on potential injury indicators
- Optional "debugging" output

SLIDE 12-14

6/28/79

## SLIDE 14

Many options for operation of the computer program have been discussed. The controls required for model operation include values for the simulation beginning time, ending time, integration time step, and tabular output time step. Physical parameters in the input data set may be in either metric or English system units, and the user denotes which by setting a switch appropriately. Digital filter specifications are entered whenever it is desired to filter occupant acceleration responses. Printout of up to fifty-one categories of quantities can be produced. The user may specify any of forty-five standard output categories, and any of six special categories. The special categories include printout of the input data set, printer-plot stick figures, and results for comparisons of potential injury indicators against test values. Finally, auxiliary "debugging" printout can be obtained from the Dynamics Solution Processor by specification of various controls.



**MVMA 2-D**  
**CRASH VICTIM SIMULATION**

**\* \* \***

**MODULE 2**

**THE BODY LINKAGE**

**MVMA 2-D**  
**CRASH VICTIM SIMULATION**

**\* \* \***

**MODULE 2**

**THE BODY LINKAGE**

**SLIDE 2-1**



## MODULE 2 -- THE BODY LINKAGE

### SLIDE 1

The MVMA-2D crash victim is represented analytically as a "lumped mass" dynamical system. That means that we approximate the body by a string of rigid links and that all viscoelastic elements affecting angulation of body parts relative to each other act at discrete points connecting the links. This approach is essentially the same as used in other crash victim simulators developed to date.

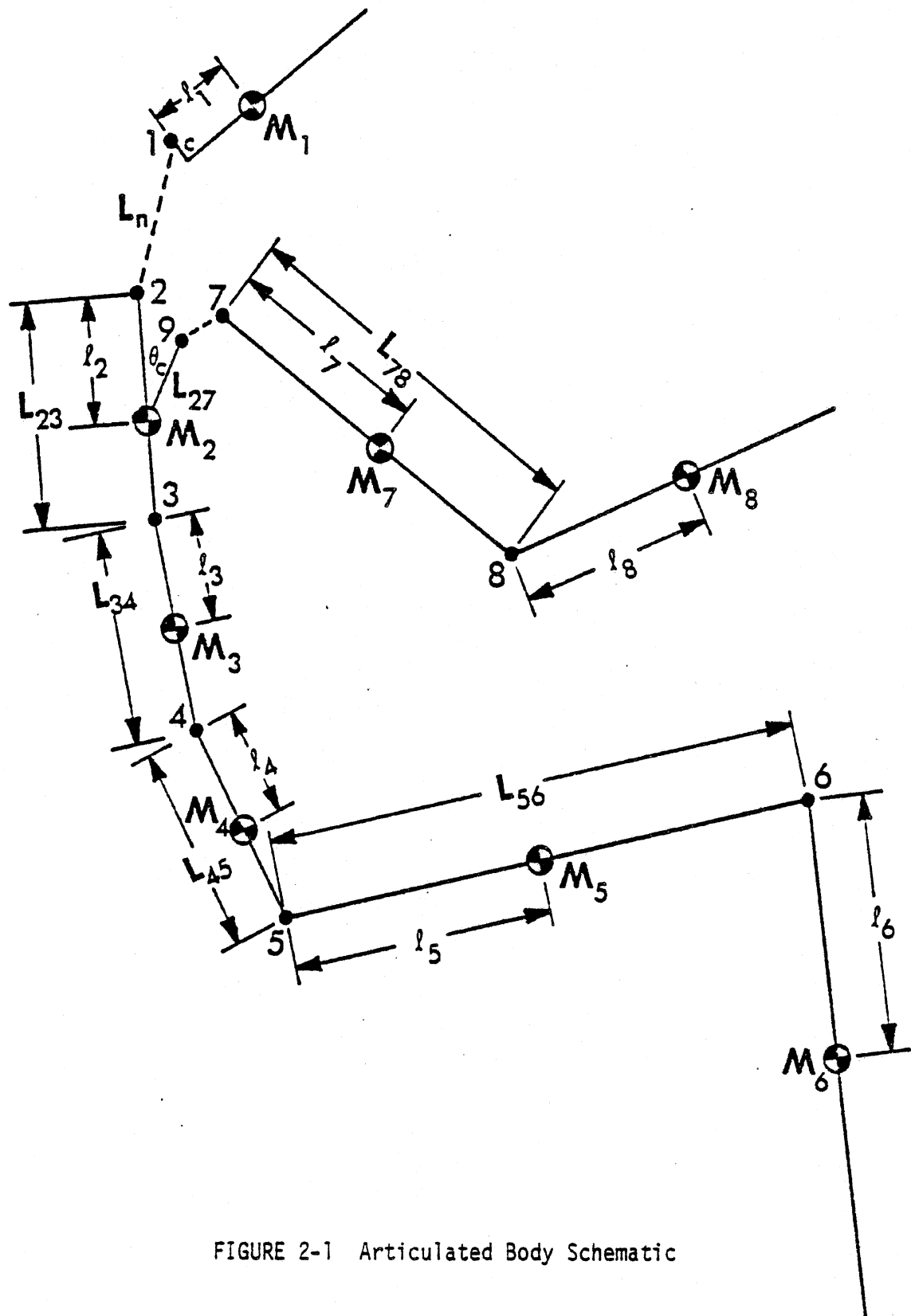
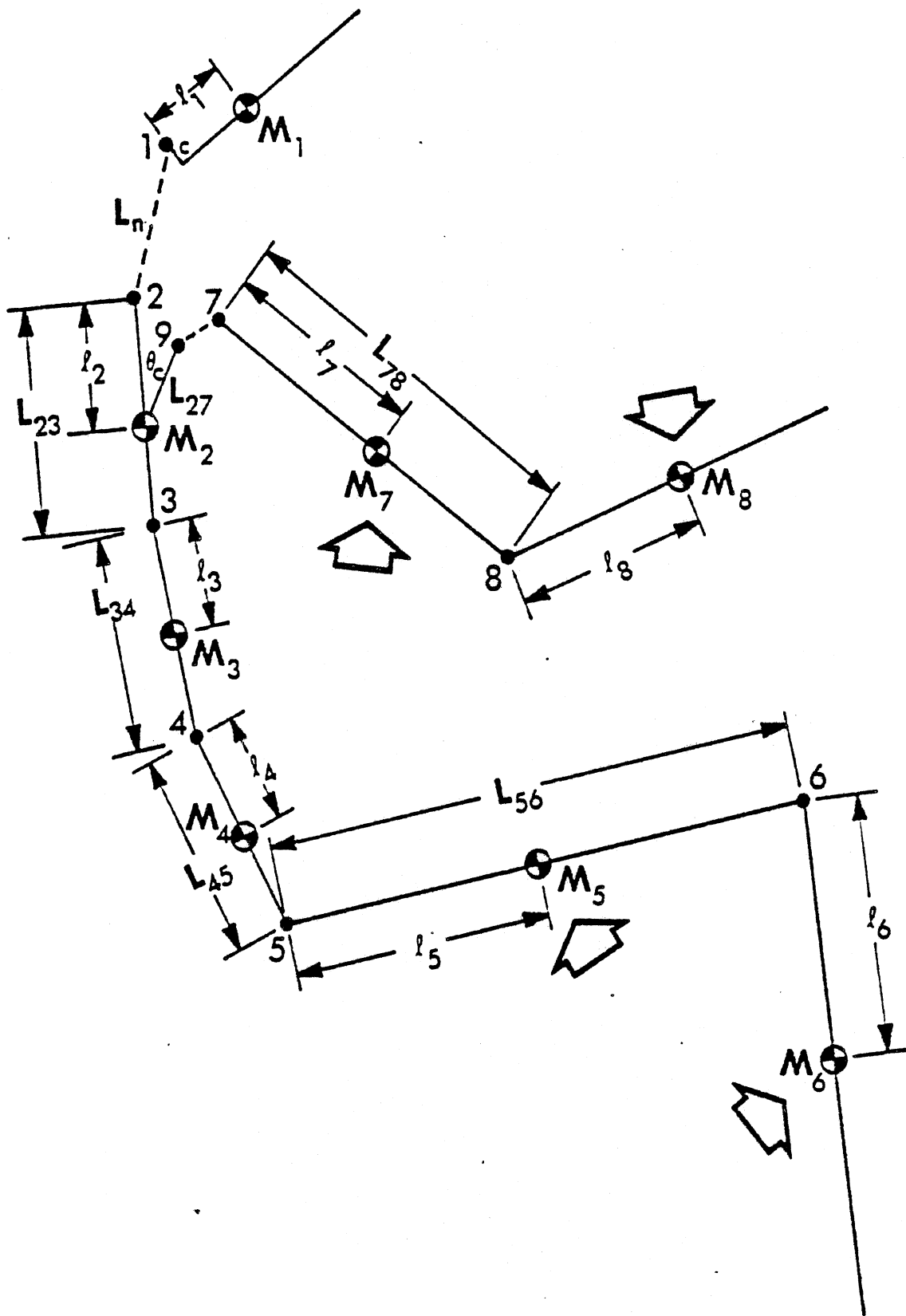


FIGURE 2-1 Articulated Body Schematic

SLIDE 2-2

SLIDE 2

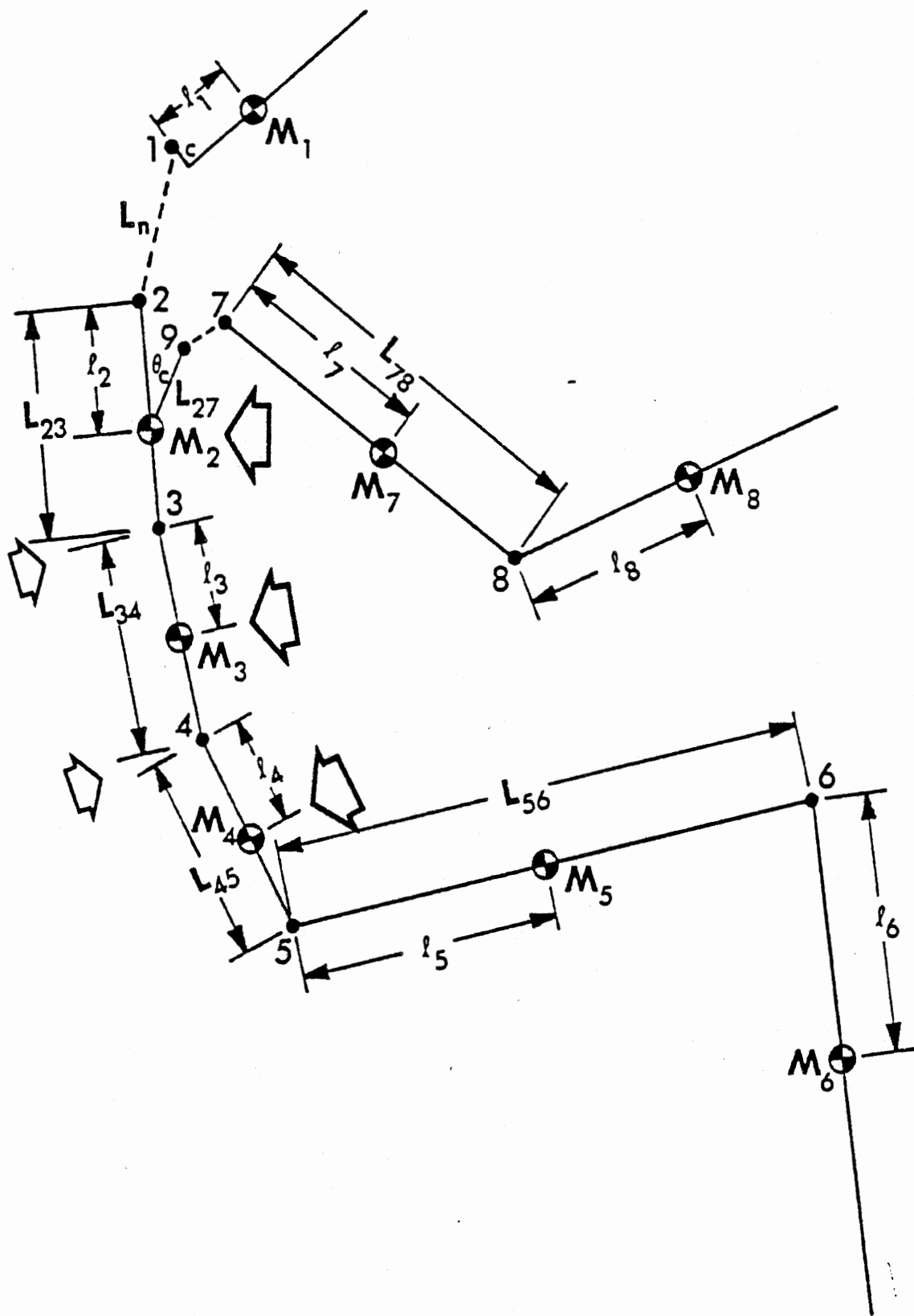
The first figure illustrates this body linkage. The crash victim is treated as an eight-mass system in which ten physical links are represented. The user of the MVMA-2D model supplies values for link lengths illustrated and specifies the location of each link center of mass with respect to a body joint. A mass and moment of inertia are specified for each body element.



SLIDE 2-3

### SLIDE 3

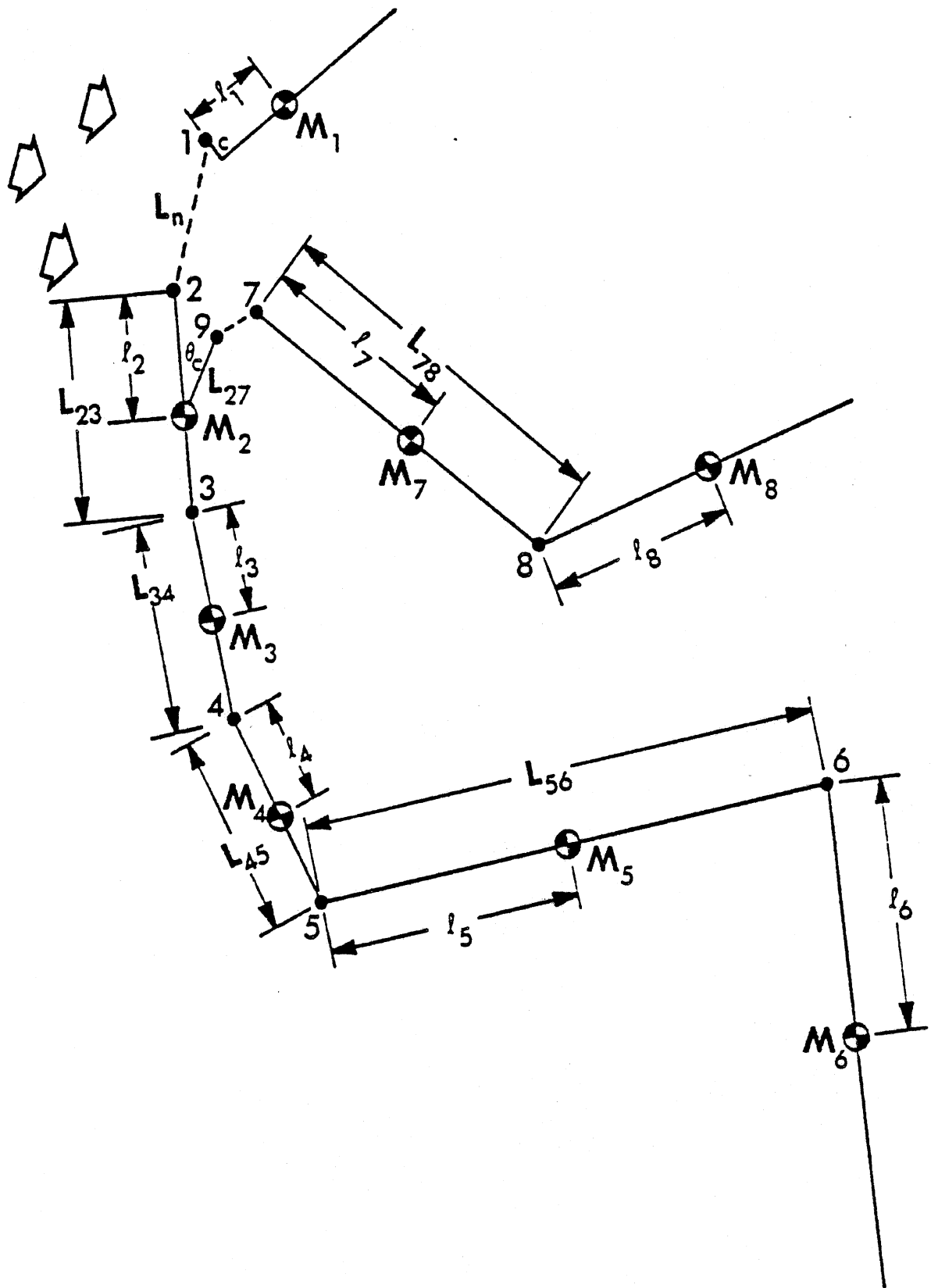
Since this is a planar model there would be no great purpose to including left and right legs separately. Consequently, a single two-link leg represents the two legs combined, as if bound together. Accordingly, the thigh and lower leg masses,  $M_5$  and  $M_6$ , should be assigned double values. The arms are similarly treated as only two links.



SLIDE 2-4

#### SLIDE 4

The human spinal column is more or less continuously flexible since it is composed of thirty-three vertebrae and intervening fibrocartilaginous discs. The model simulates flexibility of the combined thoracic and lumbar spines by two articulations which connect three torso masses. These are joints 3 and 4 in the figure. The mass  $M_2$  ordinarily represents the thorax and contents while  $M_4$  represents the pelvis and attached soft tissues. Mass  $M_3$  can be called the abdominal area as it serves as the mass between the thoracic and pelvic regions.

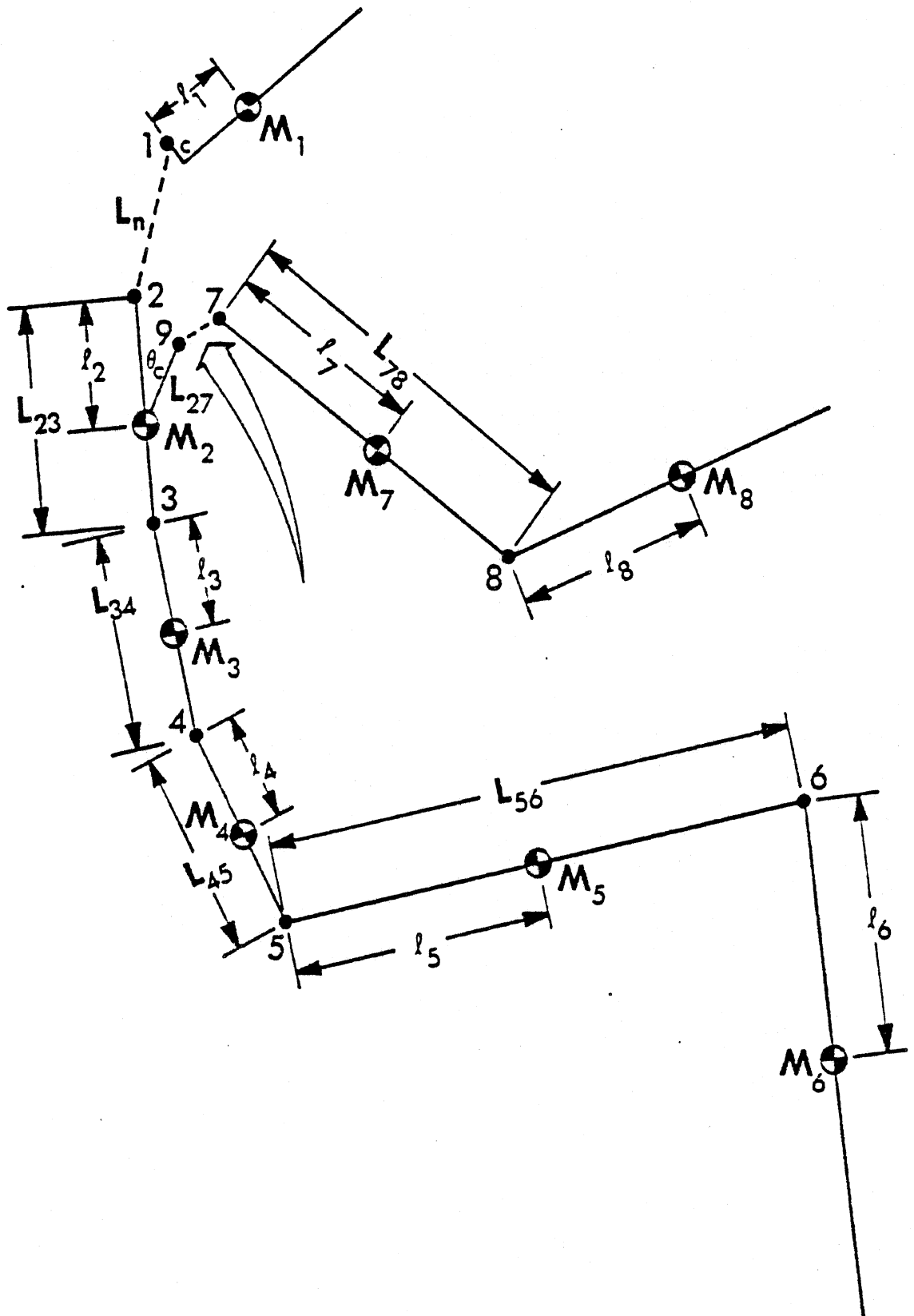


SLIDE 2-5



## SLIDE 5

Flexibility of the cervical spine (neck) is accounted for by two articulations, one at the occipital condyles at the base of the skull and one at the seventh-cervical/first-thoracic juncture, where the neck joins the chest. The neck element itself is massless in this model, but neck mass can be apportioned however desired at the head and torso junctures. This element can undergo both compression and elongation. Note that the upper neck articulation may be offset from the vertical head axis.



SLIDE 2-6

## SLIDE 6

A similar massless body link is found at the shoulder connecting joints 7 and 9 in the figure. This element allows simulation of shoulder flexibility resulting from motion of the clavicle. Neck and shoulder flexibility is discussed in detail in Module 3.

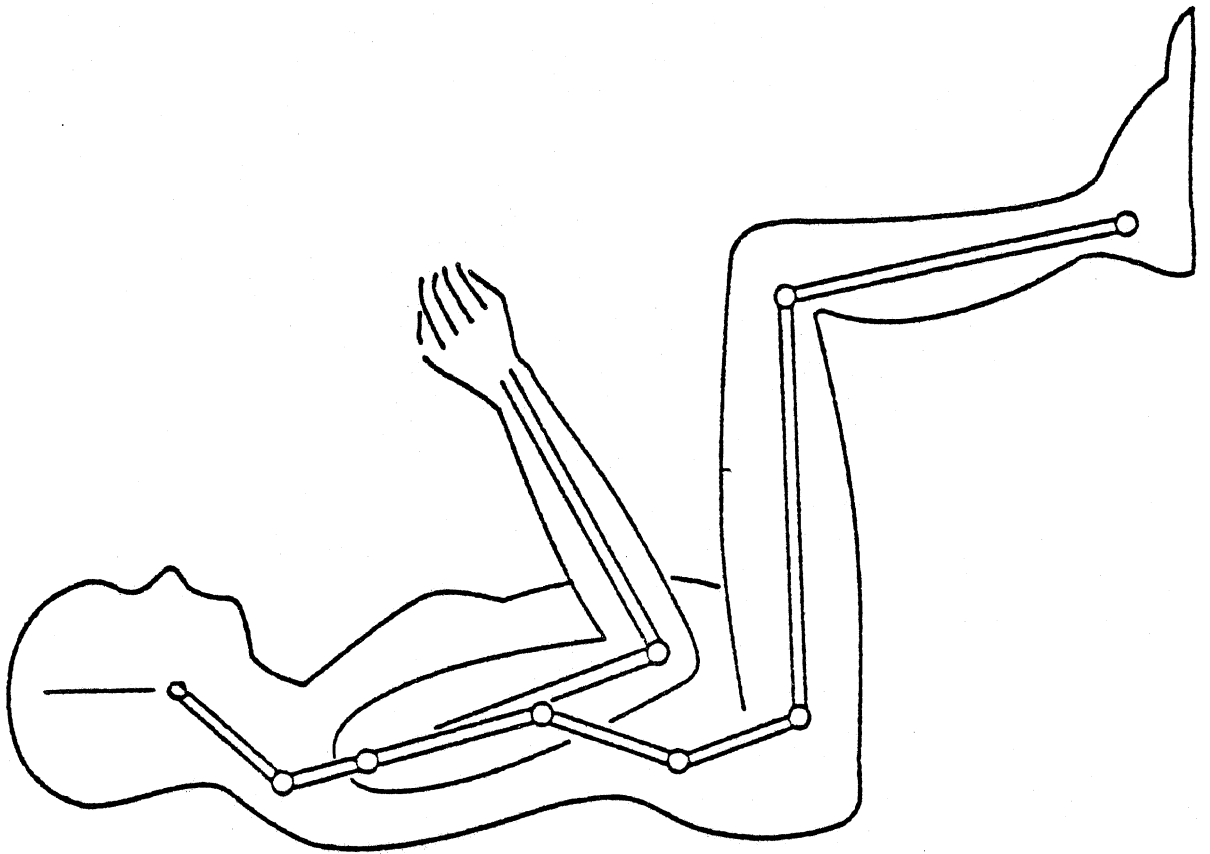
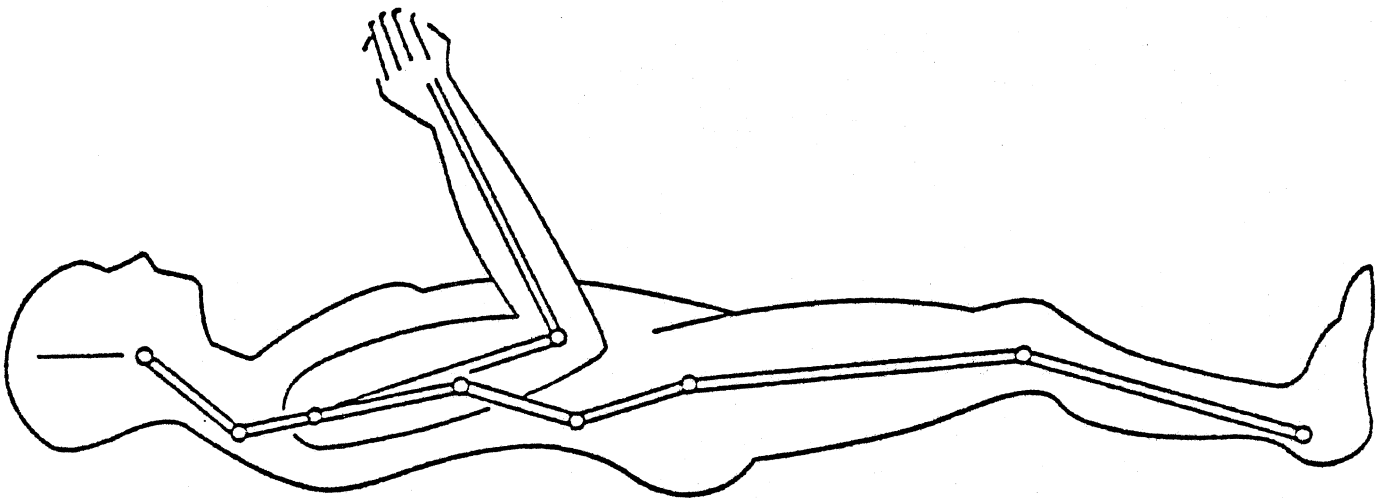
## BASIC BODY LINKAGE DATA

- **Body Segment Length**
- **Center of Gravity Position Along Length of Segment**
- **Body Segment Masses**
- **Body Segment Moments of Inertia**

SLIDE 2-7

## SLIDE 7

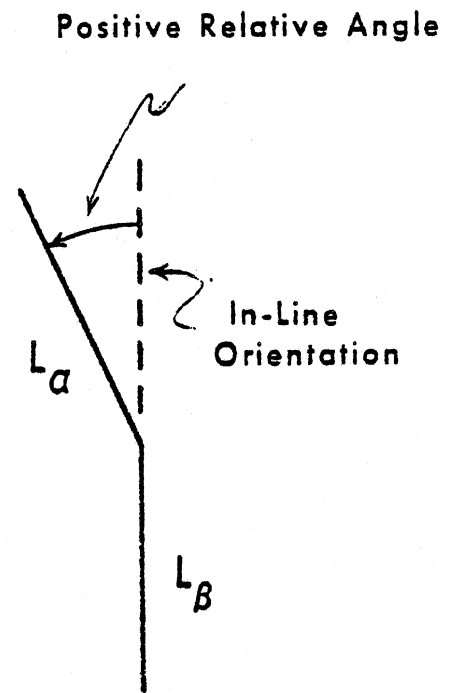
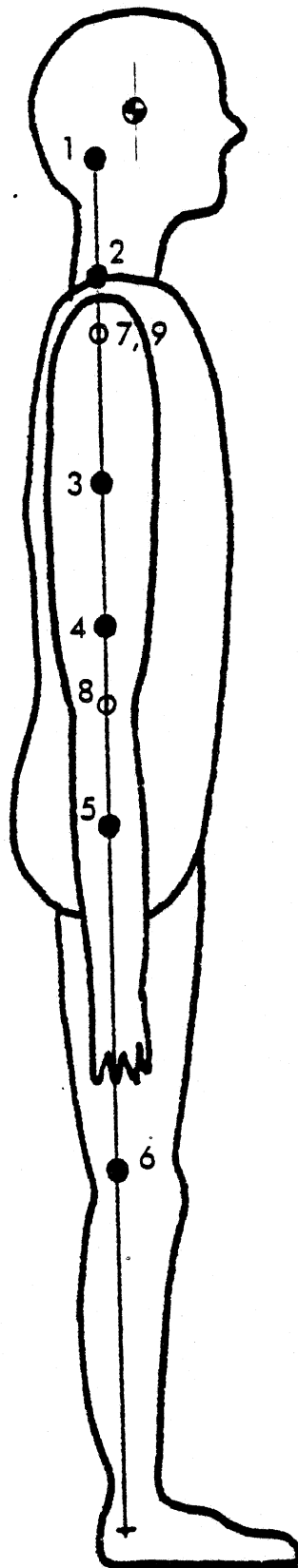
The first series of slides has dealt with physical quantities such as body segment length, mass, moment of inertia, and center of gravity location. These quantities are measured relatively easily for simulations of dummy motions as the dummy can be disassembled. The measurement of link lengths and inertial properties of human and cadaver subjects is not yet an exact science.



SLIDE 2-8

## SLIDE 8

Much of the remainder of this module deals with joint angulation. The figure shows two typical postures for a subject -- sitting and standing. The body links approximate the skeletal structure and are shown here to illustrate that they are not necessarily in alignment even in an erect posture. ▸



$L_a$  = body link nearer to head

$L_b$  = body link nearer to feet

FIGURE 2-5 In-line Orientation

SLIDE 2-9



## SLIDE 9

A so-called "in-line orientation" is defined as a reference orientation for several model input quantities. Body joints are numbered here as in the first series of slides.

Angulation at body joints is relatively free until hard-tissue resistance is encountered. Polynomial coefficients for nonlinear resistive torques are prescribed and become effective when specified range-of-motion limits are reached. A relative angle is considered positive when the link nearer the head is positioned counterclockwise from its in-line orientation as shown in the figure.

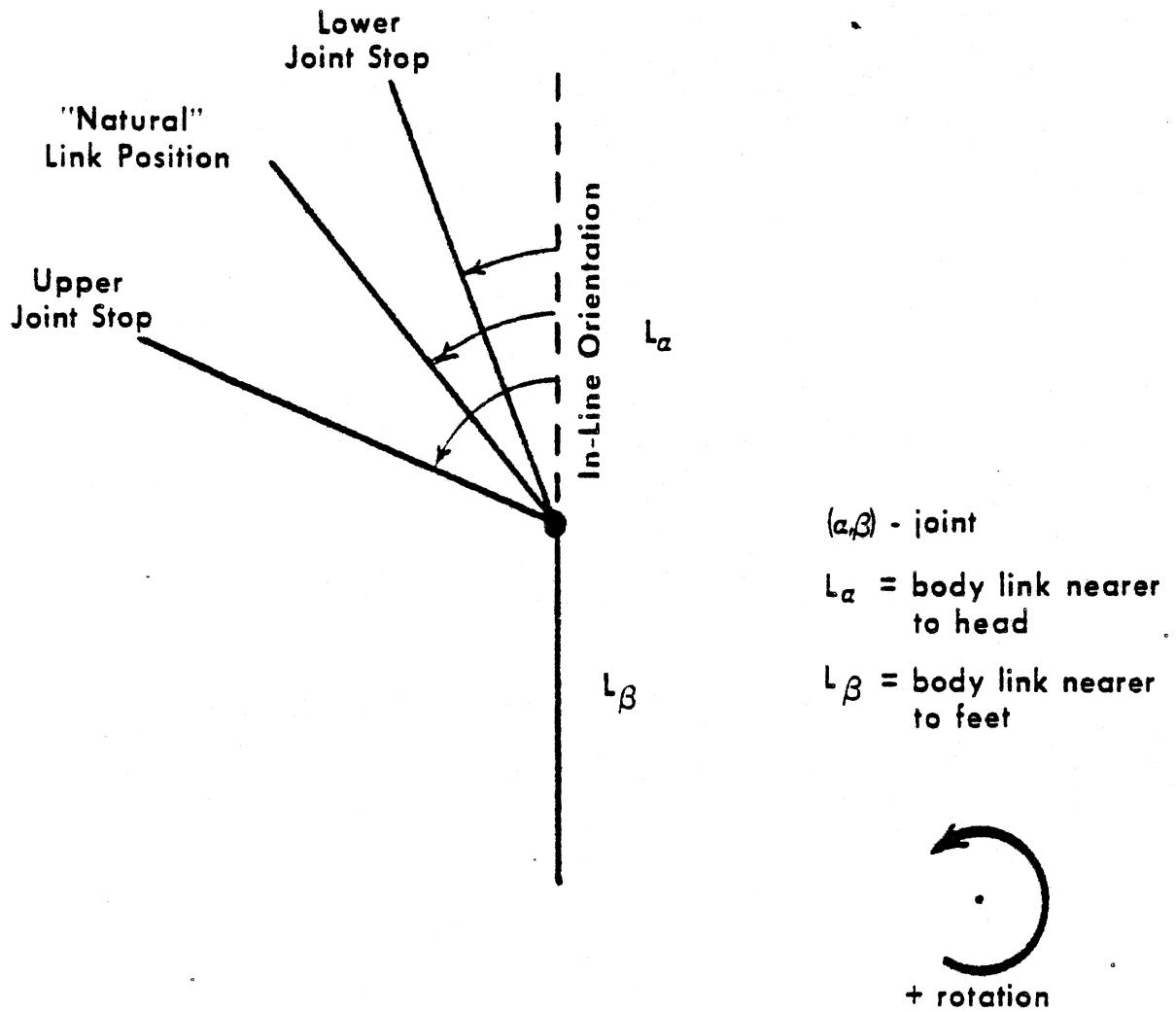


FIGURE 2-6 Definition of joint stop angles and natural link position

SLIDE 2-10

## SLIDE 10

Values for the range-of-motion limits, the so-called joint stop angles, are normally taken as the extreme angulations voluntarily assumed by human subjects. Two joint stop angles are defined for each joint so that both clockwise and counterclockwise angulations can be properly limited. For many joints, these positions are on either side of the in-line orientation, that is, one value is positive and one is negative. For this reason they are often called "positive" and "negative" joint stop angles. But since there is no general restriction on the stop values and since indeed the stops are not always on either side of the in-line orientation, they are best called "upper" and "lower" stop angles, the upper joint stop being the positive-most position as illustrated in the figure. Positions of  $L_{\alpha}$ , the upper link, requiring clockwise rotation are described by negative angles.

Another quantity illustrated by the figure is the "natural link position." A better name for this quantity might be "link equilibrium position." It is the value of the relative angle at which no linear, elastic component of spring torque results. In contrast to the nonlinear joint stop coefficients, the values normally used for elastic coefficients produce small torques except for large relative angulations. The natural link positions are most commonly set to coincide with the initial occupant configuration so that no joint torques exist at time zero. Resistance to small motion away from this configuration is normally considered to be due to soft-tissue deformation.

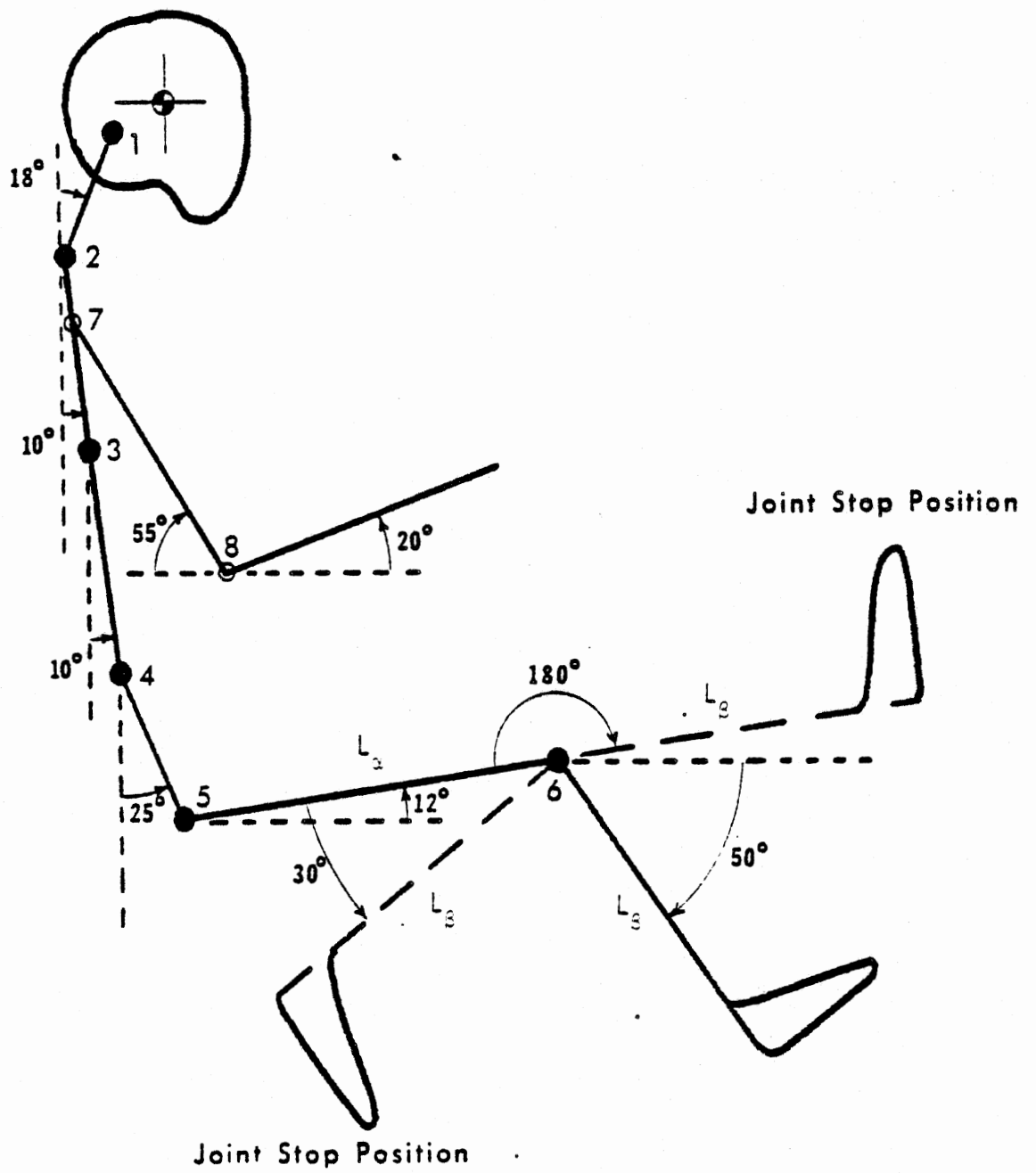
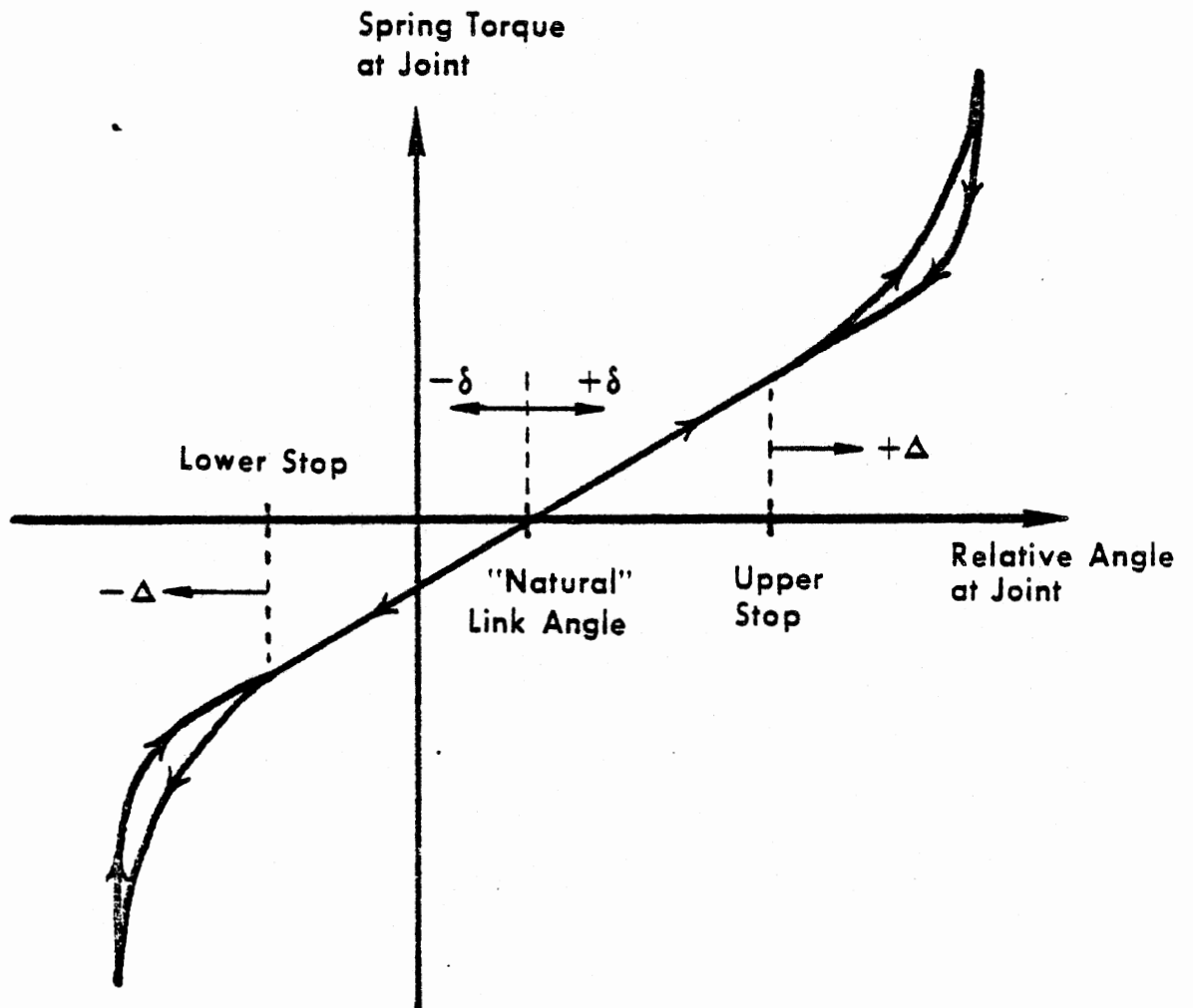


FIGURE 2-7 Joint Stop Positions for Knee

SLIDE 2-11

## SLIDE 11

This next figure is a stick-figure representation of a seated occupant. As an example of joint stop locations, consider the knee, for which a range of motion is illustrated. The lower leg is at the positive-most stop in the bent knee position. There, the upper-leg link,  $L_\alpha$ , is located  $+150^\circ$  counterclockwise from an in-line position with the lower leg element,  $L_\beta$ . The straight leg position of zero degrees angulation is the negative-most stop. The natural link angles are normally chosen for the rest position of the seated occupant. Here, the knee has a natural link position of  $62^\circ$  since the upper leg is  $62^\circ$  counterclockwise from an in-line orientation with the lower leg. The two stop angles and the natural link angle must be specified for each joint.



$$\text{SPRING TORQUE} = -k_{\text{ELASTIC}} \delta - \left\{ K_{1,\text{STOP}} |\Delta| + K_{2,\text{STOP}} \Delta^2 + K_{3,\text{STOP}} |\Delta^3| \right\} \text{sgn } \Delta$$

Linear, elastic component

Nonlinear, joint-stop component

FIGURE 2-9 Linear and nonlinear joint torques

SLIDE 2-12

## SLIDE 12

Spring torques resisting joint angulation are illustrated in this figure as functions of relative angle at a joint. A linear, elastic torque component is proportional to  $\delta$ , the angular distance from the natural link position. Linear, quadratic, and cubic joint-stop terms enter the torque computation when interaction with a motion-limiting stop is encountered.

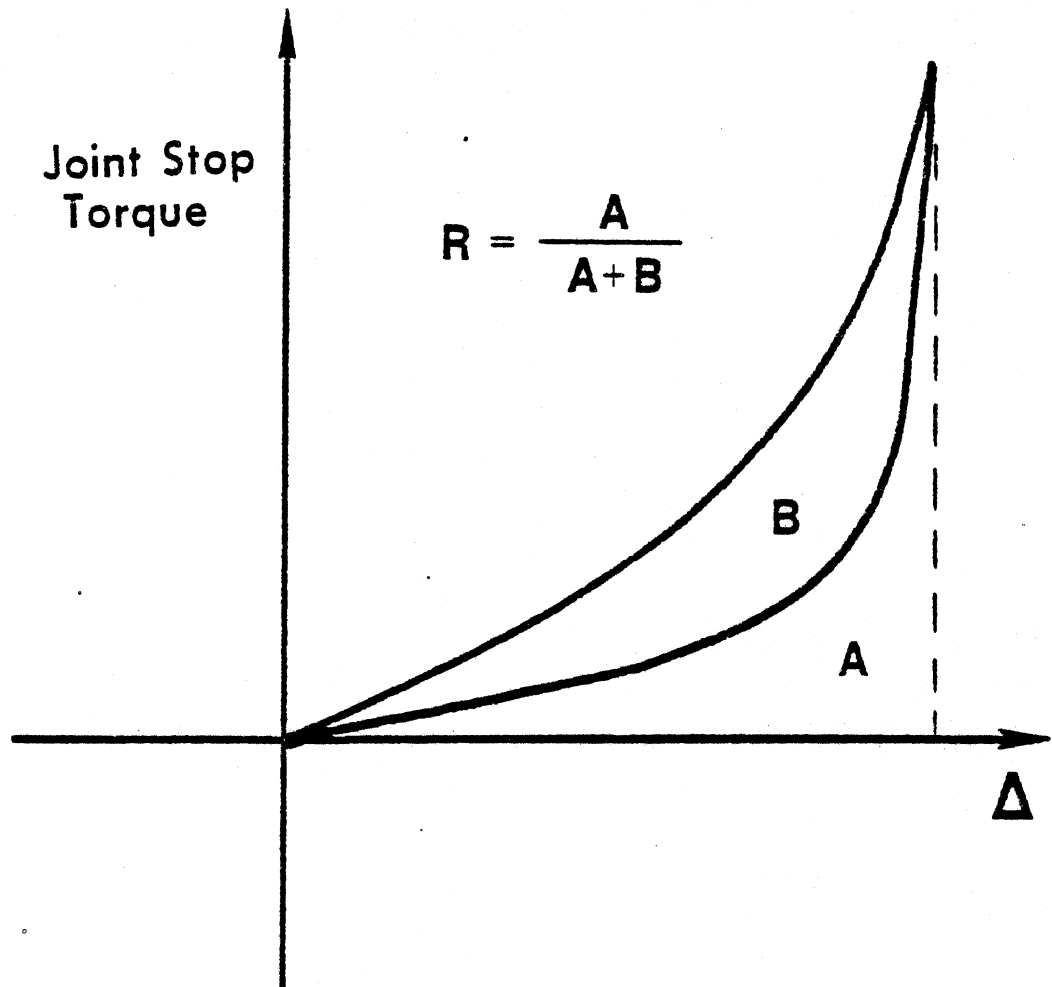


FIGURE 2-10 R-ratio for energy conserved at joint stop

SLIDE 2-13



## SLIDE 13

Four additional properties of the joint have yet to be described. These deal with energy absorption. The first property is the "R-ratio" for the joint. This is the fraction of the energy stored in the nonlinear loading of a joint stop which will be conserved upon complete unloading of the stop. A typical loading-unloading loop for the nonlinear spring torque component is illustrated in the figure. During program execution, a quadratic unloading curve is computed such that the area A is related to the total loading energy through the R-ratio.

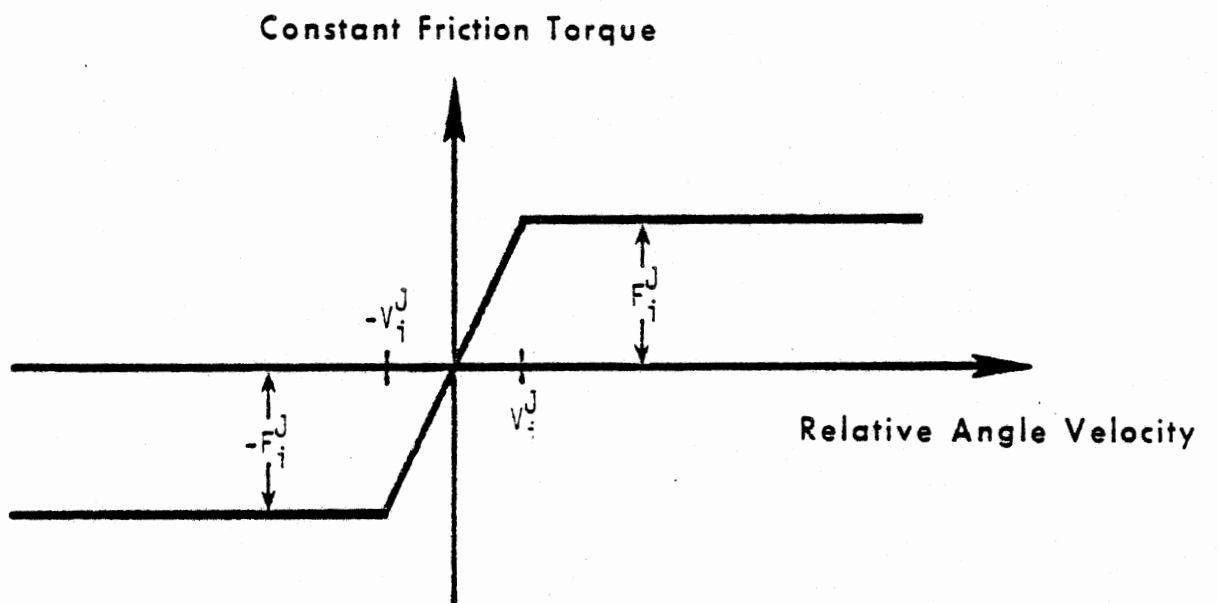


FIGURE 2-11 Joint friction at joint "i"

SLIDE 2-14

6/28/79

#### SLIDE 14

This figure defines two quantities needed for computation of a constant friction joint torque.  $F_i^J$  is the constant torque level for joint "i." The quantity  $V_i^J$  is the velocity threshold for constant friction. This is the minimum relative angle velocity for which the full friction torque results. Torques for relative angle velocities less than the velocity threshold in absolute value are calculated with a linear ramp, as illustrated in the figure. This quantity is required for computational stability. Constant friction is not a component of torque appropriately used for modeling the human being since human joints are virtually frictionless. It is very useful, however, in simulating anthropomorphic dummies. Another required coefficient, not illustrated here, is the proportionality constant for a velocity-dependent torque -- the viscous friction coefficient. This torque is directly proportional to the magnitude of the relative angle velocity and, of course, acts in a direction to resist motion.

## DATA QUANTITIES FOR JOINT DEFINITION

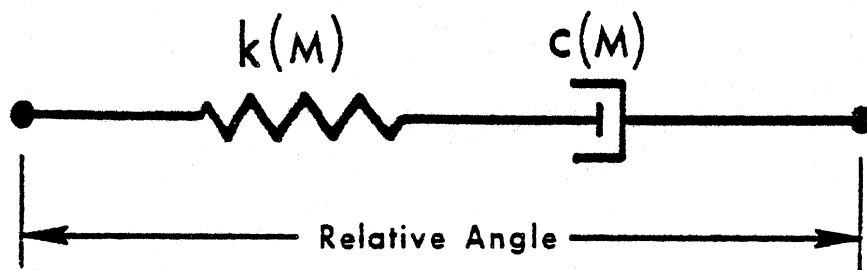
- Joint stop locations (2)
- Natural (zero-torque) position (1)
- Spring torque coefficients (3)
- Energy absorption in joint unloading (1)
- Velocity-dependent viscous motion resistance (1)
- Constant friction (2)

SLIDE 2-15

## SLIDE 15

Ten data quantities that must be specified for all joints have been described with the preceding six slides. These include joint stop locations, the natural or zero-torque position, three coefficients for computation of spring torque, the R-ratio for indicating energy absorption for joint unloading from the non-linear torque range, constant friction torque, and a viscous torque coefficient.

The upper and lower neck joints in the MVMA 2-D model are atypical joints in an important sense. They are allowed to have viscoelastic properties in flexion different from those in extension. While the "typical" joints discussed can have asymmetric joint-stop positions, still the torque-producing elements are the same for positive and negative relative angle motions.



$$k = a_1 + a_2 |M|$$

$$c = a_3 |M|$$

$M = M(t)$ , muscle activity level

FIGURE 2-12 Muscle element

SLIDE 2-16

## SLIDE 16

The remainder of the module deals mostly with data required for modeling human response to impact. The first item discussed is muscle tension. None of the previously described viscoelastic joint torque elements can be used to adequately model muscle tension. Moderate levels of muscle contraction generally have a significant effect on the crash dynamics, especially for low-g impacts, so analytical representation of the effect is of obvious value. The MVMA-2D model determines generalized forces for muscle tension torques at the eight joints. A similar torque is calculated to resist angular motion of the shoulder link. Muscle tension resistance to elongation of the neck and shoulder links is also modeled.

Experimental investigation of the knee joint indicates that this property is properly represented by a Maxwell element, i.e., a spring and damper in series as shown in the figure. The spring and damping coefficients are simple functions of the degree of muscle activation,  $M$ .

$a_1$ ,  $a_2$ , and  $a_3$  are assumed to be constants for the subject and the joint. Arguments relating these quantities to muscle tissue strength properties allow the development of scaling laws for going from joint to joint in an individual or from individual to individual for the same joint.

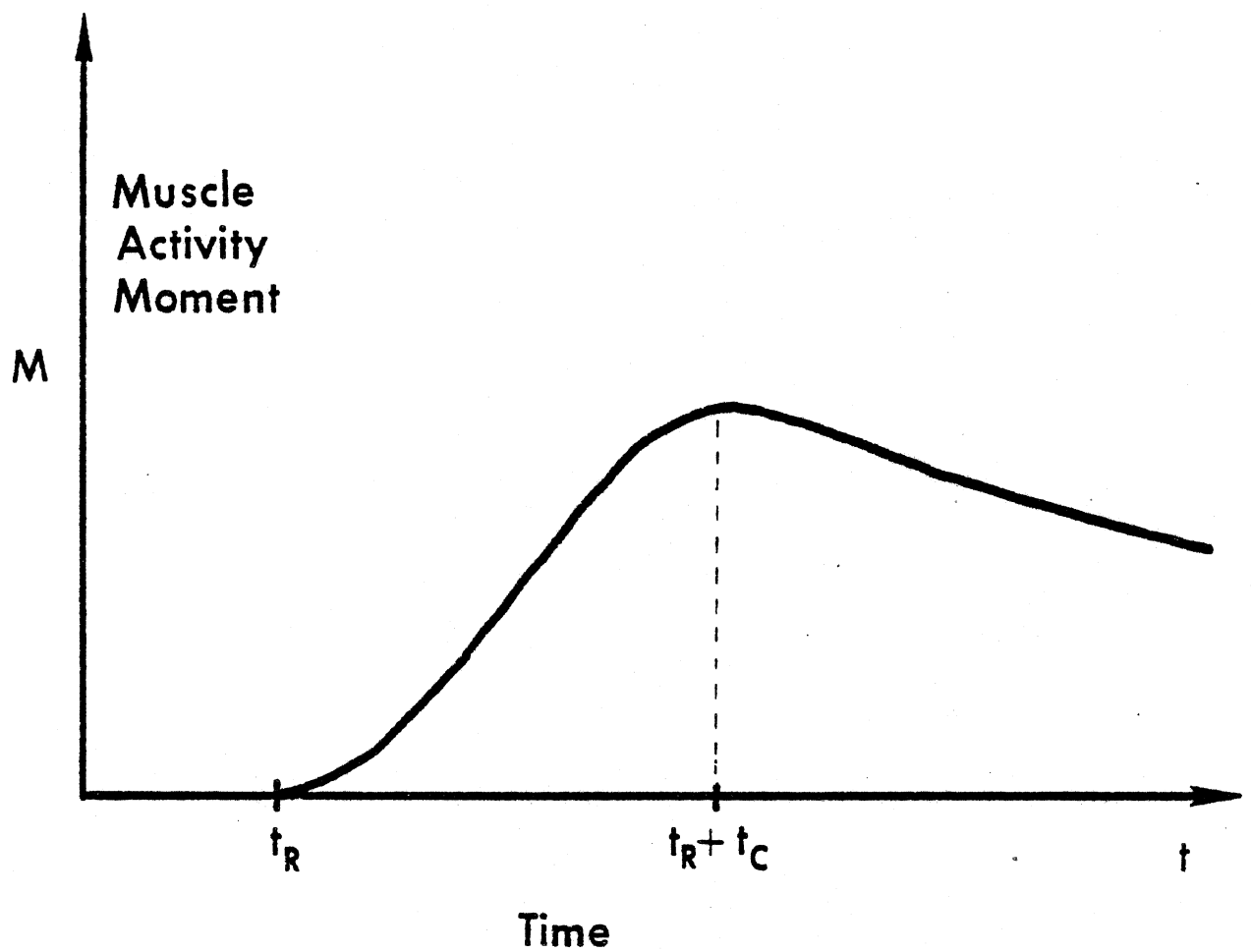


FIGURE 2-13 Muscle activity moment as a function of time

SLIDE 2-17



#### SLIDE 17

The torques  $M$  are specified by the user as time-dependent levels of muscle activation.  $M(t)$  for any particular joint is generally bounded by the maximum static moment that the vehicle occupant would be able to generate voluntarily. Typically, the dependence on time is as shown in the figure.  $t_R$  is the reflex time, a non-zero value whenever the vehicle occupant is not pre-tensed because of awareness of impending impact.  $t_C$  is the contraction time, which is the time required for muscle activity to peak from a state of rest. Values of  $t_R$  and  $t_C$  for muscles at all joints are typically 50 msec and 120 msec, respectively.

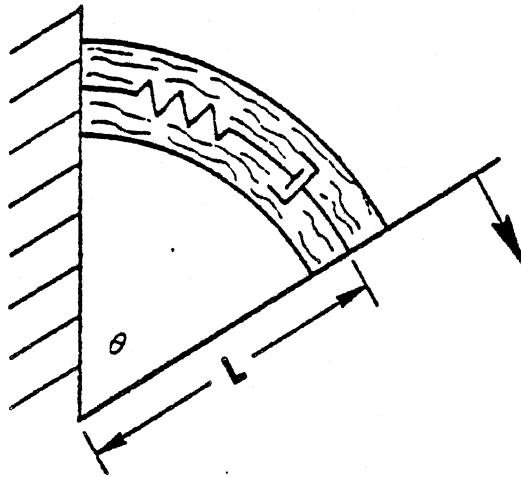


FIGURE 2-14 Muscle at a joint

SLIDE 2-18

SLIDE 18

The MVMA-2D muscle model, based directly on angular motion, is somewhat artificial in that muscle moments are really a result of lineal action of a muscle with a moment arm. This results in no analytical difficulties, however, since all lineal muscle coefficients can be related to effective angular coefficients by the effective moment arm,  $L$ .

## MUSCLE TENSION DATA

- Muscle tissue parameters,  $\alpha_1, \alpha_2, \alpha_3$
- Muscle activation level,  $M(t)$

SLIDE 2-19

SLIDE 19

Muscle tension data are required only for those cases where the user desires to simulate living human response to a dynamic environment. Required for each joint are the three coefficients  $a_1$ ,  $a_2$ ,  $a_3$  and a time-dependent table defining muscle activity moment. Example data are included with the text of Module 2.

## SCALING RELATIONS

	$M = \text{mass}$
LENGTH:	$L_1 = L_2 (M_1/M_2)^{1/3}$
AREA:	$A_1 = A_2 (M_1/M_2)^{2/3}$
VOLUME:	$V_1 = V_2 (M_1/M_2)$
MASS:	$m_1 = m_2 (M_1/M_2)$
MOMENT OF INERTIA:	$I_1 = I_2 (M_1/M_2)^{5/3}$
DAMPING COEFFICIENT:	$C_1 = C_2 (M_1/M_2)^{2/3}$
LINEAL SPRING CONSTANTS:	$K_1^{(n)} = K_2^{(n)} (M_1/M_2)^{(2-n)/3}$ where $F = K^{(1)} \delta + K^{(2)} \delta^2 + \dots$
TORSIONAL SPRING CONSTANTS:	$K_{1\theta}^{(n)} = K_{2\theta}^{(n)} (M_1/M_2)$ where $T = K_{\theta}^{(1)} \Delta\theta + K_{\theta}^{(2)} (\Delta\theta)^2 + \dots$

FIGURE 2-18 Parameter Scaling Relations

SLIDE 2-20

## SLIDE 20

Good biomechanical and anthropometric data are important for successful use of any crash victim simulator. It will often be the case that the user has established a good data set for one segment of the population, for example, middle-age males of 50th percentile stature and weight. However, he may have little data for other populations. It is generally possible by applying scaling relations to good data for one population to develop reasonable data for other populations.

It must always be kept in mind, however, that scaling is only a substitute for more direct development of biomechanical and anthropometric data.

Assumptions made in developing the relations shown in the slide are:

1) All internal and external length measures of the "scaled" biomechanical system (subscript 2) are proportionate to the corresponding measures of the "scaled to" system (subscript 1) by the same proportionality constant. That is, linear scaling in size is assumed.

2) Corresponding body parts of the two systems have equal mass densities.

3) Corresponding anatomical elements of the two systems have the same material constitutive properties. This means that material parameters such as Young's modulus ( $E$ ) are the same for corresponding elements while the strengths of the elements will not be the same if they are of different size.

It is clear from these conditions that biomechanical scaling will be better between some population segments than between others. Linear scaling in size is probably the primary weakness in human scaling. The reason is that body proportions are functions of age and sex. For example, better results can be expected for scaling from 35-44 year-old males to 18-24 year-old males than one can expect from scaling 35-44 year-old males down to 6-9 year-old females. But it is also clear from the stated assumptions that scaling between segments of the human population has a considerably firmer basis than scaling from lower primates to humans, which is a common technique used in the development of human injury tolerance data.

## SUMMARY OF REQUIRED BODY LINKAGE DATA

- Body segment lengths
- Center of gravity positions
- Body segment masses
- Moments of inertia
- Joint stop locations
- Joint zero-torque position
- Spring Torque coefficients
- Energy absorption in joint
- Viscous torque
- Constant friction torque
- Muscle tension

SLIDE 2-21



## SLIDE 21

The preceding slides have illustrated the features of the MVMA-2D body linkage and the data required for model operation. Four of these illustrate overall geometric and inertial properties. Two define joint stop locations and link equilibrium angles. Five describe force resistance properties at joints. All of the joint properties are relevant to both dummy and human simulation except for constant friction torque, which is not realistic for human joints, and muscle contraction torque, which is characteristic of human response only.



**MVMA 2-D**  
**CRASH VICTIM SIMULATION**

**\* \* \***

**MODULE 3**

**NECK AND SHOULDER MODELS**

**MVMA 2-D  
CRASH VICTIM SIMULATION**



**MODULE 3**

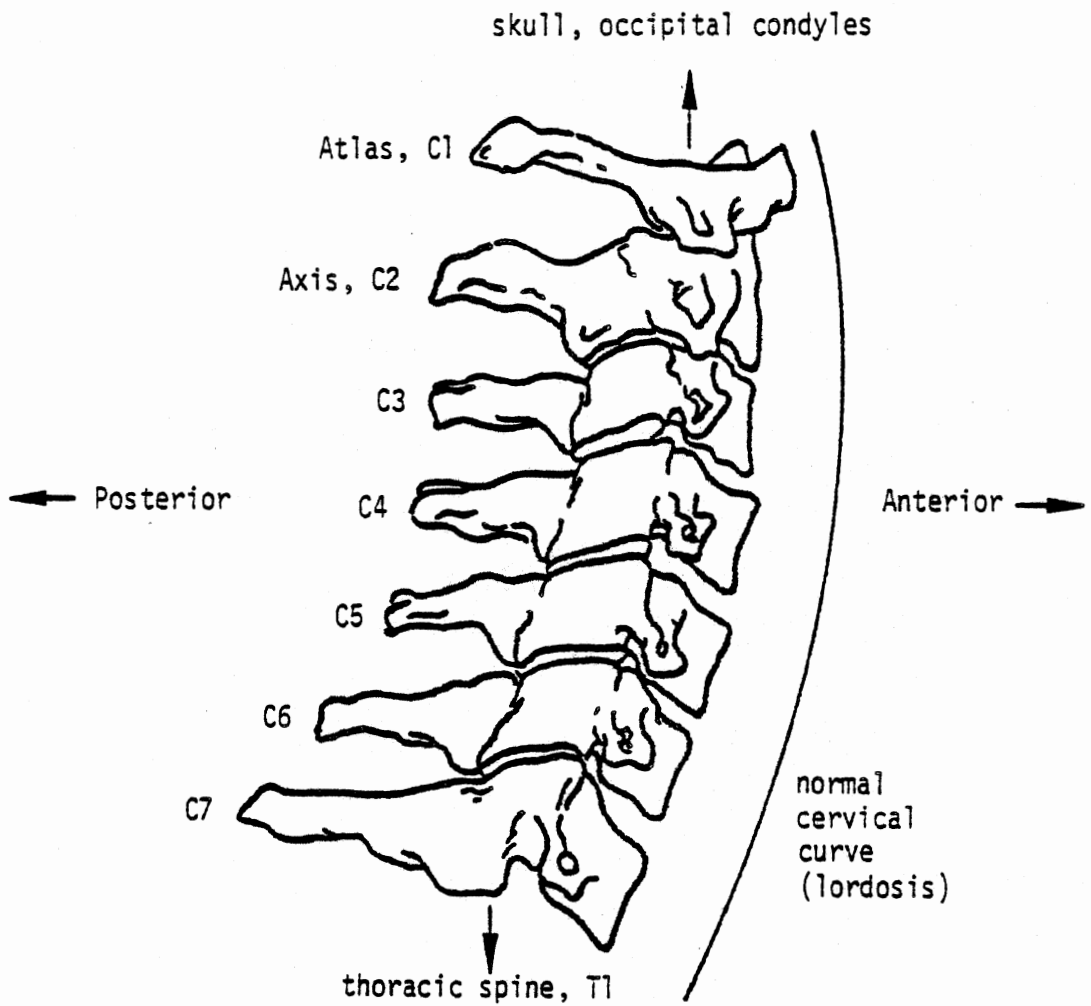
**NECK AND SHOULDER MODELS**

**SLIDE 3-1**

MODULE 3 -- NECK AND SHOULDER MODELS

SLIDE 1

In this module, the neck and shoulder models of the MVMA 2-D  
Crash Victim Simulator are discussed.



The cervical spine, lateral view

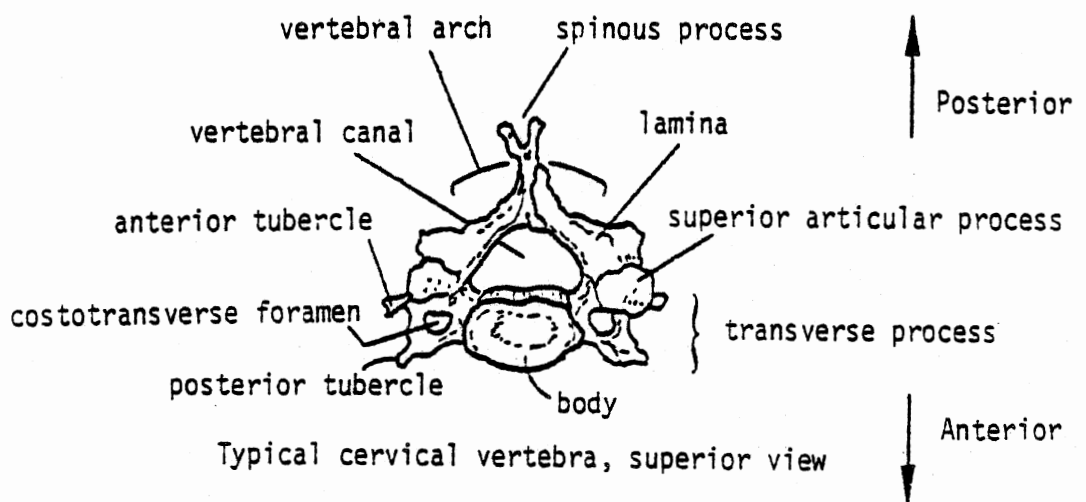


FIGURE 3-1 The cervical vertebrae

SLIDE 3-2

## SLIDE 2

The cervical spine is that portion of the spinal column from the skull to the thoracic spine. It supports the head and provides mobility and flexibility in the neck. The upper portion of the first slide shows a lateral view of the human cervical vertebral column.

Viewed as a mechanical system, the human neck is complex. The MVMA 2-D occupant model is a lumped-parameter system. While the neck representation in this model is more complex than that in most whole-body motion simulators in current use, it still adds only three degrees of freedom to the occupant model. The user is therefore neither required nor allowed to define values for more than a relatively few biomechanical neck parameters. The discussion accompanying this slide and the following four is an introduction to the anatomy of the neck. The purpose of this introduction is not to define quantities for which values must be provided, since no anatomical detail is included in the analytical neck model, but rather to help the user to develop good judgment and insight in the use of the model and interpretation of results.

There are three primary types of structural components in the cervical spine -- vertebrae, intervertebral discs, and ligaments. Of the thirty-three vertebrae in the human spinal column, seven are in the neck. The seven vertebrae are conventionally designated C1 through C7, where C1 is the uppermost vertebra, commonly called the atlas. The lower portion of this slide is a superior view of a typical cervical vertebra, any below the axis, C2. The anterior portion of each vertebra is a solid vertebral body, which imparts strength to vertebral arch is attached to the posterior portion of the body. It encloses and protects the spinal cord. This arch also furnishes bony projections and processes, to which ligaments and muscles attach. The inferior portion of the skull, or occiput, is closely attached to the cervical spine by some of these ligaments and muscles. The skull is supported on the spinal column by two rounded, bony protuberances of the occiput. These protuberances are called the occipital condyles, and they are accommodated by two hollow recesses on the superior surface of the first cervical vertebra, the atlas.



Neck Flexion



Neck in Neutral Position



Neck Extension

FIGURE 3-2 X-rays of a normal human neck in the neutral position and in full voluntary flexion and extension

SLIDE 3-3



### SLIDE 3

Here, x-rays show the cervical spine in neutral, hyperflexed, and hyperextended positions. Note that in the neutral position, the normal cervical spine is already in slight extension, a rearward bending with convexity forward. This normal cervical curvature is called lordosis, and it results from the greater depth of the intervertebral discs anteriorly rather than posteriorly. Greater articulation in the plane of symmetry can occur at the occipital condyles than at any interspace below the atlas in the cervical spine. Values of from 20 to 35 degrees of total motion are reported by various investigators. Below the atlas, there is considerable variation in the average ranges of motion at the different vertebral levels.

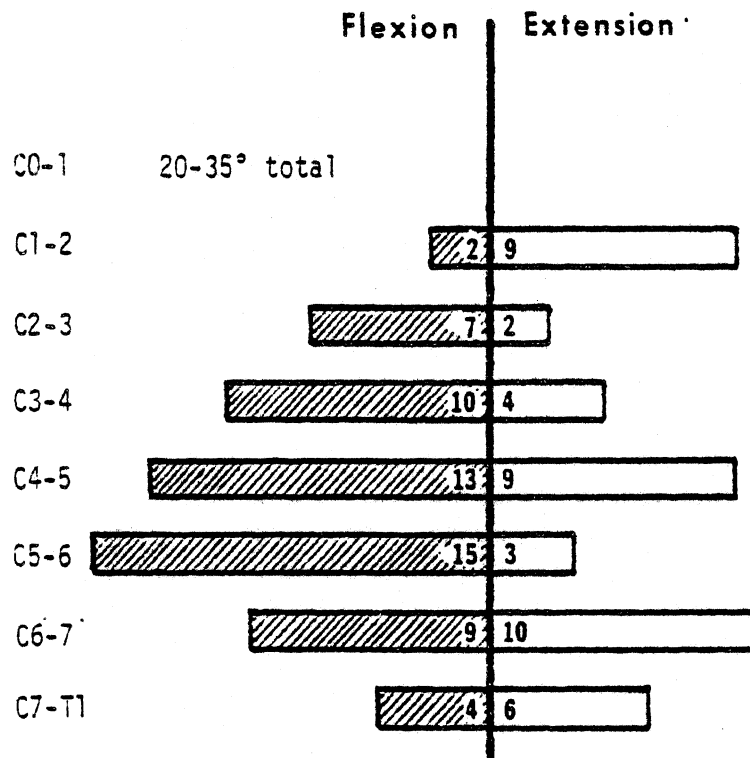
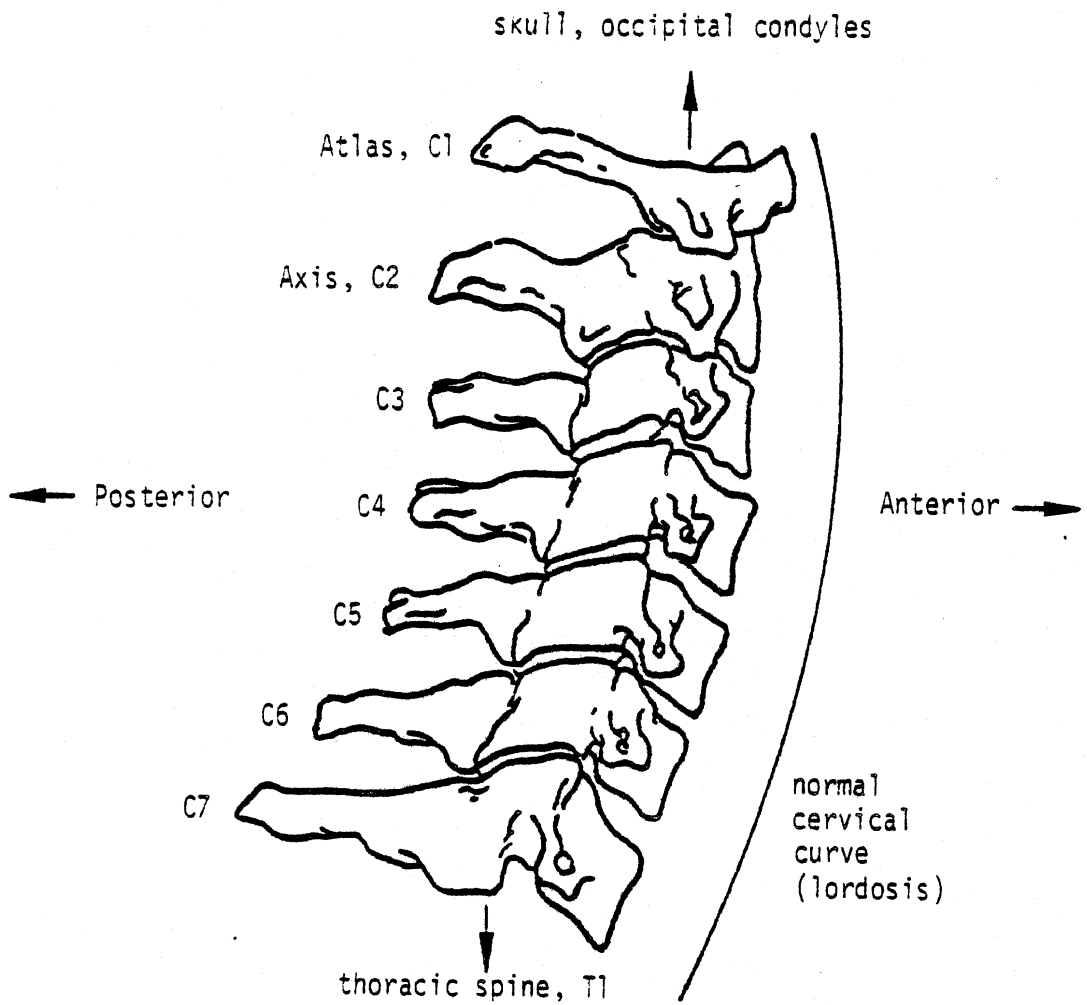


FIGURE 3-3 Average range of flexion and extension (in degrees) at each vertebral level in 20 normal adults

SLIDE 3-4

#### SLIDE 4

The range of motion values given in this slide are averages for twenty normal adults and are typical of values reported in the literature. C7 is adjacent to the first thoracic vertebra, conventionally designated T1. The thoracic part of the spinal column itself is relatively immobile, and the transition interspace C7-T1 has a smaller range of motion than the cervical interspaces above it. After the atlanto-occipital joint at the condyles, most motion occurs at the mid-levels of the cervical spine.



The cervical spine, lateral view

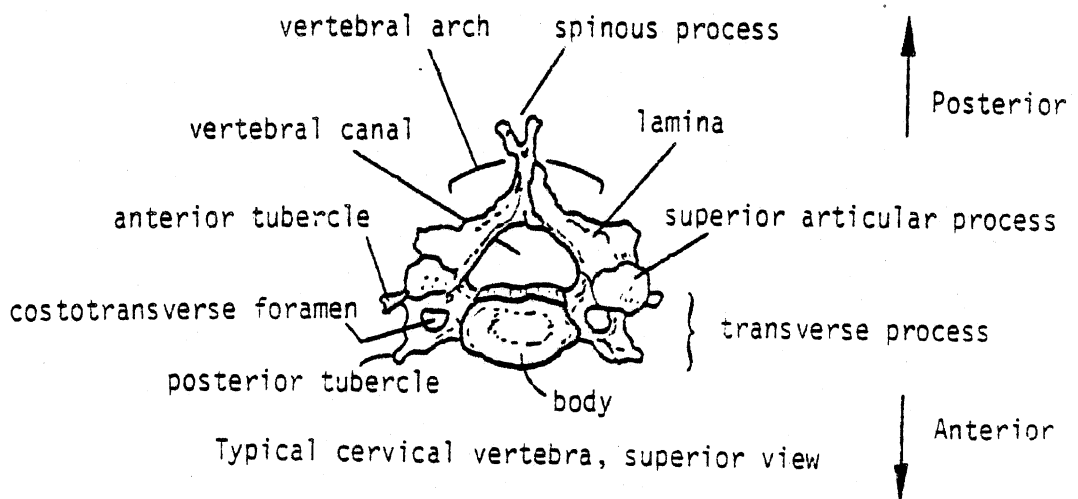


FIGURE 3-1 The cervical vertebrae

SLIDE 3-5

## SLIDE 5

Except between the occipital bone of the skull and the atlas, and between the atlas and axis, the vertebrae are separated by elastic discs of cartilage called intervertebral discs. These are firmly joined to the vertebral bodies, anterior to the spinal canal, and allow movement of the spinal column because of their elasticity. The walls of a disc, called the annulus fibrosus, are a heavy layer of fibrous cartilage. The fibers are directed obliquely and thus prevent excessive movement in any direction. The annulus fibrosus encloses a semigelatinous substance and a kernel of elastic, compressed tissue called the nucleus pulposus. The semifluid character of the interior of the disc serves to distribute compression forces equally over the surfaces of opposing vertebrae. The intervertebral discs in the neck are resilient and rugged, less likely to rupture during dynamic loading than the vertebrae are to fracture.

In addition to vertebrae and discs, ligaments are an important structural component of the cervical spine. Ligaments in the neck are bands of connective tissue -- tough, flexible, and in some cases elastic -- which extend between the vertebrae. Some connect vertebrae to the occipital region of the skull and intervertebral discs to one another. The most important function of the cervical ligaments is in maintaining stability. They serve to maintain the apposition of component parts of joints and allow and limit the appropriate range of motion for each joint.

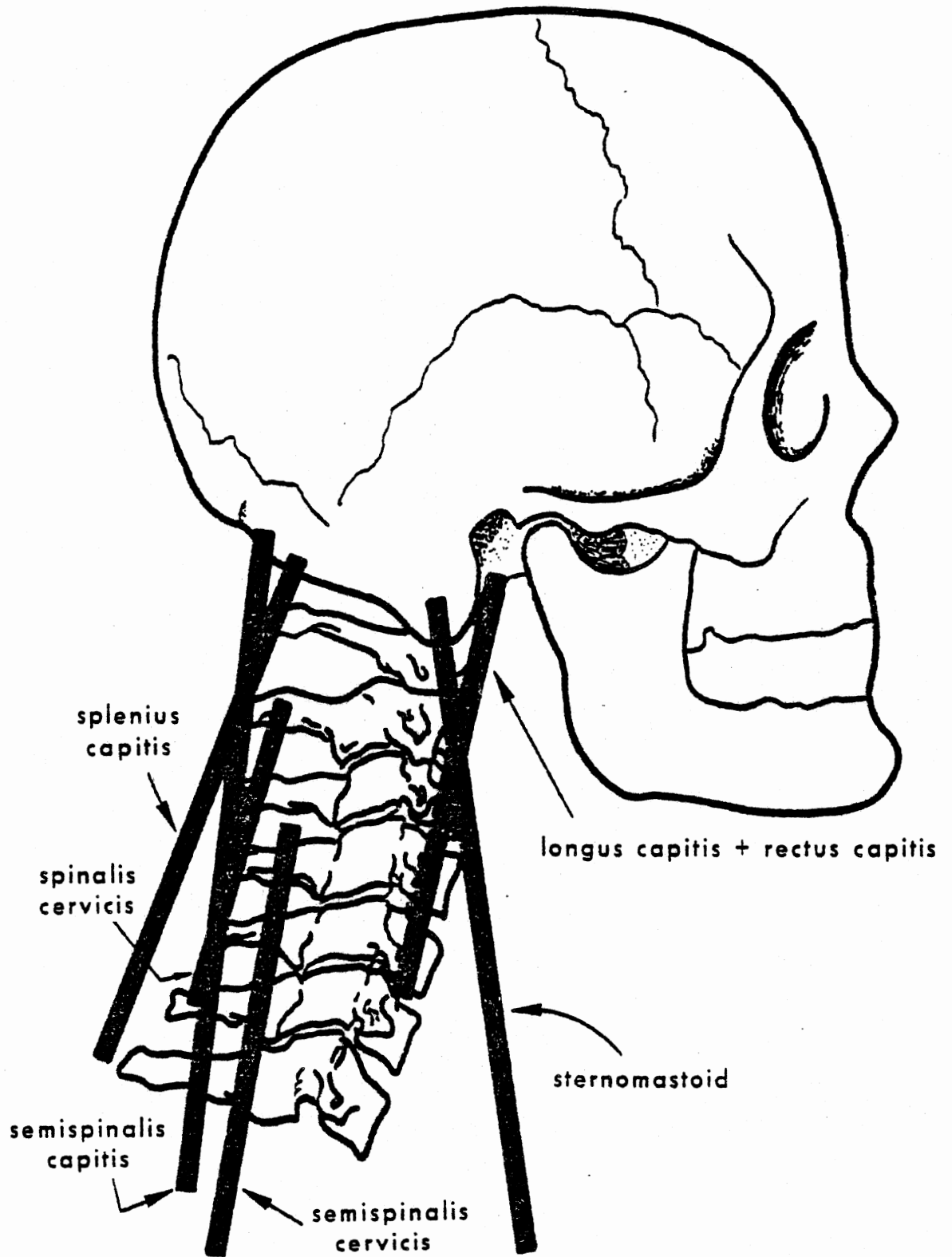


FIGURE 3-4 The major muscle groups controlling head and neck movements

SLIDE 3-6

## SLIDE 6

Muscles are not components of the cervical spine, but they do significantly affect head and neck dynamics. They assist the vertebrae, discs, and ligaments in resisting tension and torsional loads.

Six major muscles control movements of the head and seven control neck movement. The approximate origin and insertion points and the line of action of the most important of these muscles are indicated in this figure.

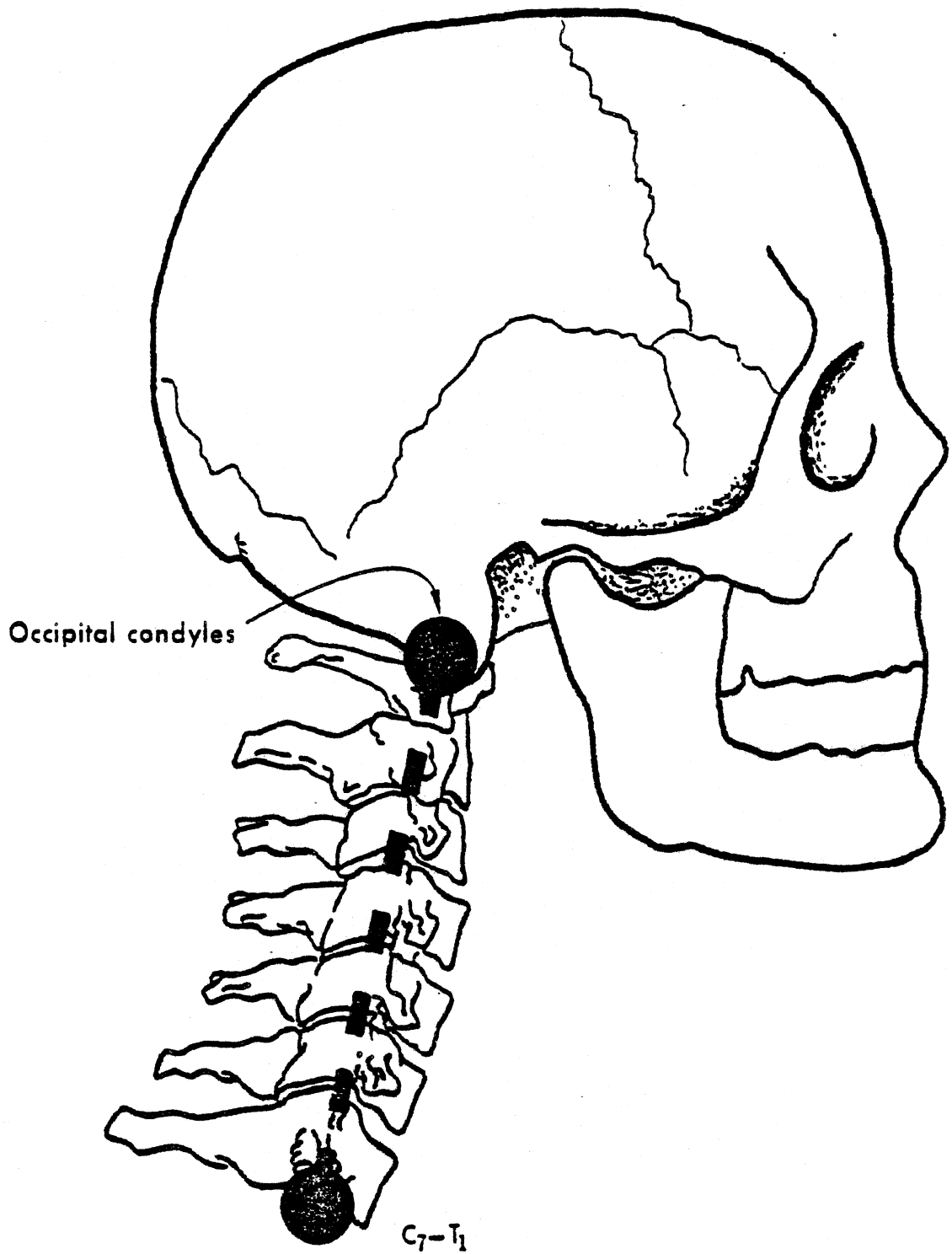


FIGURE 3-5 The MVMA-2D two-joint, extensible neck

SLIDE 3-7



## SLIDE 7

It is clear that the cervical spine has many degrees of freedom, even in motion confined to the plane of symmetry, the midsagittal plane. Even if the intervertebral discs were assumed to be non-deforming in shear, tension, and compression, eight degrees of freedom might reasonably be defined for angular motions of the seven cervical vertebrae and the skull in the midsagittal plane. In the MVMA-2D simulation, angular motions of the head and neck are lumped at two articulations. In this figure these joints are illustrated at the positions of the occipital condyles and the C7-T1 intervertebral disc. The user is free, however, to define their positions as he chooses by selecting input data appropriately. The two joints of the analytical model are not joined by a rigid link but rather by deformable viscoelastic elements, so a third degree of freedom is a mode for compression and elongation of the neck. Motion in this mode tends to be small even in high-G environments since the intervertebral discs are stiff.

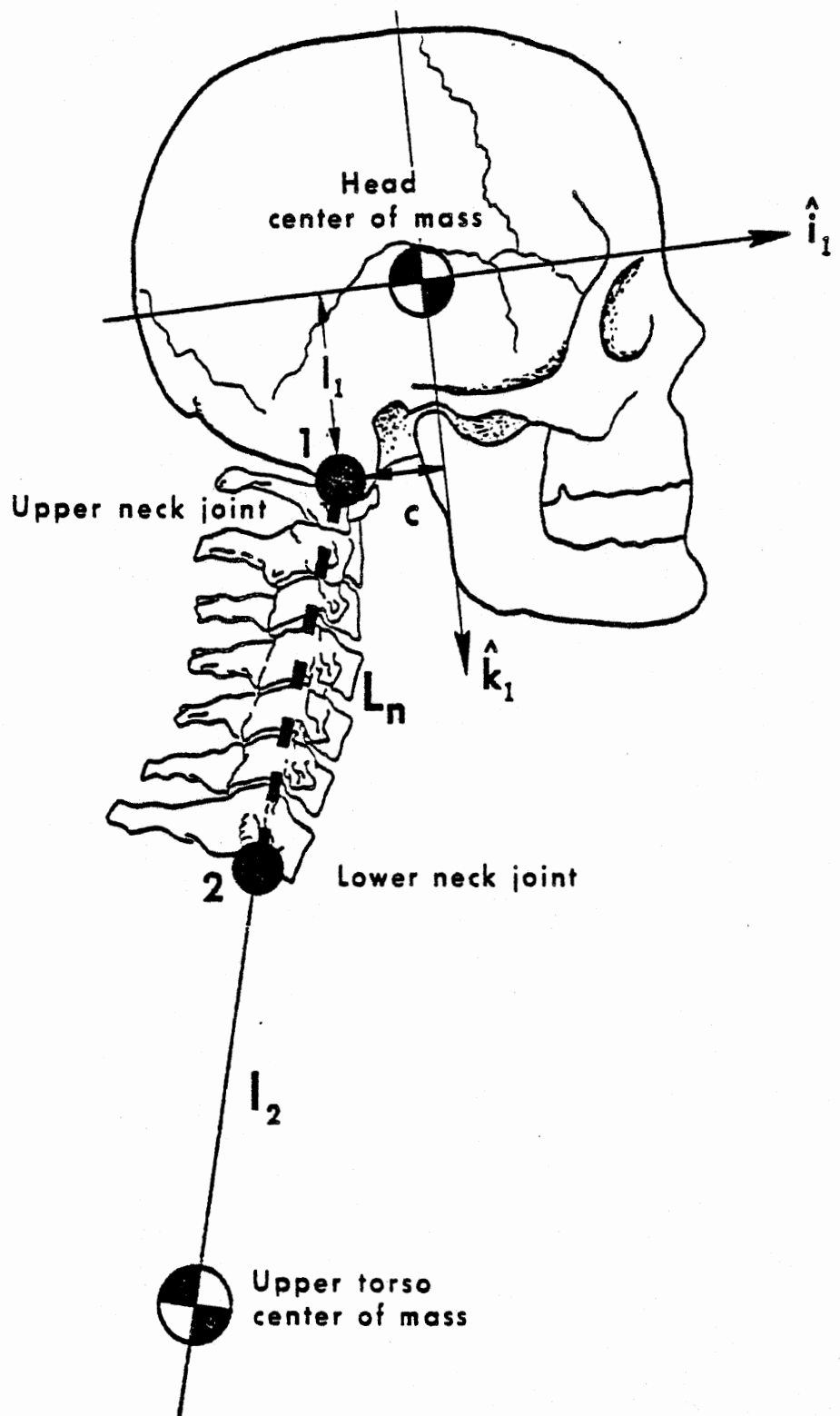


FIGURE 3-6 MVMA-2D extensible neck geometry

SLIDE 3-8

## SLIDE 8

This figure illustrates various geometrical quantities for which the user must assign values. The position of the upper neck articulation is specified with respect to the head center of mass in the head coordinate system. The quantity  $C$  is the rearward offset of the joint from the superior-inferior head axis. The quantity  $l_1$  positions the joint downward from the head center of mass. The lower neck articulation is constrained to lie on the longitudinal principal axis of the upper torso link, so a single length,  $l_2$ , is required to define its location. This is the distance of the C7-T1 joint from the center of mass of the upper torso. Additionally, the initial length of the extensible neck link, that is, the straight-line distance between the neck articulations, must be specified by the user.

The mass of the extensible neck is lumped at the extremities of the element, at the head-neck and neck-torso joints. The total neck mass and the decimal fraction which is to be placed at the upper joint are user-prescribed quantities.

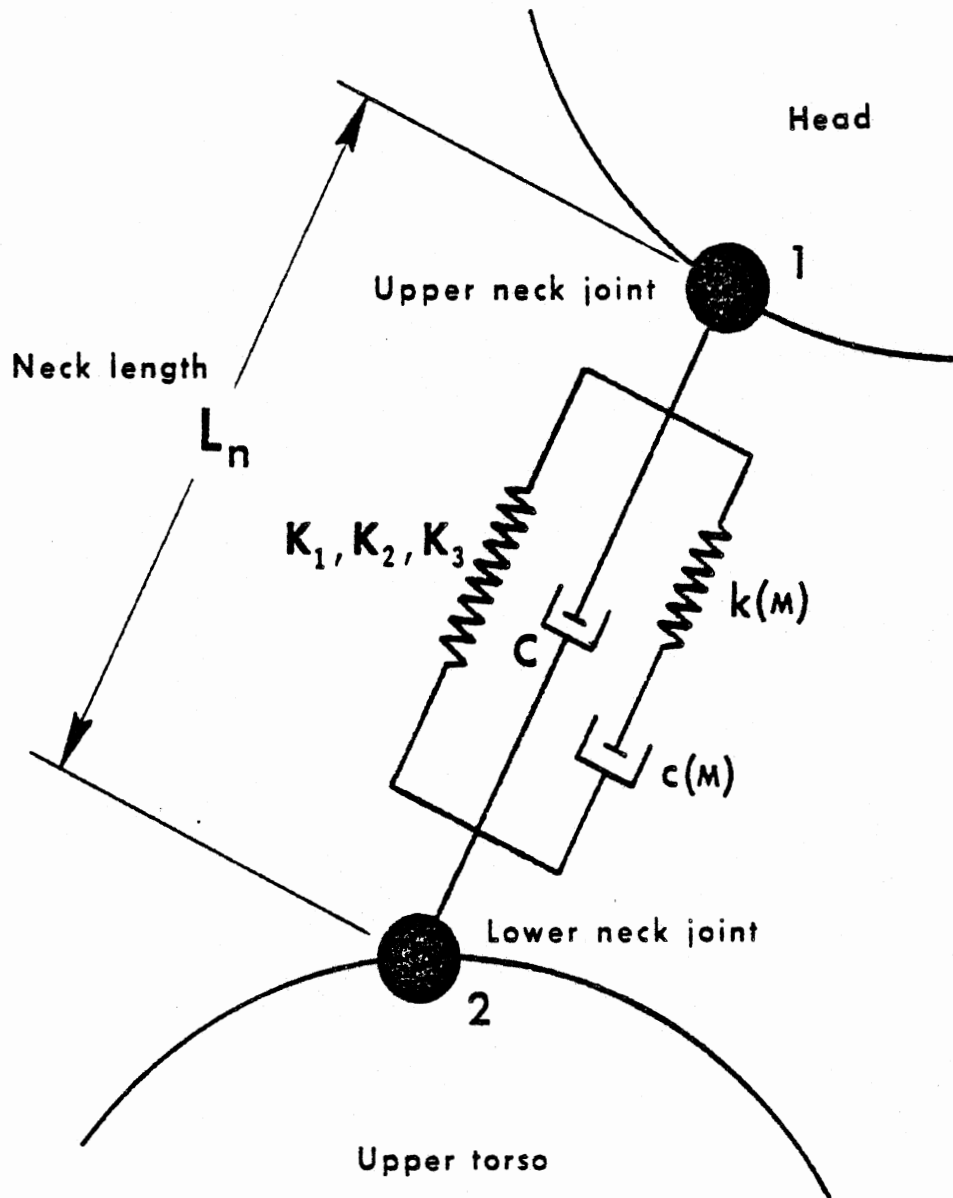


FIGURE 3-7 Lineal viscoelastic components in MVMA-2D extensible neck

SLIDE 3-9

## SLIDE 9

In the MVMA-2D model, the complex of motion-restricting elements in the cervical spine previously described is lumped by defining composite torsional viscoelastic elements at the two joints and linear viscoelastic elements between the joints. While this limits the degree to which model predictions can agree with reality, performance of the lumped-parameter, three-degree-of-freedom, head-neck system has been shown to be good. And from a practical point of view, this simplification of the real biomechanical system makes the model usable because empirical values for composite neck characteristics are much easier to determine than values required to describe an anatomically detailed analytical model.

Viscoelastic joint parameters are fully discussed in Module 2. Several types of elements are defined for each joint in the occupant linkage, including the neck joints. These include a linear spring for angulation away from an equilibrium joint angle, a nonlinear spring for angular deformation of motion-limiting "joint stops," a viscous damper, a constant-friction torque producer, and a Maxwell element with coefficients that are functions of a user-defined, time dependent level of muscle activation. Hysteretic energy loss for deformation of a joint stop can be simulated by specification of a restitution coefficient. For the neck joints, these viscoelastic elements, except for muscle tension, may have different coefficient values for flexion and extension.

The slide illustrates a viscous damper and a nonlinear spring in parallel which resist neck compression and elongation. These elements represent resistance of discs and ligaments to lineal deformation. The spring and damping coefficients need not have the same values for compression and elongation. The user prescribes spring rates for force components proportional to the magnitudes of the first, second, and third powers of neck deformation and values for the linear viscous-friction coefficients.

## SUMMARY OF REQUIRED NECK MODEL DATA

- Neck length
- Neck mass
- Joint locations
- Joint stop angles
- Joint zero-torque positions
- Spring torque coefficients
- Energy absorption in joints
- Viscous torque
- Muscle properties
- Time-dependent level of muscle activation

SLIDE 3-10

## SLIDE 10

The preceding slides have illustrated characteristics of the human cervical spine and of the neck model of the MVMA 2-D simulator. The data requirements for the neck model include geometry and mass properties, the relative angulations at the neck joints for which elastic torques are zero, joint stop locations, passive viscoelastic properties for both angular and linear deformations of the neck, and muscle characteristics.

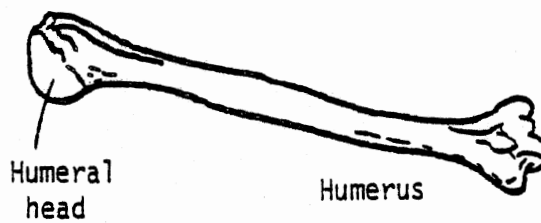
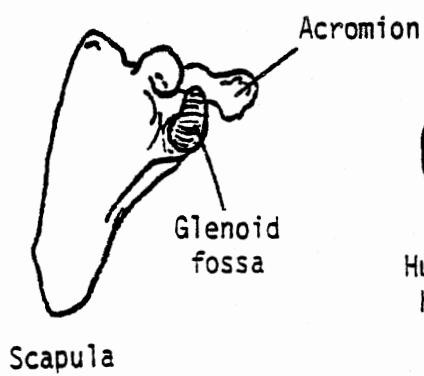
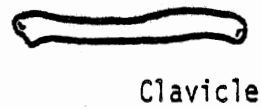
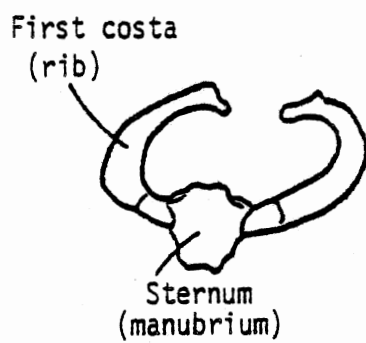
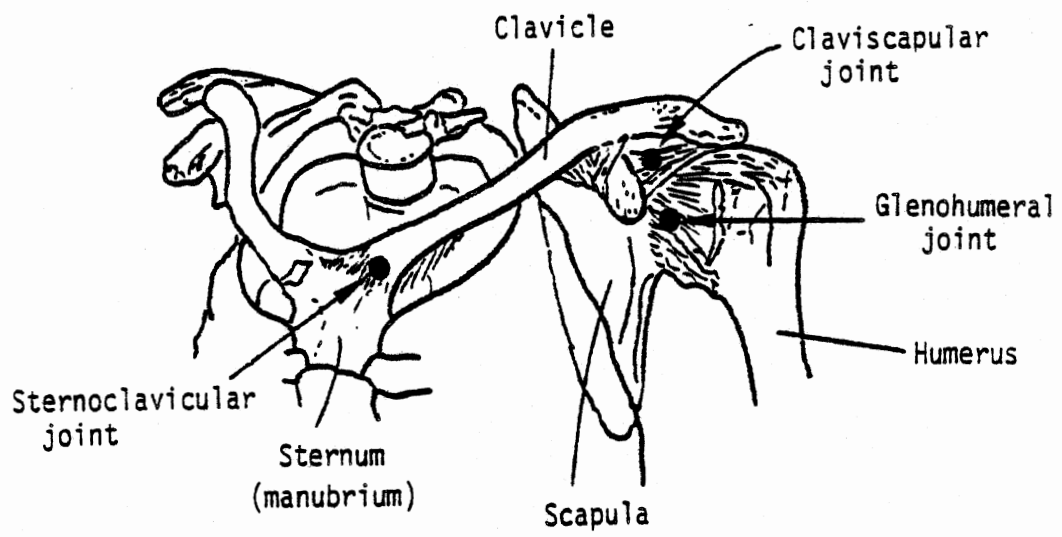


FIGURE 3-12 The shoulder complex and its skeletal parts

SLIDE 3-11



## SLIDE 11

The shoulder is a composite system that consists of four skeletal elements and three joints. In order of their positions in the linkage, the skeletal elements are: 1) the sternum, or breastbone; 2) the clavicle, or collar bone; 3) the scapula, or shoulder blade; and 4) the humerus, or upper arm bone. The three joints are the articulations between these four skeletal parts, and their names are derived from the skeletal parts that they join. Thus, the first two joints are the sternoclavicular joint and the claviscapular joint. The third is called the glenohumeral joint. Its name is derived from the glenoid fossa, the depressed surface on the scapula in which the head of the humeral bone rotates.

Twelve separate ligaments affix to the four skeletal elements. They transmit torques from one element to another as muscles are contracted, and they limit the motions that the shoulder complex can undergo freely. The continuous boundary of the range of relatively free motion that can occur at a single joint or a composite of several joints is called a "joint sinus." It is sometimes called an "excursion cone" since in three-dimensional space the extreme range of the motion pattern is typically a conical surface swept out by a skeletal link.

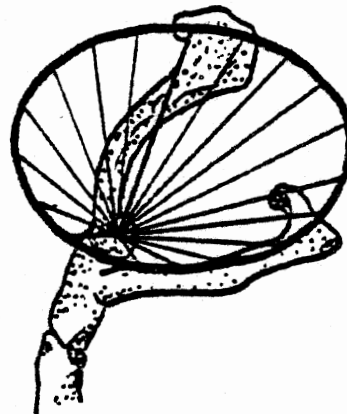
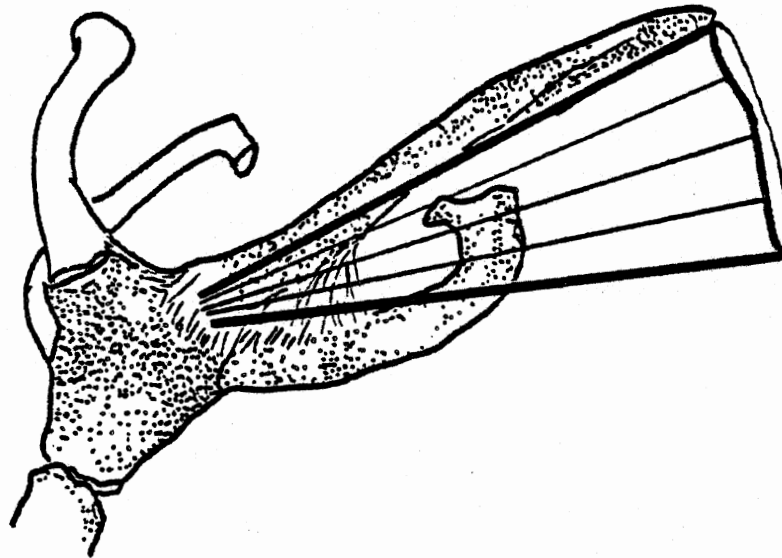


FIGURE 3-13 Joint sinus of sternoclavicular joint

SLIDE 3-12

## SLIDE 12

The clavicle, when moved to its extreme positions in all directions permitted by the sternoclavicular joint, describes a conical joint sinus with an elliptical opening. The elliptical base of the cone is shown in the lower figure. Motion of the clavicle tending to enlarge the sinus is resisted by the binding of ligaments and by the pressing together of articular surfaces.

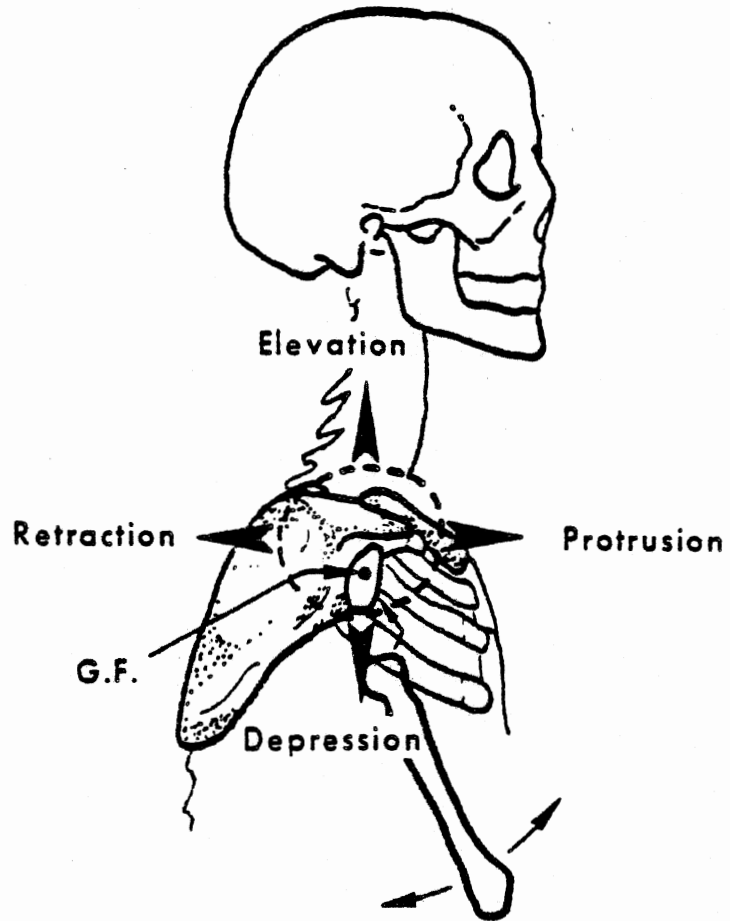


FIGURE 3-14 Maximum range of motion of the glenoid fossa (shoulder socket) in shrugging movements

SLIDE 3-13

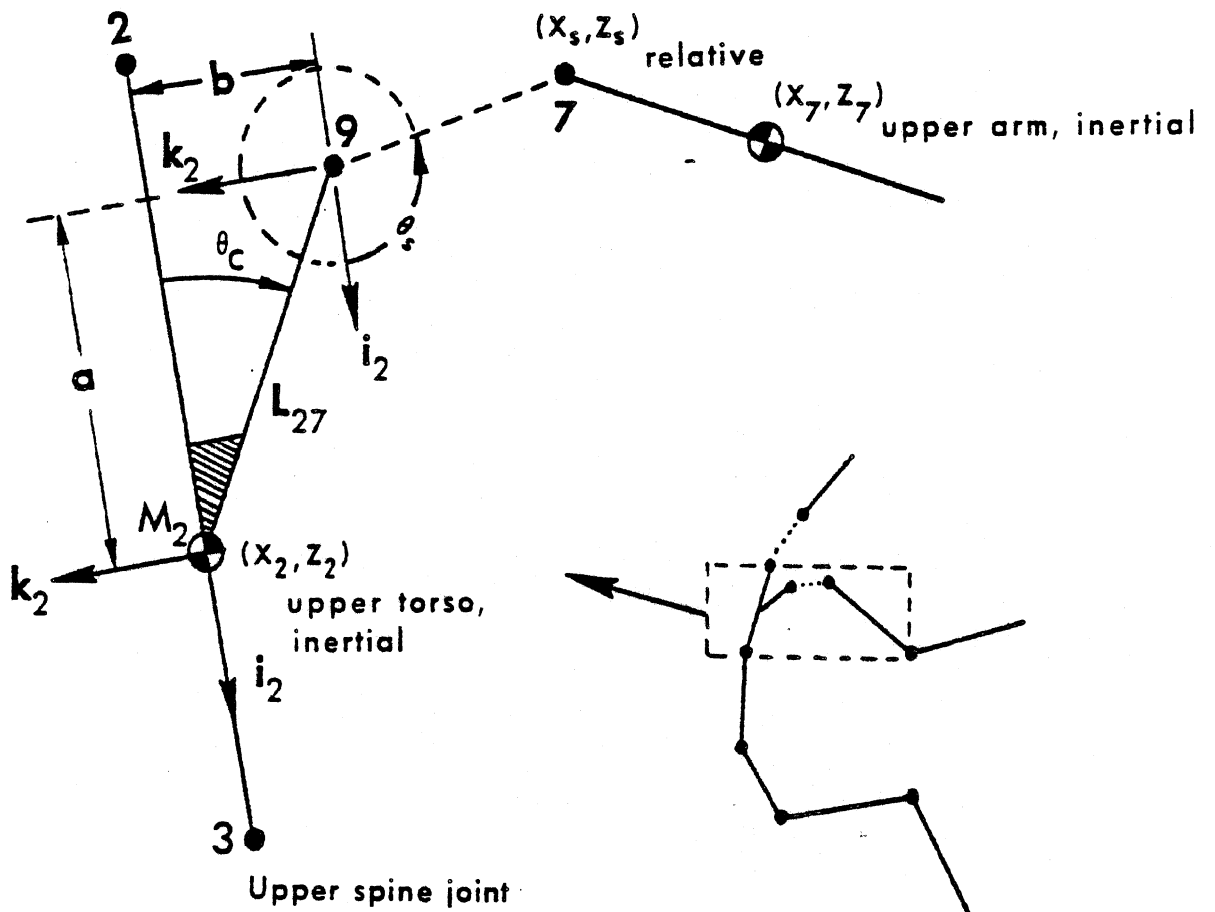
### SLIDE 13

This figure shows actions that result in direct translatory, or "shrugging," motions of the shoulder mass. These are shoulder protrusion, shoulder retraction, shoulder elevation, and shoulder depression. They are combined motions of the clavicle and scapula. The point marked "G.F." is the rest position of the mean center of the glenoid fossa on the scapula, the socket in which the humeral head articulates. The dashed ellipse is the maximum range of motion of this point when the arm is hanging straight down.

More or less independently from these claviscapular motions, articulations of the humerus occur at the glenohumeral joint. The joint sinus is large since ligaments between the scapula and the humerus allow the arm considerable freedom of movement. As long as the humerus is not rotated axially, the glenohumeral sinus from anterior to posterior is about 160 degrees. With axial rotation of the humerus, the range of motion of the upper arm can exceed 180 degrees, being limited to an approximately overhead position in the one extreme and to a position somewhat back of vertical when downward.

The shoulder model used in the MVMA 2-D Simulator has three degrees of freedom which represent the motions illustrated in the figure. The model is simplified by the assumption that the joint sinus for clavicle and scapula translatory movements is circular in cross section rather than elliptical as shown. Further, the rest point of the glenoid fossa is assumed to be at the center of the circle rather than below it.

Lower neck joint



$$\vec{l}_{9 \rightarrow 7} = x_s i_2 + z_s k_2$$

$$\theta_c = \text{constant}$$

$$L_{27} = \text{constant}$$

FIGURE 3-16 Shoulder Joint

SLIDE 3-14

## SLIDE 14

The geometry of the planar shoulder model is illustrated in this figure. Joint 9 is the rest position of the glenoid fossa. Its fixed location on the upper torso link is defined by the constants  $\theta_c$  and  $L_{27}$ , both determined from user-specified input data. This point is at the center of a circle with radius specified by the user which represents the translatory range of motion of the glenoid fossa. Joint 7 is the time-varying position of the glenoid fossa, together with the humeral head. Excursion of this point away from point 9 is resisted by linear spring and damping elements until the joint sinus circle is reached. Excursions exceeding the radius of this circle are resisted further by quadratic and cubic spring elements since such motions can occur only with stretching of clavicular and scapular ligaments. The dashed line between joints 7 and 9 is most accurately pictured as the projection onto the X-Z plane of the straight line joining the sternoclavicular joint (9) with the glenohumeral joint (7). The angle between this dashed line and the upper arm has no physical significance. Thus, sagittal-plane articulation of the upper arm at the shoulder socket, i.e.,  $\theta_7$  - motion about point 7, is restricted by viscoelastic elements fixed to the upper torso. Joint stop positions of the upper arm with respect to the upper torso as well as all viscoelastic elements are user-prescribed input data.

These data include a restitution coefficient for hysteretic unloading from excursions beyond the joint sinus circle. As it may not be true that resistance to motion of point 7 away from point 9 is the same in all directions, the linear, quadratic, and cubic spring coefficients are allowed to be specified as functions of the angle  $\theta_s$  having periods of  $360^\circ$ .

Three muscle elements can be defined for the shoulder complex. One is a force producer which limits excursion of joint 7. Two are torque producers, limiting  $\theta_s$ -motion and motion of the upper arm relative to the torso.

## **SUMMARY OF REQUIRED SHOULDER MODEL DATA**

- **Location of the sternoclavicular joint relative to the upper torso CG**
- **Radius of the sinus for claviscapular motions**
- **Joint stop angles**
- **Joint zero-torque positions**
- **Spring torque coefficients**
- **Hysteretic and viscous-force energy absorption**
- **Muscle properties**
- **Time-dependent level of muscle activation**

**SLIDE 3-15**



## SLIDE 15

The last four slides have illustrated characteristics of the sagittal-plane kinematics of the shoulder complex and also characteristics of the shoulder model used in the MVMA 2-D simulator. The data that must be specified by the user include shoulder geometry, the positions of motion-limiting stops, passive viscoelastic properties, and muscle characteristics.



**MVMA 2-D  
CRASH VICTIM SIMULATION**

**\* \* \***

**MODULE 4**

**CONTACT SURFACES ATTACHED TO THE OCCUPANT**

**MVMA 2-D**  
**CRASH VICTIM SIMULATION**

**\* \* \***

**MODULE 4**

**CONTACT SURFACES ATTACHED TO THE OCCUPANT**

**SLIDE 4-1**

## MODULE 4 - CONTACT SURFACES ATTACHED TO THE OCCUPANT

### SLIDE 1

Modules 2 and 3 describe the occupant linkage adequately only for the simulation of free motion problems. In those modules, link lengths, joint characteristics, and mass and moment of inertia properties are defined. No part of the occupant description in those modules is directly relevant to the application of external forces to the linkage. While one can imagine problems of free motion of the human linkage that would be of interest in certain types of studies, they are of no interest in crash simulations. Means must be provided for generating forces for occupant interactions with restraint systems and surfaces of the vehicle interior. In general, this necessitates description of the geometry of the interacting systems.

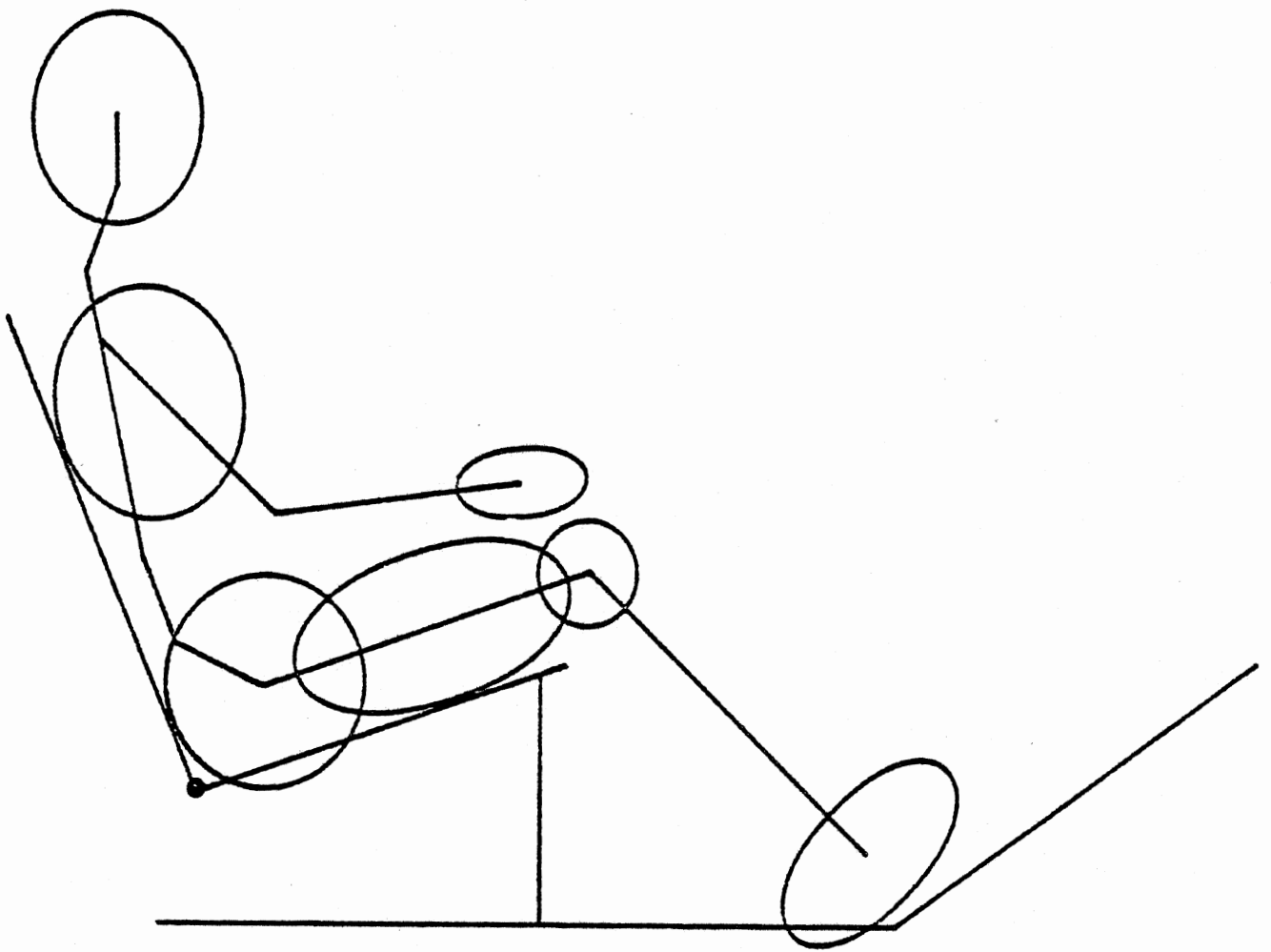


FIGURE 4-1 Example Occupant Profile of Contact Sensing Ellipses for Interaction with Vehicle Interior Surfaces

SLIDE 4-2

## SLIDE 2

This module deals with the description of occupant geometry, that is, with the definition of the planar occupant profile. The MVMA 2-D model provides for generation of forces from belts, airbag, occupant contact with vehicle surfaces, and interaction between body parts. The MVMA 2-D belt models, discussed in Module 9, do not require the definition of an occupant profile. The other force producers mentioned do depend on an occupant profile, and their descriptions are discussed in this module. Since it was convenient to use different analytical techniques for each of the force producers, the occupant contact-sensing profile is defined for each, independently, by a different set of input parameters.

## OCCUPANT PROFILE FOR INTERACTION WITH VEHICLE INTERIOR SURFACES

- **Ellipses**
  - **Arbitrary number**
  - **Arbitrary dimensions**
  - **Fixed to body links at any position**
  - **Major or minor axes parallel to body link line**
  
- **Load-deflection properties**
  - **General material properties for each ellipse**
  - **Any ellipse can be rigid**

SLIDE 4-3



### SLIDE 3

The most important of the three occupant profiles to be discussed in this module is for sensing occupant interaction with vehicle-interior surfaces. It is the most important in that it will be defined for virtually all crash simulations while the occupant profiles discussed in the last two sections of this module are associated with special options of the model and are far less commonly used.

This contact-sensing occupant profile is a set of ellipses of arbitrary number and dimensions, fixed to body links at arbitrary positions. The only restriction is that either the major or minor axis of each ellipse must be parallel to the body link to which it is attached. Material properties may be assigned for each ellipse, or an ellipse can be specified as rigid.

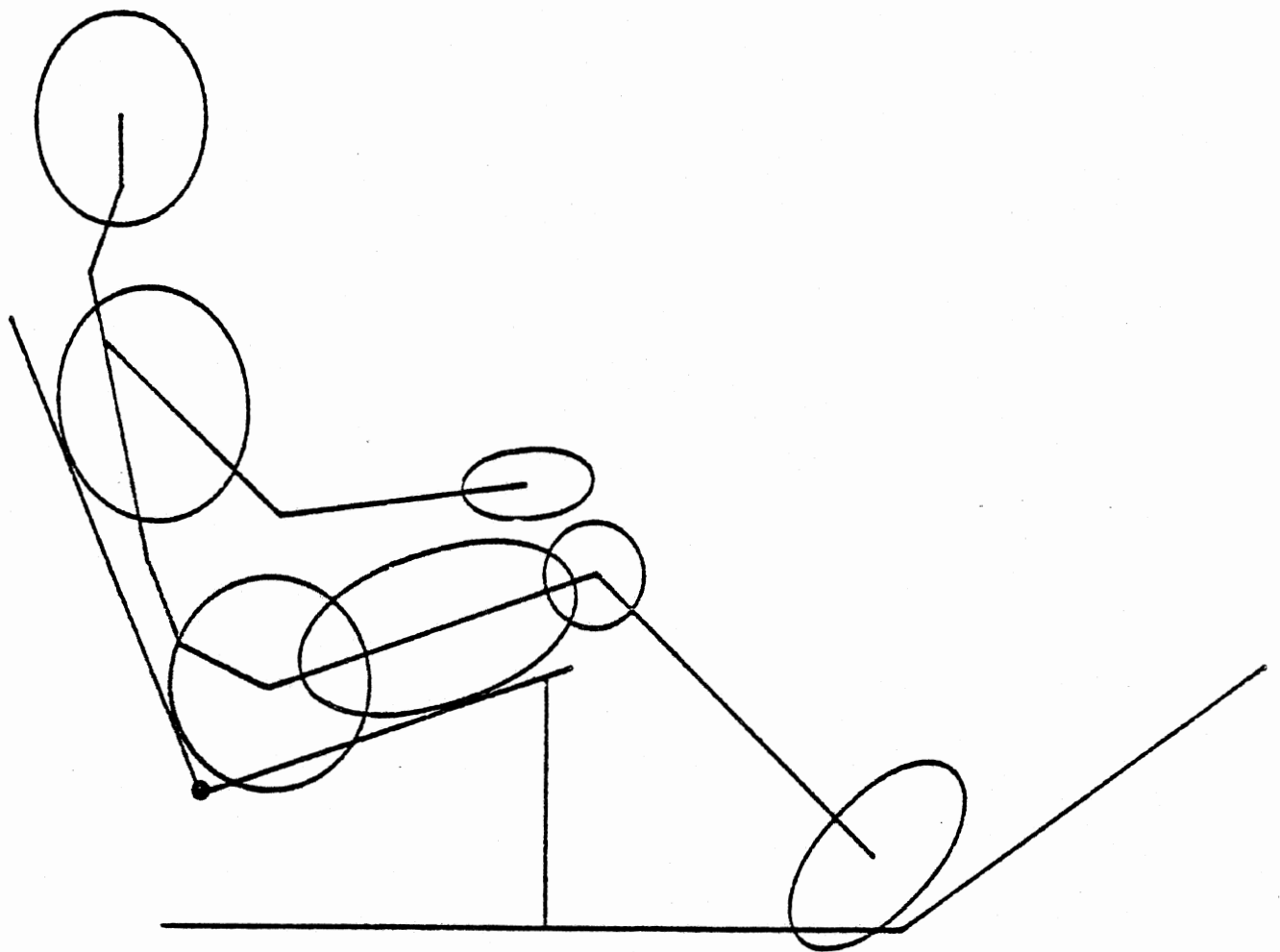


FIGURE 4-1 Example Occupant Profile of Contact Sensing Ellipses for Interaction with Vehicle Interior Surfaces

SLIDE 4-4

#### SLIDE 4

Forces between the occupant and the vehicle interior are generated by the model as a result of interaction of a profile of occupant ellipses, such as the example set illustrated, with a user-defined vehicle-interior profile. Module 5 details the description of this profile so it will be only summarized here. This profile is a set of connected or disconnected straight-line segments. An example profile of five segments is illustrated in this figure, but any number may be prescribed and their lengths and locations are arbitrary. As with contact ellipses, they may be assigned material properties or may be specified as rigid.

An untutored user of the MVMA 2-D model would soon develop, on his own, a proficiency in defining occupant ellipse profiles appropriate for his various simulations. Nonetheless, a discussion is presented here of several considerations that are normally made. Several points can be made by examining the figure. The following discussion pertains to these points.

The first point deals with specification of unnecessary ellipses. For the vehicle-interior profile shown, the head ellipse is probably unnecessary for simulation of a front-end collision, even for a restrained occupant. It seems unlikely that any head contacts could occur within the time frame of a crash history. While the specification of this head ellipse can do no harm, the only need for its presence is to sense possible contacts; hence, its presence may represent a modeling inefficiency since wasted computations and storage result. Similarly, the knee and hand ellipses are probably unnecessary for a frontal impact. The careful user will seldom go wrong in trying to model a crash event as efficiently as possible.

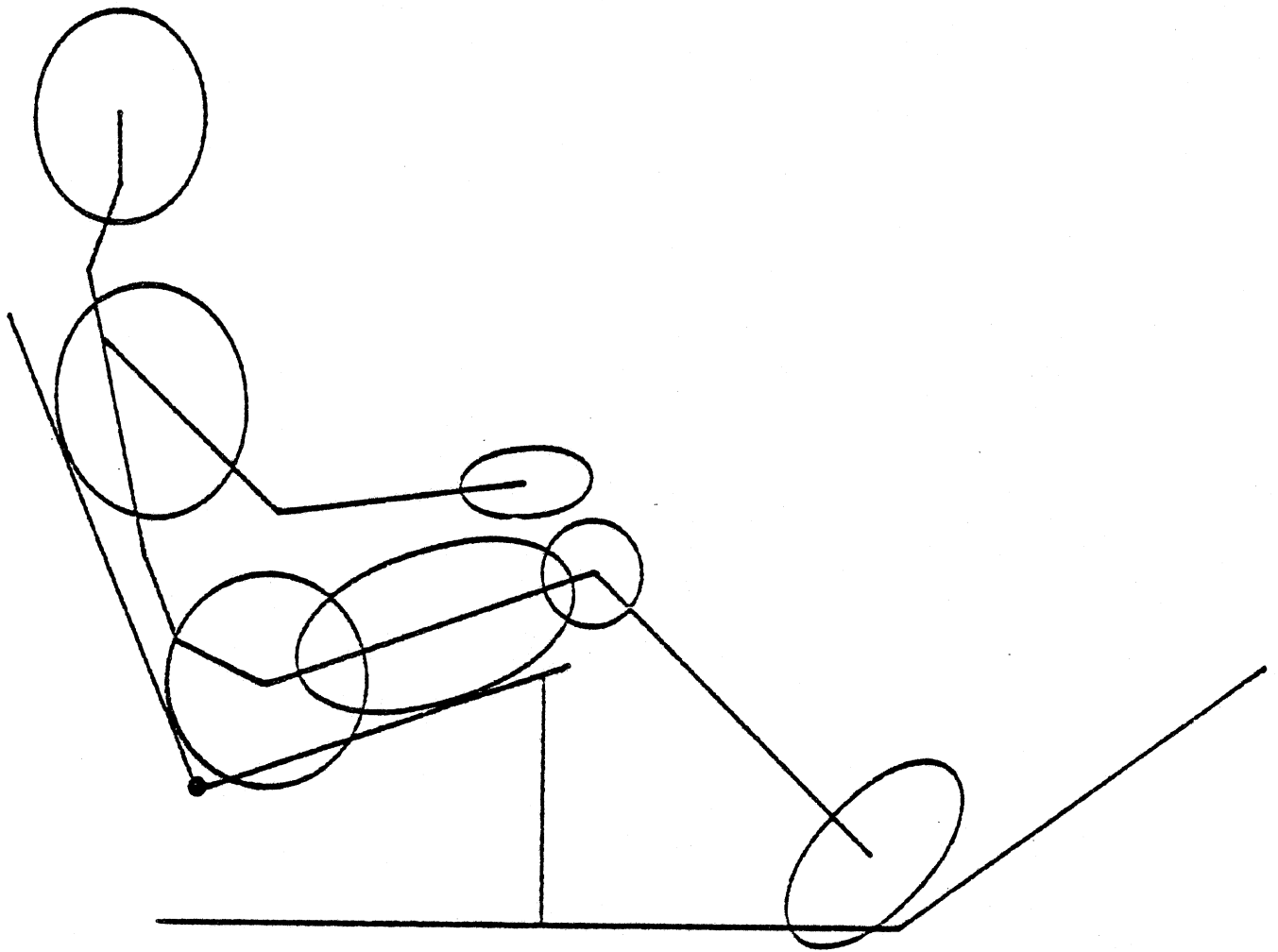


FIGURE 4-1 Example Occupant Profile of Contact Sensing Ellipses for Interaction with Vehicle Interior Surfaces

SLIDE 4-4

The second point deals with incomplete specification of ellipses. The figure illustrates such a modeling deficiency for the case of a rear impact simulation. The addition of an elbow ellipse might be appropriate as the elbow joint might otherwise pass unimpeded through the seatback line. However, the effect of arm contacts on overall body dynamics is often considered not to be of importance, so this may not be necessary.

Third, so-called "inhibition switches" for contact interactions should be used for most simulations. Contact inhibition switches can be used to specify either allowed interactions or interactions that are not to be considered by the model, that is, "inhibited" interactions. The purpose of specifying allowed or disallowed interactions is usually to make it unnecessary for the computer model to check all combinations of occupant ellipses and vehicle-interior regions for potential interaction. In many simulations, the user can be sure that certain interactions will not occur, so this will effect a reduction in computation expense. For example, for a frontal impact involving the occupant in the figure, restrained by a lap belt, it would be reasonable to specify the following allowed interactions: THORAX against SEATBACK, HIP against SEATBACK, HIP against SEATCUSHION, THIGH against SEATCUSHION, KNEE against SEATCUSHION, FOOT against FLOORPAN, and FOOT against TOEBOARD. These are seven interactions for which forces could result. Since there are potentially seven ellipses interacting with five vehicle-interior regions, or 35 total potential interactions, use of inhibition switches reduces in this instance by 80% the number of potential interactions that the computer model must consider.

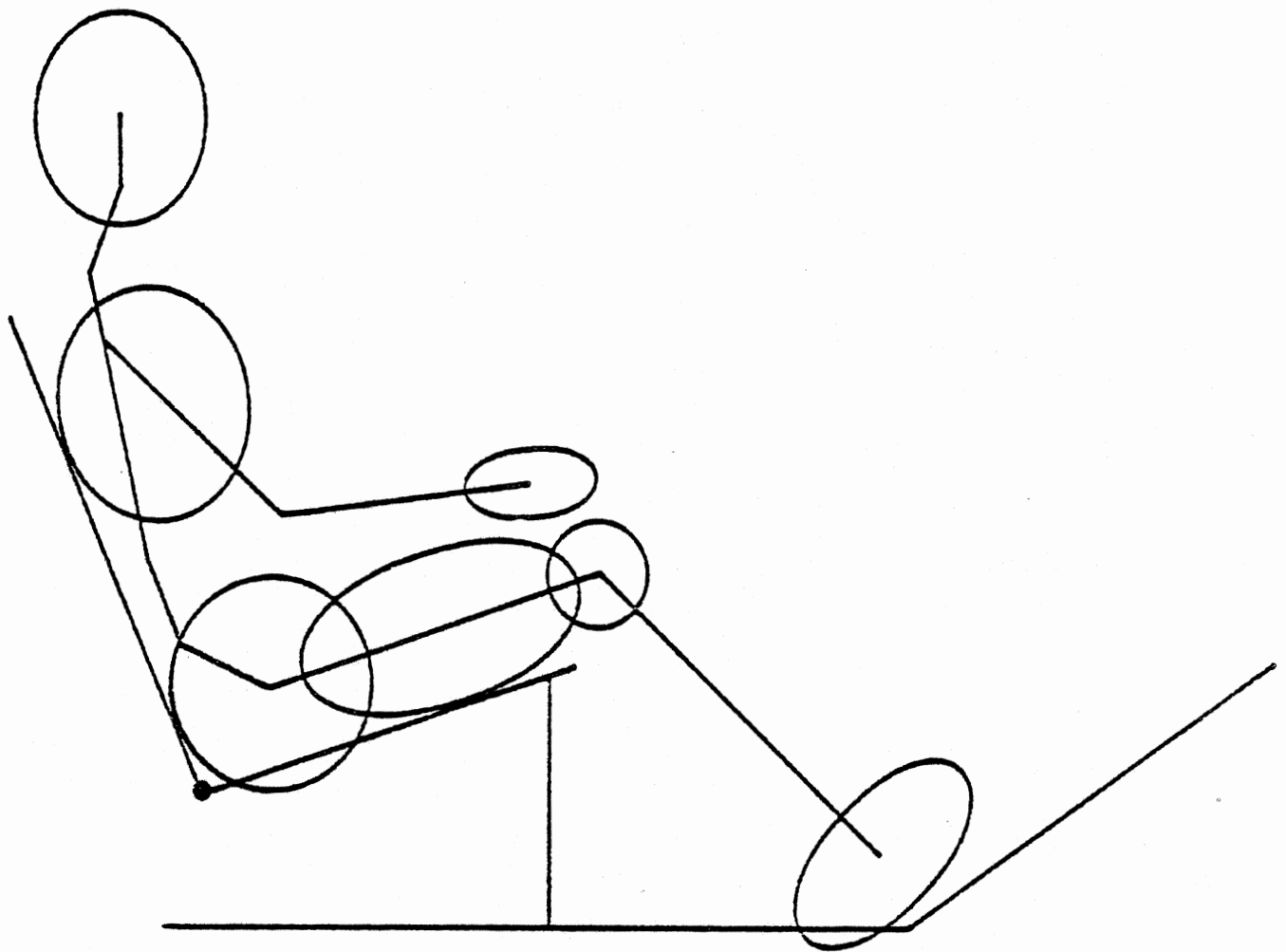


FIGURE 4-1 Example Occupant Profile of Contact Sensing Ellipses for Interaction with Vehicle Interior Surfaces

SLIDE 4-4

Fourth, "holes" in the occupant profile are sometimes of consequence and sometimes not. For example, the figure shows several spaces between ellipses along the occupant linkage, but the ellipses present are adequate for reasonable interaction with the defined vehicle-interior profile. No ellipse should be required at a mid-torso location because the hip and thorax ellipses at either end of the torso adequately account for interaction against the single line of the seat back. Holes in the occupant profile at the neck, arms, and lower legs are of no consequence for this case because there are no vehicle surfaces which are likely to pass through the interspaces. If, on the otherhand, the vehicle-interior profile included a panel region in front of the occupant, it would probably be important to add a contact-sensing profile for the lower leg, which might otherwise pass upward through the panel area with the knee and foot straddling the panels. An ellipse might be needed at a mid-torso location for a rear collision.

Fifth, a contact-sensing circle is often just as suitable as an ellipse. The thorax ellipse in the figure is a true ellipse, not a circle. But there is clearly no advantage in using an ellipse here. The only possible interaction of the thorax is with the seat back, and a circle could be attached to the upper torso link which would produce virtually identical deflections of the seat back for all likely positions and orientations of the body linkage. Use of a circle instead will result in a negligible reduction in computation expense, but the circle may be somewhat easier to position properly on the upper torso link.

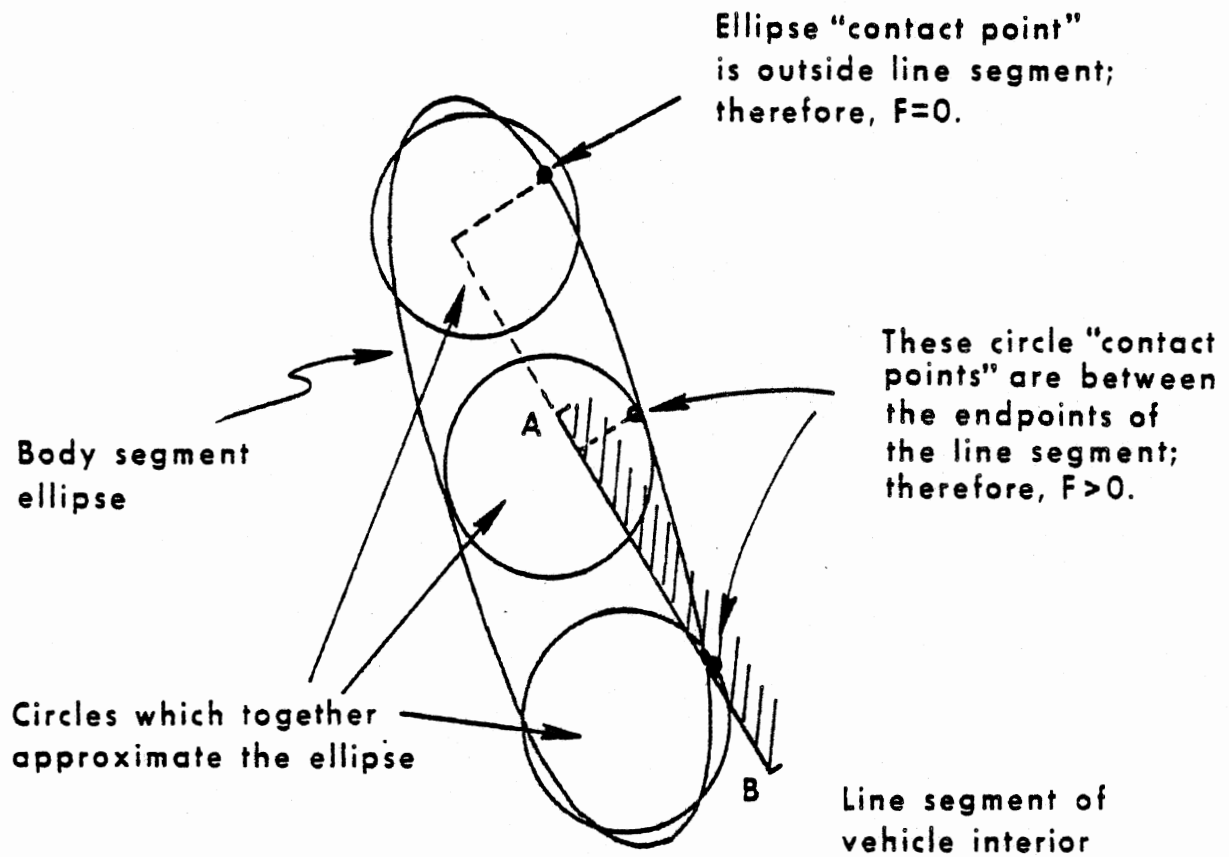


FIGURE 4-2 A Contact Sensing Ellipse and a Better Representation of the Body Segment Profile With Circles

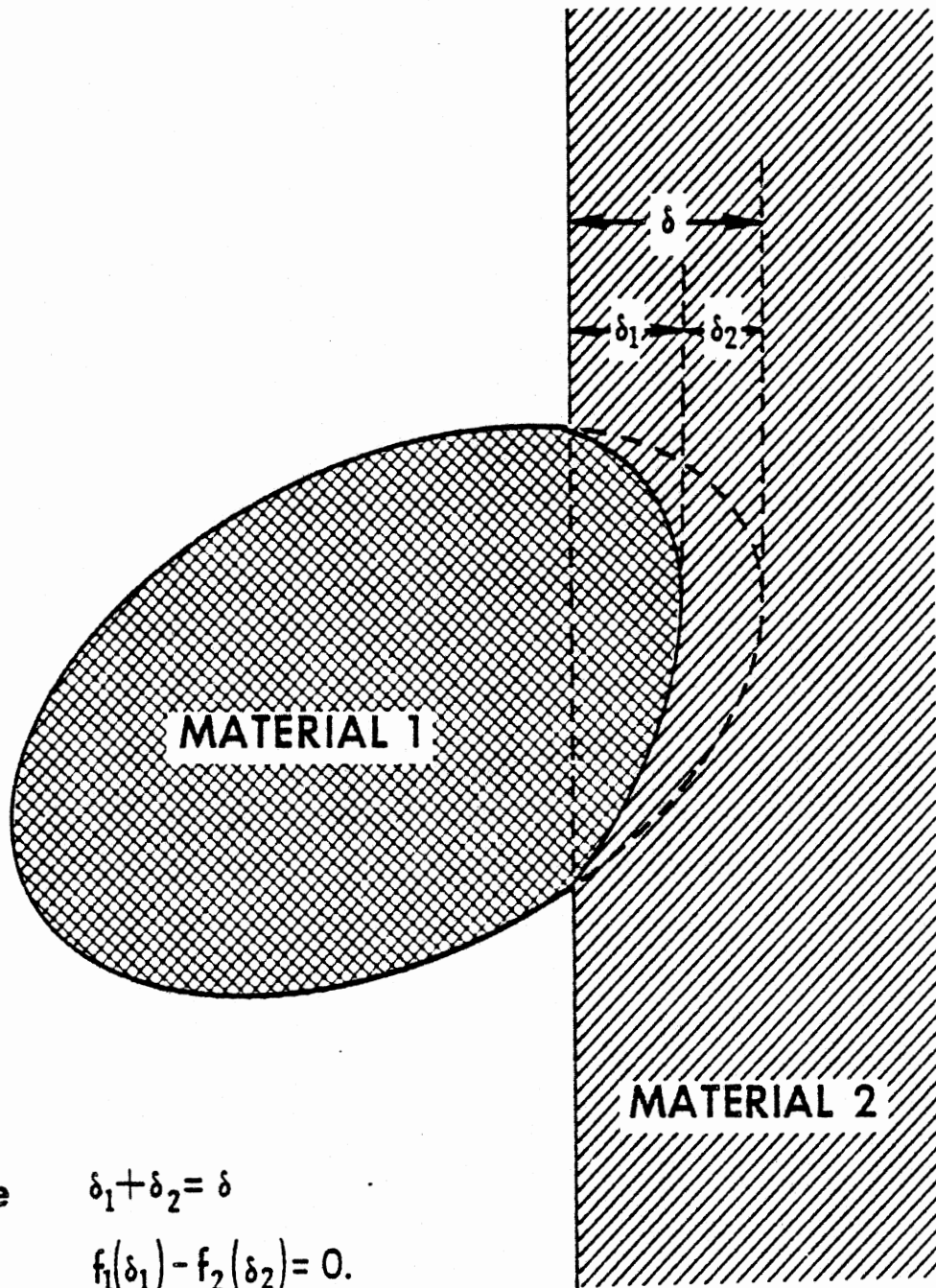
SLIDE 4-5



## SLIDE 5

Sixth, a single narrow ellipse sometimes defines a segment of the occupant profile inadequately and should be replaced by two or more circles. This figure illustrates such a case. The point on each ellipse and circle perimeter of maximum distance into the material side of the line segment is called a "contact point," and, for each, the maximum penetration distance defines the deflection. For the line segment and ellipse illustrated, the deflection is  $\delta_E$ .

The algorithm for determining contact forces, discussed in Module 6, will normally find a non-zero force for a deflection  $\delta$  greater than zero whenever the contact point is between the endpoints of the line segment. The force is normally zero whenever the contact point is outside the line segment. The ellipse shown clearly should have an interaction force with the line segment AB. But it will not, even though the "deflection"  $\delta_E$  is greater than zero, since the contact point lies outside the line segment. Use of the three circles in place of the narrow ellipse is superior since, while the contact point of one circle is outside the segment AB, two circles lie within the segment. The deflection  $\delta_C$  will produce a reasonable force. A general rule to follow is that a contact-sensing ellipse should not be longer than any line segment that it must contact for there to be proper resistance to occupant motion.



Solve  $\delta_1 + \delta_2 = \delta$

$$f_1(\delta_1) - f_2(\delta_2) = 0.$$

Then,  $F = f_1(\delta_1) = f_2(\delta_2).$

SLIDE 4-6

## SLIDE 6

Seventh, it is important when assigning material properties to keep in mind that forces for contacts of the occupant with the vehicle interior can be influenced significantly by the force-deflection characteristics of the portion of the body involved. Very often users of crash simulation models concern themselves only with the force-deflection characteristics of elements of the vehicle interior and use rigid contact ellipses or circles on the occupant. This invariably results in effective stiffnesses for occupant-interior interactions that are too large. Consequently, resulting model predictions of peak forces and G-levels are generally too high. The MVMA 2-D model allows separate definition of material properties for contact ellipses and vehicle-interior surfaces. The user should define a material for both elements of an interaction whenever data is available unless one element is considerably softer than the other. In this case, the stiffer element may reasonably be specified as rigid.

The figure illustrates an interaction between a non-rigid body ellipse and a non-rigid vehicle-interior surface. Both interacting elements deform. The total relative displacement,  $\delta$ , is the sum of the separate deflections,  $\delta_1$  and  $\delta_2$ .

## MATERIAL PROPERTIES

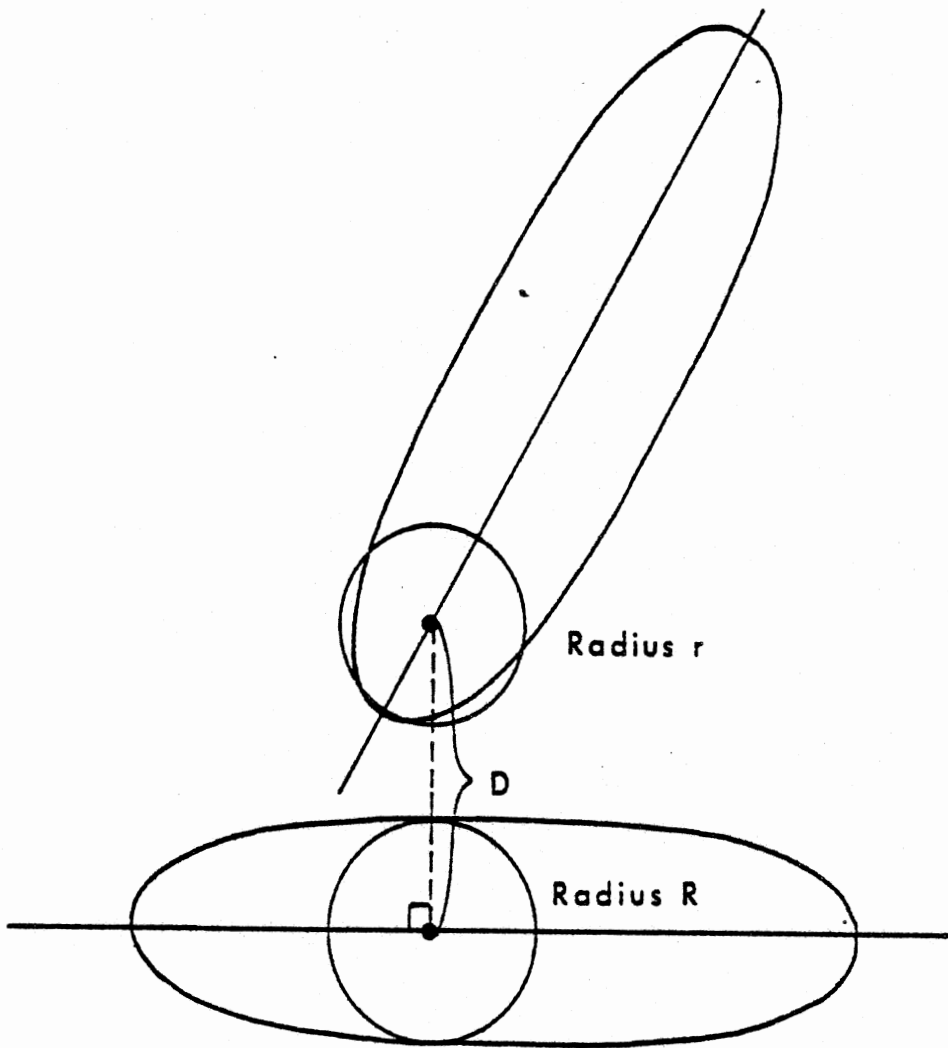
- Static force-deflection loading curve
- Hysteretic unloading
  - Permanent deformations:  $G = G(\delta_{\max})$
  - Absorbed energy:  $R = R(\delta_{\max})$
- Inertial spike loading curve
- Friction class

SLIDE 4-7

## SLIDE 7

Specification of material properties for ellipses of the body contact-sensing profile, and also for elements of the vehicle interior, is discussed in detail in Module 6, which deals specifically with the generation of forces between interacting occupant and vehicle systems. However, a general description of specifiable material properties will now be given.

For each material, values must be prescribed for deflections at the yield point and at the beginning and end of material breakdown. A force saturation level can be defined if desired. Provision is made for tabular or polynomial representation of: 1) the static force-deflection loading curve; 2) the ratio of permanent deformation to maximum deformation upon complete unloading, as a function of maximum deflection; 3) the fraction of total loading energy not lost to hysteretic absorption upon complete unloading, as a function of maximum deflection; and 4) the so-called "inertial spike" curve, a force-deflection loading curve which may be superimposed upon the static loading curve to represent the effects on impact forces of mass and loading rate. Friction characteristics are also prescribed, but friction coefficients are defined not for materials but rather for pairings of "classes" of potentially interacting ellipses and vehicle-interior regions. For example, knee and chest ellipses might be of the same ellipse friction class if both are covered with cloth. The head would probably be of a different friction class. Similarly, a seat back and a padded panel would likely belong to different region friction classes because of different surface roughnesses.



$$\delta = R + r - D$$

$$\text{Deflection} = \begin{cases} \delta & \text{if } \delta > 0 \quad (\text{circles overlapping}) \\ 0 & \text{if } \delta \leq 0 \quad (\text{circles separated}) \end{cases}$$

FIGURE 4-7 Ellipse Replacement Circles at Positions of Nearest Approach

SLIDE 4-8

## SLIDE 8

A second type of interaction which involves body ellipses is contact between body parts. Examples of such an interaction are the head striking the knee, the chest striking the upper leg, and the chin striking the sternum.

In any simulation, the same ellipses defined for interaction with vehicle surfaces may be used for determining contact forces between body parts. This is not required, however. Separate ellipses can be defined for this purpose only, if desired. Any ellipse can be made invisible to any other ellipse and to any region of the vehicle interior by inhibition specifications previously described.

The deflection for an interaction between two ellipses is determined by a computer program algorithm that models the interaction as one circle against another. This algorithm replaces a user-supplied ellipse by a circle which is positioned along the major axis of the ellipse so that its distance from a similar circle on another body element is minimum. The figure shows two ellipses at an instant of time when there is no deflection between the ellipses because the centers of the ellipse-replacement circles are further apart than the sum of their radii. Approximating an ellipse by a circle positioned along the major axis essentially reduces the ellipse to parallel lines with a semicircular cap at each end.

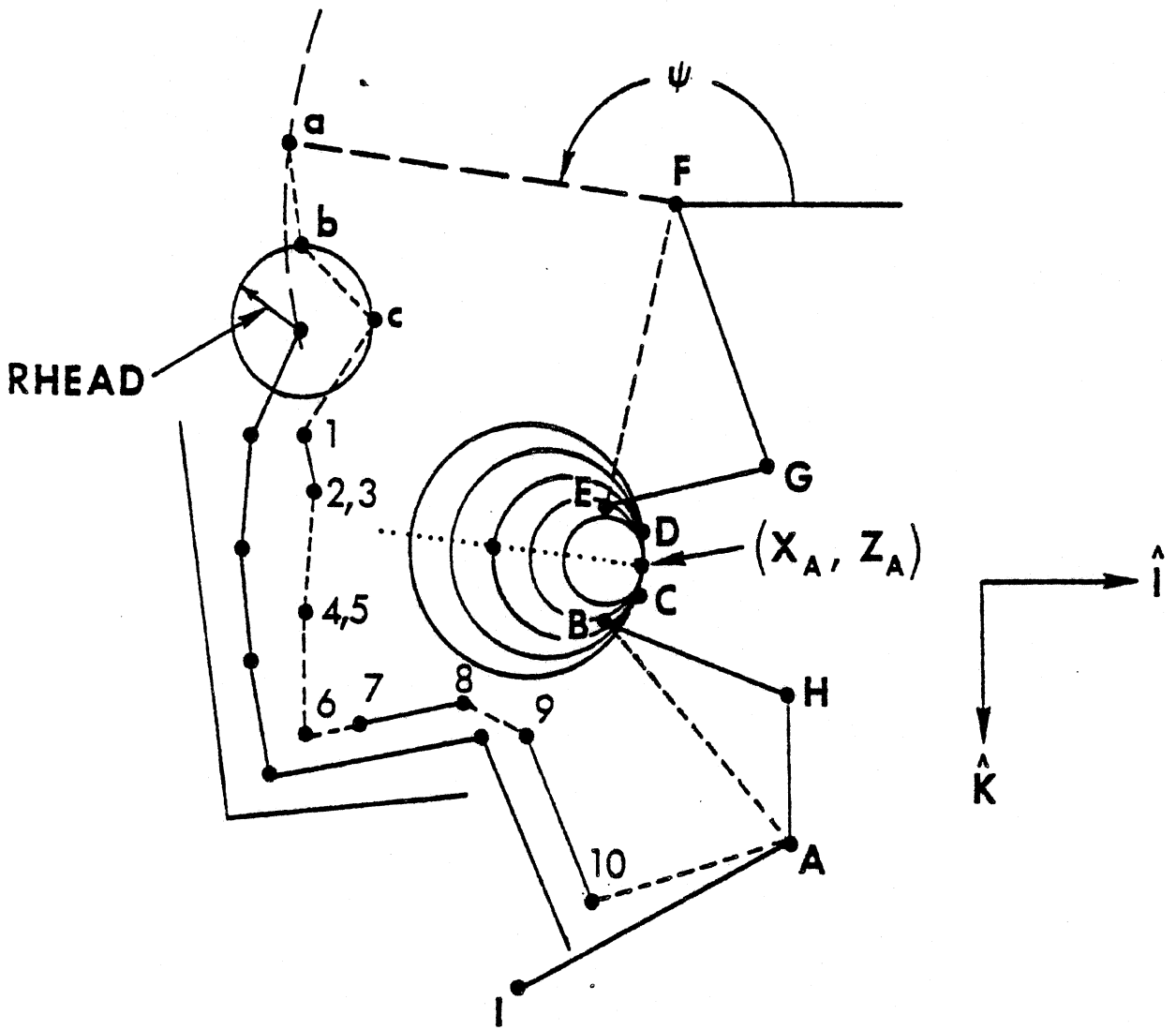


FIGURE 4-11 MVMA 2-D Airbag Model

SLIDE 4-9



## SLIDE 9

The third type of occupant profile senses contact with the airbag. The figure illustrates the profile, which consists of the line segments from b-c at the head to 9-10 at the lower legs. Airbag forces and moments are applied to the occupant only at segments C-1, 1-2, 3-4, 5-6, and 7-8, but the airbag submodel makes use of the entire profile. The user is required to define the locations of eight points on the occupant frontal profile, each fixed with respect to some body link as indicated in the next slide.

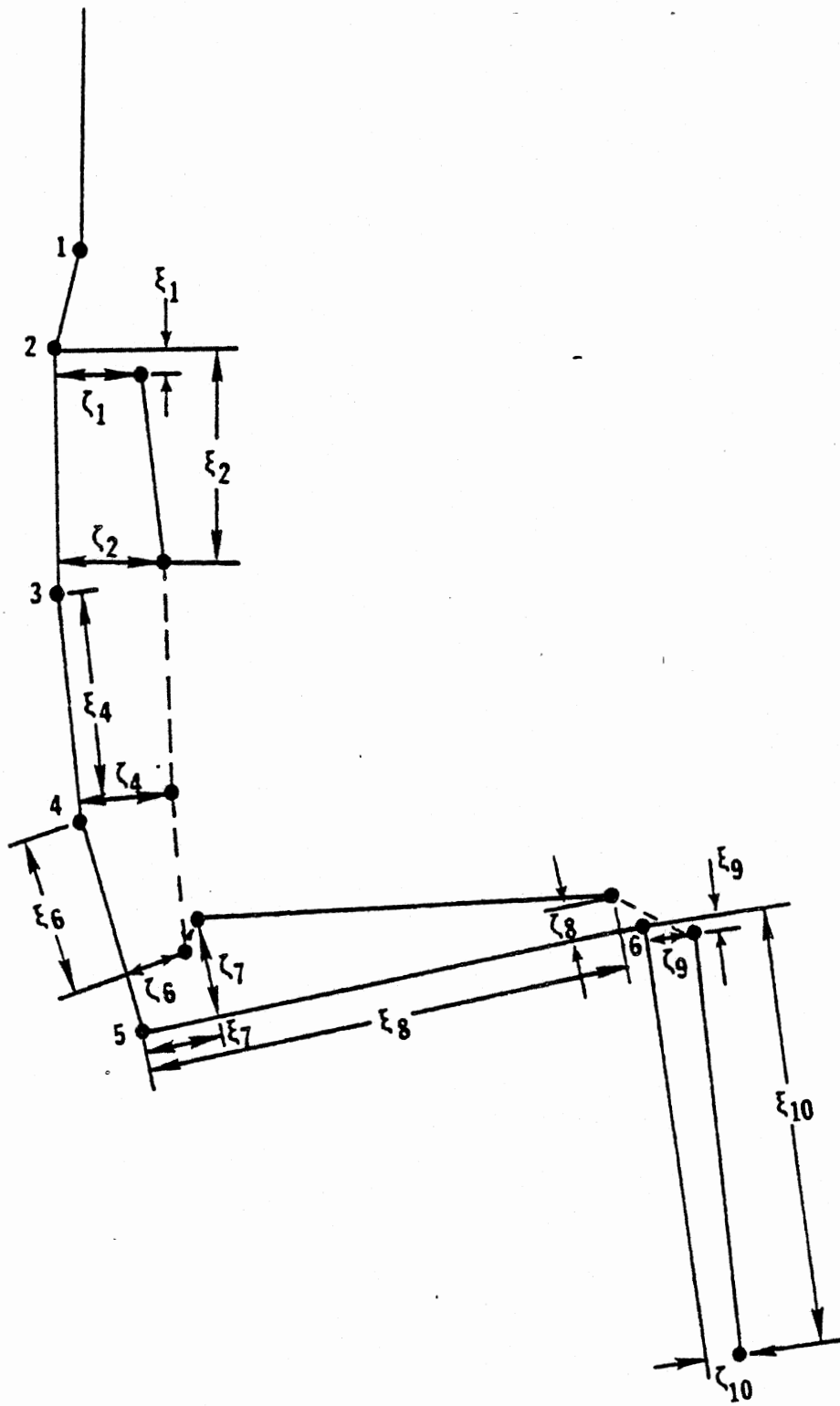


FIGURE 4-12 Airbag Contact Lines on Occupant

SLIDE 4-10

## SLIDE 10

The coordinates  $\xi_i$  and  $\zeta_i$ , with "i" equal to 1, 2, 4, 6, 7, 9, and 10, define these points. It is clear that as articulation occurs at body joints, any successive points of this group that are not defined with respect to the same body link will undergo relative motion. Solid line segments in the contact-line profile are fixed in length and orientation by the input data. Dashed lines will vary in both length and orientation with respect to all body links; these are determined by the computer model from the input data so as to make the contact profile continuous. Contact lines at the head are established by the computer model from a user-prescribed head radius.

## **SUMMARY OF OCCUPANT CONTACT SURFACE SPECIFICATIONS**

- **Ellipse and line segment dimensions**
- **Positions of attachments to body links**
- **Loading and unloading properties of body parts**

**SLIDE 4-11**

## SLIDE 11

The preceding slides have illustrated the three occupant profiles that sense contact with surfaces within the occupant compartment. The first of these is a set of ellipses that are fixed to body links and which sense interaction with vehicle-interior surfaces. This profile must be defined for virtually all crash simulations. The second profile consists of similarly prescribed ellipses and is needed only if significant forces are expected from interactions between body parts. The third profile is a set of straight-line segments attached to body segments. These are needed only if the airbag submodel is used. Except for this third profile, all contact-sensing lines on the occupant may be assigned a set of material properties for determination of interaction forces. For all occupant profiles, the user must specify the dimensions of the set of contact-sensing elements and the positions of attachments to the body links.



**MVMA 2-D  
CRASH VICTIM SIMULATION**

**\* \* \***

**MODULE 5**

**CONTACT SURFACES ATTACHED TO THE VEHICLE**

**MVMA 2-D  
CRASH VICTIM SIMULATION**

**\* \* \***

**MODULE 5**

**CONTACT SURFACES ATTACHED TO THE VEHICLE**

**SLIDE 5-1**



## MODULE 5 - CONTACT SURFACES ATTACHED TO THE VEHICLE

### SLIDE 1

The MVMA 2-D model is a predictive tool for estimating the dynamic response of a human or an anthropomorphic dummy in a crash environment. The mathematical simulation of a specific event requires the definition of: 1) an occupant model; and 2) a crash environment. The occupant model is described primarily in Modules 2, 3, and 4 while the elements of the expansive term "crash environment" are described in the remaining modules. The crash environment is comprised of all elements of the total system which cause external forces to be developed on the occupant. These include: 1) surfaces of the vehicle-interior profile; 2) restraint systems; and 3) vehicle motion. This module deals with the first of these, occupant-compartment surfaces.

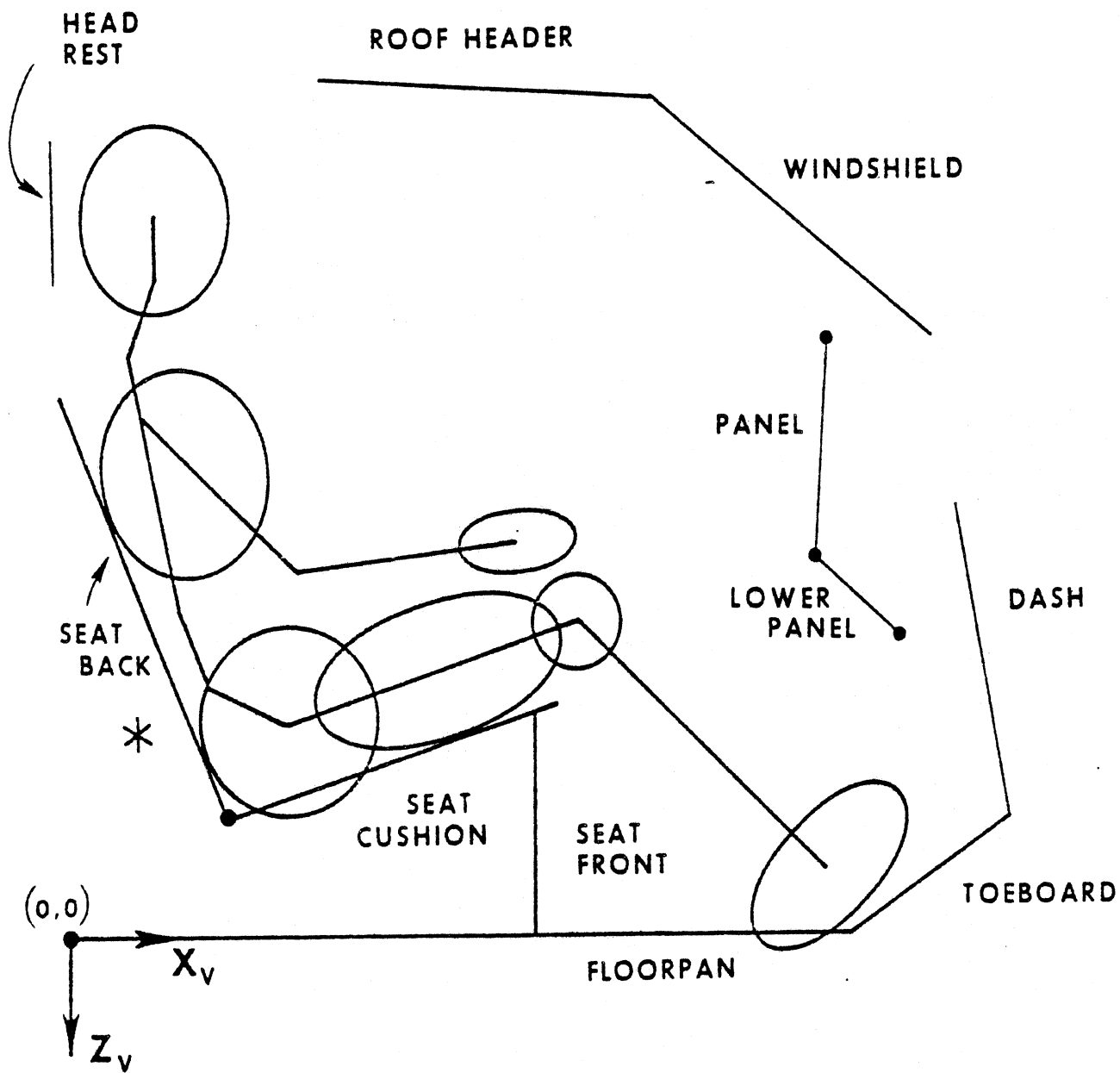


FIGURE 5-1 Example Profile of Vehicle-Interior Surfaces

SLIDE 5-2

## SLIDE 2

Forces between the occupant and the vehicle interior are generated by the model as a result of interaction of a profile of occupant ellipses with the user-defined vehicle-interior profile. This profile is a set of connected or disconnected straight-line segments. An example profile of eleven segments is illustrated in the figure, but any number may be prescribed and their lengths and locations are arbitrary. The line segments may be assigned material properties or they may be specified as rigid.

In most instances, the model user will specify line segments of fixed position within a coordinate frame which has three degrees of freedom for user-prescribed occupant-compartment motion. This is appropriate for simulation of any crash with a human or human analog inside an occupant compartment that does not suffer intrusion or collapse as a result of the impact. However, model options allow the user two variations. First, motion of segments of the vehicle-interior profile within the original space of the occupant compartment can be prescribed. Time-dependent positioning of the segments might model either direct intrusion in the case of a side-impact simulation or secondary frontal interior displacements resulting from gross deformation of the engine compartment. For the occupant compartment illustrated, this would most likely involve the elements PANEL, LOWER PANEL, DASH, and TOEBOARD. Second, the time-dependent position of any line segment can be defined with respect to the inertial frame, if desired, instead of with respect to a vehicle-fixed coordinate frame. This option is only a convenience for users with occasional diverse applications for the model. With vehicle motion taken into account, it is always possible to make any such simulation without the use of this option.

## VEHICLE INTERIOR REGIONS

- A set of straight-line segments
- Arbitrary number of segments
- Segments connected end to end
- All segments have same material properties

SLIDE 5-3

### SLIDE 3

The user defines a contact-sensing vehicle-interior profile as a set of "regions." A region is a set of straight-line segments characterized by the following features.

1) The line segments comprising a region are connected end to end. There may be an arbitrary number of segments in a region, with as few as one.

2) All line segments in a region are considered to have the same load-deflection characteristics since materials are prescribed for regions, not for segments.

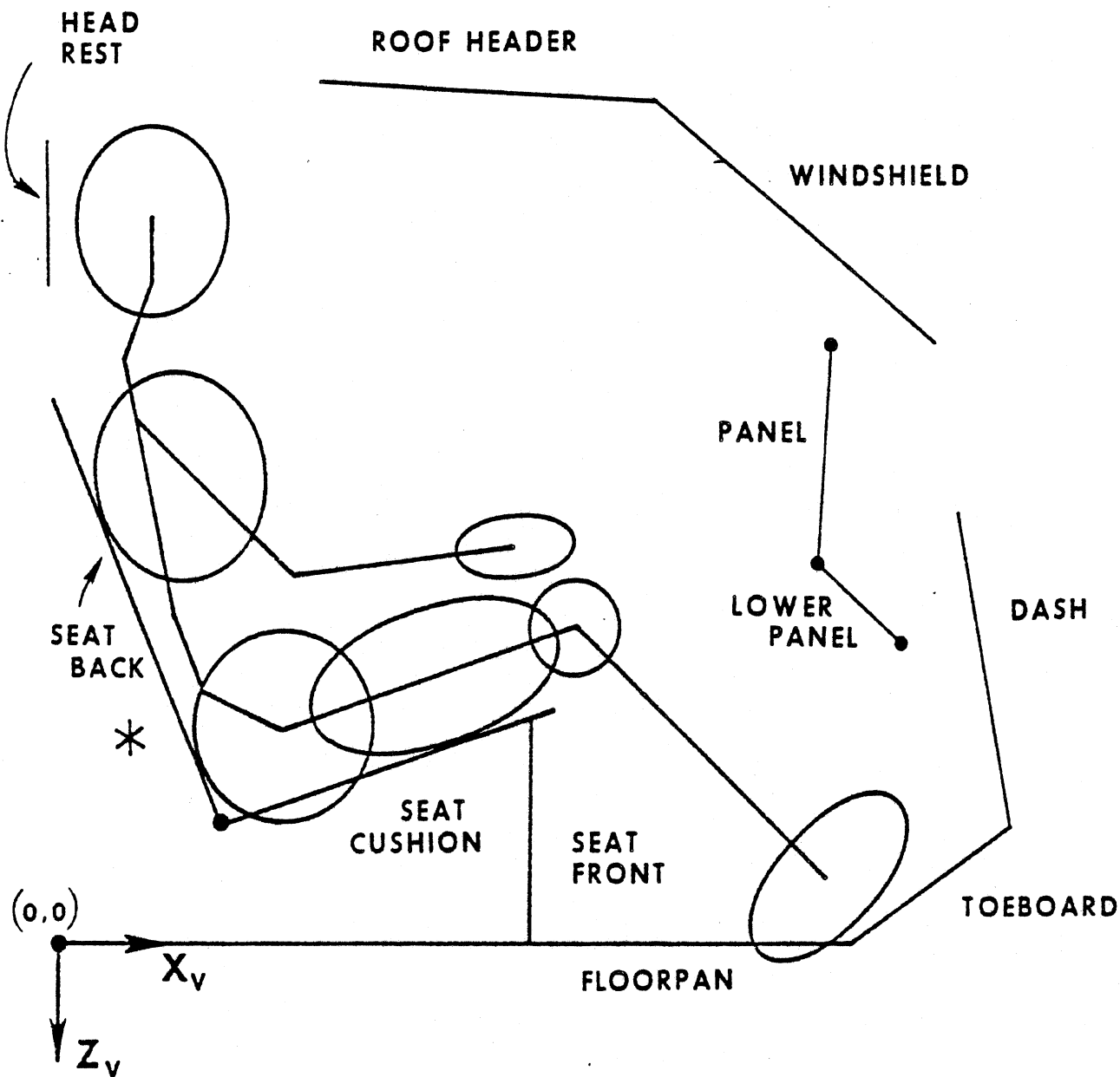


FIGURE 5-1 Example Profile of Vehicle-Interior Surfaces

SLIDE 5-4

#### SLIDE 4

Several points pertinent to specification of regions are illustrated by this slide. a) First, the roof and windshield lines, although connected, would surely be separate regions in any reasonable simulation. The reason is that these surfaces should have different load-deflection properties. b) Second, the two panel segments, the seat back plus seat cushion, and the floorpan plus toeboard might reasonably be made two-segment regions since the line segments are connected and may very well have the same load-deflection properties. c) Third, regions in the profile may be disconnected even though segments within a region cannot be.

## REQUIRED SPECIFICATIONS FOR REGIONS

- Identification of line segments comprising region plus frame of reference
- Material loading and unloading characteristics
- Friction class
- Specification of ellipses with which interactions are allowed or disallowed

SLIDE 5-5



## SLIDE 5

A number of specifications must be made for each region. These include, first, identification of the line segments which comprise the region and the frame of reference in which they are prescribed.

Second, as mentioned previously, material properties are prescribed for each region. This is discussed in detail in Module 6. The specifiable properties include a static loading curve, parameters which characterize hysteretic unloading, and an "inertial spike" loading curve for representing the effects on impact forces of mass and loading rate.

Third, friction characteristics are prescribed. However, friction coefficients are defined not for surfaces but rather for pairings of "classes" of potentially interacting body ellipses and regions. Each region of the vehicle interior must be assigned to a region friction class. Vehicle-interior regions with similar surface roughnesses are normally assigned to the same friction class. Finally, "inhibition switch" settings are usually prescribed. This option makes it possible to limit the body ellipses that must be considered by the model for potential interaction with the region to a subset of the total number of ellipses. Either allowed or disallowed interactions may be specified. In many simulations, the user can be sure that certain interactions will not occur. In such cases, use of this option will reduce computation expense.

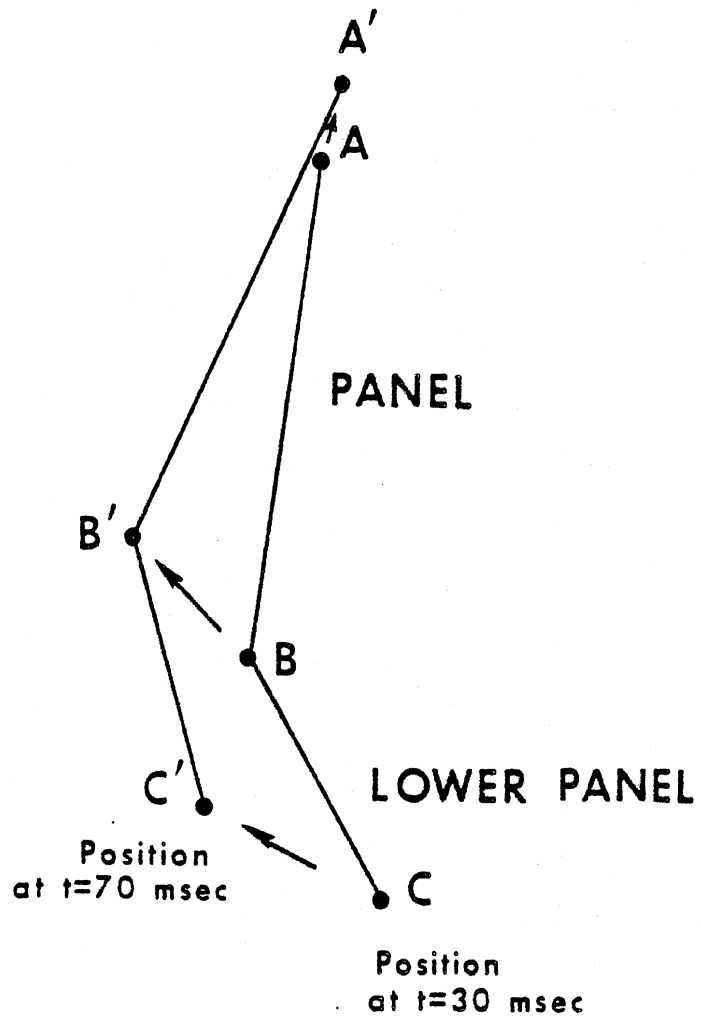


FIGURE 5-3 Padded Panel Region Displacement for Example Data

SLIDE 5-6

## SLIDE 6

Various specifications are required for each line segment in a region. First, the line segment endpoint positions must be prescribed. If the segment is stationary with respect to the reference frame indicated, whether the vehicle frame or the inertial frame, then of course, only a single pair of coordinates is needed for each endpoint of the segment. If the segment is moving perhaps for the representation of intrusion as discussed earlier, then a tabular, time-dependent, motion history is prescribed for each endpoint. The figure illustrates a rotation and displacement of a two-segment instrument-panel region into the occupant compartment. Such motion can occur with severe structural deformations that might result from a frontal impact.

## REQUIRED SPECIFICATIONS FOR LINE SEGMENTS OF A REGION

- Segment end point coordinates as tabular functions of time
- "Direction factor" to indicate material side of line segment
- "Penetration limit" to help identify cases where an apparent deflection should produce no force

SLIDE 5-7

## SLIDE 7

In addition to endpoint coordinates, two other quantities must be specified for each line segment. These are the so-called "direction factor," which indicates the side of the line segment that is capable of producing contact forces, and the "penetration limit," which is used by the computer model to identify cases where a deflection is only apparent and should produce no force.

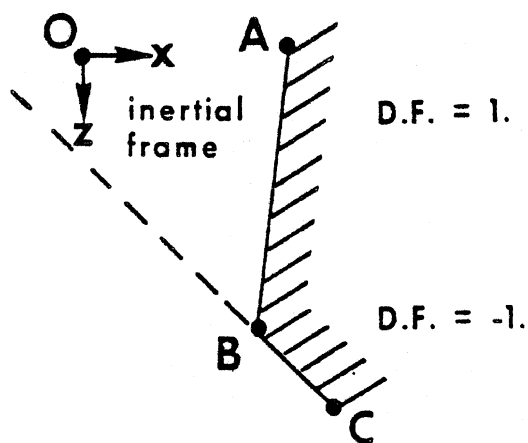
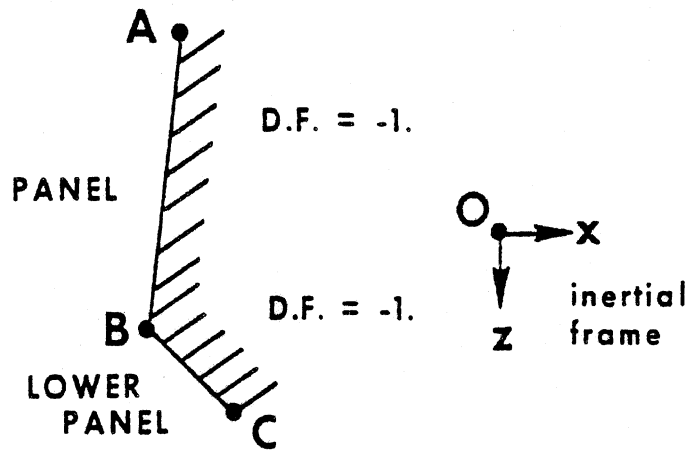
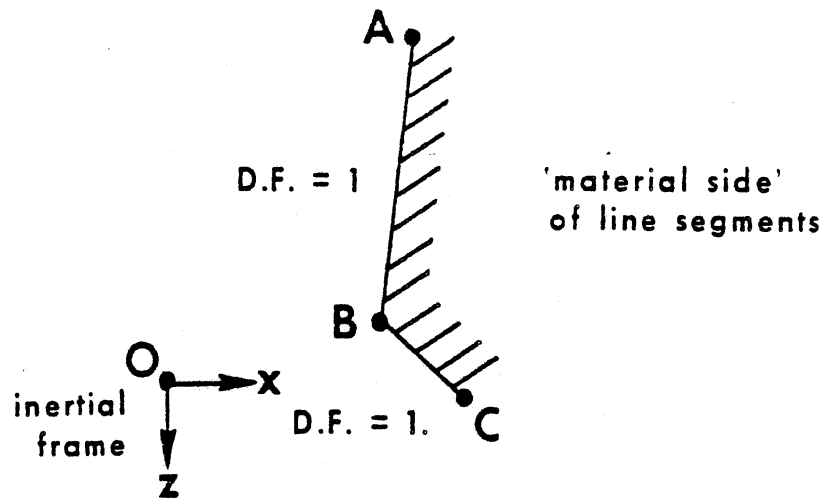


FIGURE 5-5 Line-Segment Direction Factors, Defined at  $t = 0$

SLIDE 5-8

## SLIDE 8

The first quantity, the "direction factor," is explained by this slide. It is necessary for the user to specify the "material side" of each line segment so that the computer model can properly determine an interaction force between an ellipse and the line segment. This is done by indicating whether the inertial origin lies behind or in front of the contact surface at time zero. If the inertial origin is on the side of the surface which should be contacted, that is, away from the "material side," then the direction factor is  $D. F. = +1$ . The figure illustrates three different cases for a two-segment panel region. In the upper figure, the direction factor for both segments is  $+1$ . In the middle figure the inertial origin is behind both contact surfaces, so for this case both direction factors would be assigned values of  $-1$ . The line segments in the lower figure have direction factors of different sign.

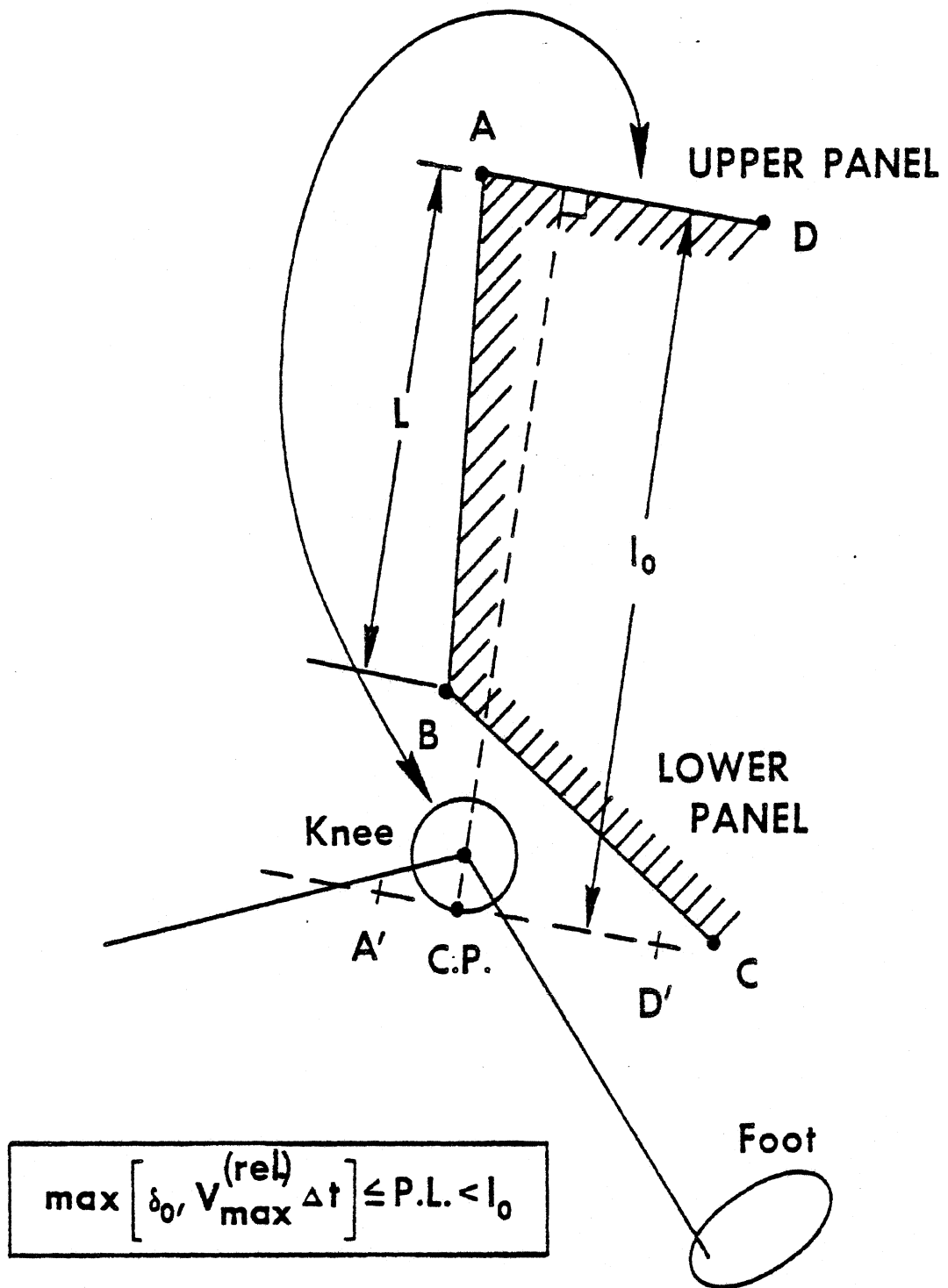


FIGURE 5-6 Selection of Value for Line-Segment Penetration Limit

SLIDE 5-9



## SLIDE 9

This slide illustrates one case in which a contact force would not be properly determined by the computer model unless an appropriate value were specified for the line-segment parameter called the "penetration limit." The figure shows a three-segment instrument panel and the upper and lower legs of the occupant. The knee has an apparent deflection of  $\lambda_0$  into the UPPER PANEL in the position shown, but a legitimate non-zero force should be predicted only if the knee passes around the panel area and strikes the UPPER PANEL from above. Since the knee location in the normal seated position might very well be as shown in the figure, the penetration limit has pertinence to the specification of conditions at time zero. In particular, the penetration limit must have a value less than the initial distance,  $\lambda_0$ .

Extreme attention need not be given to the selection of a value for this quantity. The computer logic only requires a value which satisfies the following inequality shown with the figure.

There, P.L. is the penetration limit.  $\Delta t$  is the integration time step,  $\lambda_0$  is the maximum initial apparent deflection of all ellipses against the line segment, and  $\delta_0$  is the maximum real initial deflection of all ellipses against the line segment.  $v_{\max}^{(rel.)}$   $\Delta t$  is the maximum change of deflection which is expected in one time integration step, which is to say that  $v_{\max}^{(rel.)}$  is the maximum speed at which an ellipse is expected to approach the contact surface. Since  $v_{\max}^{(rel.)}$  is limited roughly to the crash impact velocity, a reasonable lower bound for P.L. is easily established for a surface that has no real initial deflections, that is, for the case that  $\delta_0$  equals 0. If, for example, the impact velocity is 30 mph, or 528 in/sec, and the integration time step is 1. msec, then P.L.  $\geq$  .528 inches. In practice, P.L. is best set equal to its lower bound:  $P.L. = \max(\delta_0, v_{\max}^{(rel.)} \Delta t)$ . The small value will eliminate the possibility of a sudden, large, anomalous force when an ellipse is near the edge of a contact surface. This is explained in Module 6, which deals with the generation of contact forces.

## **SUMMARY OF CONTACT SURFACE DATA REQUIREMENTS**

- **Specification of vehicle-interior regions**
- **Material properties**
- **Specification of allowed or disallowed interactions**
- **Endpoint coordinates for moving or fixed line segments**
- **Line segment direction factors**
- **Line segment penetration limits**

**SLIDE 5-10**

## SLIDE 10

In summary, the user of the MVMA 2-D model must prescribe geometry and several special parameters for the vehicle-interior profile. The occupant-compartment surfaces are specified by "regions," which are comprised of arbitrary numbers of line segments, connected end to end, which have the same material properties. The line segments may be fixed or moving with respect to either an inertial or a vehicle frame of reference. Material loading and unloading characteristics must be prescribed for each region, and it is normal, although optional, to specify either allowed or disallowed interactions with ellipses for each region in order to eliminate unnecessary computational expense. In addition to endpoint coordinates, quantities which must be prescribed for each line segment are its "direction factor" and "penetration limit," both of which are used by the computer model to help determine whether a force-producing interaction exists between the line segment and a body ellipse.



**MVMA 2-D**  
**CRASH VICTIM SIMULATION**

**\* \* \***

**MODULE 6**

**GENERATION OF CONTACT FORCES**  
**ON THE OCCUPANT:**

**PART 1**

**MVMA 2-D**  
**CRASH VICTIM SIMULATION**

**\* \* \***

**MODULE 6**

**GENERATION OF CONTACT FORCES  
ON THE OCCUPANT:**

**PART 1**

**SLIDE 6-1-1**

MODULE 6 -- GENERATION OF CONTACT FORCES ON THE OCCUPANT: Part 1

SLIDE 1

Module 6 is in two parts. Part 1, which follows, deals primarily with two subjects: first, the determination of deformations of the occupant and elements of the vehicle interior that occur in an interaction between them; and second, the general force-deflection characteristics that may be prescribed for the interacting elements.

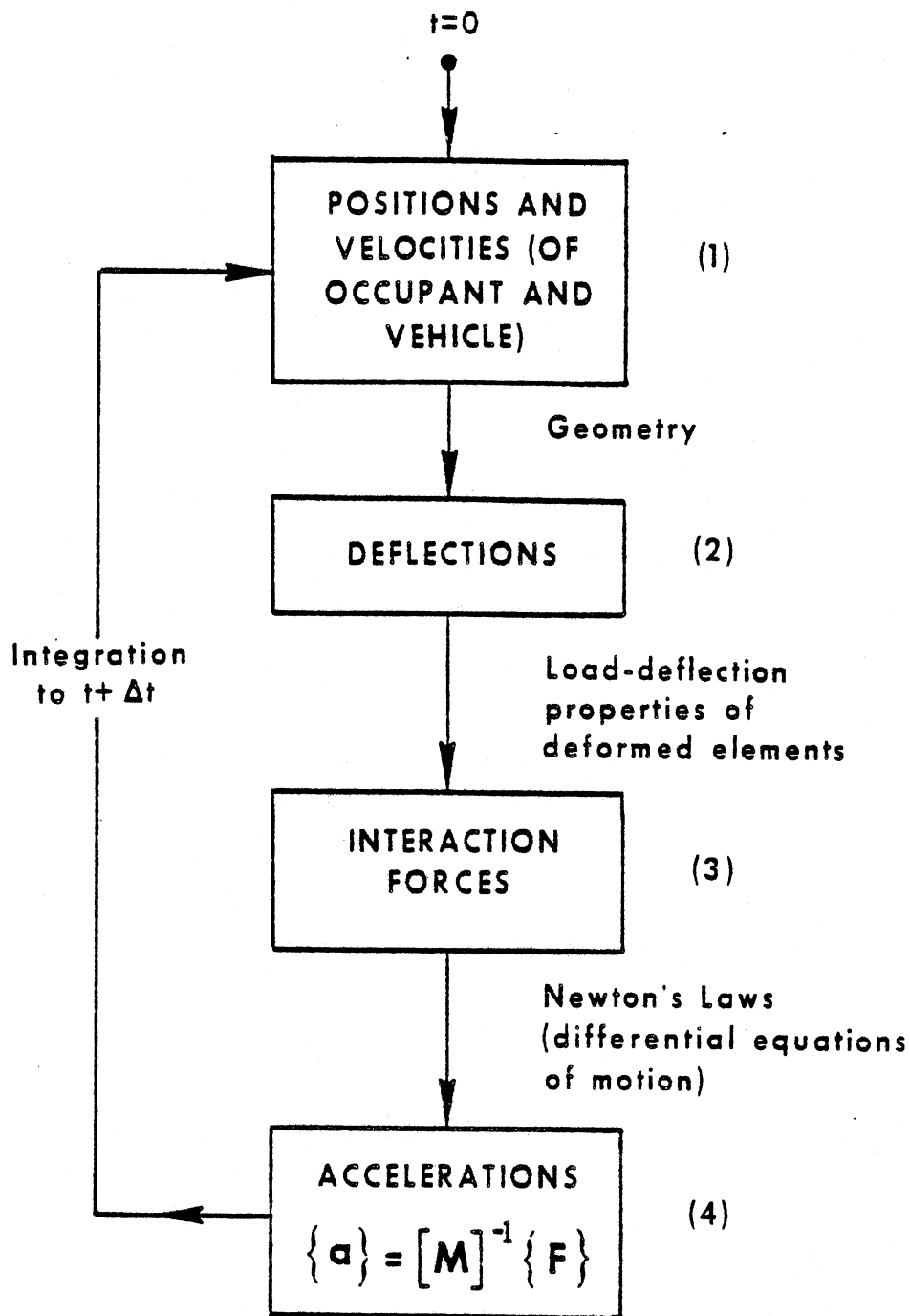


FIGURE 6-1 Relationship of Position Conditions and Interaction Forces Within the Framework of an Initial Value Problem

SLIDE 6-1-2



## SLIDE 2

Occupant motion within the vehicle both determines and is determined by forces acting on the occupant linkage. This slide illustrates the relationship between the motion and the forces. At some instant of time, usually called  $t = 0$ , the position and velocity conditions of the occupant relative to a vehicle-fixed reference frame must be known. From these, the instantaneous state of displacements between body and vehicle elements, and hence the interaction forces, may be determined. Further, the instantaneous interaction forces thus found, together with the motion equations of classical mechanics, namely Newton's Laws, determine the instantaneous accelerations essentially as force divided by mass. Integration of the accelerations then yields the occupant velocities and positions at a new time, different from the time at which forces were determined by an arbitrarily small amount,  $dt$  or  $\Delta t$ . New position and velocity conditions having been determined, new deflections can be determined and so forth so that the entire time histories for motion and forces are established.

The vector  $\{F\}$  in block 4 of the figure is a function of position and velocity coordinates and the interaction forces from block 3. The interaction forces include restraint system loads, which are discussed in Modules 9 and 10, and "contact forces," with which this module deals. Contact forces are those forces resulting from direct interaction between body parts or between a body part and a surface of the occupant compartment. Block 1 indicates that occupant and vehicle positions and velocities must be known before interaction forces may be determined. Modules 2, 4, and 7 are relevant to occupant conditions for block 1, and pertinent vehicle specifications are described in Modules 5 and 8. The subject of this module is determination of contact-interaction deflections and resulting forces in blocks 2 and 3.

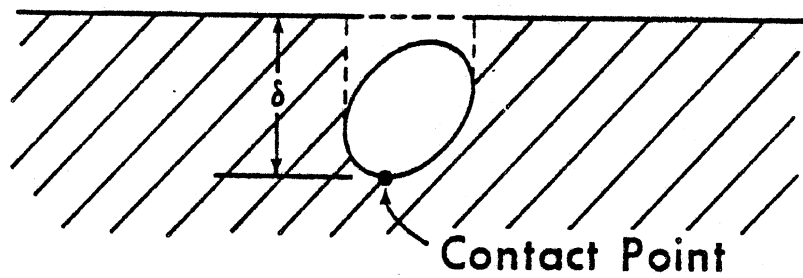
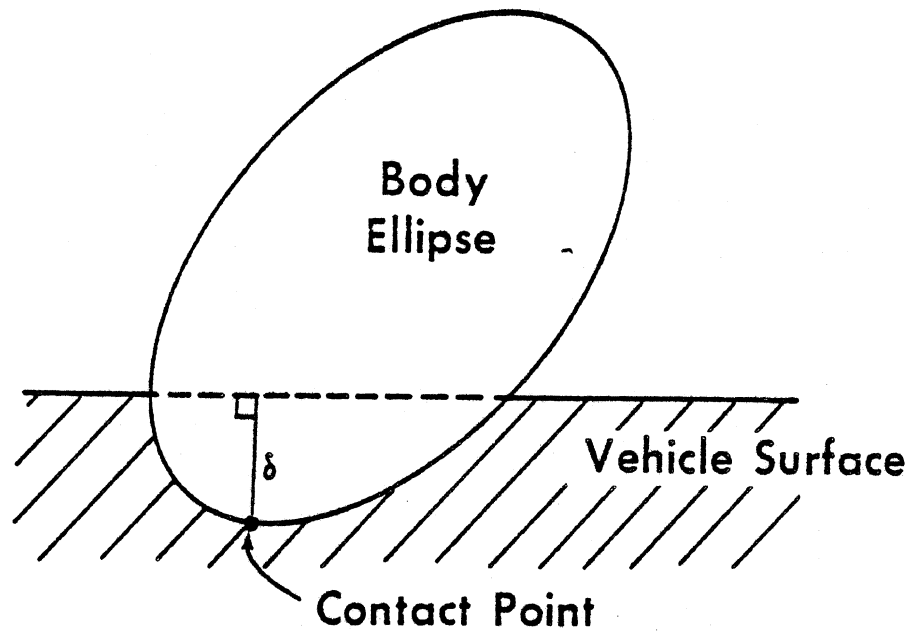


FIGURE 6-3 Deflection Between a Straight-Line Segment and an Ellipse

SLIDE 6-1-3

### SLIDE 3

A contact force vector is generated whenever a body ellipse intersects a vehicle-interior line segment. The figure illustrates such a case. The deflection  $\delta$  is defined as the distance of maximum penetration of the ellipse beyond the line. Note from the lower figure that this definition still applies if the body ellipse has passed completely beyond the resisting surface.

Whether the deforming element in a contact interaction is the ellipse or the line segment is not implicit in the definition of deflection. This is dependent upon material specifications. The figure illustrates a rigid ellipse against a deforming line segment, but with different material specifications the deflection could be shared or could be solely in the ellipse.

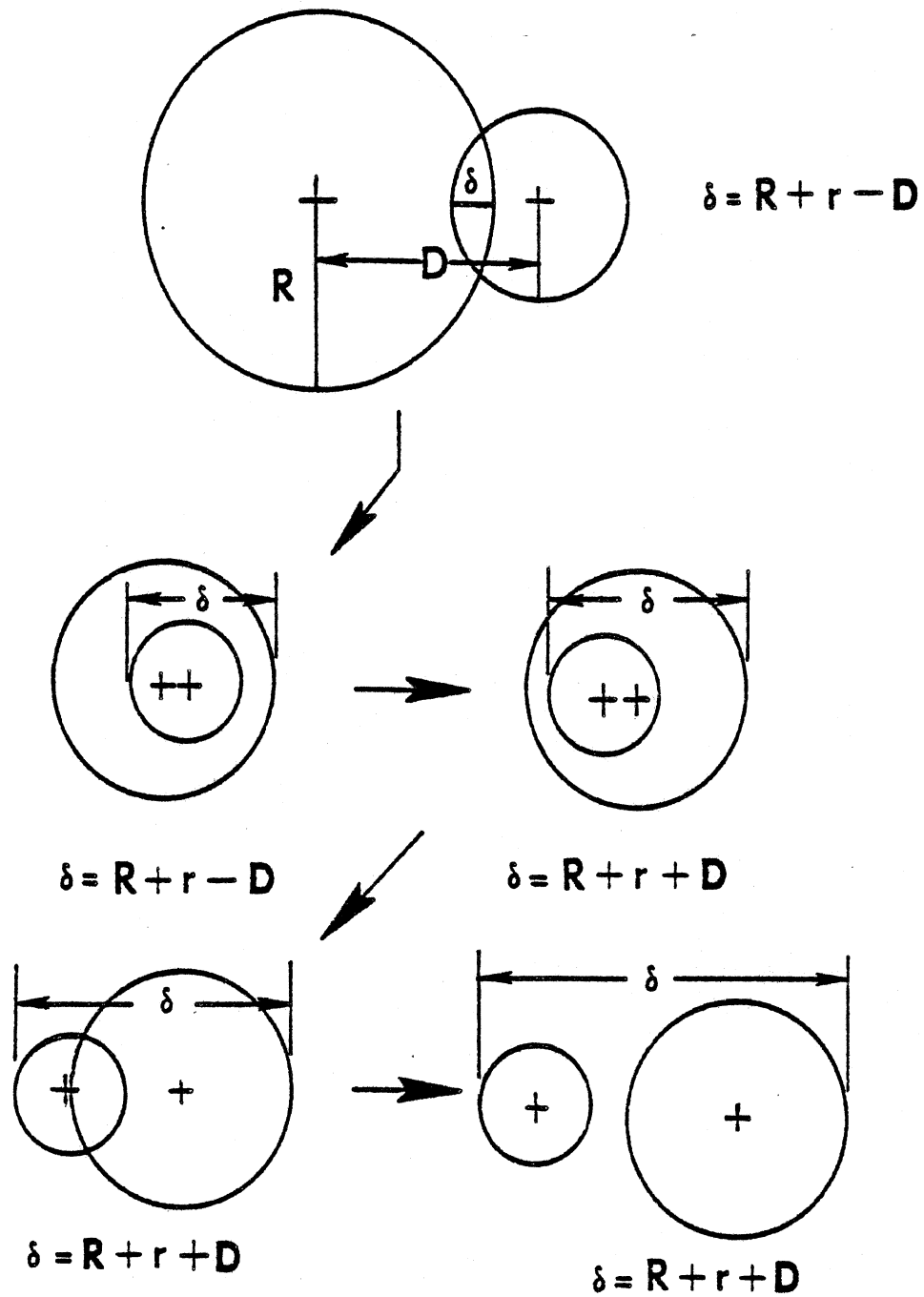


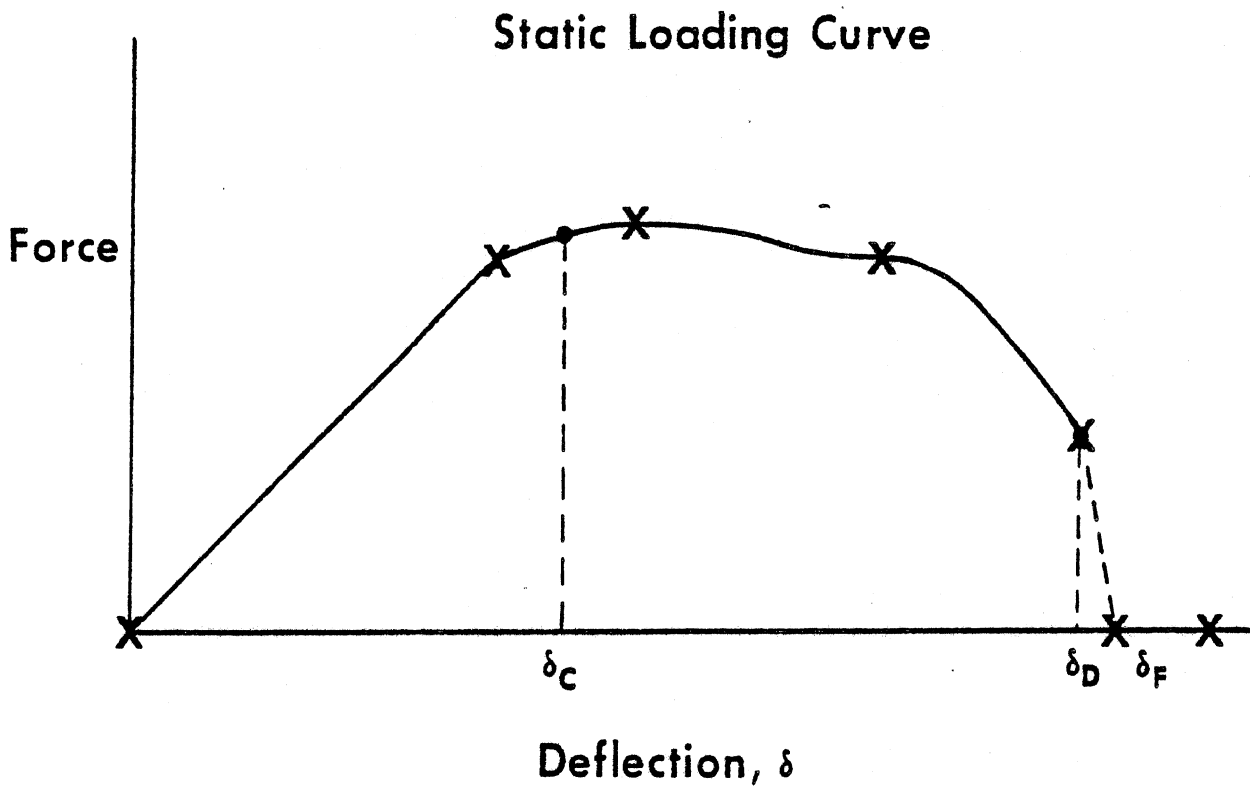
FIGURE 6-7 Deflection Between Ellipse Replacement Circles

SLIDE 6-1-4

#### SLIDE 4

Module 4 explains how ellipses attached to different body segments are approximated, for the purpose of considering potential interactions between ellipses, by circles of varying position. An ellipse-ellipse contact force will be produced if the ellipse replacement circles overlap.

This figure illustrates contact interactions between replacement circles for progressively greater deflections. In each instance,  $R$  and  $r$  are the radii of the circles, and  $D$  is the distance between their centers. A resulting force is applied to the body link of each ellipse as a vector along the line between the centers of the circles.



$\delta_c$  = yield point (elastic limit)

$\delta_D$  = breaking point

$\delta_F$  = end of breakdown curve

FIGURE 6-8 Static Loading Curve

SLIDE 6-1-5

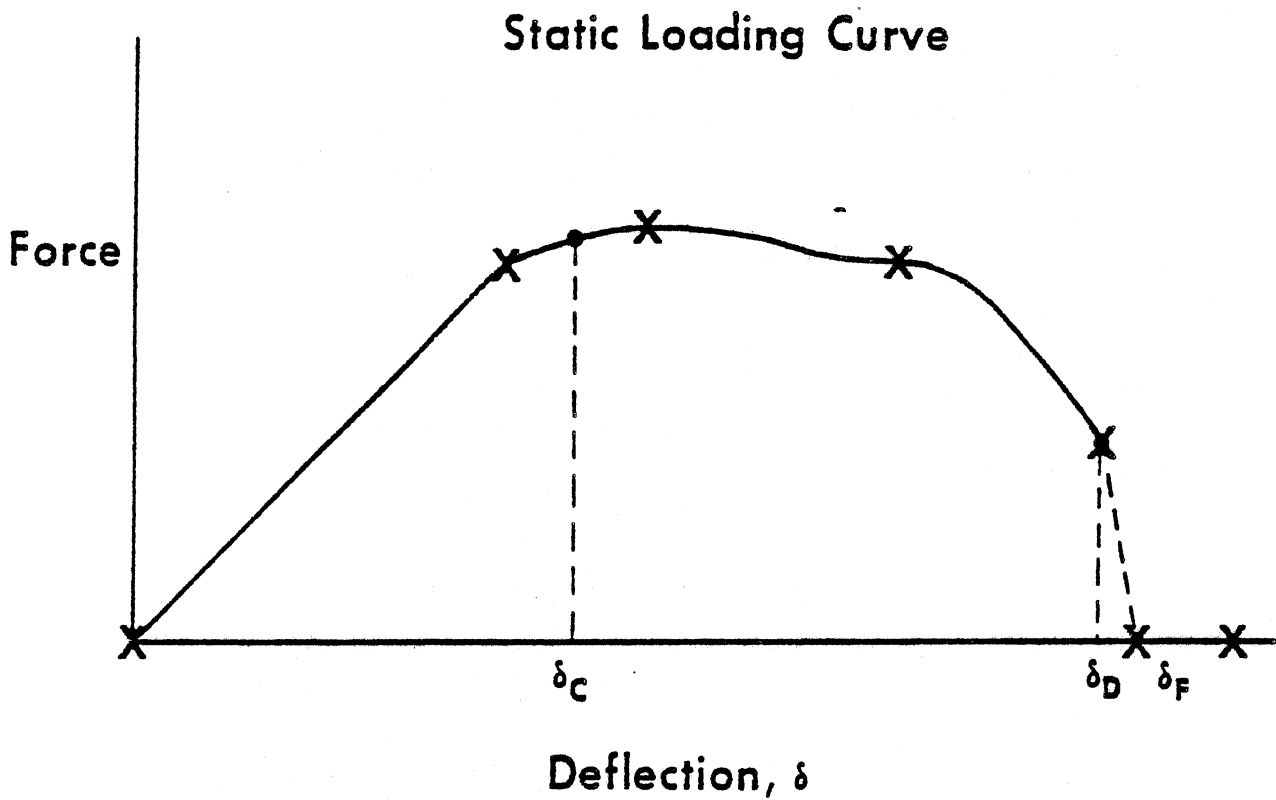
## SLIDE 5

Contact forces in the MVMA 2-D model are directly dependent on deformations of the interacting elements but not on deformation rates. The user prescribes for each body-segment ellipse and each vehicle-interior region a material with resistive properties that depend only on deflection. This is not to say that the loading history of a material is not considered; deformations beyond a user-defined yield point, or "elastic limit," can result in hysteretic energy loss and permanent deformation of the element upon unloading. Also, reloading from a partially unloaded state is complex.

The various material properties that can be specified by the user will be explained in the remainder of this module. All material characteristics described here pertain equally to vehicle-interior region materials, body ellipse materials, and belt webbing materials. It might be noted at this point, however, that belt material specifications can be made optionally in terms of strain, instead of deflection.

An element is undergoing "loading" whenever its material deformation is increasing with time. Note that this does not mean that the load, or force, is necessarily increasing with time or with deflection. The user is required to prescribe a static loading curve for each material defined for a simulation.

Suppose that an element is tested in quasi-static loading by pressing against it a rigid form, either flat, elliptical, or circular in shape in accordance with the definitions of deflections previously illustrated. A load-deflection curve such as illustrated in this figure could be established. It can be represented as accurately as necessary by a piecewise-linear approximation. For example, the curve shown is adequately defined for simulation purposes in tabular form by coordinate pairs of force and deflection values of the points marked with an "X." The user may prescribe a tabular static loading curve, or optionally, a polynomial curve of order six. The tabular form of the curve is generally used, but sometimes it is convenient to fit a polynomial to the load-deflection data. The most common use of the polynomial is for specifying a constant load-deflection slope.



$\delta_c$  = yield point (elastic limit)

$\delta_D$  = breaking point

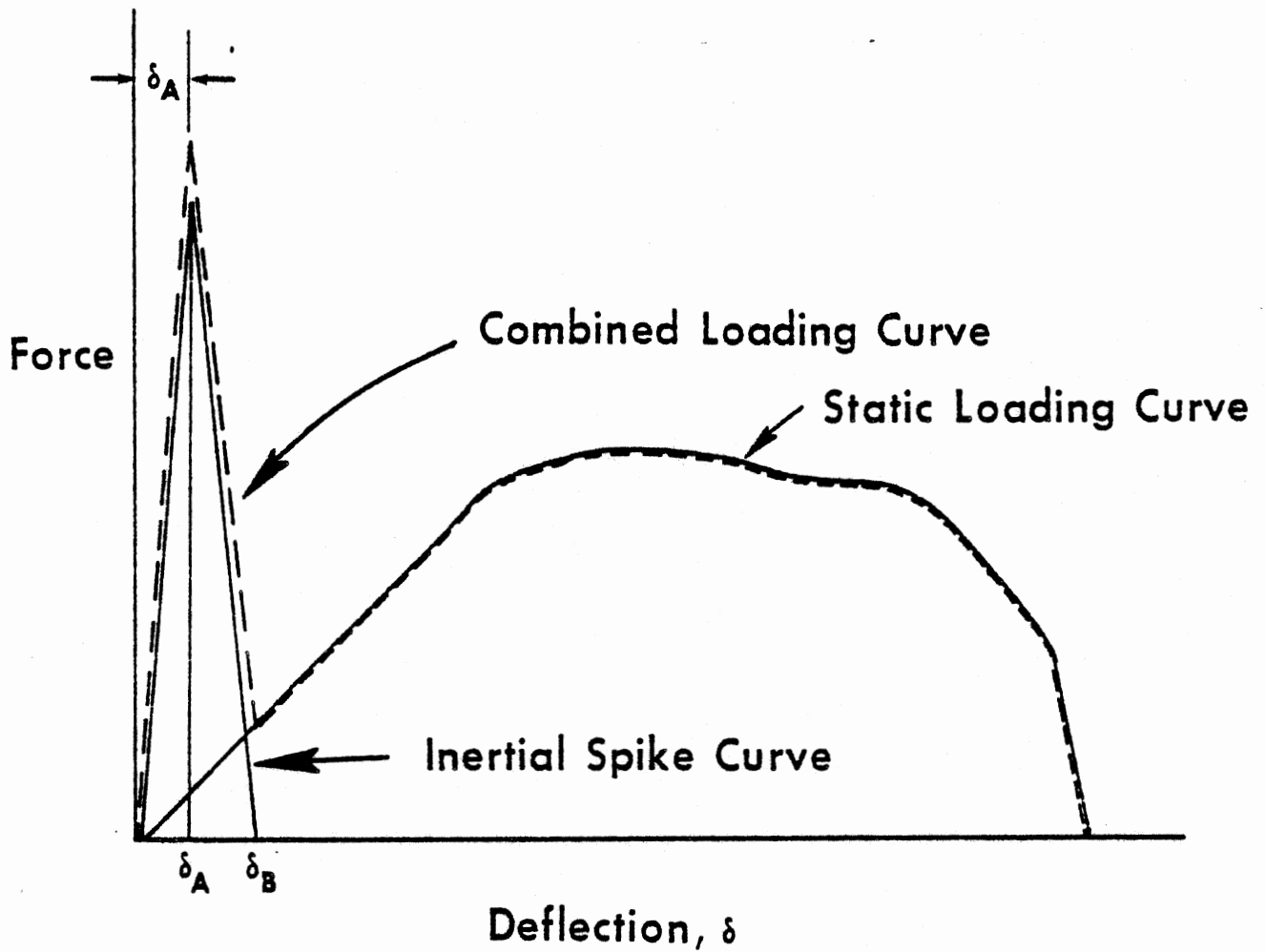
$\delta_F$  = end of breakdown curve

FIGURE 6-8 Static Loading Curve

SLIDE 6-1-5



Three points pertinent to continued static loading are shown on the figure as deflections  $\delta_C$ ,  $\delta_D$ , and  $\delta_F$ , all user-defined input parameters.  $\delta_C$  is the deflection at the material yield point, or "elastic limit." Note that it is not identified with the limit of material linearity. Its proper definition relates to characteristics of the material in unloading. Unloading from peak deflections less than  $\delta_C$  are backward along the loading curve, that is, they occur without permanent deformation of the material and without energy loss. There are no restrictions on  $\delta_C$  except that it be greater than or equal to zero. The deflections  $\delta_D$  and  $\delta_F$  relate to material, or structural, breakdown. All points on the user-defined static loading curve beyond  $\delta_D$  are ignored by the computer model. This value is the deflection at which the material begins to fail. Continued loading to  $\delta_F$  or beyond will complete breakdown of the material, as illustrated in the figure.



$\delta_A$  = deflection at peak of inertial spike curve

$\delta_B$  = deflection at cutoff of inertial spike curve

FIGURE 6-9 Inertial Spike Curve

SLIDE 6-1-6

## SLIDE 6

The so-called "inertial spike curve" is a model feature which can be used to account for dynamic effects on the force-producing capability of a material. This is the only model feature through which mass- and rate-dependence of material properties can be represented, even indirectly. It is observed that initial impact against a deforming surface is sometimes accompanied by a high force spike which diminishes rapidly with increasing deflection and which does not reappear with repeated loadings. Such an inertial spike force can be specified by the user as a tabular or polynomial function of deflection. This curve is added to the static load-deflection curve previously discussed.

The figure illustrates an inertial spike curve and the combined loading curve. Values for  $\delta_A$  and  $\delta_B$  in the figure are supplied by the user.  $\delta_A$  is the deflection at which inertial effects of the surface break down irreparably. This means that once deflection exceeds  $\delta_A$ , subsequent re-loadings from deflections less than  $\delta_A$  will be along the static curve, not the combined curve.  $\delta_B$  is the deflection at which all inertial effects cease.

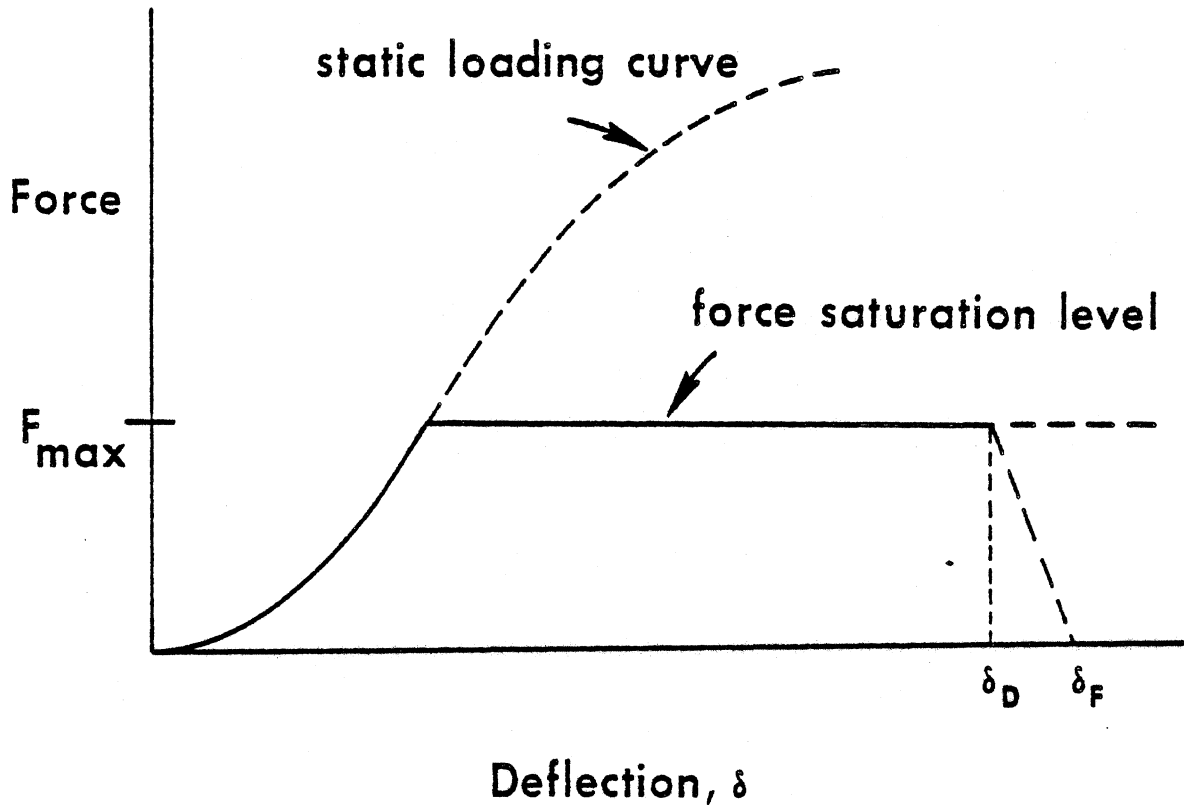


FIGURE 6-10 Static Loading Curve with Force Saturation

SLIDE 6-1-7

## SLIDE 7

This slide illustrates a loading curve for an element which deforms plasticly once the load has reached a specific value. The force saturation level is at load  $F_{\max}$ , an input parameter. Whenever the saturation force limit is exceeded by the static curve, the regular loading sequence is superceded. Force saturation affects only static loading. The inertial spike curve is unaffected. If loading is on the combined static and inertial spike curve when  $F_{\max}$  is reached, only the static component will be limited to  $F_{\max}$ .

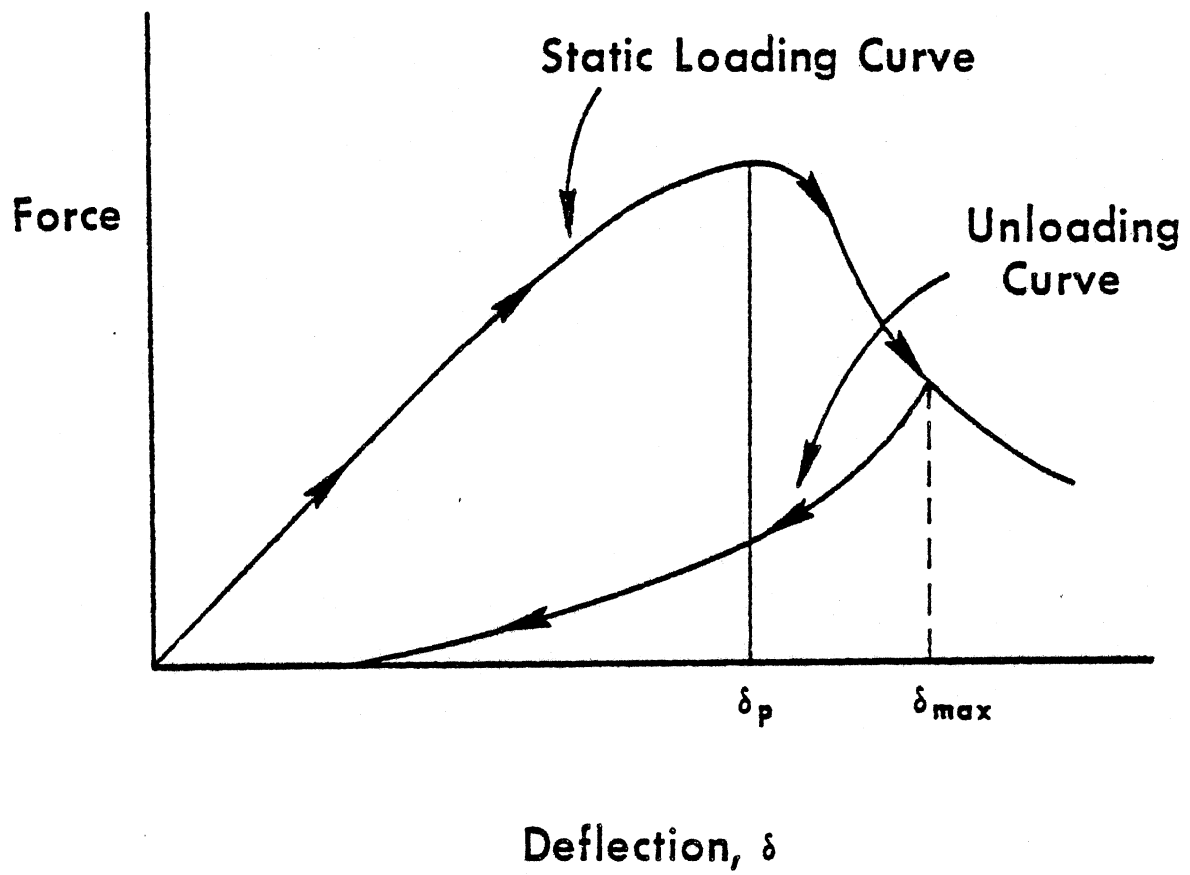


FIGURE 6-11 Unloading From Deflections Greater Than  $\delta_p$

SLIDE 6-1-8

6/28/79

## SLIDE 8

An element is undergoing "unloading" whenever its material deformation is decreasing with time. While it is not necessarily true that force increases with deflection in a loading material, the decreasing deflection for unloading of a reasonably specified material will be accompanied by decreasing force. The figure illustrates the loading curve for a material which surely requires hysteretic unloading specifications because unloading back along the loading curve from any deformation which exceeds  $\delta_p$  would involve force increase for decreasing deflection. Unloading curves are calculated by the computer model from user-prescribed specifications. These will be explained after one additional point is made from this figure.

$\delta_c$ , the deflection at the material "elastic limit," was discussed earlier in this module. If material deflection once exceeds  $\delta_c$ , then any subsequent unloading will not be back along the loading curve but instead will be along a curve which lies below the loading curve. It is noted in connection with the figure that, while there are no restrictions on the user-supplied value for  $\delta_c$ , it cannot reasonably be greater than  $\delta_p$  for a material with a loading peak as illustrated.

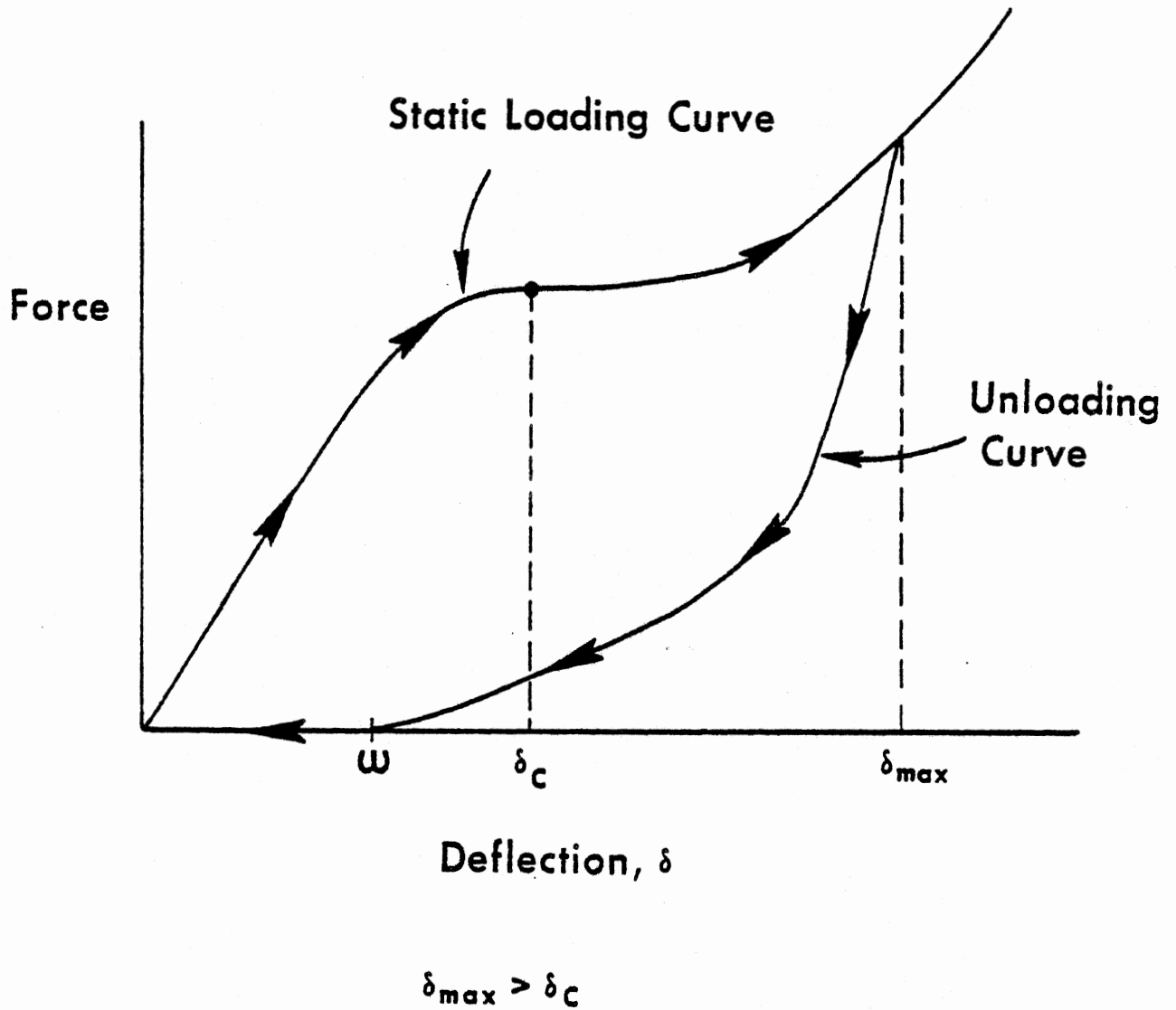


FIGURE 6-12 Unloading With Permanent Deformation from Deflections Greater Than  $\delta_c$

SLIDE 6-1-9



SLIDE 9

This figure illustrates unloading from a turnaround deflection  $\delta_{\max}$  greater than  $\delta_c$ . On complete unloading from beyond the elastic limit, the force usually returns to zero before the deflection. In other words, there is usually a permanent deformation of the surface, represented in the figure by the deflection  $\omega$ . In general, the permanent deformation increases with increasing turnaround deflections.

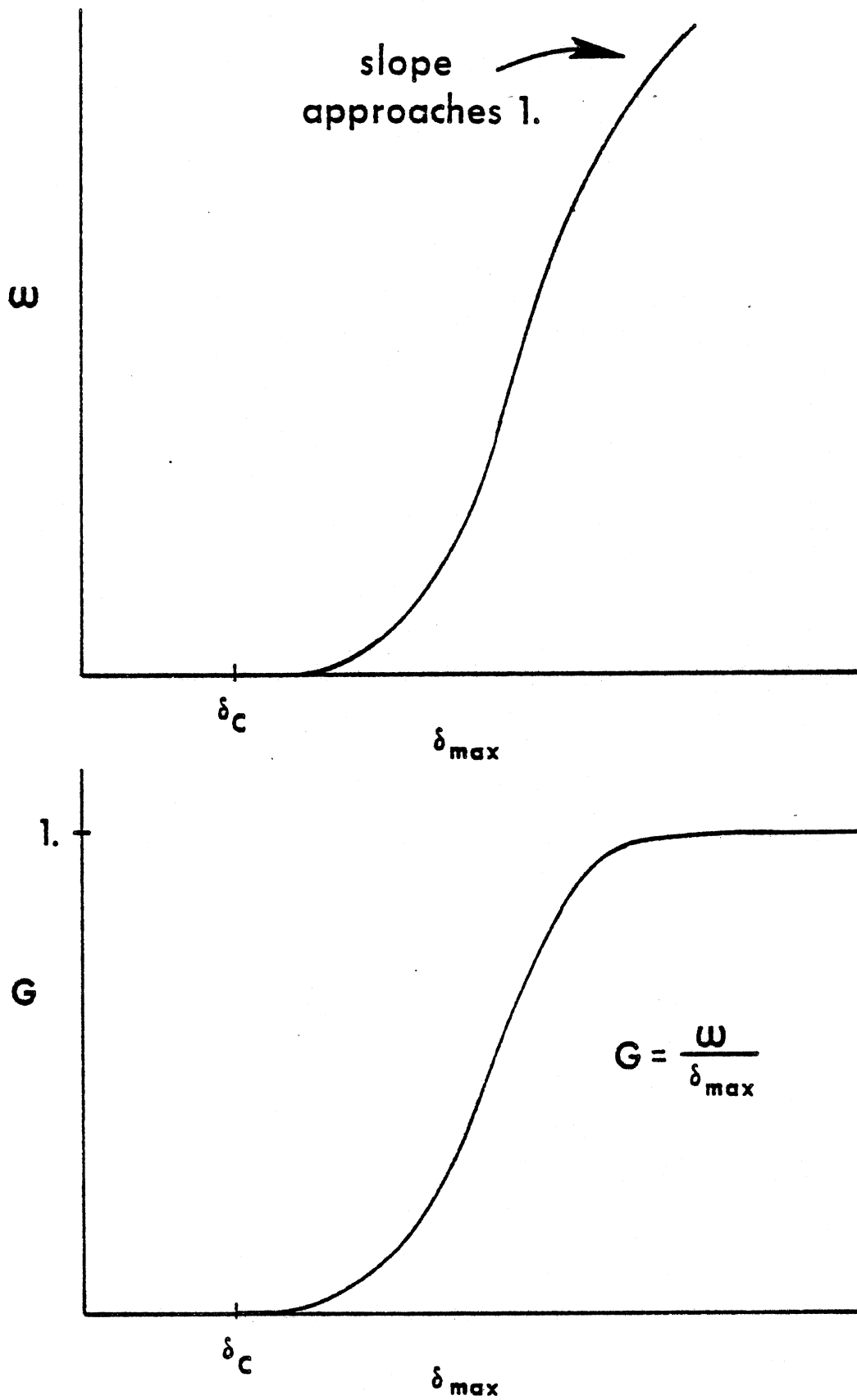


FIGURE 6-13 Permanent Deformation  $\omega$  and G-ratio As Functions of Maximum Deflection

SLIDE 6-1-10

## SLIDE 10

The upper portion of the next figure illustrates the typical dependence of permanent deformation on deflection. For deflections up to the elastic limit, the permanent deformation is zero. As deflection increases without bound, the permanent deformation approaches the value of the turnaround deflection. This characteristic of the material is illustrated in a completely equivalent way in the lower figure. The lower curve is simply the upper curve divided by deflection, point for point. That is, the lower curve defines, as a function of  $\delta_{\max}$ , a non-dimensional ratio of the permanent deflection to the turnaround deflection. This function is zero for deflections up to the elastic limit and approaches 1. as  $\delta_{\max}$  increases without bound. The function has been called the "G-ratio," and in the MVMA 2-D model it is a user-supplied input for each material. It may be entered in tabular form or it may be assigned a constant value. It should be noted, however, that a constant can be used with safety only if there are a priori reasons to expect a particular approximate maximum deflection of the material for the specific crash simulation. The reason for this is that for most materials the G-ratio changes rapidly with increasing deflection past the yield point.

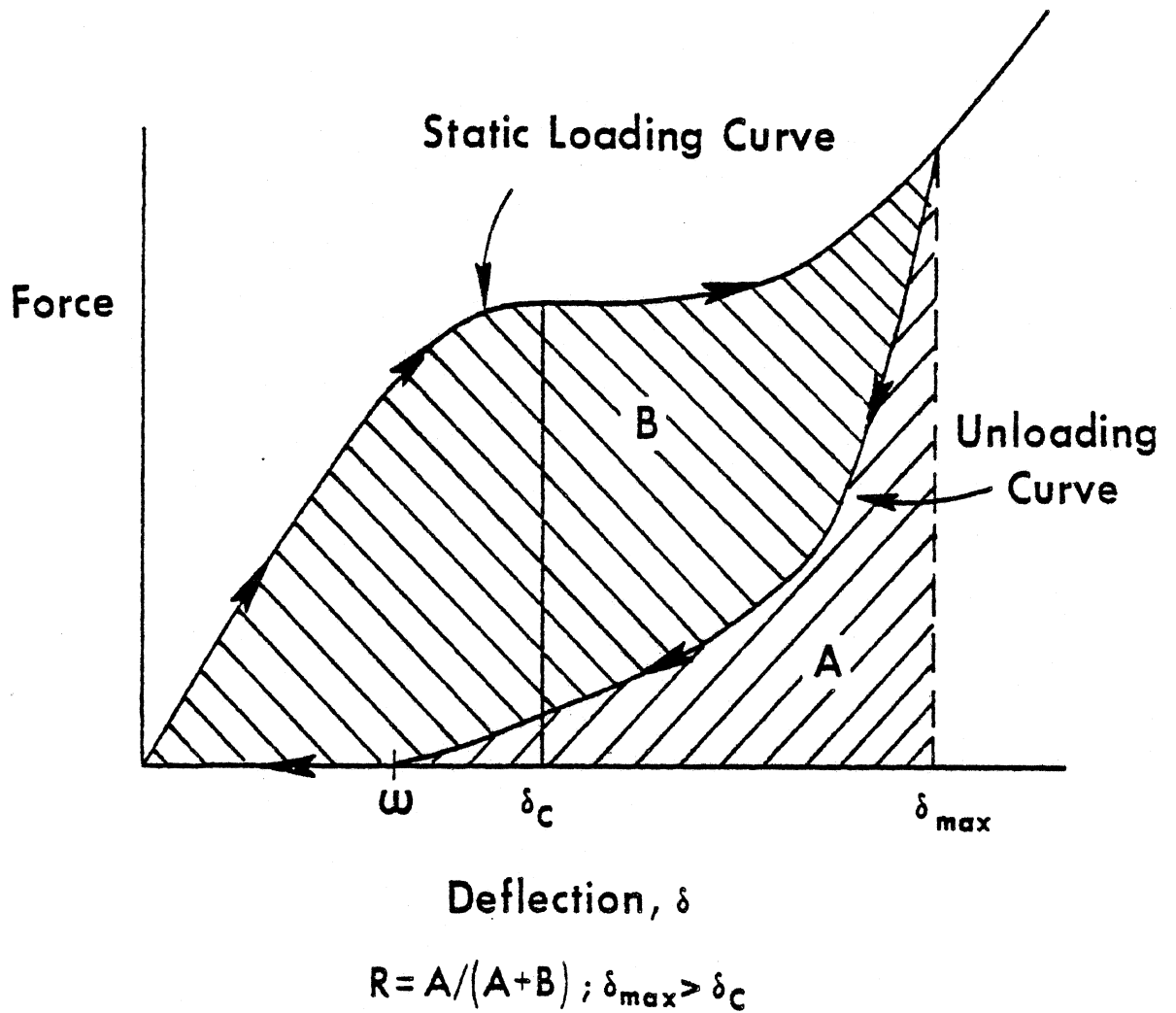


FIGURE 6-14 Unloading with Energy Loss from Deflections Greater Than  $\delta_c$

SLIDE 6-1-11

## SLIDE 11

This slide again illustrates an example loading-unloading cycle. Since the integral to  $\delta_{\max}$  of the force times an incremental deflection, namely, the area under the static loading curve, is the work done in reaching the turnaround deflection,  $\delta_{\max}$ , unloading along a curve which lies under the loading curve means that there is a hysteretic energy loss. Energy is absorbed by heating or by mechanical breakdown of the material. In the figure, area B equals the absorbed energy. Area A is the restored, or conserved, energy. Just as permanent deformation is in general a function of turnaround deflection, so is the amount of energy restored upon complete unloading. For each material, a nondimensional ratio of restored energy to total loading energy can be defined in parallel to the G-ratio for permanent deformation. This quantity is called the "R-ratio" and it is clearly a function of turnaround deflection, namely the ratio of area A to the sum A plus B, where A and B are both functions of the turnaround deflection. The model user supplies the R-ratio either as a tabular function of  $\delta_{\max}$  or as a constant. The next slide illustrates the typical dependence of the R-ratio on  $\delta_{\max}$ .

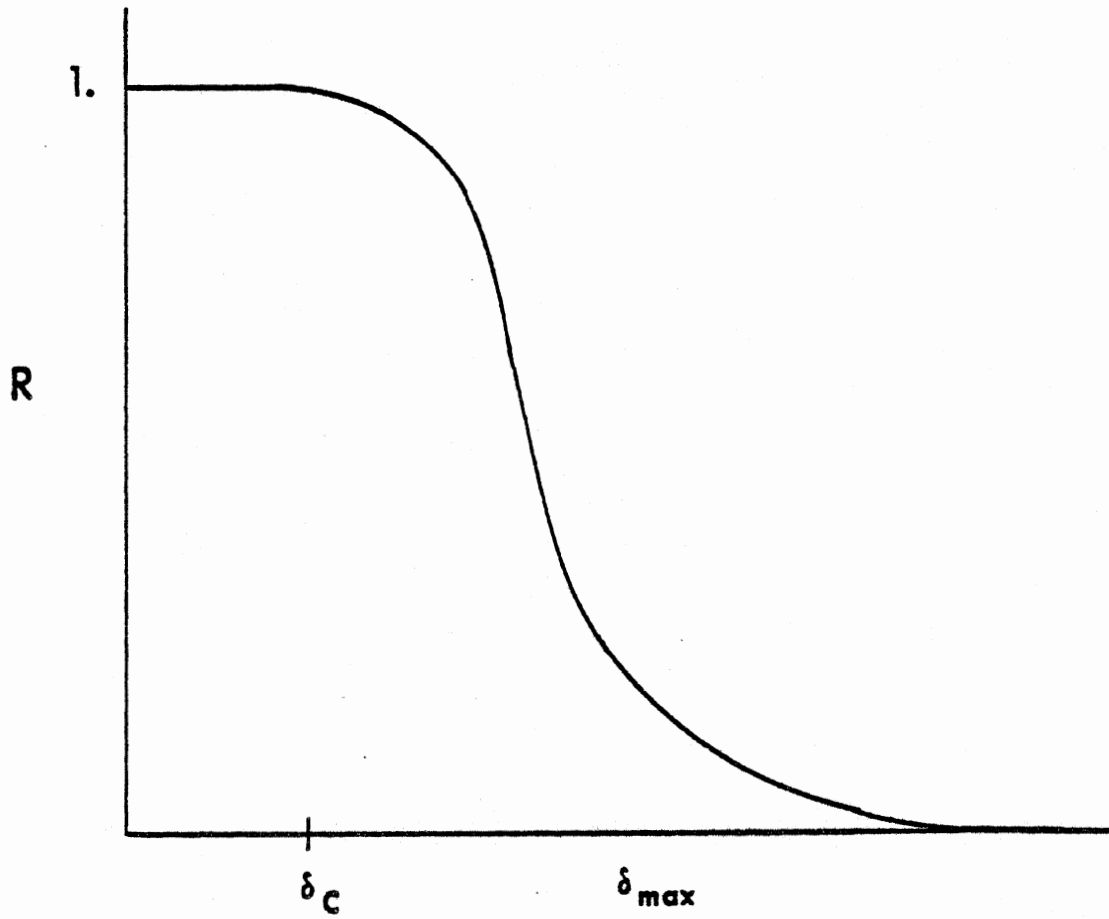


FIGURE 6-15 R-ratio as a Function of Maximum Deflection

SLIDE 6-1-12

## SLIDE 12

The R-ratio is used together with the G-ratio by the computer model for calculating an unloading curve whenever unloading from a deflection greater than  $\delta_c$  begins. The unloading curve is normally quadratic in form, and its coefficients are determined so that unloading occurs with the appropriate permanent deformation and restored energy. Strictly, the G- and R-ratios are not independent quantities as there exists a constraint between their values. This is discussed in Module 6, Part 2.

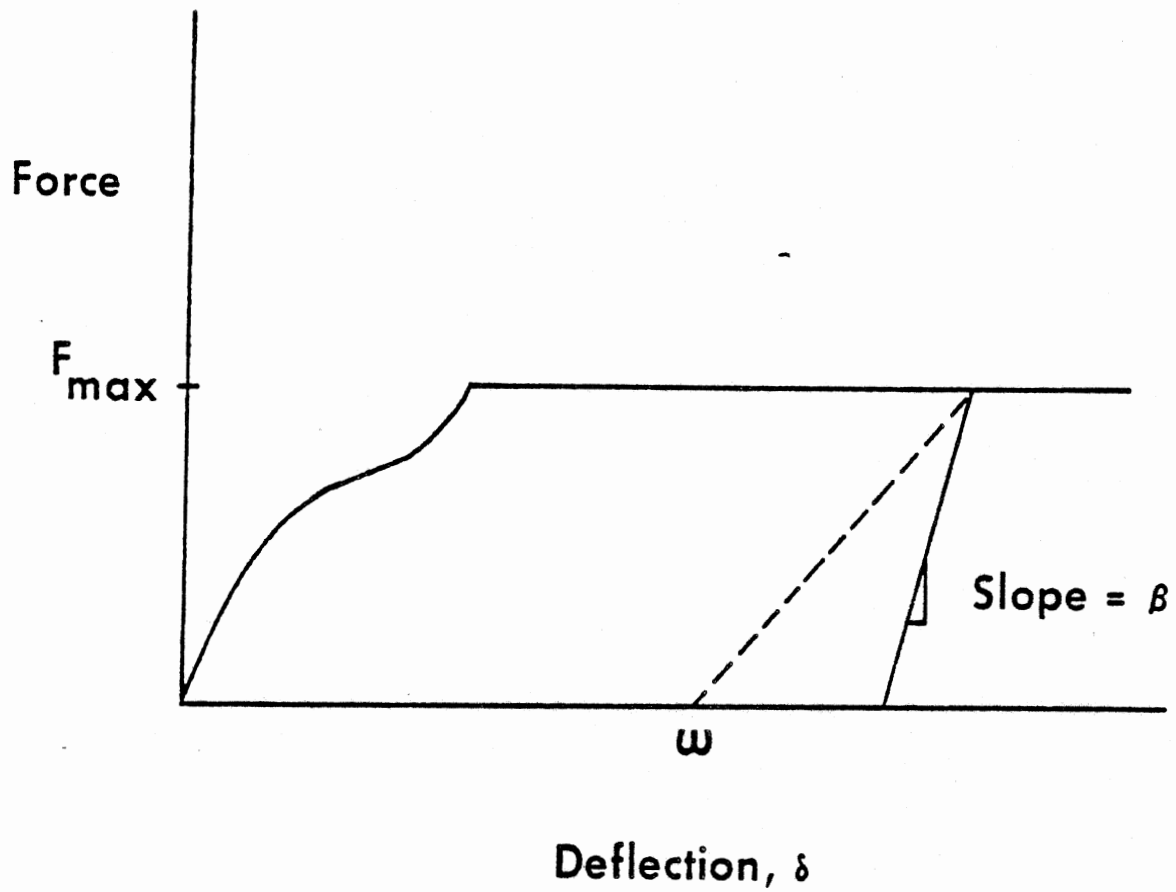


FIGURE 6-16 Unloading from Force Saturation

SLIDE 6-1-13



SLIDE 13

Either of two types of unloading from a force-saturation level can be specified by the model user. Both are illustrated in this figure. The standard method is to unload with a specified slope,  $\beta$ , an input parameter. Alternatively, the G-ratio is used to determine a permanent deformation, to which unloading occurs along a straight-line segment.

## SUMMARY OF DATA REQUIREMENTS FOR MATERIAL SPECIFICATIONS

- Tabular or polynomial static loading curve
- Tabular or polynomial inertial-spike loading curve
- Deflections at the material yield point and beginning and end of material breakdown
- Force saturation level and unloading slope
- G-ratio for permanent deformation as a function of turnaround deflection
- R-ratio for restored energy upon unloading, as a function of turnaround deflection

SLIDE 6-1-14

## SLIDE 14

The subject of this module has been the loading and unloading characteristics of elements of the occupant profile, the vehicle-interior profile, and the belt restraint systems. While any such element may be specified as rigid if desired, material specifications should always be made for deformable elements if data are available. Static and inertial-spike loading curves are prescribed, together with associated parameters such as the yield-point deflection and deflections at the beginning and end of material breakdown. An optional force saturation level may be specified independently. Hysteretic unloading characteristics are specified by the user by G- and R-ratios, from which permanent deformation and conserved energy can be calculated as functions of maximum deflection.



**MVMA 2-D**  
**CRASH VICTIM SIMULATION**

**\* \* \***

**MODULE 6**

**GENERATION OF CONTACT FORCES**  
**ON THE OCCUPANT:**

**PART 2**

**MVMA 2-D  
CRASH VICTIM SIMULATION**

**\* \* \***

**MODULE 6**

**GENERATION OF CONTACT FORCES  
ON THE OCCUPANT:**

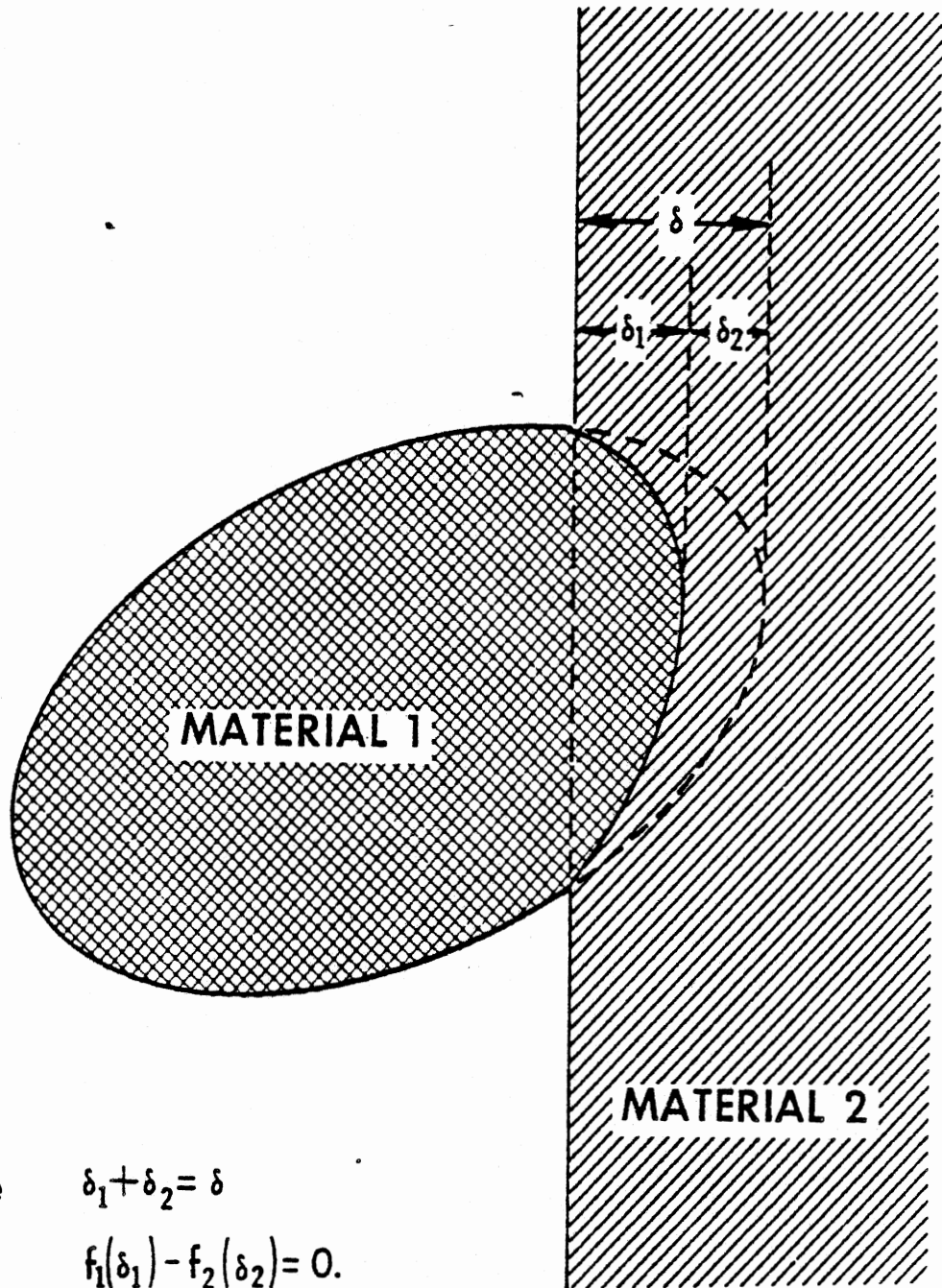
**PART 2**

**SLIDE 6-2-1**

MODULE 6 -- GENERATION OF CONTACT FORCES ON THE OCCUPANT: Part 2

SLIDE 1

Part 1 of Module 6 deals primarily with the definitions of deflections and material properties of elements of the occupant profile and the vehicle-interior profile. Part 2, which follows, deals with various features of the algorithms in the MVMA 2-D model which generate occupant contact forces.



Solve  $\delta_1 + \delta_2 = \delta$   
 $f_1(\delta_1) - f_2(\delta_2) = 0$ .

Then,  $F = f_1(\delta_1) = f_2(\delta_2)$ .

FIGURE 6-18 Mutual Deformation of an Ellipse and a Line

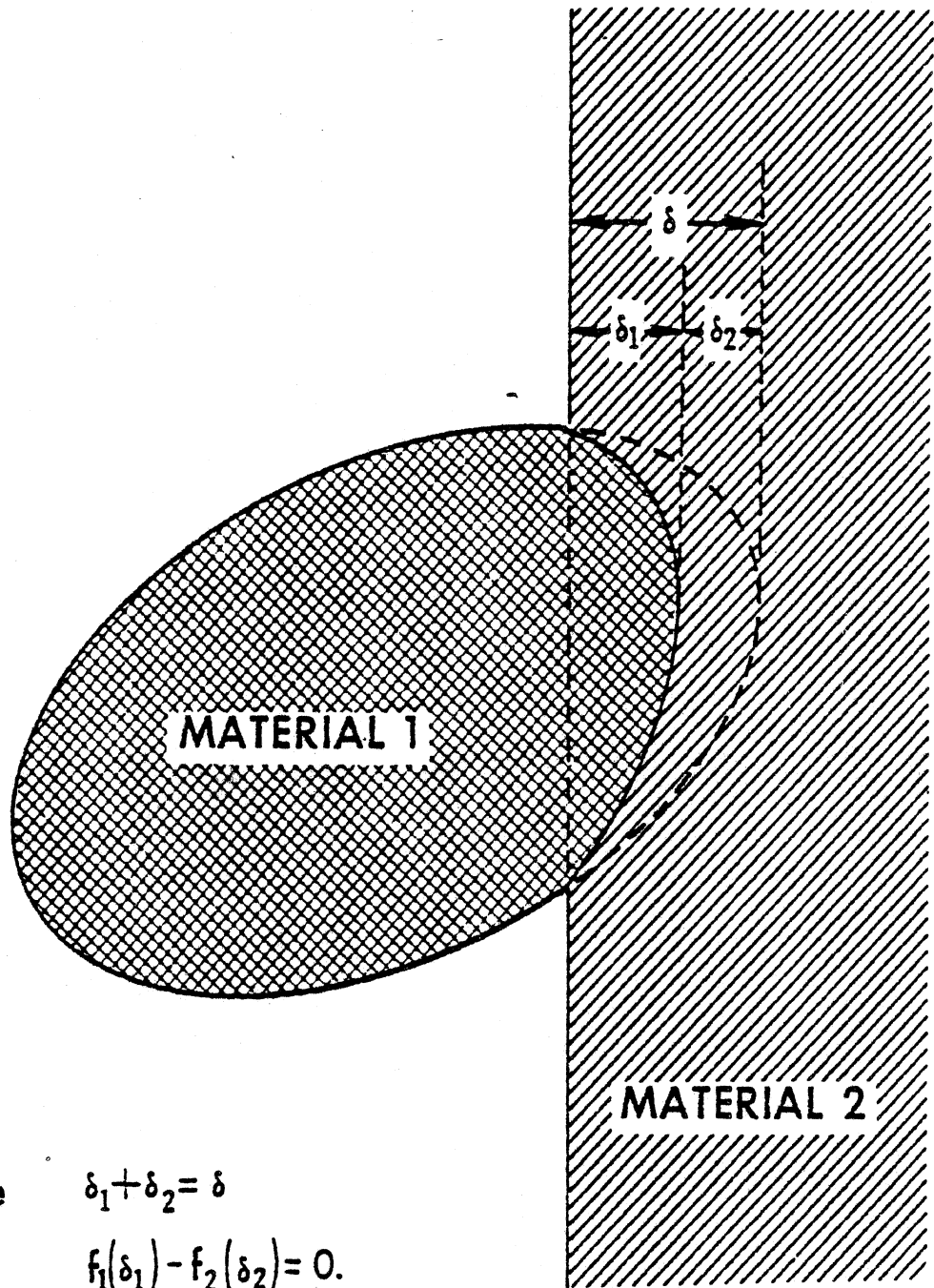
SLIDE 6-2-2



## SLIDE 2

Whenever two deformable elements contact each other, both will deform. In the MVMA 2-D model, this is called "shared deflection" or "mutual deformation." The figure illustrates such an interaction for an ellipse and a line segment. Interacting ellipses could be considered just as well. Given only the position of the ellipse and the position of the line, the total deflection  $\delta$  is determined. The component deflections  $\delta_1$  and  $\delta_2$ , however, depend on the material properties of the interacting elements. The compressive forces in the elements will be equal. In order to determine the interaction force, the computer model solves the equations shown with the figure for  $\delta_1$  and  $\delta_2$ . The total deflection  $\delta$  is a known value at each instant of time.  $f_1$  and  $f_2$  are the functional relationships between force and deflection for the two materials, specified by the user in polynomial or tabular form as explained in Module 6, Part 1.

The solution algorithm involves an iterative procedure, and it requires five control values specified by the user. Two are convergence epsilons,  $\epsilon_1$  and  $\epsilon_2$ , one for each material. The force balance is considered to be good enough when  $f_1(\delta_1)$  is within  $\epsilon$  of  $f_2(\delta_2)$ , where  $\epsilon = \min\{\epsilon_1, \epsilon_2\}$ . Other values required are for the maximum and minimum allowed trial adjustments of the component deflection values at any iteration step and the maximum number of deflection adjustments allowed for finding force balance at any time step. Guidance in choosing values for these parameters is provided in the text for this module.



Solve  $\delta_1 + \delta_2 = \delta$   
 $f_1(\delta_1) - f_2(\delta_2) = 0.$

Then,  $F = f_1(\delta_1) = f_2(\delta_2).$

FIGURE 6-18 Mutual Deformation of an Ellipse and a Line

SLIDE 6-2-2

It is important to keep in mind that forces for contacts of the occupant with the vehicle interior can be influenced significantly by the force-deflection characteristics of the portion of the body involved. Very often users of crash simulation models concern themselves only with the force-deflection characteristics of elements of the vehicle interior and use rigid contact ellipses or circles on the occupant. This invariably results in effective stiffnesses for occupant-interior interactions that are too large. Consequently, resulting model predictions of peak forces and G-levels are generally too high. Both materials for an interaction should be defined whenever data are available unless one is considerably softer than the other. In this case, the stiffer element, whether ellipse or line, may reasonably be specified as rigid.

The definition of deflection for a contact interaction has been given in Module 6, Part 1. An explanation was also given of material specifications from which a contact force can be determined when deflections and deflection histories are known. This slide illustrates a contact interaction between two deformable bodies, and the means by which the contact force is determined in such a case has been outlined.

Nothing has yet been said about the precise circumstances under which a force will be calculated. That is, when is a contact interaction considered to have taken place?

Only the interaction between an ellipse and a line needs to be discussed. One obvious requirement for production of a contact force by the simulation model is that there be a positive relative displacement between the ellipse and the line. A non-zero force should clearly be determined for the deflection  $\delta$  shown in the figure.

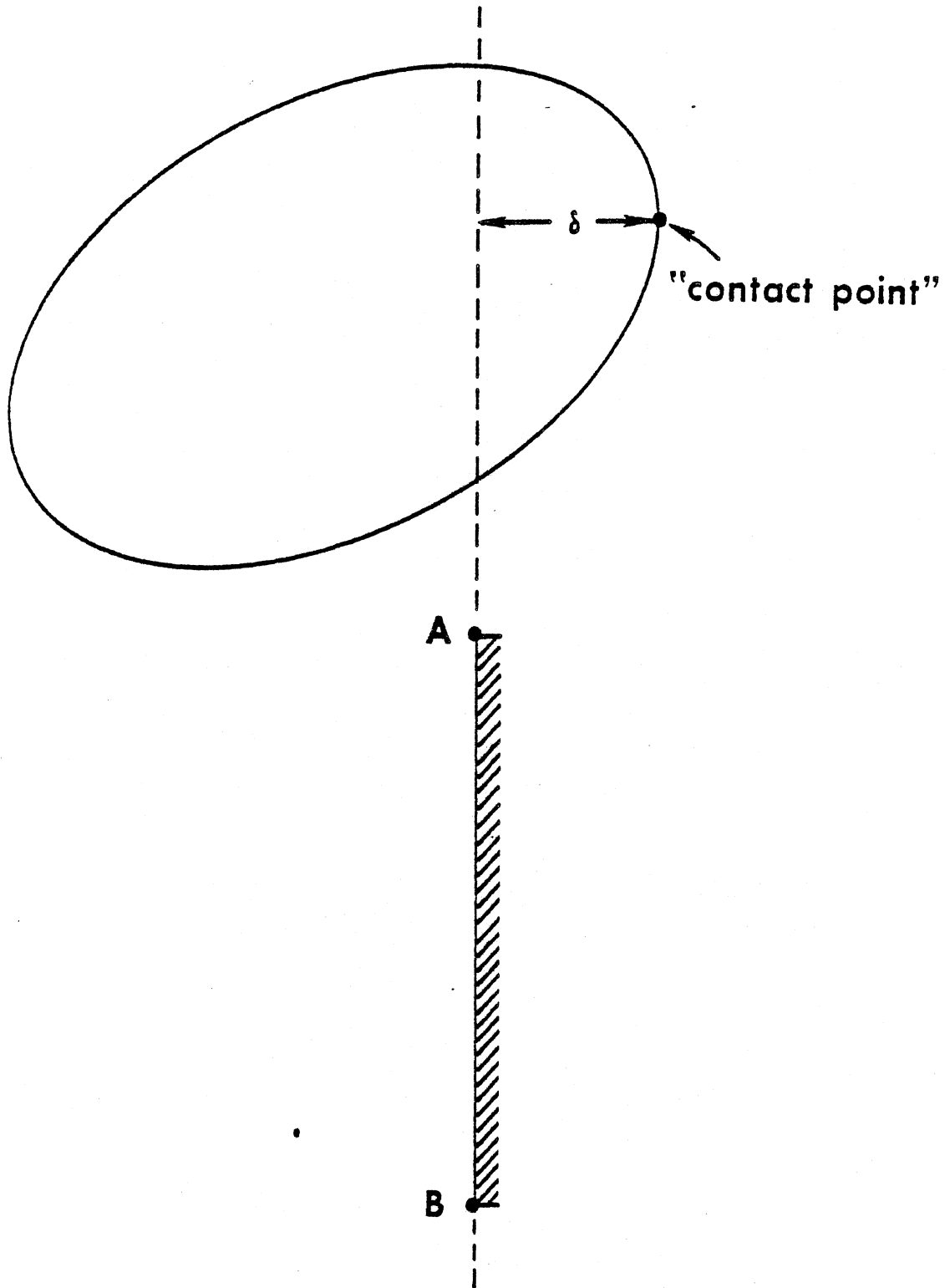


FIGURE 6-19 An Ellipse Which Misses a Line Segment to the Side

SLIDE 6-2-3

### SLIDE 3

This slide illustrates a case where the deflection  $\delta$ , as previously defined, is positive yet there should be no interaction force because the ellipse passes to one side of the line segment. It is obviously necessary to consider not only deflection against the extended line defined by the segment endpoints A and B but also the position of the ellipse relative to the endpoints themselves.

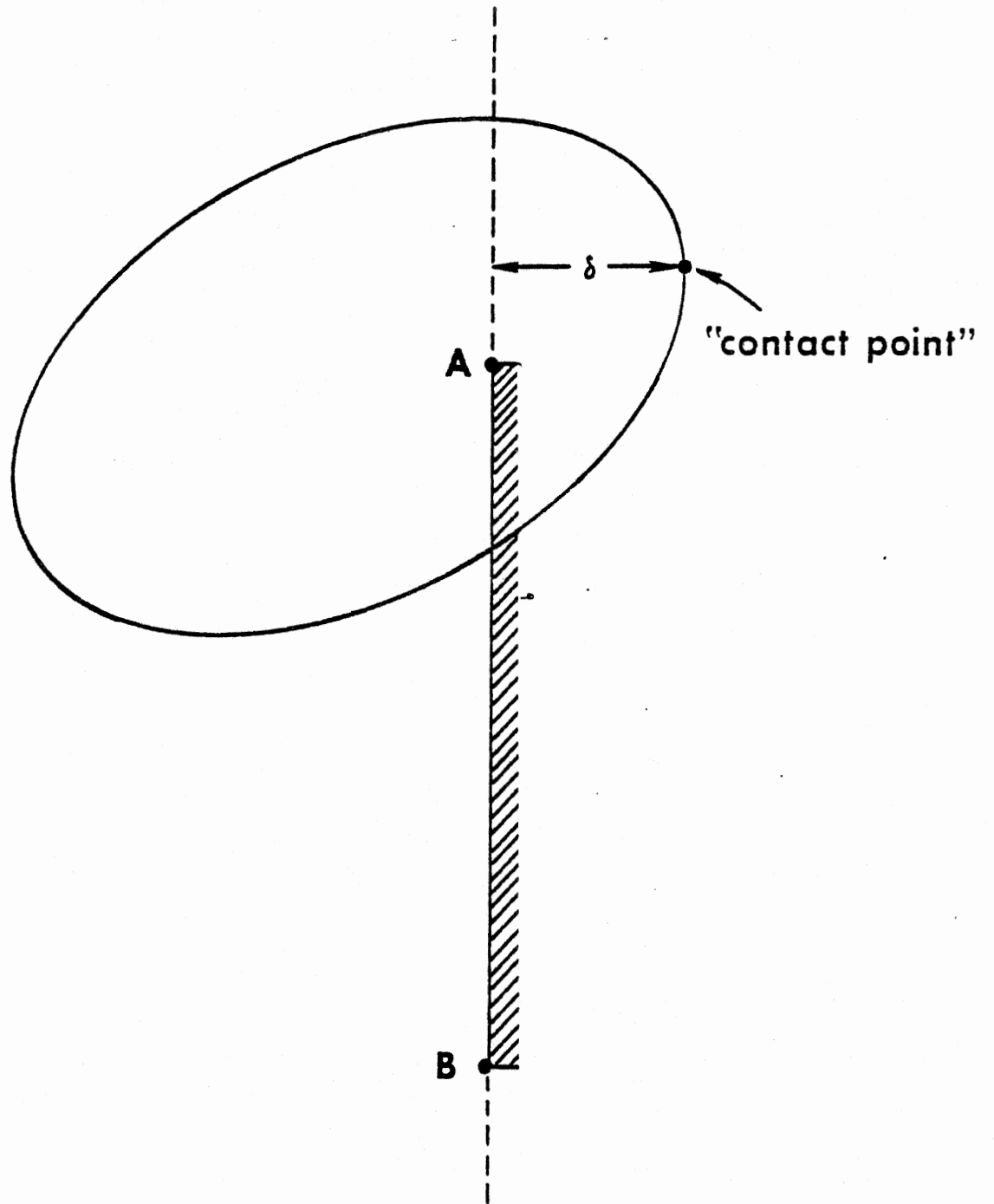
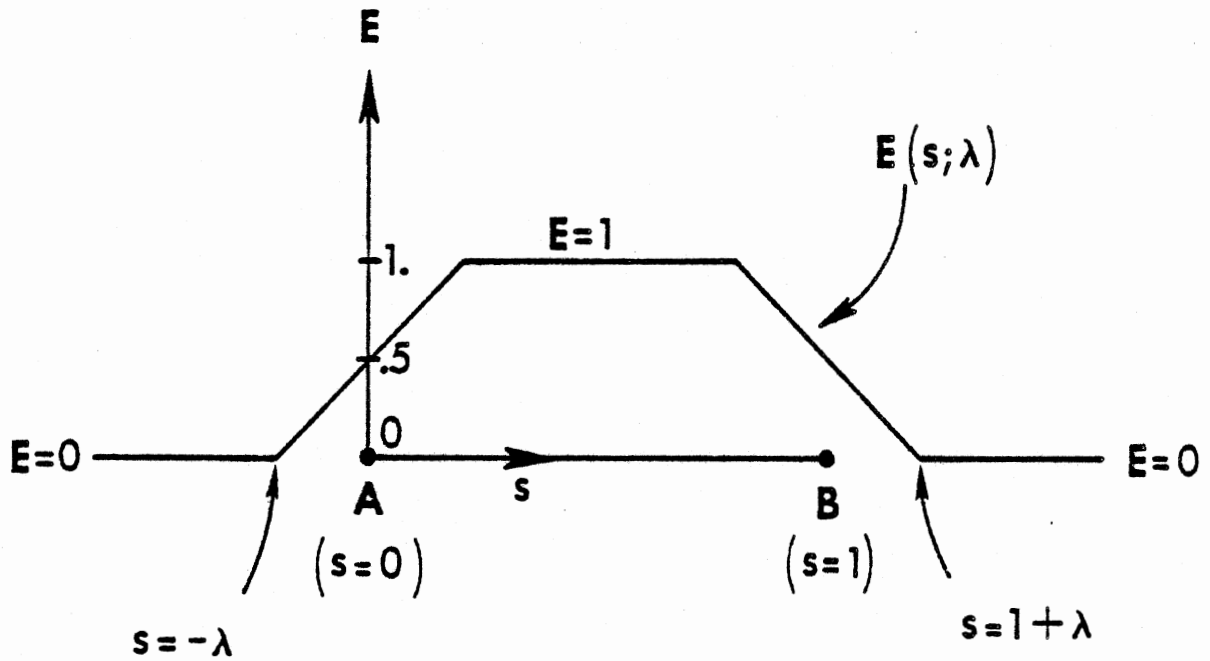


FIGURE 6-20 An Ellipse Contacting a Line Segment Near Its Edge

SLIDE 6-2-4

#### SLIDE 4

An intermediate condition is shown here. While the so-called "contact point" is beyond the endpoint A, still there is an apparent interaction between the ellipse and the segment and a means should be provided for estimating an appropriate force. If the ellipse in the figure were moved upward so that the contact point lay far beyond the edge of the line segment, a zero interaction force should clearly be predicted. Such a condition has already been illustrated in the previous slide. If, on the other hand, the ellipse were moved downward so that the contact point lay halfway between the line-segment endpoints, then an interaction force appropriate for firm contact should be predicted. The model provides a means by which diminishing normal forces can be calculated as an ellipse moves from firm contact through intermediate positions such as illustrated in this figure to positions off the edge of the segment where forces become zero.



$$F_{\text{eff}} = EF(\delta)$$

FIGURE 6-21 Effectiveness Factor  $E$  as a Function of  $s$ , the Position of Contact Point with Respect to Line Segment, With Edge Constant  $\lambda$  as a Parameter

SLIDE 6-2-5



## SLIDE 5

The user supplies for each line segment a value for a parameter called an "edge constant." Whenever there is a positive relative displacement between an ellipse and the line, a so-called "effectiveness factor" is calculated for the interaction as a function of the edge constant and of the position of the contact point relative to the extent of the segment. The effective force is found by multiplying the deflection-dependent normal force determined from material properties by the effectiveness factor,  $E$ .

The definition of the effectiveness factor is illustrated by this slide. The figure shows  $E$  as a function of a non-dimensional coordinate called " $s$ ," which ranges from 0 to 1 as the position of the contact point varies from endpoint A of the line segment to endpoint B. The quantity  $s$  takes on negative values for contact point positions beyond endpoint B. The effectiveness factor is symmetric about the midpoint of the line segment, and it has the value 1 for contact point positions near the middle of the segment, that is, where ellipse contact with the segment is firm. Unit value for the effectiveness factor results in undiminished forces for contacts near the middle. The extent of the firm area of the segment is defined by the user-prescribed edge constant,  $\lambda$ , which is a parameter of the graph for  $E$ . The effectiveness factor increases linearly from 0 to 1 from a contact point position of non-dimensional distance  $\lambda$  beyond an endpoint to a position of distance  $\lambda$  within the endpoint. Thus, the effectiveness factor is always .5 for contact precisely at an endpoint, and the effective force is zero for any contact beyond an endpoint by a non-dimensional distance greater than  $\lambda$ .

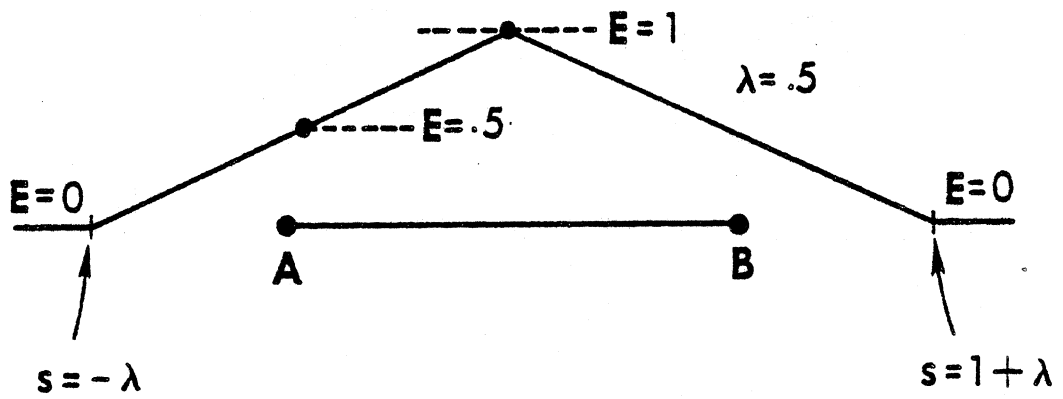
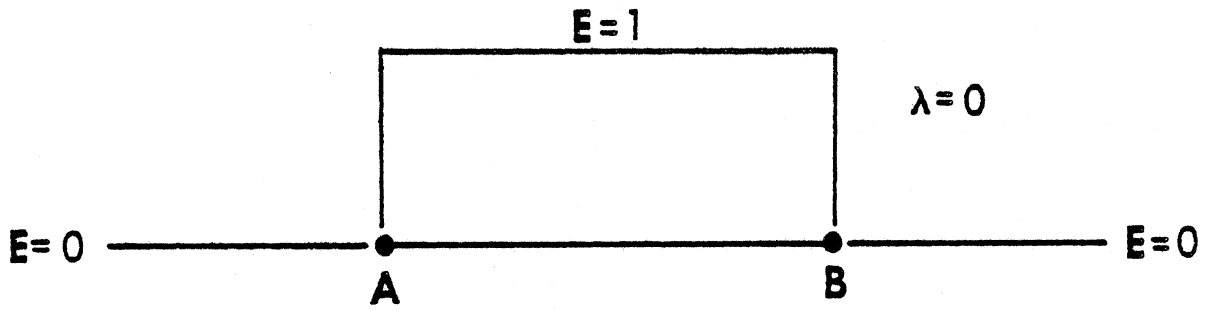


FIGURE 6-22 Effectiveness Factors for Edge Constant Values of 0. and .5

SLIDE 6-2-6

## SLIDE 6

The two extreme forms of the effectiveness factor are illustrated here. In the upper figure, for an edge constant of 0, an undiminished force results for all contacts within the segment endpoints, but the effective force is zero for any contact beyond an endpoint. In the lower figure, the surface softens away from the center. The user prescribes an edge constant value for each line segment of the vehicle interior. Each edge constant must be from 0. to .5.

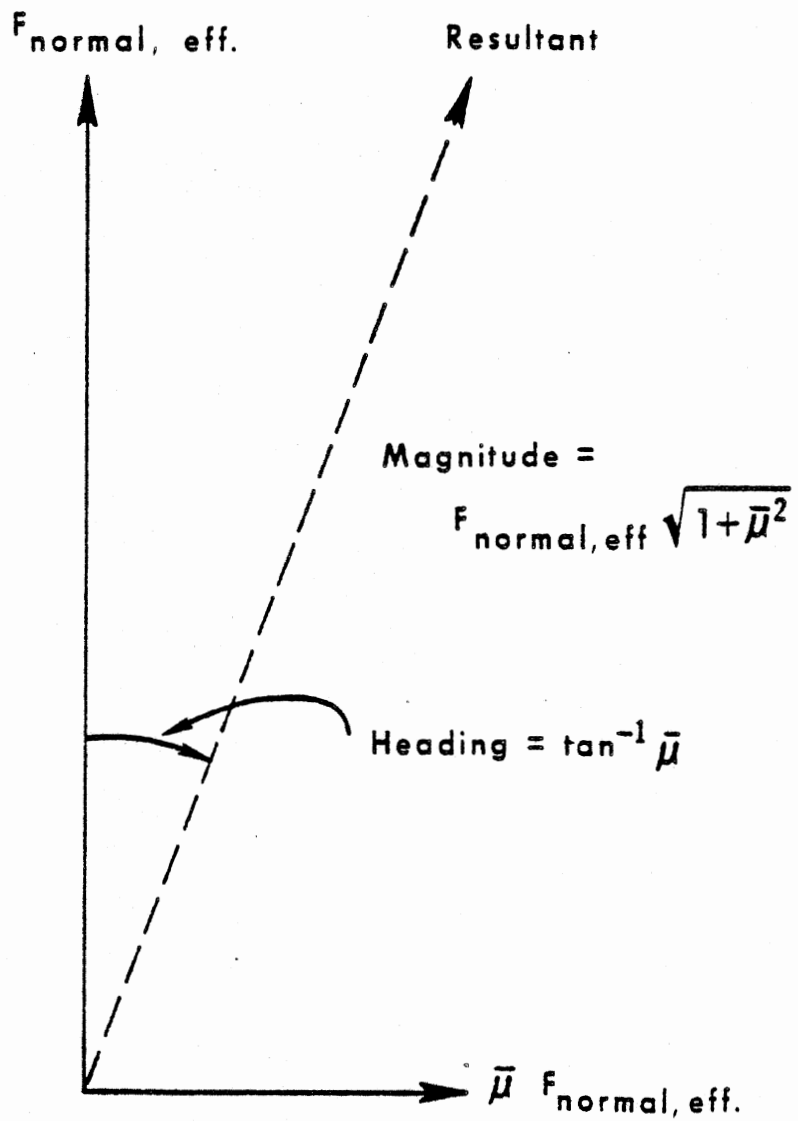


FIGURE 6-23 Resultant Interaction Force Vector For Friction Coefficient  $\bar{\mu} = .4$ : Resultant =  $1.08 F_{\text{normal}}$ , Heading =  $21.8^\circ$

SLIDE 6-2-7

## SLIDE 7

In addition to a force component normal to the contact surface, the interaction force vector includes a friction component parallel to the surface for interactions between an ellipse and a line. This component is determined as the product of a user-defined coefficient of friction and the effective normal force resulting from edge-factor adjustment. The figure illustrates the friction force as the horizontal component of the resultant force vector.

Modeling of friction should not be neglected by the user since it can sometimes significantly affect results. Friction coefficients for interactions within the occupant compartment are typically in the range .25 to .75. The figure is proportioned for a coefficient value of .4 and shows that while the magnitude of the resultant force vector may be very little different from the normal component alone, the direction of the resultant may be significantly different.

In the MVMA 2-D model, friction coefficients are defined not for materials but rather for pairings of "classes" of potentially interacting ellipses and regions. For example, a seat back and a seat cushion might be of the same region friction class if they are covered with the same fabric. On the otherhand, the head and foot ellipses would likely belong to different ellipse friction classes because of different surface characteristics. Each region of the vehicle interior is assigned to one of ten friction classes. Ellipses are similarly assigned to one of five ellipse friction classes. Thus, up to 50 combinations of ellipse and region classes can be assigned friction coefficients. Friction coefficients may be constant or they may be specified as polynomial functions of deflection in order to represent "plowing" at the ellipse-region interface.

- **Small values, 0.1 or less, are appropriate for the energy restitution coefficient ( R-ratio) for most biological tissues.**

**SLIDE 6-2-8**

## SLIDE 8

As the user gains experience, improvement in modeling technique will result in more effective and more efficient simulation of the crash event. Points relevant to effective modeling procedure are made throughout the modules of the MVMA 2-D Tutorial System. The remaining slides and discussion of this module address modeling considerations that relate to contact forces and are largely miscellaneous.

The first point deals with assigning values for R-ratios, or energy restitution coefficients, for body ellipse materials. The energy restitution coefficient for soft biological tissues in general decreases rapidly as a function of deflection. While the appropriate value for zero deflection is 1., values of .1 or less are appropriate for peak deflections which might occur in a crash. This can be understood intuitively by considering a fall victim who lands on a concrete surface in a prone, face-down orientation from a fall height of ten feet. His bounce height divided by ten feet provides a rough estimate for an average overall R-ratio.

$$\omega = G(\delta_{\max}) \delta_{\max}$$

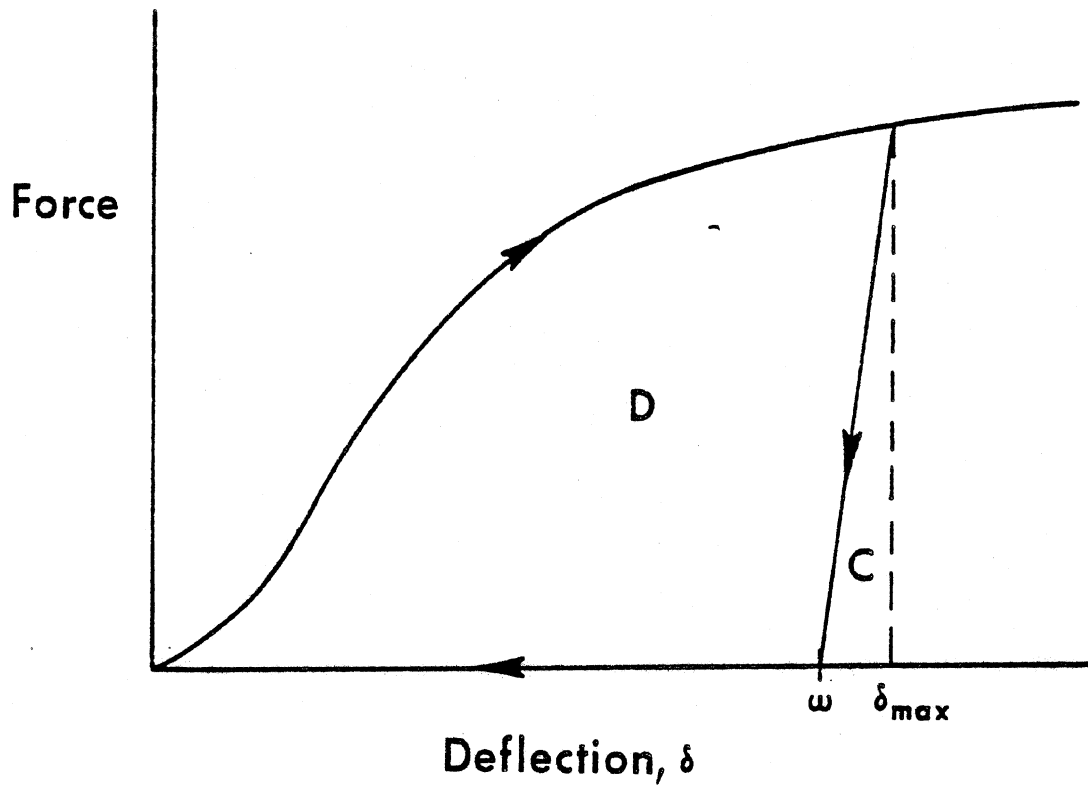


FIGURE 6-27 Maximum-Energy Unloading for a G-Ratio Near to 1.

SLIDE 6-2-9



## SLIDE 9

Second, while the user of the MVMA 2-D model is required to provide R-ratios and G-ratios separately for the calculation of unloading curves, they cannot in reality be independent. For example, a G-ratio near 1. can be consistent only with R-ratios near zero. This follows from the following argument and is illustrated by the figure.

Although an unloading curve for any combination of G and R values could be determined which would satisfy both the permanent deflection and restored-energy requirements, only concave-upward unloading curves are reasonable for deflections beyond the yield point. The straight-line unloading to  $\omega$  shown in the figure is thus the limit of reasonable curves. Since the area under the curve is maximized by straight-line unloading, the R-ratio for any value of maximum deflection should always be less than or equal to the energy ratio  $C/(C+D)$ . Since the area C approaches zero as  $\omega$  approaches  $\delta_{max}$ , that is, as the G-ratio approaches 1., the R-ratio must approach 0.

The user may occasionally specify incompatible G- and R-ratios for unloading from a particular loading curve. Should G and R be incompatible for some  $\delta_{max}$ , then the computer model will by default accept the G-ratio and unload to  $\omega$  on a straight-line curve, ignoring the R value. A warning is printed, and results will normally be reasonable, but the condition can be corrected if desired by reducing either G or R. Experience has shown that reducing G is generally better.

- (1)  $\delta_{\max}$  = maximum deflection
- (2)  $G = g(\delta_{\max})$  [G-ratio; input]
- (3)  $R = r(\delta_{\max})$  [R-ratio; input]
- (4)  $F_{\max} = f(\delta_{\max})$  [loading curve; input]
- (5)  $\omega = G\delta_{\max}$  [permanent deformation]
- (6)  $C = (\delta_{\max} - \omega) F_{\max}/2$  [area under straight line unloading]
- (7)  $A_L = C + D = a(\delta_{\max}) = \int_0^{\delta_{\max}} f(x) dx$   
[area under loading curve]
- (8)  $R \leq C/A_L$  for all  $\delta_{\max}$

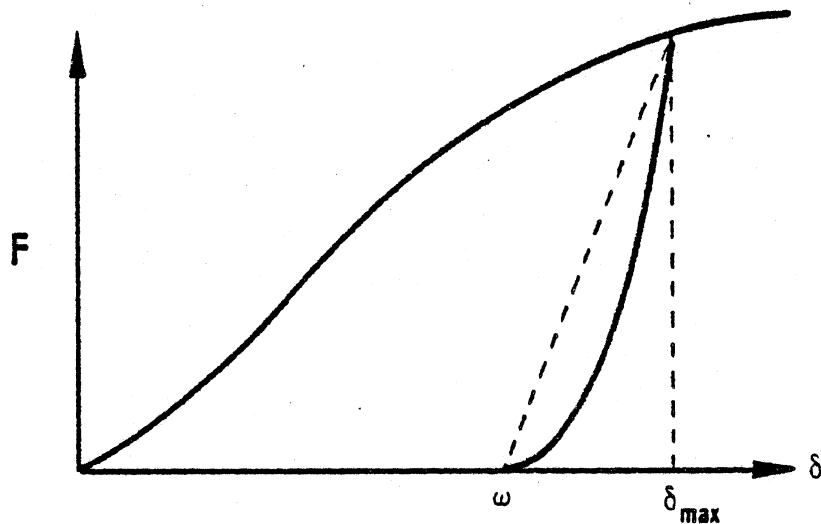
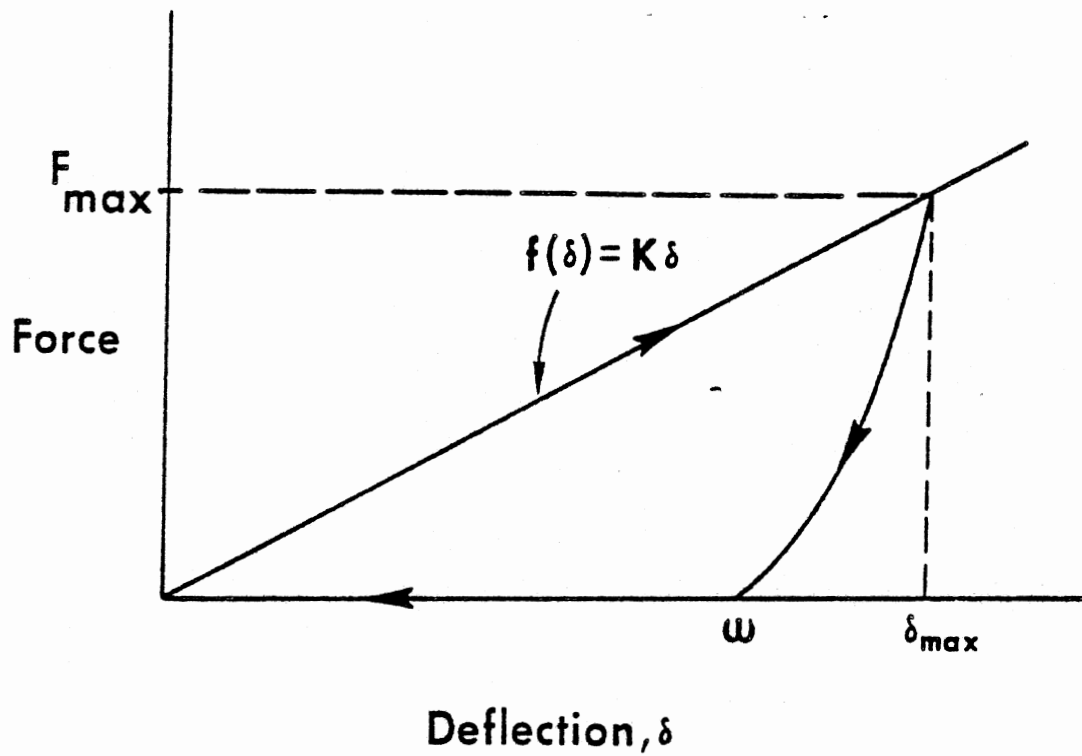


FIGURE 6-28 Determination of Compatibility of R-Ratio with a Specified G-Ratio

SLIDE 6-2-10

SLIDE 10

If the user wants to be entirely certain that G and R functions are compatible, it is necessary to verify that condition (8) on this slide is satisfied for all values of  $\delta_{\max}$ .



$$R(\delta_{max}) \leq 1 - G(\delta_{max})$$

FIGURE 6-29 G-R Compatibility Constraint for Constant Stiffness Loading Curve

SLIDE 6-2-11

SLIDE 11

A commonly used loading curve is one of constant slope, or stiffness. The curve for a stiffness  $K$  is illustrated here. It is easily demonstrated, for such a loading curve, that the inequality relating  $G$  and  $R$  which should be satisfied for all turnaround deflections  $\delta_{\max}$  is:  $R \leq 1 - G$ .

Various other modeling considerations pertinent to generation of contact forces are discussed in the text for this module; and one final point will be discussed here in some detail, but first an additional note might be made relative to  $G$ - and  $R$ -ratios.

It should be kept in mind that  $G$ - and  $R$ -ratios determined quasi-statically may be different from values appropriate for a dynamic interaction. If statically determined values are used, an implicit assumption is that the material is capable of responding instantaneously to changes in deflection, that is, that there is no dependence on rate of unloading. The degree to which static and dynamic values differ depends, of course, on the material, but in general, the  $G$ -ratio will be larger and  $R$  smaller for fast unloading, such as would occur in a crash.

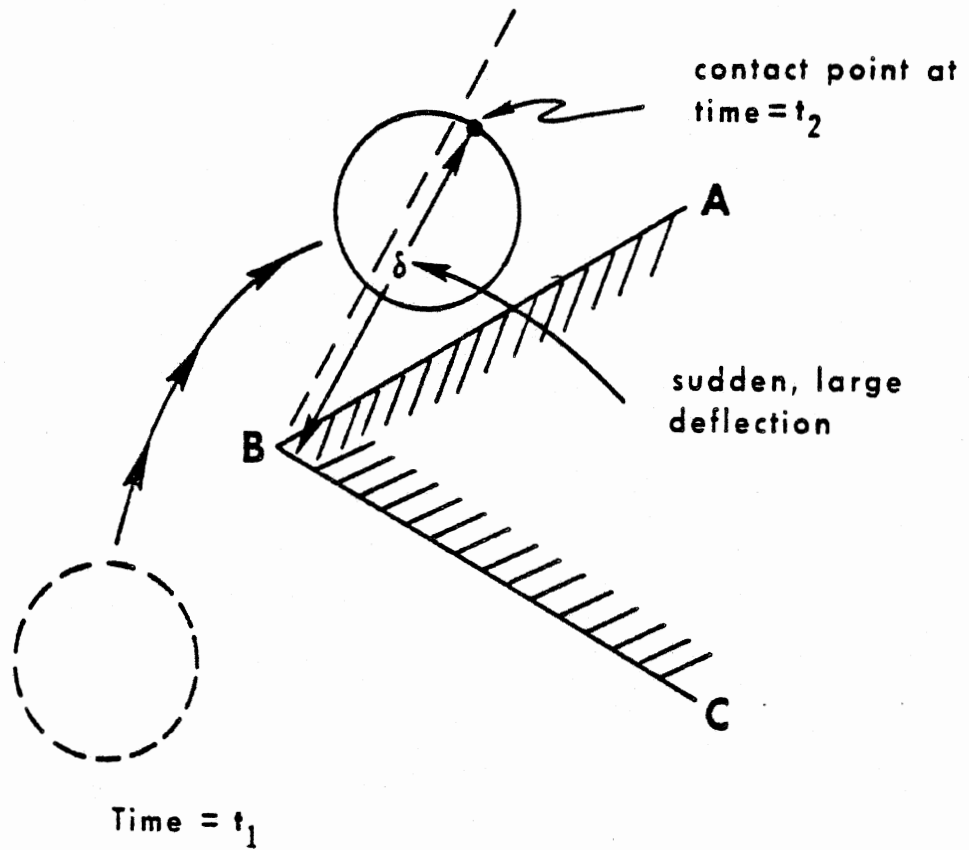


FIGURE 6-30 A Sudden, Large Deflection Near an Acute Angle

SLIDE 6-2-12

SLIDE 12

The final modeling consideration that will be discussed relates to a particular use of the so-called "penetration limit." One use of this line-segment input parameter has already been discussed in Module 5.

The figure illustrates how the contact force generation algorithm in the model can have difficulty in defining an interaction when the user has represented some part of the vehicle-interior profile by line segments which meet at an acute angle. Use of acute angles may result in sudden, unreasonably large forces on the occupant after an ellipse passes near the vertex. Such forces can result if the ellipse passes around the corner, as illustrated, so that the first effective deflection between the line segment and the ellipse contact point is large.

The most effective way of lessening the likelihood of occurrence of this problem in the case that acute angles must be used in the vehicle interior is to set the "penetration limits" for the line segments to properly small values. One way of recognizing as "false" a sudden, large deflection such as shown in the figure for line segment BC is to compare it with the maximum change of deflection which is possible in one time integration step. If the first effective deflection is larger than the maximum possible change in one time step, then the deflection is false and no forces should be calculated while the ellipse remains behind the line segment. Clearly, the smallest false deflections which can be recognized in this manner are just larger than the product of the time step  $\Delta t$  and the speed at which an ellipse approaches the contact surface, say  $v^{(rel)}$ . Therefore, the computer model will recognize most false deflections by comparing the deflection with a penetration limit set to  $v_{max}^{(rel)} \Delta t$ , where  $v_{max}^{(rel)}$ , the maximum speed at which an ellipse is ever expected to approach the surface, can be taken as the crash impact velocity, a reasonable limiting value. Thus, for an impact velocity of 30 mph, or 528 in/sec, and an integration time step of 1. msec, penetration limits may be set to .528 inches and no false deflections greater than .528 inches will be accepted as real by the computer model. Penetration limit values should not be taken as significantly less than  $v_{max}^{(rel)} \Delta t$  since real interactions between ellipses and line segments might then be identified as false.

## **SUMMARY OF DATA REQUIREMENTS OF CONTACT FORCE ALGORITHMS**

- **Specification of loading properties of materials with compatible G- and R-ratios for unloading**
- **Shared-deflection (mutual -deformation) iteration controls**
- **Friction class specification for each ellipse and region**
- **Deflection-dependent friction coefficient for each pairing of friction classes**
- **An edge constant and a penetration limit for each line segment**

**SLIDE 6-2-13**



### SLIDE 13

In summary, the user must supply a variety of data relating directly to the determination of contact forces. Module 6, Part 1, dealt primarily with loading and unloading properties of elements of the occupant profile and the vehicle-interior profile. Special parameters that have been discussed here in Module 6, Part 2, include five quantities that are used by the model in determining the component deflections in interacting, mutually deforming elements. The most important of these are force-convergence "epsilon" for the iteration procedure which finds the force balance and a limit to the number of allowed iterations. Each body ellipse and each vehicle-interior region is assigned to a friction class. For each pairing of friction classes, a friction coefficient is specified as a polynomial function of deflection so that plowing can be represented. Finally, for each line segment, an edge constant and a penetration limit must be prescribed. The first of these may be used to soften a line segment near its edges, and a primary use of the second is to prevent the calculation of large, anomalous contact forces near corners or edges in the vehicle-interior profile.



**MVMA 2-D**  
**CRASH VICTIM SIMULATION**

**\* \* \***

**MODULE 7**

**OCCUPANT POSITIONING**  
**WITH RESPECT TO THE VEHICLE**

**MVMA 2-D**  
**CRASH VICTIM SIMULATION**

**\* \* \***

**MODULE 7**

**OCCUPANT POSITIONING**  
**WITH RESPECT TO THE VEHICLE**

**SLIDE 7-1**

MODULE 7 - OCCUPANT POSITIONING WITH RESPECT TO THE VEHICLE

SLIDE 1

This module deals with the description of occupant position and orientation.

**COMPUTER SIMULATION  
OF OCCUPANT DYNAMICS  
IN A CRASH ENVIRONMENT**

**GIVEN (Input):**

- 1) Description of a biomechanical system representing the occupant
- 2) Description of a mechanical system representing the occupant compartment
- 3) Time-history of occupant compartment motion
- 4) Occupant position at onset of crash

**DETERMINED (Output):**

- 1) Occupant motion
- 2) Forces on Occupant
- 3) Derived descriptions and measures of the crash dynamics

FIGURE 7-1 Computer Simulation of Occupant Dynamics

## SLIDE 2

The problem of determining occupant dynamics in a crash environment can be simply stated. A description of a mechanical or biomechanical system, the occupant, is given. A description of potentially interacting mechanical system, the occupant compartment, is given. The motion in space of the occupant compartment as a function of time is specified. And finally, the occupant's position and orientation and their rates of change are specified for some single instant of time. It is required to determine the motion of the occupant and the forces which describe his interaction with the vehicle interior.

Since the user of the simulation model is required to specify occupant position and orientation and their rates of change for some instant of time, arbitrarily assigned the value  $t = 0$ , this module is pertinent to preparation of input data sets. It is also pertinent to interpretation of model output since "occupant motion" is nothing more than time-histories of occupant position and orientation. Rates of change with respect to time of these histories, namely, velocities and accelerations, are equivalent descriptions of the motion and are normally printed together with the position history.

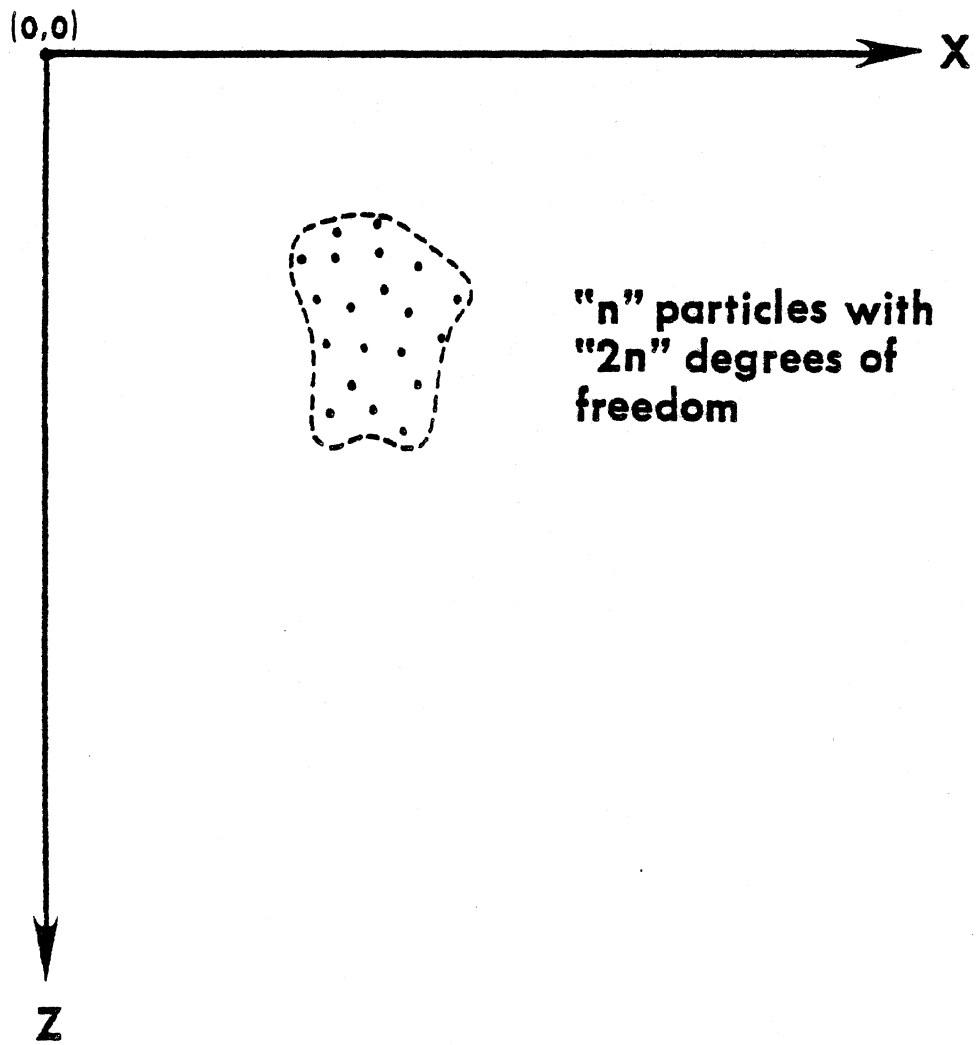


FIGURE 7-2 "n" Free Particles in an Inertial Coordinate Frame

SLIDE 7-3



### SLIDE 3

Consider a system of "n" particles confined to a plane, and let the positions of all points in the plane be defined in an arbitrarily positioned, non-accelerating orthogonal axis system with coordinates X and Z. This is a so-called "inertial coordinate frame." In general, "2n" coordinate values must be specified to completely define the state of the system at any instant of time, that is, there are "2n" degrees of freedom. However, if constraints exist on the positions of particles relative to each other, then fewer than "2n" coordinate values are sufficient.

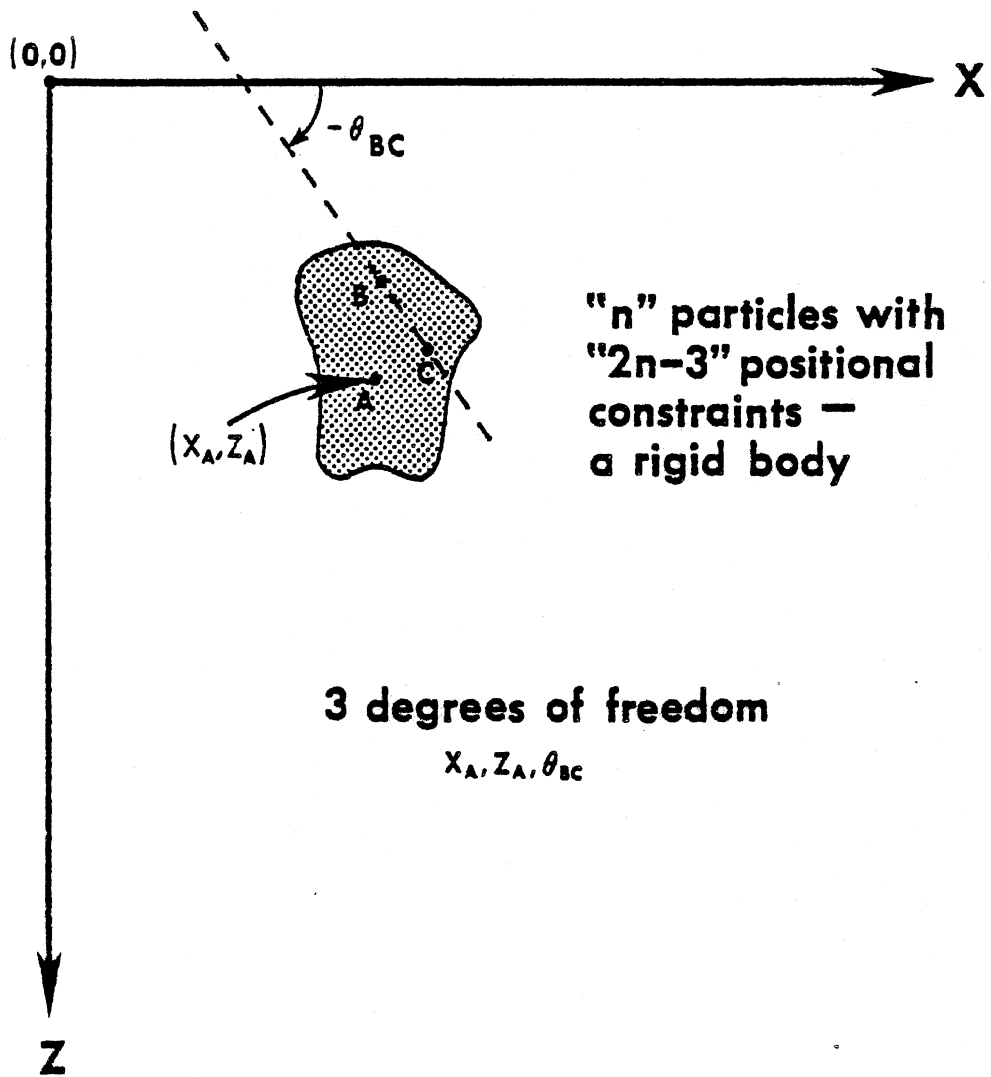
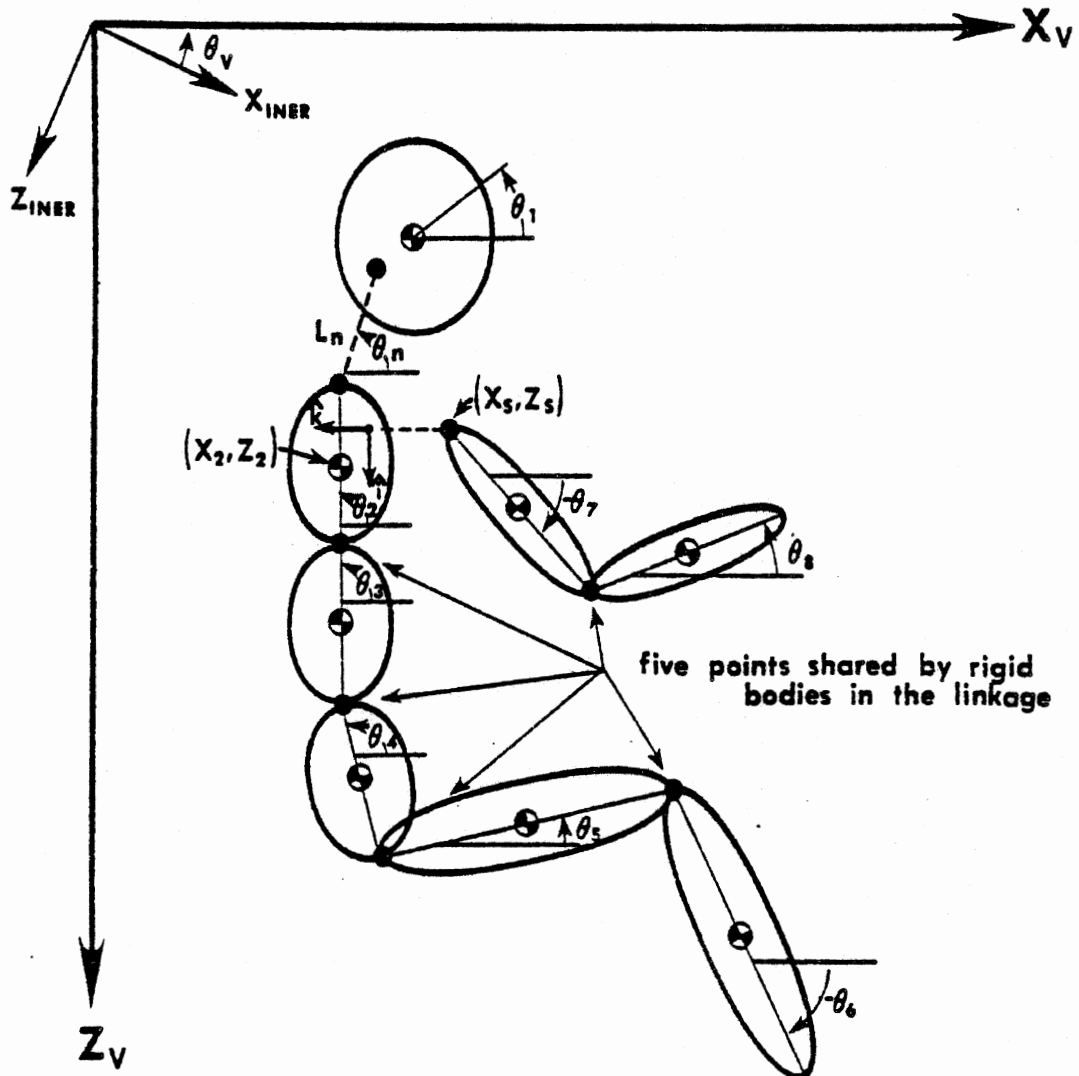


FIGURE 7-3 A Rigid Body in 2-Space, with Three Degrees of Freedom

SLIDE 7-4

#### SLIDE 4

If there exist " $2n - 3$ " independent positional constraints, then the system of particles is called a "rigid body." There remain three independent modes of motion of this system, and as " $n$ " approaches infinity there are infinitely many equivalent ways that three independent degrees of freedom may be defined. It is most convenient and conventional to locate an arbitrary point in a rigid body, normally the center-of-mass point, by the two cartesian coordinates  $x$  and  $z$ . The third coordinate is the angle of intercept between the  $x$ - or  $z$ -axis of the inertial frame and an extended line drawn between two specified but arbitrary points in the rigid body. In the figure, the three quantities  $x_A$ ,  $z_A$ , and  $\theta_{BC}$  are so-called "generalized coordinates" for the rigid body.



14 generalized coordinates:  $X_2, Z_2, \theta_1, \theta_2, \theta_3, \theta_4, \theta_5, \theta_6,$   
 $\theta_7, \theta_8, \theta_n, L_n, X_5, Z_5$

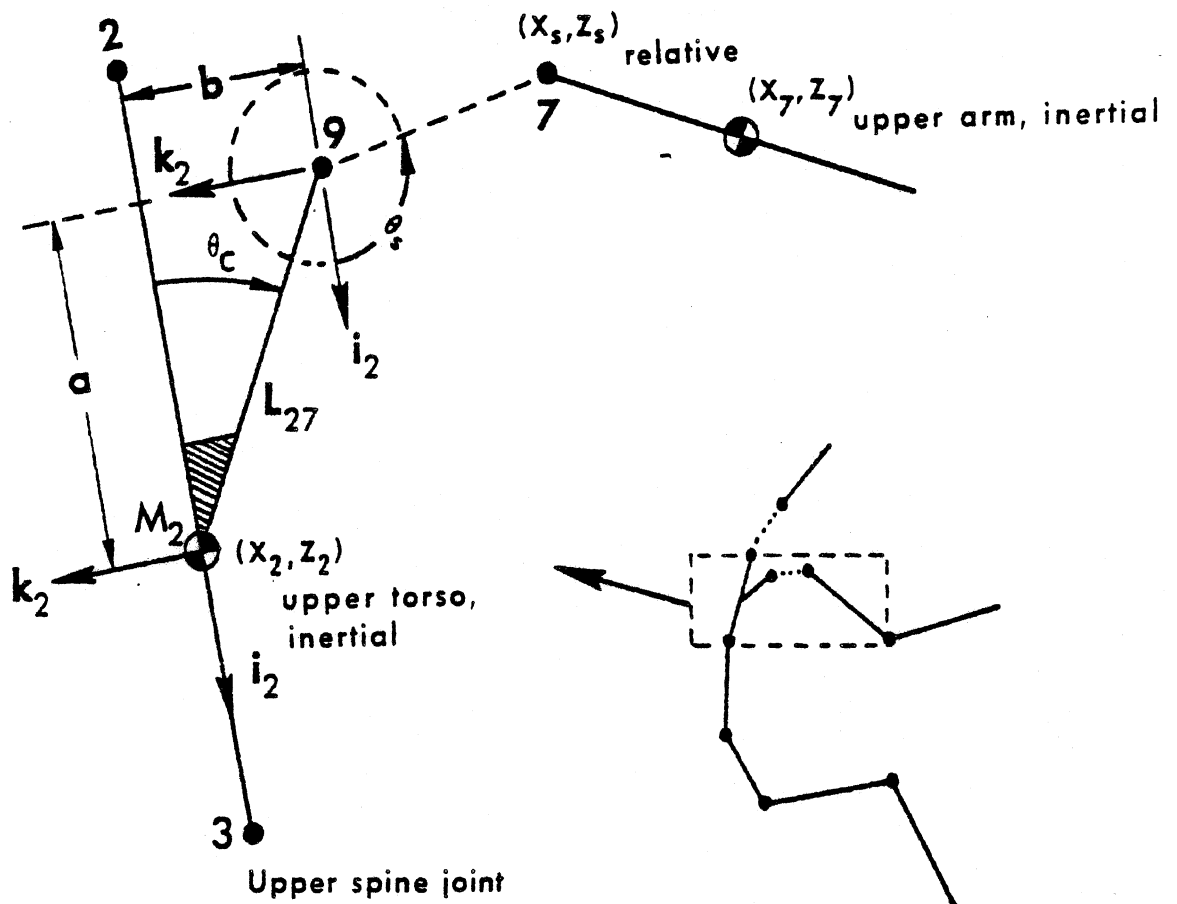
FIGURE 7-4 Occupant Model Generalized Coordinates for Input and Output (absolute coordinates defined with respect to vehicle axes)

SLIDE 7-5

## SLIDE 5

If a system of particles is not rigid, then one additional generalized coordinate must be defined for each positional constraint fewer than  $2n - 3$  which exists for the system. The MVMA 2-D man model linkage consists of eight rigid-body elements. If this were not a kinematically constrained linkage, twenty-four generalized coordinates would be required to define the position and orientation of the system, three for each rigid-body element. There are, however, five points shared by the rigid-body elements, at body joints, and for each, the X and Z coordinate values of one particle point are made redundant. Thus, there are ten positional constraints. Consequently, the linkage shown has only fourteen degrees of freedom, and fourteen suitable generalized coordinates are indicated. Eleven have been chosen to be relative to the axis system  $(X_V, Z_V)$ . They are nine link angles,  $\theta_1$  to  $\theta_8$  plus  $\theta_n$ , and two cartesian coordinates of the upper torso element center of mass,  $X_2$  and  $Z_2$ . Three coordinates were more conveniently defined as relative to points in the linkage. They are  $L_n$ , the length of the extensible neck link, and  $(X_S, Z_S)$ , the coordinates in a coordinate frame fixed to the upper torso element of the end of the upper arm element. Initial values for all fourteen of these occupant coordinates must be specified by the user, together with fourteen initial velocities.

Lower neck joint



$$\vec{r}_{9 \rightarrow 7} = x_s i_2 + z_s k_2$$

$$\theta_c = \text{constant}$$

$$L_{27} = \text{constant}$$

FIGURE 7-5 Shoulder Joint

SLIDE 7-6

## SLIDE 6

The coordinates  $X_s$  and  $Z_s$  represent shoulder flexibility in the linkage and they are more clearly illustrated here. These coordinates are normally initialized to zero because zeroes define a rest position for the shoulder linkage -- that is, point 7 then coincides with point 9. Joint properties and dimensional parameters of the shoulder linkage as well as the rest of the body linkage are discussed fully in Modules 2 and 3.

$\theta_1, \theta_2, \theta_3, \theta_4, \theta_5, \theta_6, \theta_7, \theta_8, \theta_n = 0$  (input or output)

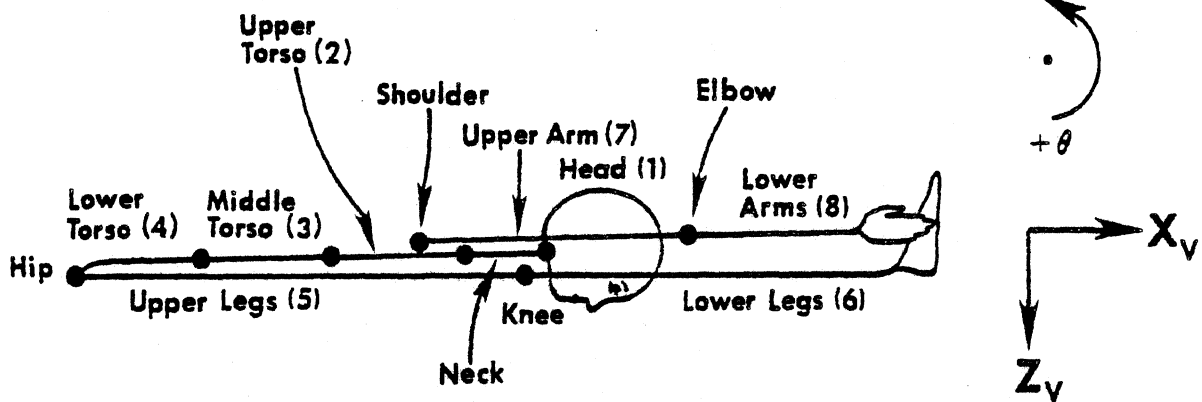


FIGURE 7-6 Occupant Model Configuration with all Body Link Angles Equal to Zero, for INPUT or OUTPUT

SLIDE 7-7



## SLIDE 7

The differential equations of motion for the occupant which are numerically integrated by the computer model are derived in terms of generalized coordinates defined relative to an inertial frame. This definition of coordinates is pertinent to the analytical equations of motion in Volume 1 of the MVMA 2-D manuals and to the computer model code. The average user of the MVMA 2-D simulation, however, will be concerned only with model input and output, and for both, coordinate values are relative to an arbitrarily positioned coordinate frame in the vehicle.

A vehicle-relative coordinate frame is shown in this slide, and the illustrated occupant orientation is for all link angles equal to zero. The body linkage of a person touching his toes while doing sit-ups approximates this orientation. The legs are straight out to the right, parallel to the vehicle x-axis, and the torso is completely forward and down, with articulation at the hip only. The arms are extended straight ahead toward the feet. Unfolding the occupant illustrated into an approximation of a seated position would clearly require specification of head, neck, and torso link angles of about  $+90^\circ$  and a lower leg angle of about  $-90^\circ$ . As explained and illustrated earlier, the cartesian coordinates  $(X_2, Z_2)$  of the upper torso element are also specified with respect to the axis system  $(X_V, Z_V)$  in the vehicle.

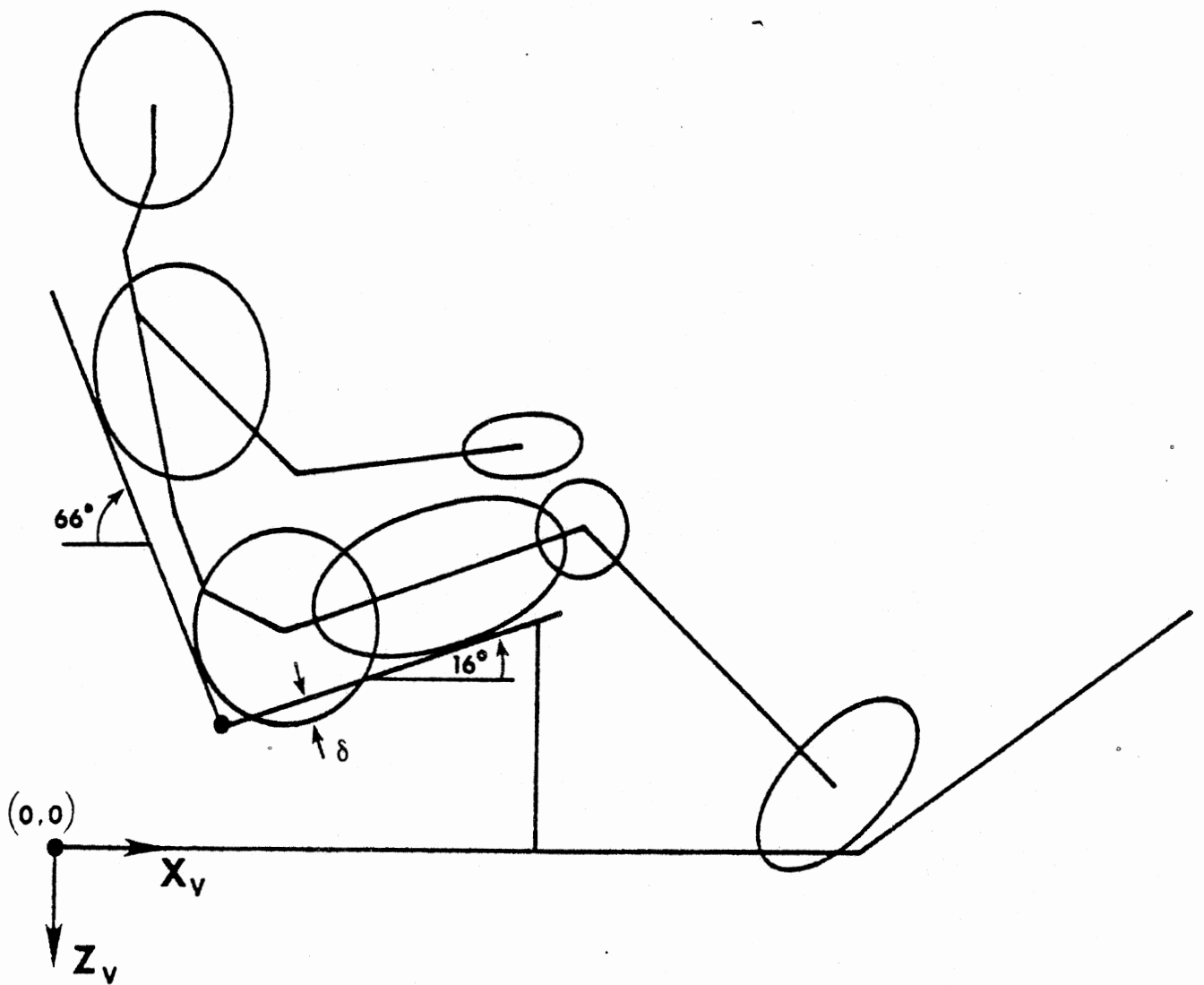


FIGURE 7-9 Seated Occupant in Position of Approximate Equilibrium

SLIDE 7-8

## SLIDE 8

The MVMA Two-Dimensional Crash Victim Simulator has been applied in various ways for the modeling of dynamical systems. A broad range of front, rear, and even side impacts for driver and passenger have been simulated. The applications include simulating anthropomorphic dummy drops onto a hard surface and human fall victims striking yielding and unyielding surfaces. They include simulating pedestrians struck by a vehicle. Simulations have been done of laboratory tests in which lateral neck response of human subjects was measured when the head jerked to the side by a falling weight. Use of the MVMA 2-D model need not be restricted to simulating human or human-analog systems. While it could be used to simulate a hanging to help determine force levels for vertebral fracture, it could also be used to model a particle subject to a two-dimensional force field or a three-ball billiards shot on a four-cushioned table. Diverse applications are possible if the user is clever in utilizing the many features of the model.

It is unfortunate that the most common application of the model, simulation of vehicle occupant dynamics, presents a difficulty presented by few of the special model applications -- namely, proper specification of the initial position and orientation of the mechanical linkage. The special model applications, while often requiring a certain amount of ingenuity and imagination in the construction of input data sets, normally involve simpler mechanical systems than the occupant/vehicle-interior system; and in particular there is normally no special difficulty in initializing the simpler systems for the desired state of force balance or imbalance. On the other hand, initial positioning of the occupant within the occupant compartment requires special care by the user because several variously-directed force vectors are required on the seated-occupant linkage to balance gravity. In practice it is not possible to specify the initial position so that the sums of all moments and all forces on all body parts are equal to zero. The user should attempt to approximate this condition of equilibrium, however, if it is intended that the occupant be seated at rest at crash onset. The best measure of his success is probably the nearness to zero of the values calculated by the model

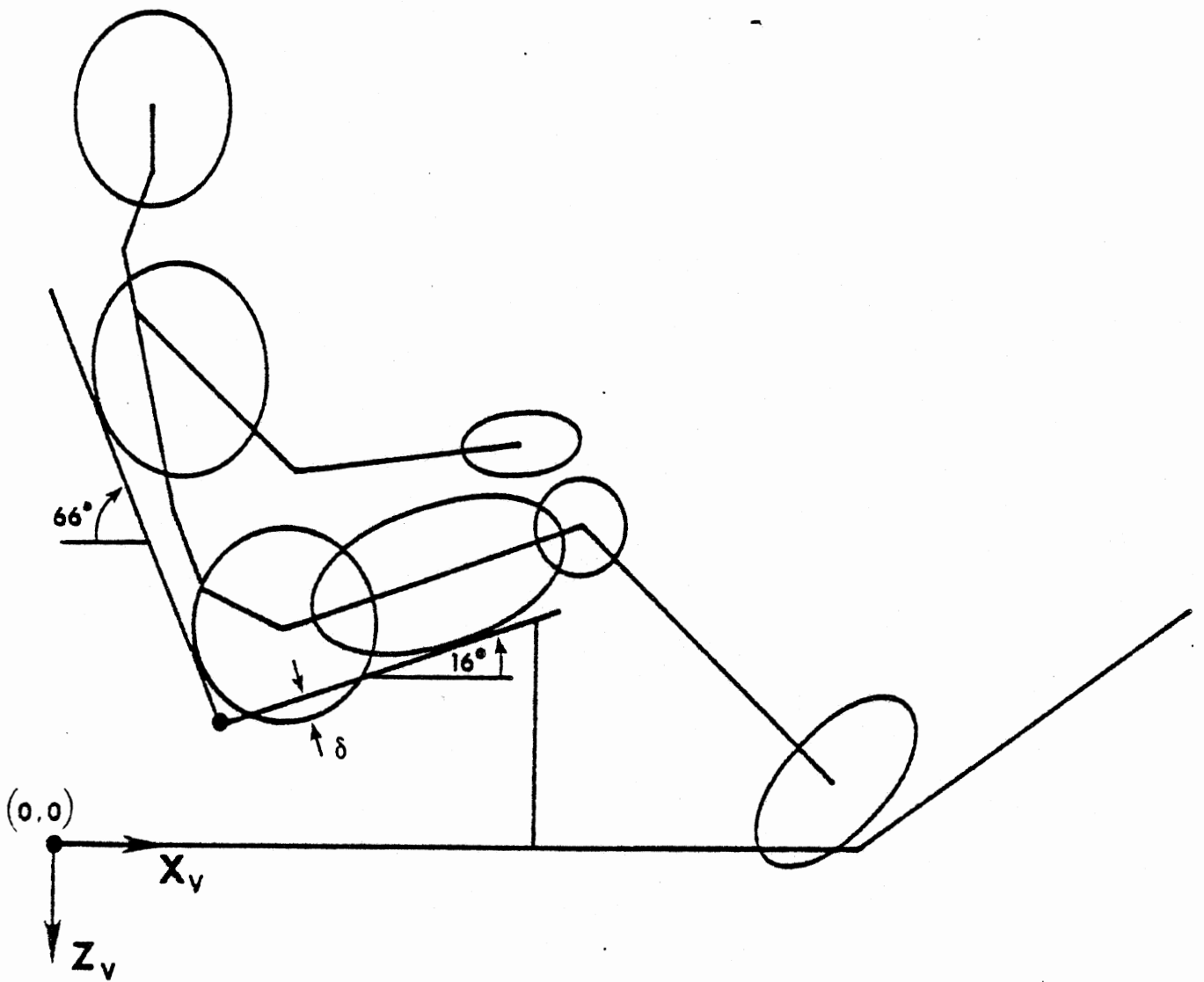


FIGURE 7-9 Seated Occupant in Position of Approximate Equilibrium

SLIDE 7-8

at time zero for body link angular accelerations and upper-torso and hip resultant linear accelerations. If these values are small in comparison with the maximum values attained in the simulation, then the initial imbalance is probably not significant.

## **INITIAL POSITIONING OF OCCUPANT FOR APPROXIMATE EQUILIBRIUM: FIXED DATA**

- **Establish body link lengths and masses**
- **Establish occupant contact-sensing profile , including ellipse sizes and attachment positions**
- **Establish vehicle-interior profile**
- **Establish static load-deflection relations for all ellipses and vehicle-interior regions**

**SLIDE 7-9**

## SLIDE 9

In lieu of a pre-processor computer model or special subroutines, the user himself must establish an initial positioning for approximate equilibrium. It should be made clear that various approaches are equally good. One reasonable way to proceed is as follows. First decide on all body-segment masses and body dimensions, including link lengths and sizes and attachment positions of ellipses which define the contact-sensing profile. Decide on the positions in the vehicle of all segments of the vehicle-interior profile. Next, determine what material stiffnesses will be assigned for all ellipses and vehicle-interior line segments.

## INITIAL POSITIONING OF OCCUPANT FOR APPROXIMATE EQUILIBRIUM

- Determine total deformation of hip ellipse and seat cushion line required to balance the torso weight plus half the upper leg weight
- Determine total deformation of foot and floorpan for balancing lower leg weight plus half the upper leg weight
- Use scale drawings or equations to determine the hip-joint coordinates and upper and lower leg angles which give the required initial deformations
- Use scale drawings or equations to find torso link angles which make torso ellipses tangent to the seat back or produce desired deflections
- Determine required input coordinates for the upper torso center of gravity from the established hip joint position and torso link angles
- Assign head, neck, and arm angles

SLIDE 7-10



## SLIDE 10

Next, on the basis of the material stiffnesses of the hip ellipse and the seat cushion line, determine the total hip plus seat cushion deformation required to produce a vertical component of seat force which will balance the weight of the torso segments plus one half of the upper legs segment. Similarly determine the total deformation required for the materials of the floorpan and of a contact ellipse at the foot in order to produce a force which will balance the weight of the lower legs plus half the upper-leg weight. It is reasonable to position the hip ellipse so that it is tangent to the seat back, producing no normal force. Thus, it is now possible, using scale drawings or analytic geometry, to establish the coordinates of the hip joint and upper and lower leg angles which will result in the desired initial deformations at the seat cushion and floorpan.

With the hip-joint position already established, values for the torso link angles can next be determined which will make the torso contact ellipses tangent to the seat back. If desired, they can instead be determined so that torso-ellipse deformations of the seat back produce forces with moments about the hip which balance torso gravitational moments about the hip. However, the force and moment imbalances that result from assuming a zero initial deflection, or simply from making a reasonable estimate of the non-zero initial deflection, will not be significant to the crash dynamics.

Finally, the coordinates of the hip joint position together with the established torso link angles and dimensions completely determine the coordinates  $X_2$  and  $Z_2$  of the upper torso center of gravity. It is necessary in assigning initial head, neck and arm angles to be certain that contact ellipses attached to the head and arm segments are not in position to interact with a head rest, the seat back, the seat cushion, or any other vehicle-interior segment. The procedure described here can be modified if thigh or knee ellipses are present and in potential contact with the seat.

Details for an example initial-positioning problem are included with the text of this module. Only one further point will be discussed here.

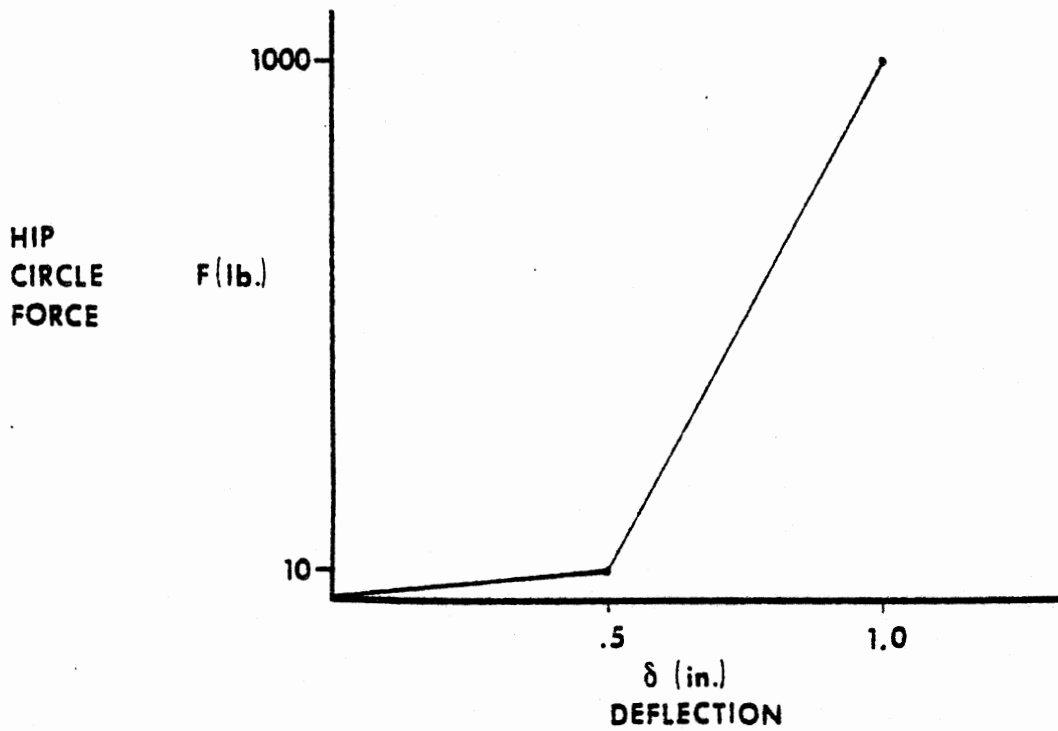
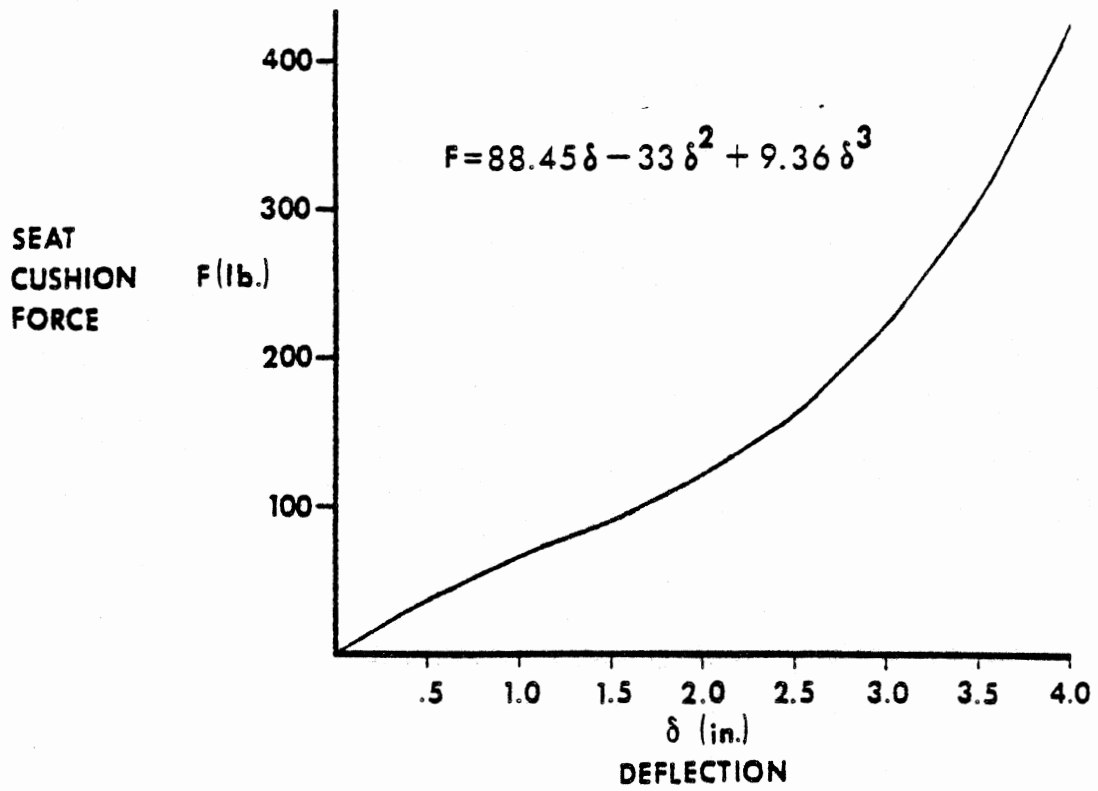


FIGURE 7-10 Force-Deflection Curves for Seat Cushion and Hip Circle

SLIDE 7-11

## SLIDE 11

One step in the foregoing procedure is to determine the combined deformation of the hip ellipse and the seat cushion line required to balance the torso weight plus a portion, say half, of the upper leg weight. If both the hip circle and the seat cushion are modeled as deformable, then two static force-deflection curves must be considered. Example curves are illustrated.

If the torso weight is 77 lb and the upper legs weight is 37 lb, the force to be balanced in the z-direction is 95.5 lb. The force normal to a seat cushion line at an angle of  $16^\circ$  from the horizontal should be 95.5 times the cosine of  $16^\circ$ , or 91.8 lb. From the force-deflection equation for the seat cushion, shown with the figure, the seat cushion deflection which will produce this force is found as the solution of the first equation on the next slide.

**Weight to be balanced: 95.5 lb**

**Component normal to 16° seat cushion: 91.8 lb**

$$1) 91.8 = 88.45\delta - 33\delta^2 + 9.36\delta^3$$

$$2) \delta_{sc} = 1.533$$

$$3) 91.8 = 10 + (\delta - .5) 990 / .5$$

$$4) \delta_H = .541$$

$$5) \delta = \delta_{sc} + \delta_H = 2.074$$

**SLIDE 7-12**

SLIDE 12

Its solution may be found iteratively, graphically, or by other means to be  $\delta_{SC} = 1.533"$ . The hip-circle deflection necessary for 91.8 lb is found similarly as the solution of the third equation as  $\delta_H = .541"$ . The total deflection, that is, the sum of the component deflections, has thus been determined as 2.074".

## **SUMMARY OF DATA REQUIREMENTS FOR INITIAL POSITIONING OF OCCUPANT**

- **Nine body link angles**
- **x and z coordinates of upper torso center of gravity**
- **Two shoulder-joint coordinates**
- **Neck length**
- **Condition of approximate equilibrium**

**SLIDE 7-13**

## SLIDE 13

This module has described the position coordinates for which initial values must be specified for the 14-degree-of-freedom occupant model. These include nine body link angles and the two cartesian coordinates of the upper torso center of gravity. Those eleven are prescribed with respect to a coordinate frame fixed to the occupant compartment. The three other position values required are for the cartesian shoulder-joint coordinates, specified in a frame fixed to the upper torso element, and the initial neck length. In addition, initial velocities must be specified for each of these coordinates. The user must position the occupant carefully within the occupant compartment so that the occupant will be seated at rest in a condition approximating force and moment equilibrium at crash onset.





**MVMA 2-D**  
**CRASH VICTIM SIMULATION**

**\* \* \***

**MODULE 8**

**CRASH DECELERATION PROFILES**  
**AND HEAD APPLIED FORCES**

**MVMA 2-D**  
**CRASH VICTIM SIMULATION**



**MODULE 8**

**CRASH DECELERATION PROFILES**  
**AND HEAD APPLIED FORCES**

**SLIDE 8-1**

## MODULE 8 -- CRASH DECELERATION PROFILES AND HEAD APPLIED FORCES

### SLIDE 1

The crash victim's environment is made to be dynamic by specifying a vehicular motion. If the crash victim is a pedestrian, the vehicle might be moving with constant speed or it might be accelerating or decelerating. If the crash victim is an occupant of either a struck vehicle or a striking vehicle, he is normally initially at rest with respect to the vehicle. He interacts dynamically with the vehicle interior and restraint systems only as a result of occupant compartment acceleration or deceleration. Therefore, unless the model is being used to solve a free motion problem, it is always necessary to prescribe a vehicular motion.

Inertial reference frame

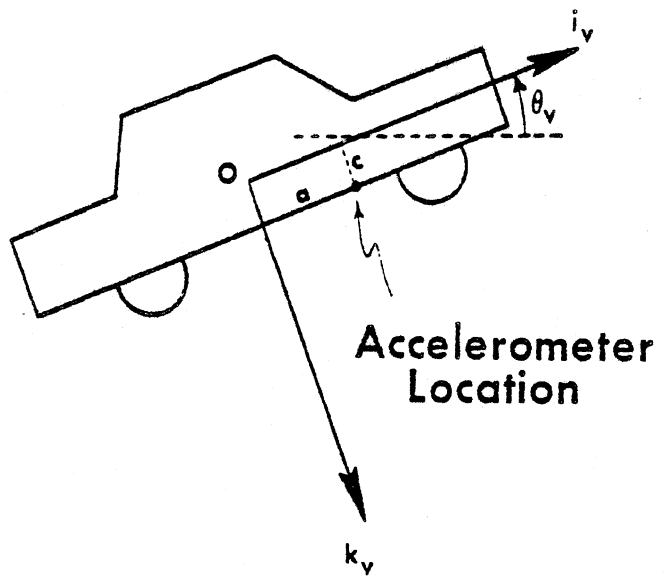
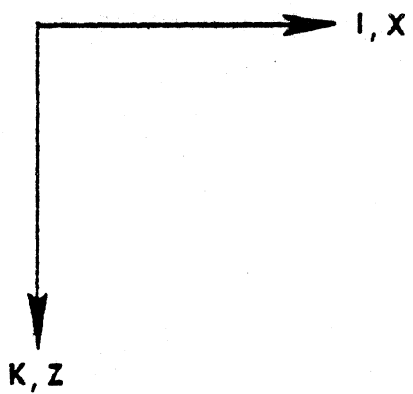


FIGURE 8-1 Vehicle Coordinates

SLIDE 8-2

## SLIDE 2

The figures shows a schematic of the planar vehicle. Point "0" is the origin of a coordinate system fixed to the occupant compartment. Its location in the vehicle is arbitrary; it might, for example, be a point on the toeboard. In the illustration, the vehicle-fixed coordinate frame is just behind the front seat and at knee level. While occupant position and the location of points defining the vehicle interior are prescribed with respect to this point, vehicle motion is prescribed by specifying the position of point "0" within an inertial reference frame. In addition to horizontal and vertical motions, an angular pitching motion must also be defined. In the MVMA 2-D simulator, the pitch angle is positive when measured counterclockwise from the inertial x-axis, as illustrated.

In order to define these three motions, the user first specifies for each an initial position and an initial velocity. It is often convenient to define the inertial frame reference point as coincident with the vehicle origin at time zero. The initial vehicle x- and z-coordinate values will obviously both be 0. in this case. If velocities of the vehicle degrees of freedom are to vary with time, then acceleration histories must also be prescribed. Only for a simulated pedestrian impact would it be reasonable to hold vehicle velocities constant. In order that vehicle accelerations can be specified with greatest possible ease, it is not required that the linear accelerations be defined at the point "0," but rather at an arbitrary point in the occupant compartment, where, for example, a biaxial accelerometer might be mounted. The location of that point in vehicle coordinates, that is, relative to point "0," must be specified. Its coordinates are (a,c) in the figure.

## OCCUPANT COMPARTMENT ACCELERATIONS

- Accelerations for three vehicle degrees of freedom as tabular functions of time
- Linear accelerations defined with respect to either the vehicle frame of reference (biaxial accelerometer) or the inertial frame
- Linear accelerations in g's,  $\text{in}/\text{sec}^2$ , or  $\text{m}/\text{sec}^2$
- Pitching acceleration in  $\text{rad}/\text{sec}^2$  or  $\text{deg}/\text{sec}^2$

SLIDE 8-3

### SLIDE 3

Acceleration histories are entered in tabular form as functions of time. For user convenience several options are available with regard to their specification. Linear accelerations, that is, x and z, may be defined if desired as the responses of a biaxial accelerometer mounted on a part of the frame that is fixed with respect to the occupant compartment. Alternatively, the accelerations may be prescribed as motion components for the vehicle origin within an inertial frame of reference. The x- and z-accelerations may be entered in g's or, depending on whether the simulation is being made with English or metric system units,  $\text{in}/\text{sec}^2$  or  $\text{m}/\text{sec}^2$ . Pitching accelerations may be in  $\text{rad}/\text{sec}^2$  or  $\text{deg}/\text{sec}^2$ . It might be noted here that definition of the beginning of the crash, that is,  $t = 0$ , is arbitrary, but is reasonably taken as the time at which accelerations begin to deviate from zero.

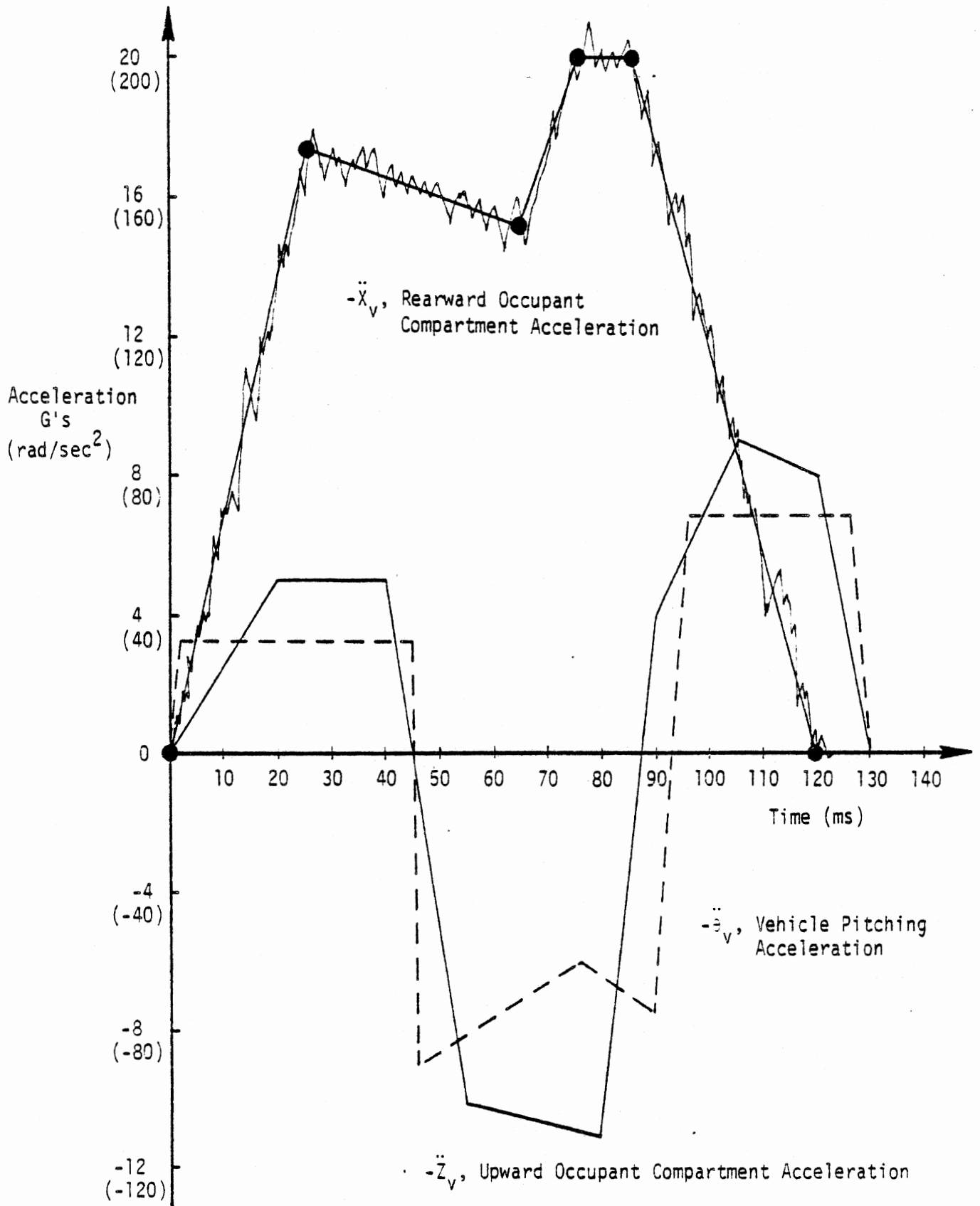


FIGURE 8-3 Vehicle Acceleration Profiles

SLIDE 8-4



#### SLIDE 4

The user can approximate a continuous accelerometer trace to any desired degree of accuracy by connected straight-line segments. Piecewise-linear approximations are shown of hypothetical accelerometer traces for a 30 mph frontal barrier collision. Seven input points are sufficient to accurately approximate the horizontal component of acceleration. The first six are at times of 0 msec, 25, 65, 75, 85, and 120 msec. Since the acceleration profile is identically zero after 120 msec, the seventh point should be for an acceleration of zero at some time exceeding the end of the crash. This coordinate might be 1000 msec, arbitrarily, since simulations are normally terminated at 200 to 250 msec. There is seldom any occupant dynamics of interest after 250 msec.

The pitching acceleration trace illustrated might have been obtained from an angular accelerometer, from analysis of non-coincident linear accelerometer data, or from film analysis. Like the x- and z-accelerations in the figure, this trace is a piecewise-linear approximation of a more complex profile.

Whether the model user inputs vehicle acceleration components relative to the inertial frame or in the vehicle frame of reference generally depends on the source of his data. The linear acceleration profiles may be entered in whichever form is more convenient. It is unnecessary for the purpose of defining input data for the user to understand the analytical relationship between acceleration components in these two reference frames. It is not a consideration in the specification of data. But an analytical relationship between them does exist.

## VEHICLE ACCELERATION TRANSFORMATIONS

$\theta_v$  = vehicle pitch angle

$$\begin{aligned}\ddot{x}_{v,"0"}^{(\text{inertial})} &= \ddot{x}_{v,"0"}^{(\text{vehicle frame})} \cos \theta_v + \ddot{z}_{v,"0"}^{(\text{vehicle frame})} \sin \theta_v \\ \ddot{z}_{v,"0"}^{(\text{inertial})} &= -\ddot{x}_{v,"0"}^{(\text{vehicle frame})} \sin \theta_v + \ddot{z}_{v,"0"}^{(\text{vehicle frame})} \cos \theta_v\end{aligned}$$

where

$$\begin{aligned}\ddot{x}_{v,"0"}^{(\text{vehicle frame})} &= \ddot{x}_{\text{accelerometer}} - c \ddot{\theta}_v + a \dot{\theta}_v^2 \\ \ddot{z}_{v,"0"}^{(\text{vehicle frame})} &= \ddot{z}_{\text{accelerometer}} + a \ddot{\theta}_v + c \dot{\theta}_v^2\end{aligned}$$

SLIDE 8-5

6/28/79

## SLIDE 5

The simple transformation shown here relates the inertial components to components measured in the rotating vehicle coordinate system. These relations are pertinent to understanding the printed output of vehicle motion. Although the user is allowed to prescribe acceleration components in the vehicle-fixed frame, inertial components are calculated by the computer model for output and for use in the equations of motion. The inertial components are, of course, identical to the vehicle-relative components whenever the vehicle is not pitched.

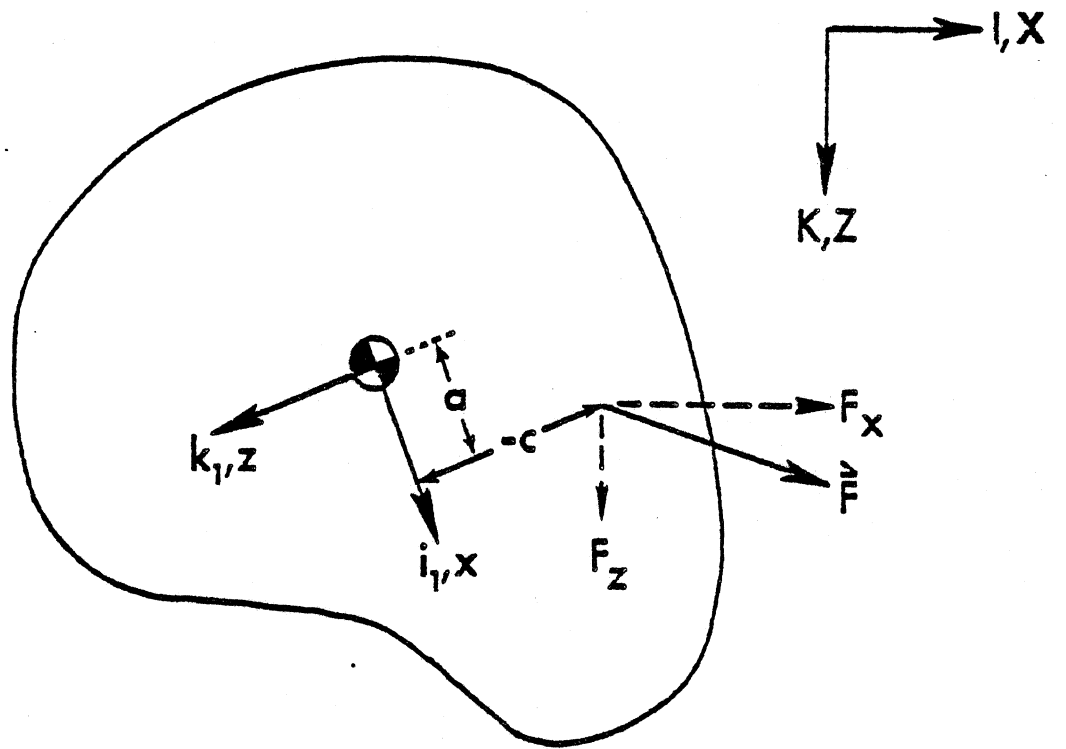


FIGURE 8-5 Schematic of Force Applied to Head

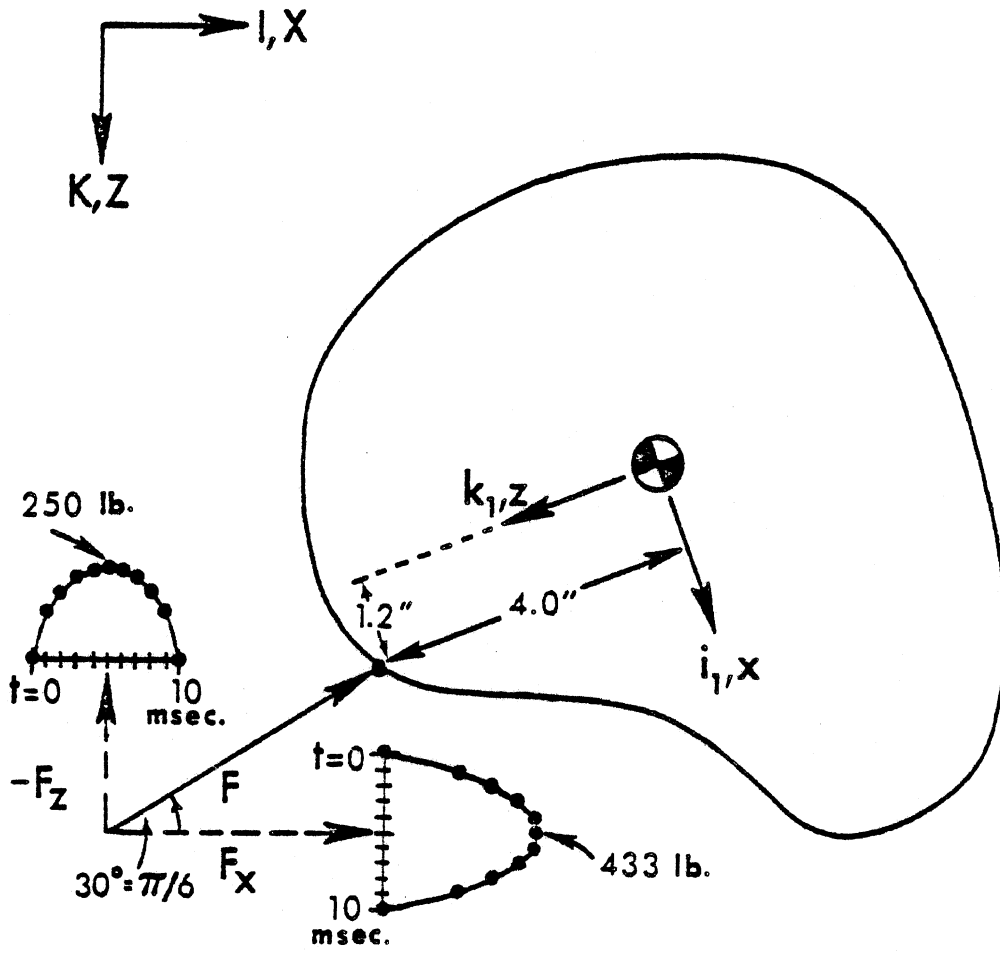
SLIDE 8-6

6/28/79

## SLIDE 6

Crash deceleration profiles provide an indirect forcing excitation to the occupant linkage. It is indirect in that crash forces on the occupant result only when prescribed vehicle motion causes interaction with occupant-compartment surfaces and restraint systems. The MVMA Two-Dimensional Crash Victim Simulator provides as well for a special, direct forcing excitation that has found occasional use. This is the direct application of a time-dependent force vector to any desired point on the head. Both the magnitude and direction of the vector can be time dependent since the X- and Z-components are separately specified.

These components are prescribed as tabular functions of time and they may be defined with respect to either the inertial axes or the rotating head system. The point of application of the force vector cannot change with time since its coordinates in the head system, "a" and "c" in the figure, are user-defined constants.



$$F_x = 500 \cos \pi/6 \sin \left( \frac{2\pi}{.02} t \right)$$

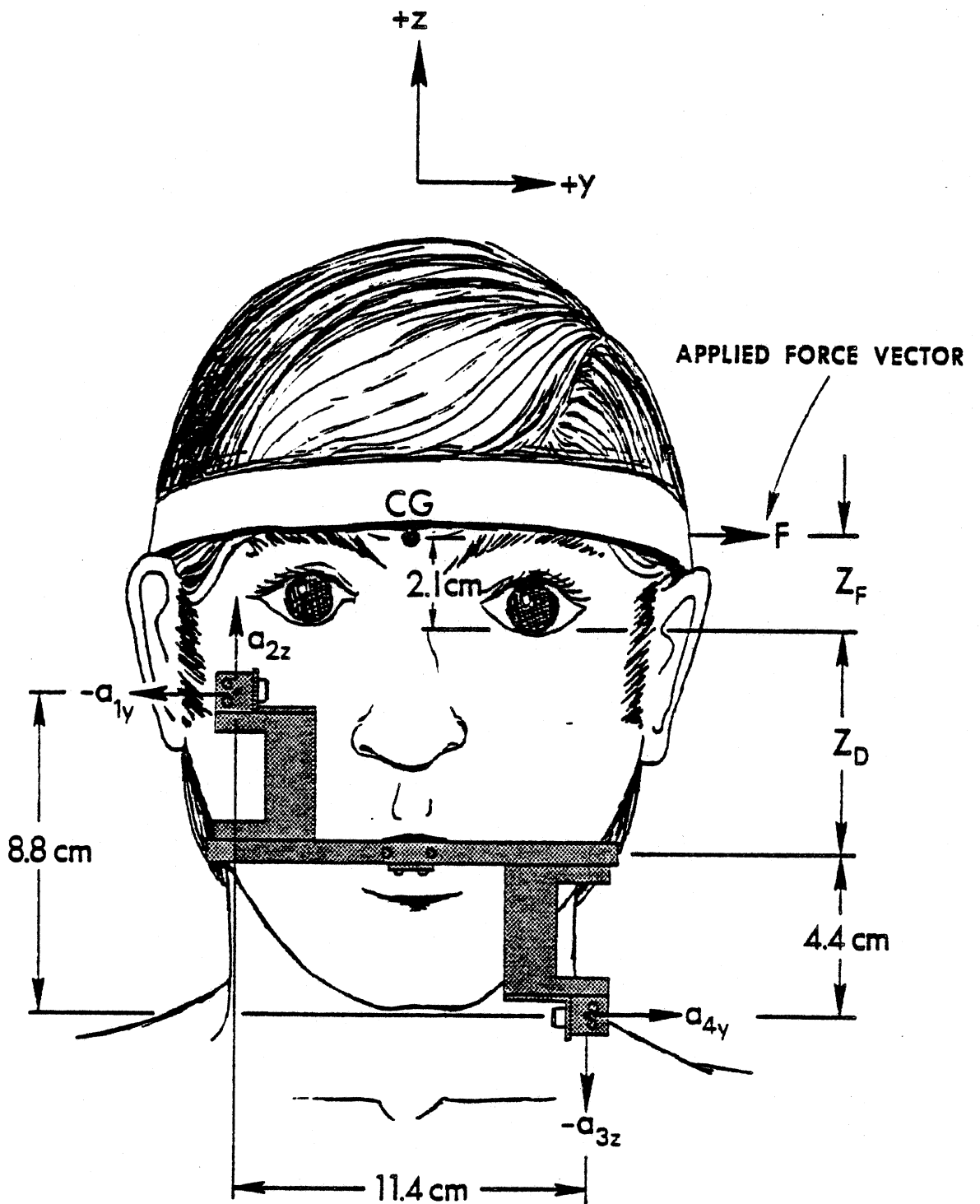
$$F_z = -500 \sin \pi/6 \sin \left( \frac{2\pi}{.02} t \right)$$

FIGURE 8-6 Example of Data for Force Applied to Head

SLIDE 8-7

## SLIDE 7

This figure illustrates a 500 lb., 10 msec half-sine force applied at the base of the skull in a superior and anterior direction,  $30^\circ$  above the inertial horizontal axis. The force is applied at a point 4 inches posterior and 1.2 inches inferior of the head center of gravity. The sinusoidal force pulses are approximated by piecewise-linear forms.



SLIDE 8-8



## SLIDE 8

Diverse applications might be made of this model feature. One use to which it has been put was to aid in the empirical determination of a composite lateral bending stiffness of the neck for small deformations. An experiment was devised in which a short-duration, low-level force could be applied laterally to a subject's head. The subject was seated, and a sideboard prevented any torso motion. The force pulse was recorded as a function of time, and angular head acceleration was determined from accelerometers mounted on a bite-bar structure. The experiment was then simulated with the MVMA 2-D model. Primary inputs to the model were head mass and moment of inertia and neck mass, all estimated from cadaver data, and neck length, determined from x-rays of the subjects. The elastic torsional stiffness coefficients at the upper and lower neck joints were considered to be adjustable parameters for a series of computer simulations which used measured head force as a driving excitation. Neck stiffnesses appropriate for small lateral bending deflections of the head and neck were thus determined as the coefficients which gave the best fit of simulated angular acceleration response to experimentally measured response.

## **SUMMARY OF DATA REQUIREMENTS FOR VEHICLE MOTION AND HEAD APPLIED FORCES**

- **Horizontal acceleration history plus initial position and velocity**
- **Vertical acceleration history plus initial position and velocity**
- **Pitching acceleration history plus initial position and velocity**
- **Linear accelerations in inertial frame or in rotating vehicle frame**
- **Accelerometer location in vehicle**
- **Time-dependent components of head applied force**
- **Location on head of point at which force is applied**

**SLIDE 8-9**

## SLIDE 9

This module has explained the specification of motion for the occupant compartment and also a special feature that allows a time-dependent force vector to be applied to any point of the occupant head. The vehicle has three degrees of freedom, horizontal and vertical linear coordinates plus a pitching coordinate. The motion for each of these is specified as a tabular acceleration history together with initial position and velocity values. The linear acceleration components may be defined either as relative to an inertial frame of reference or as relative to a rotating coordinate frame fixed to the vehicle. If the latter option is selected, then the acceleration histories represent the motion that would be sensed by a biaxial accelerometer fixed within the rotating frame. In either case, the user must also locate a simulated accelerometer within the vehicle-fixed coordinate system. Direct application of a time-dependent force vector to the head of the occupant requires specification of time histories of the two force components and the location on the head of the point of application.



**MVMA 2-D**  
**CRASH VICTIM SIMULATION**

**\* \* \***

**MODULE 9**

**BELT RESTRAINT SYSTEMS**

**MVMA 2-D**  
**CRASH VICTIM SIMULATION**

**\* \* \***

**MODULE 9**

**BELT RESTRAINT SYSTEMS**

**SLIDE 9-1**

## MODULE 9 -- BELT RESTRAINT SYSTEMS

### SLIDE 1

The MVMA Two-Dimensional Crash Victim Simulator includes two independent belt system models for optional usage. The first is illustrated by the next slide. The second, a more complex system, will be discussed later.

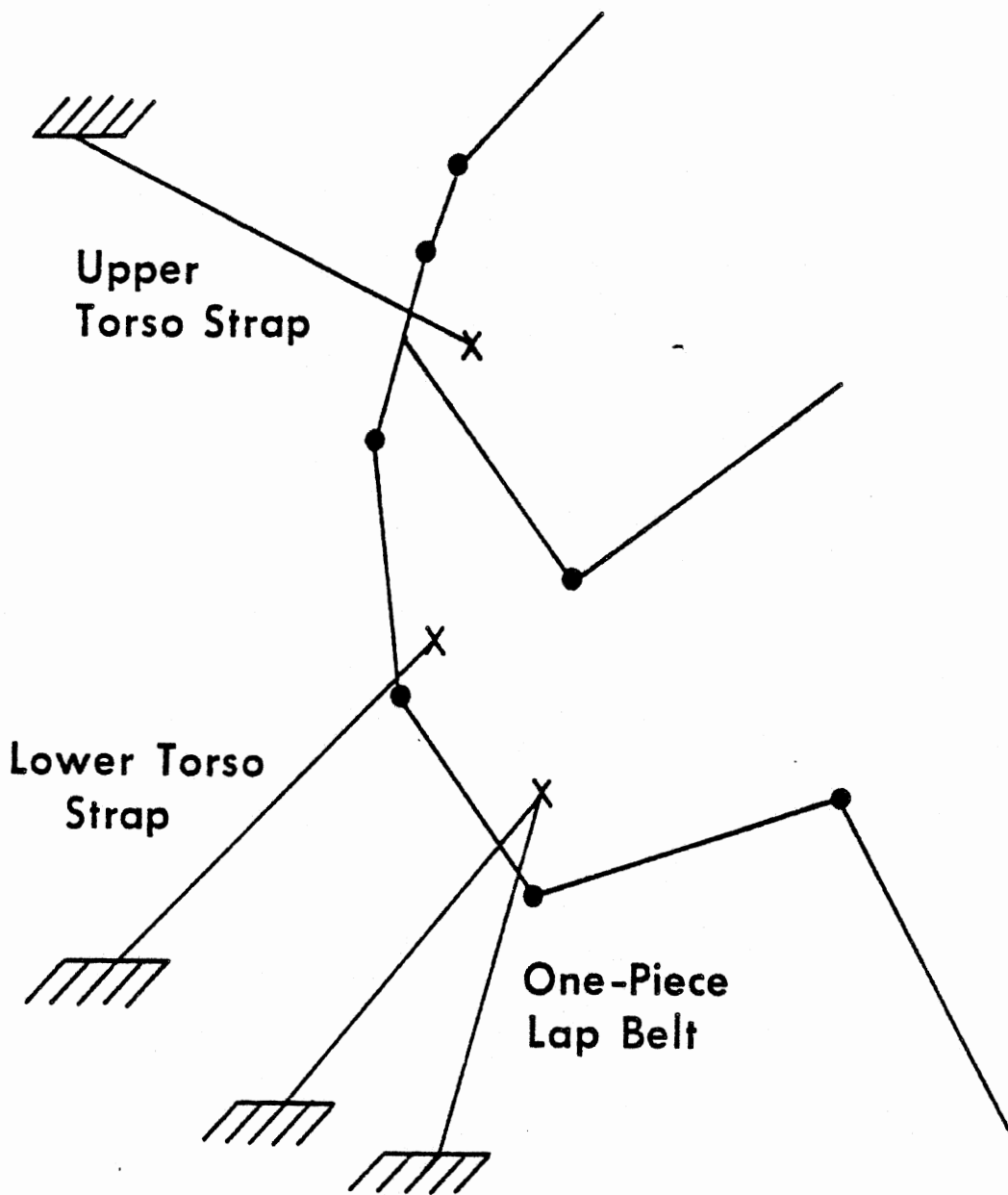


FIGURE 9-1 Simple Belt System

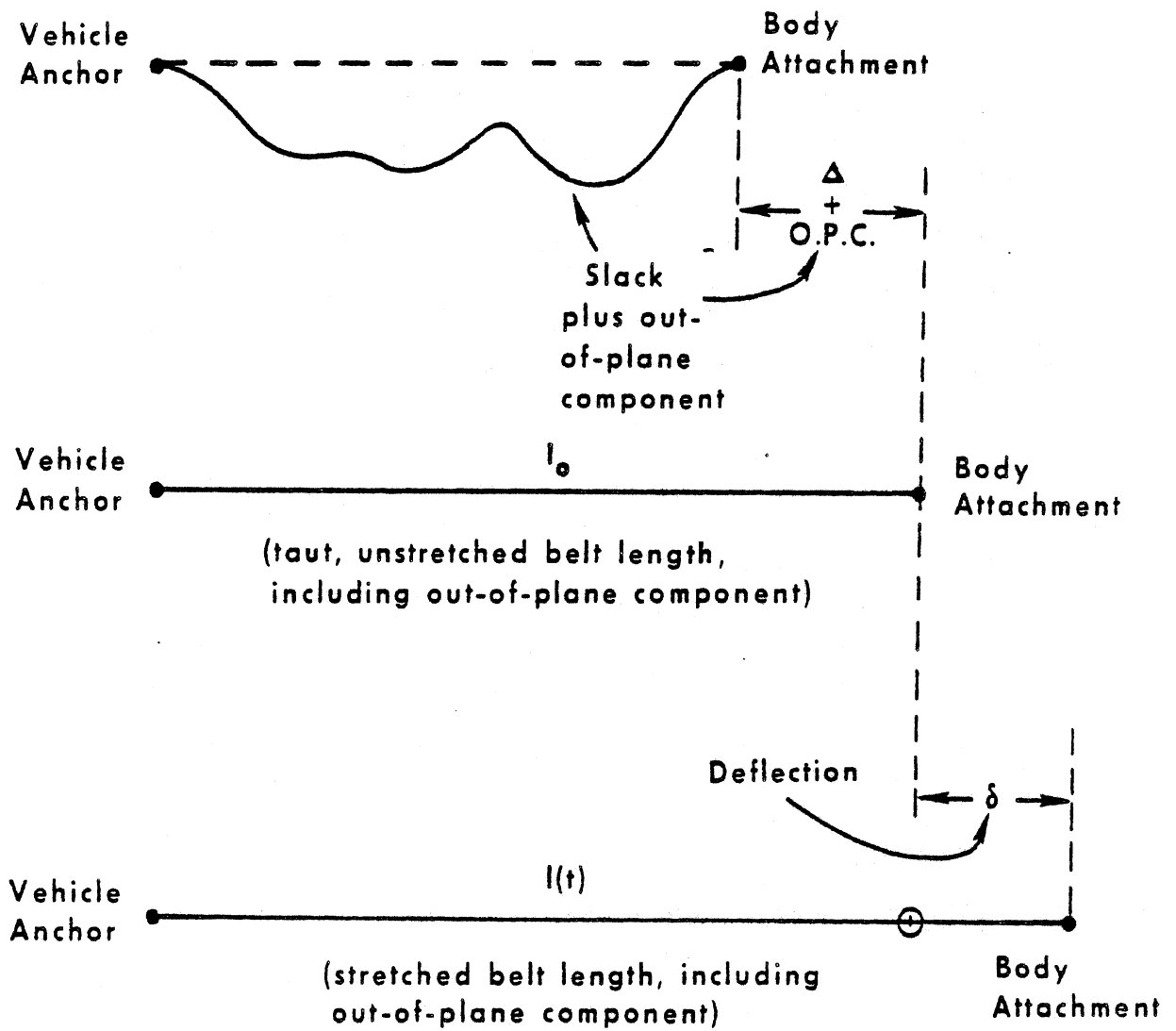
SLIDE 9-2



## SLIDE 2

This belt system consists of: a) a one-piece lap belt attached to the lower torso element and anchored at each end to the vehicle; b) an upper torso harness strap attached to the upper torso element and anchored to the vehicle; c) a lower torso harness strap attached arbitrarily to any torso element and anchored to the vehicle. The simpler of the two belt-restraint submodels is effectively a three-belt system. The two-segment lap belt shown in the figure is treated by the computer model as a single piece of webbing that slides freely over the pelvis through a user-specified point, called an "attachment point," on the lower-torso element. Thus, a lap-belt tension is determined from the elongation or strain of the total belt length, with no adjustment for possible friction effects, and the established tension is applied at the attachment point on the body through both the inboard and outboard segments. The lap belt anchor positions in the vehicle, as well as the attachment point on the lower-torso segment, can be specified arbitrarily by the user.

The torso harness restraint consists of two individual straps: an upper strap attached to a fixed point on the upper torso segment and a lower strap attached to a fixed point on the upper-, mid-, or lower-torso segment. Unlike for the lap belt, the two segments of the torso harness are independent pieces of webbing. Each extends from an anchor point positioned arbitrarily in the vehicle to an attachment point fixed on a torso element. Thus, a "no-slip" condition is assumed at the torso for each belt segment, and entirely independent belt tensions are calculated for the two segments. There is no necessity to define equivalent webbing properties for the two segments. Indeed, specification of different force-producing characteristics for these two segments is a means sometimes used for simulating slipping and friction for the torso restraint of the three-belt submodel. It is also possible to simulate belt slipping by allowing the body segment to deform together with the belt at the attachment point. Thus, the attachment point is made to relax, in a sense, in the direction of the applied belt tension.



$$\delta = l(t) - l_0$$

$$\epsilon = \frac{l(t) - l_0}{l_0}$$

FIGURE 9-3 Definition of Belt Deflection

SLIDE 9-3

### SLIDE 3

Loading curves for the three pieces of webbing may be prescribed either as force-deflection relations or force-strain relations. The type of specification must be the same for all belts in the system. Whether force-deflection or force-strain relations are used generally depends on the form of available data.

For determination of belt forces, belt deflection is defined as the difference between stretched belt length and the length of the taut, but unstretched, webbing. For each belt in the three-belt system, the input parameters pertinent to determination of belt deflection are the unstretched webbing length  $\ell_0$ , the initial slack  $\Delta$ , and the vehicle coordinates and body segment coordinates, respectively, of the belt anchor and the attachment point on the body. These values do not over-specify the belt geometry, as might be thought, because the defined belt length  $\ell_0$  should not in general be a projection onto the x-z plane but rather is the total belt length in three dimensions. The specification of both unstretched belt length and initial slack along with initial endpoint coordinates allows calculation by the computer model of the proper initial "out-of-plane" component of webbing length, O.P.C. in the figure. The stretched belt length  $\ell(t)$  is calculated as the straight-line distance in the x-z plane between the instantaneous positions of the belt anchor and attachment point plus the constant value determined for the initial out-of-plane length.

Since the input constant  $\ell_0$ , the unstretched belt length, includes the out-of-plane component by definition, the belt deflection at time  $t$  is  $\ell - \ell_0$ . The strain is defined as the ratio of belt elongation to total initial belt length, as shown by the equation with the figure.

For the second optional belt restraint-system submodel, which will be discussed later, required inputs relating to belt lengths are the same except that out-of-plane length is specified instead of the total, unstretched belt length.

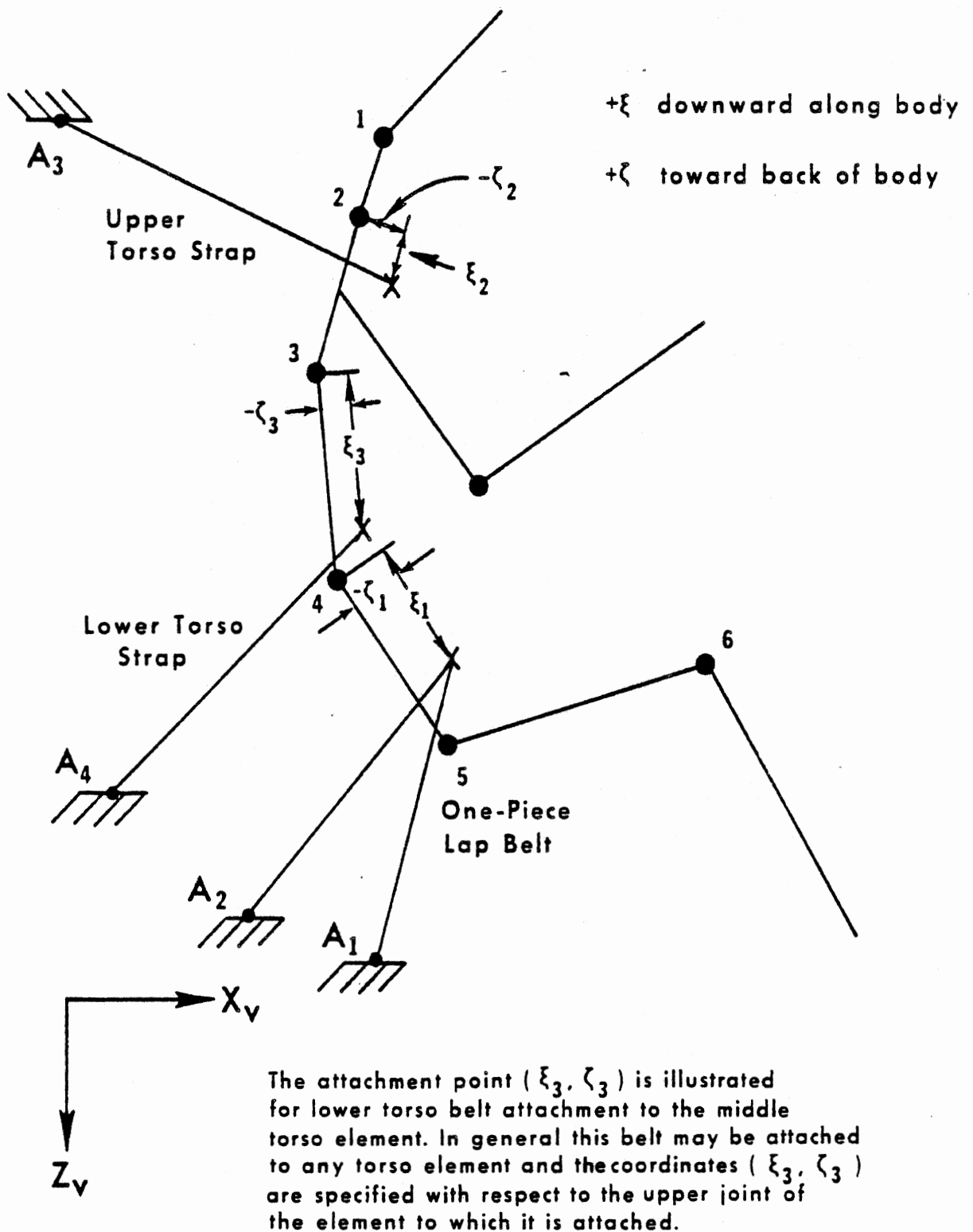


FIGURE 9-4 Three-Belt System Geometry

SLIDE 9-4

#### SLIDE 4

This figure illustrates belt geometry for the three-belt submodel. All belt anchor points, shown as  $A_1$ ,  $A_2$ ,  $A_3$ , and  $A_4$ , are prescribed by the user in the vehicle coordinate frame. Anchors 1 and 2 are interchangeable; either may be considered the inboard or outboard lap belt anchor. The three belt attachment points are defined relative to body joints by  $\xi$ - $\zeta$  coordinates. The upper torso-harness strap must be attached to the upper torso element and the lap belt attachment must be on the lower torso element. The lower torso-harness strap, however, may be attached to any desired torso element. The point  $(\xi_3, \zeta_3)$  is illustrated in the figure for attachment to the middle torso element. For the belt-restraint submodel which will be discussed later, belt attachment points on the occupant are specified in the same manner except that the coordinate perpendicular to the link line is positive toward the front of the body.

## BELT MATERIAL PROPERTIES

- Loading curves as functions of deflection or strain
- Unloading characteristics
  - Permanent deformation as function of maximum deformation
  - Hysteretic energy absorption
- Belt-failure characteristics

SLIDE 9-5

## SLIDE 5

Loading curves for belts, whether in terms of deflections or strains, may be defined either in polynomial or tabular form. Specification of loading curves is described in detail in Module 6, Part 1, and will not be discussed here. Both static and "inertial spike" loading curves may be assigned for belt materials, and unloading characteristics may be prescribed in terms of deflection-dependent "G- and R-ratios," which determine permanent deformation and restored energy upon complete unloading.

Three input parameters unrelated to the specified loading curves pertain to belt failure of the three-belt system. Two are the lap-belt and torso-belt breaking forces. The third is the time duration for belt failure, which ensures that after a belt force exceeds its breaking level the force will be reduced gradually to zero. A value of 1. ms is often used. The belt-failure mechanism can be defined alternatively by specifying the webbing loading curves so that loads reduce to zero after breaking deflections, or strains, are reached. Only this latter method can be used for the second optional belt system.

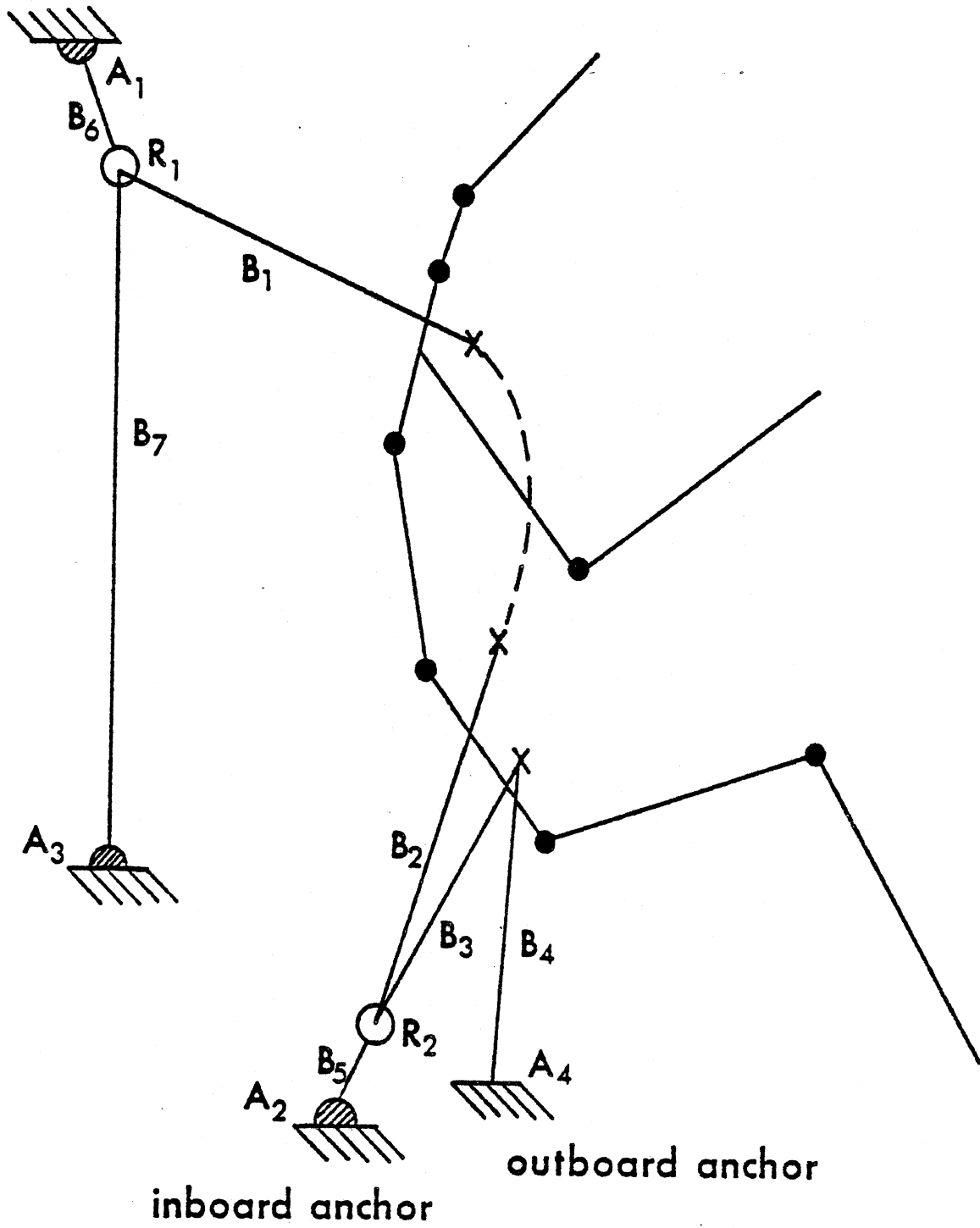


FIGURE 9-6 Advanced Belt System

SLIDE 9-6



## SLIDE 6

Whether or not belt restraint-system data are present in a data set for an MVMA 2-D simulation, a belt-system control switch must be properly set. If the switch value is 0., then no belt forces will be determined even though the data set may include cards with belt-system specifications. A value of 1. or 2. indicates that the three-belt submodel is to be used. If a 1. is entered, then only lap-belt forces will be determined. Lap-belt and shoulder-harness forces will all be determined if a 2. is entered. This switch should be set to 3. whenever belt forces are to be determined for the so-called "advanced belt-system submodel."

A schematic of this second optional belt-restraint system is shown. It includes the following features: a) seven belt segments which may be independent or, at option, may be paired in certain combinations to act as a lesser number of separate lengths of webbing by use of various free slipping and friction elections at the torso and lap and at slip points; b) a slip point in the three-belt upper harness system; c) a slip point between the lower torso and lap sections; d) optionally, inertia reels, either vehicle-sensitive or webbing-sensitive, at three of the four anchor locations.

The anchor  $A_4$  cannot have an inertia reel; the outboard lap belt segment, if present, fastens securely to this anchor. Here, and on slides to follow, a solid semi-circle at an anchor position indicates an optional inertia reel.

The system includes two slip points where three belt segments come together. One is in the upper harness system and one is between the lower-torso and lap sections. The slip points are shown as open circles, rings  $R_1$  and  $R_2$ . The rings may be fastened to ring straps, which lead to anchors  $A_1$  and  $A_2$ , or they may be fixed to the vehicle

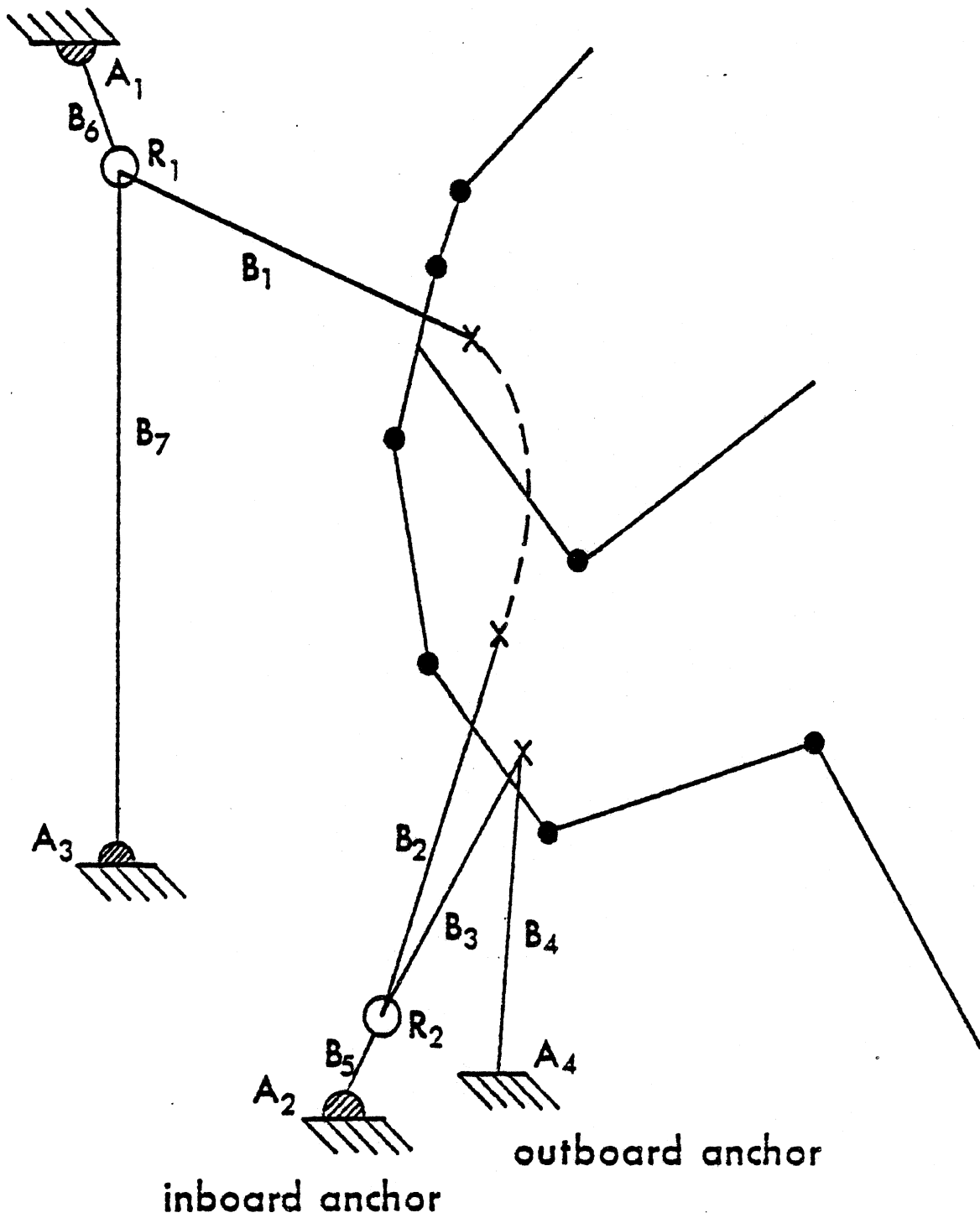


FIGURE 9-6 Advanced Belt System

SLIDE 9-6

frame at anchor locations  $A_1$  and  $A_2$ , in which case the corresponding ring straps,  $B_6$  and  $B_5$ , are absent. Belt segments  $B_5$  and  $B_6$  are always "independent" of other belt segments since they fasten to the slip rings. Through each ring, however, passes a strap of webbing shown in the figure as a pair of belt segments, either  $B_1$  and  $B_7$  or  $B_2$  and  $B_3$ . At option, the members of these pairs can be made independent by prohibiting slipping of the combined strap through the ring. In this case the ring location is a juncture of three independent straps of webbing. The pairs  $B_1$ - $B_7$  and  $B_2$ - $B_3$ , however, may be considered common straps that may slip freely through their respective rings or with an amount of frictional resistance which depends on the resultant normal force at the ring. The tension in any one-piece segment pair is determined from the total deflection, or total strain, of the combined lengths of webbing.

Various possibilities for combinations of anchor type and type of belt-segment interaction at a ring are illustrated in the next two slides.


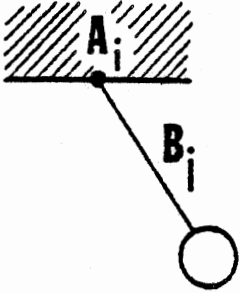
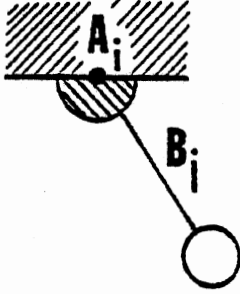
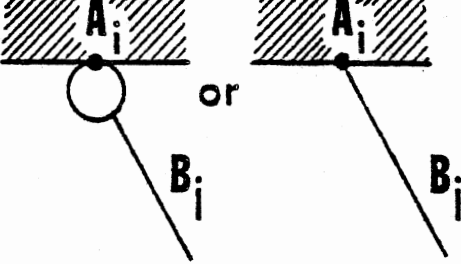
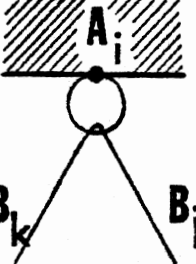
SCHEMATIC	ANCHOR TYPE DESIGNATION	ALLOWED INDEX VALUES
 <p style="text-align: center;">no belt</p>	ANCHOR <sub>i</sub> = 0	i = 1, 2, 3, 4
	ANCHOR <sub>i</sub> = 1	i = 1, j = 6 i = 2, j = 5 i = 3, j = 7 i = 4, j = 4 (no ring)
	ANCHOR <sub>i</sub> = 2	i = 1, j = 6 i = 2, j = 5 i = 3, j = 7
	ANCHOR <sub>i</sub> = 3	i = 1 or 3, j = 1, RING <sub>1</sub> = 1 i = 2, j = 2 and/or 3, RING <sub>2</sub> = 1
	ANCHOR <sub>i</sub> = 3	i = 1, j = 1, k = 7, RING <sub>1</sub> = 2 or 3 i = 2, j = 2, k = 3, RING <sub>2</sub> = 2 or 3

FIGURE 9-7 Belt Anchor Type Designation for Anchor "i"

SLIDE 7

For each anchor, an anchor type designation must be made, and for each ring, a ring type designation is made.

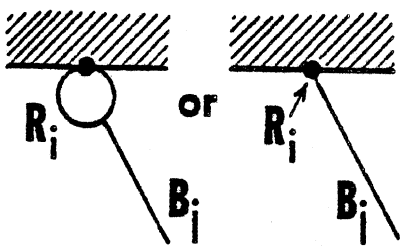
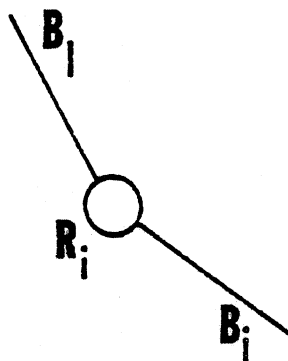
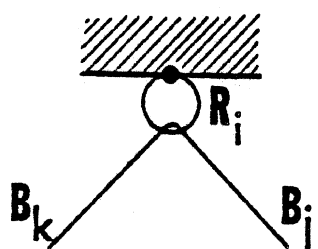
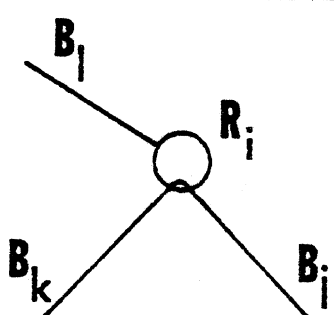
SCHEMATIC	RING TYPE DESIGNATION	ALLOWED INDEX VALUES
	RING <sub>i</sub> = 1	$i = 1, j = 1, \text{ANCHOR}_1 = 3$ $i = 2, j = 2 \text{ or } 3, \text{ANCHOR}_2 = 3$ $i = 2, j = 2 \text{ and } 3, \text{ANCHOR}_2 = 3$
	RING <sub>i</sub> = 1	$i = 1, j = 1, l = 6, \text{ANCHOR}_1 = 1 \text{ or } 2$ $i = 1, j = 1, l = 7, \text{ANCHOR}_3 = 1 \text{ or } 2$ $i = 1, j = 1, l = 6 \text{ and } 7, \text{ANCHOR}_1 \text{ and } \text{ANCHOR}_3 = 1 \text{ or } 2$ $i = 2, j = 2, l = 5, \text{ANCHOR}_2 = 1 \text{ or } 2$ $i = 2, j = 2, l = 3 \text{ and } 5, \text{ANCHOR}_2 = 1 \text{ or } 2$
	RING <sub>i</sub> = 2 or 3	$i = 1, j = 1, k = 7, \text{ANCHOR}_1 = 3 \text{ (or } 0)$ $i = 2, j = 2, k = 3, \text{ANCHOR}_2 = 3$
	RING <sub>i</sub> = 2 or 3	$i = 1, j = 1, k = 7, l = 6, \text{ANCHOR}_1 = 1 \text{ or } 2$ $i = 2, j = 2, k = 3, l = 5, \text{ANCHOR}_2 = 1 \text{ or } 2$

FIGURE 9-8 Designation of Ring-Belt Relationship for Slip Point "i"

SLIDE 9-8

SLIDE 8

(pause)

## INTERBELT INFLUENCE OPTIONS

- Normal-Force Friction
  - Static coefficient of friction
  - Sliding coefficient of friction
- Force Difference Saturation
  - Maximum allowed difference between belt segment tensions (saturation force difference)
- Percentage Influence
  - Designation of "influencing belt"
  - Positive or negative fractional force-adjustment coefficient
  - Maximum force-adjustment bound

SLIDE 9-9



## SLIDE 9

The upper and lower torso belts,  $B_1$  and  $B_2$ , may be made independent. Or, optionally, free slipping can be modeled through use of a force-equalization option for torso-belt or lap-belt pairs. This option for the advanced belt system is identical to the standard treatment of the combined two-segment lap belt discussed earlier for the three-belt submodel.

In general, however, friction and belt-system geometry factors lead to unequal belt tensions. Three optional methods are available to allow the tension in one torso belt to influence the tension in the other. These are called "interbelt influence options," and they will now be described.

The first interbelt influence option is intended to simulate the effect of static and sliding friction between belts and the occupant. This is done by allowing the torso-belt pair to "relax," in effect, toward the belt segment of greater tension. Normal-force friction effects are approximated from an estimate of the normal force where the webbing is in contact with the occupant. Two system parameters prescribed by the user for this option are static and sliding coefficients of friction for the belt-occupant interface. The static friction coefficient is in general at least as large as the sliding friction coefficient although this is not a requirement. Free slipping results if both coefficients are specified as zero. A non-slip condition is guaranteed by specifying a very large value for the static coefficient.

An interbelt influence option can be selected which will simulate the effect of belt friction in an entirely different manner. Here, a "saturation force difference" is prescribed by the user for the torso belt pair. Whenever the difference in tension between the two belts exceeds this force saturation value, the greater of the forces is reduced by an amount such that the difference in tensions is equal to the saturation value. The tension in the other belt is unchanged. This adjustment of the force difference is intended to represent partial slipping against static friction. The only quantity that the user must define if this option is used is the value for the saturation force difference.

## INTERBELT INFLUENCE OPTIONS

- Normal-Force Friction
  - Static coefficient of friction
  - Sliding coefficient of friction
- Force Difference Saturation
  - Maximum allowed difference between belt segment tensions (saturation force difference)
- Percentage Influence
  - Designation of "influencing belt"
  - Positive or negative fractional force-adjustment coefficient
  - Maximum force-adjustment bound

SLIDE 9-9

The third interbelt influence option allows the user to specify a positive or negative fraction of the tension of one torso belt which will be applied as an additive adjustment to the tension of the other. Thus, one belt is designated by the user as an "influencing belt." Its tension is not adjusted, but it determines the adjustment to the other belt of the pair. In conjunction with this option, the user supplies a "maximum influence-force bound." If the force adjustment, in absolute value, is greater than this bound, then the bound itself is applied as the adjustment. The "percentage influence" option is more artificial than the other torso interbelt influence options, but it has nevertheless found useful application.

## INERTIA REELS

- At any anchor except outboard lap
- Vehicle-sensitive reel
  - Locks at specified time, or
  - Locks when inertial acceleration or vehicle pitch exceeds specified limit
- Webbing-sensitive reel
  - Locks when rate of belt feedout exceeds specified limit, or
  - Locks when acceleration of belt feedout exceeds specified limit

SLIDE 9-10

## SLIDE 10

This slide summarizes the input data requirements of a model feature which has been mentioned briefly -- inertia reels.

Any anchor except for the outboard lap-belt anchor may have an inertia reel of either the vehicle-sensitive or webbing-sensitive type. A vehicle-sensitive reel can be made to lock at some specified time, or alternatively, when either of two conditions occurs: a) the resultant inertial acceleration at the anchor location exceeds, in absolute value, a specified limit; or b) vehicle pitch exceeds, in absolute value, a specified limit. A webbing-sensitive reel will lock either when the rate of belt feed-out or the acceleration of belt feed-out exceeds a specified limit. Once a reel of either type locks it will remain locked for the duration of the crash history.

## **SLIP POINT PARAMETERS**

- **Controls for force-balance iteration**
- **Ring type designation**
- **Anchor type designation**
- **Coefficients of friction for belts slipping through rings**

**SLIDE 9-11**

## SLIDE 11

Finally, a few additional points are made here relative to the upper and lower slip points, rings  $R_1$  and  $R_2$  in foregoing slides. The rings, if present, are fixed to the vehicle frame or fastened to the end of ring straps,  $B_5$  and  $B_6$ . If a ring is not anchored to the vehicle, then its location at any value of time is determined by the condition that x- and z-forces at the ring location sum to zero. This involves solving simultaneous nonlinear equations for the ring coordinates, and some of the required input data are specifications for the numerical solution algorithm. Guidance in selecting values for the less obvious of these parameters, such as controls for an iteration process by which a force balance is determined, is provided with the text for Module 9.

A primary characteristic of the rings is that the webbing straps passing through them can be allowed to slip either freely, or with a desired amount of frictional resistance, or not at all. In addition to ring type and anchor type designations, which were illustrated in two foregoing slides and are explained fully in the text, pertinent input quantities are coefficients of friction for belt slipping at the two rings.

## SUMMARY OF DATA REQUIREMENTS FOR BELT-SYSTEM SUBMODELS

### THREE-BELT SYSTEM and ADVANCED BELT-SYSTEM SUBMODEL:

- Anchor locations
- Body attachment locations
- Initial belt slacks
- Unstrained belt lengths or out-of-plane components
- Webbing properties for either strain or deflection deformation

### ADVANCED BELT-SYSTEM SUBMODEL only:

- Seven optional belt segments
- Anchor "type" designation
- Ring "type" designation
- Inertia reel characteristics
- Interbelt influence options
  - Normal-force friction
  - Force difference saturation
  - Percentage influence
- Slip ring friction
- Force-balance iteration controls

SLIDE 9-12



## SLIDE 12

In summary, the MVMA 2-D Crash Victim Simulator includes two independent belt system models for optional usage. These are a three-belt system and a more complex system that may have up to seven belt segments. Many of the data requirements for these two submodels are basically similar. These include anchor locations in vehicle coordinates, belt segment attachment points on torso elements, initial belt slacks, unstrained belt lengths or out-of-plane components, and either force-strain or force-deflection webbing properties. Data requirements specific to the advanced belt-system submodel include a description of overall system design by designation of: 1) belt segments present in the system; 2) anchor "types"; and 3) upper and lower slip ring "types." For any inertia reel present in the system, various specifications must be made. Three optional methods are available for simulating slipping and friction effects for the torso-belt pair. These are the so-called "interbelt influence options." Each requires different input data. Finally, coefficients of friction are needed for belts slipping through the slip rings and, in the case that a ring is present but not fixed to the vehicle frame, force-balance iteration controls are required.



**MVMA 2-D**  
**CRASH VICTIM SIMULATION**

**\* \* \***

**MODULE 10**

**AIRBAG RESTRAINT SYSTEM**

**MVMA 2-D**  
**CRASH VICTIM SIMULATION**

**\* \* \***

**MODULE 10**

**AIRBAG RESTRAINT SYSTEM**

**SLIDE 10-1**

## MODULE 10 -- AIRBAG RESTRAINT SYSTEM

### SLIDE 1

An airbag submodel may be used optionally with the MVMA 2-D Crash Victim Simulator. The estimation of bag forces is based on solution of the differential equations of gas thermodynamics. The airbag can contact both the occupant and vehicle interior. Restraining forces due to the internal pressure and skin tension are generated when the bag is fully inflated. The shape of the bag is allowed to conform to that of the occupant and the vehicle interior with free sections of the perimeter defined as circular segments. When the pressure in the bag reaches a specified level, gas is allowed to flow out of the bag through defined orifices.

## SUMMARY OF ASSUMPTIONS IN AIRBAG SUBMODEL ANALYSIS

- The occupant feels constraint forces only after bag is fully expanded.
- The skin of the bag does not stretch.
- The bag cross-section perimeter is circular except where it conforms to the shape of the vehicle interior or to the occupant.
- Tangential bag forces are negligible.
- Adiabatic expansion of ideal nitrogen is assumed.
- Bag pressure does not affect the rate of inflation, which is specified by the user.
- The attachment point is fixed in the occupant compartment.
- The effect of skin tension can be approximated from bag pressure, occupant width, and depth of penetration into the bag.

FIGURE 10-2 Summary of Assumptions in Airbag Submodel Analysis

SLIDE 10-2

## SLIDE 2

The approach chosen for developing an analytical submodel for inflatable occupant restraints was to produce the simplest model that would provide acceptable agreement with experimental data. Assumptions made in the formulation of the analytical model were based upon both analysis of the physical processes involved and observation of high-speed movies of tests of prototype inflatable safety restraints. User experience with the model may suggest alteration of some of the assumptions or generalization of some of the algorithms used to cover a wider variety of physical situations. Observation of high-speed movies of tests led to three assumptions.

First, no restraint force is exerted upon the occupant until the occurrence of full bag inflation, which is defined as the condition in which the calculated perimeter of the deformed or undeformed bag equals the specified filled-bag perimeter. This is equivalent to stating that the mass of the bag and its contents can be neglected.

Second, the skin of the bag does not stretch.

Third, the perimeter of the bag cross section in the plane of motion conforms to the shape of the automobile interior or to the occupant wherever they touch. Elsewhere the perimeter is described by circular arcs.

## SUMMARY OF ASSUMPTIONS IN AIRBAG SUBMODEL ANALYSIS

- The occupant feels constraint forces only after bag is fully expanded.
- The skin of the bag does not stretch.
- The bag cross-section perimeter is circular except where it conforms to the shape of the vehicle interior or to the occupant.
- Tangential bag forces are negligible.
- Adiabatic expansion of ideal nitrogen is assumed.
- Bag pressure does not affect the rate of inflation, which is specified by the user.
- The attachment point is fixed in the occupant compartment.
- The effect of skin tension can be approximated from bag pressure, occupant width, and depth of penetration into the bag.

FIGURE 10-2 Summary of Assumptions in Airbag Submodel Analysis

SLIDE 10-2



Five other assumptions were made to simplify the model.

First, tangential forces between the occupant and the bag are assumed negligible in comparison with normal forces.

Second, thermodynamic properties of the gas in the bag are calculated using adiabatic expansion of ideal nitrogen, neglecting potential energy of the gas. Flow of gas through the deflation membranes is calculated assuming unchoked flow through a converging nozzle.

Third, bag pressure does not affect the rate of inflation by the gas generator, which delivers gas at a predetermined rate. This implies that the area of the cross section of the bag increases at a predetermined rate until the bag is filled.

Fourth, the point at which the bag attaches to the automobile interior is fixed with respect to the interior. This means that the bag may not be attached to a collapsible steering column.

Fifth, restraint force due to tension in the skin of the bag, caused primarily by the bag wrapping around the sides of the occupant, is approximated by a simple algorithm which takes into account the most important variables: pressure in the bag, width of the occupant and depth of penetration into the bag.

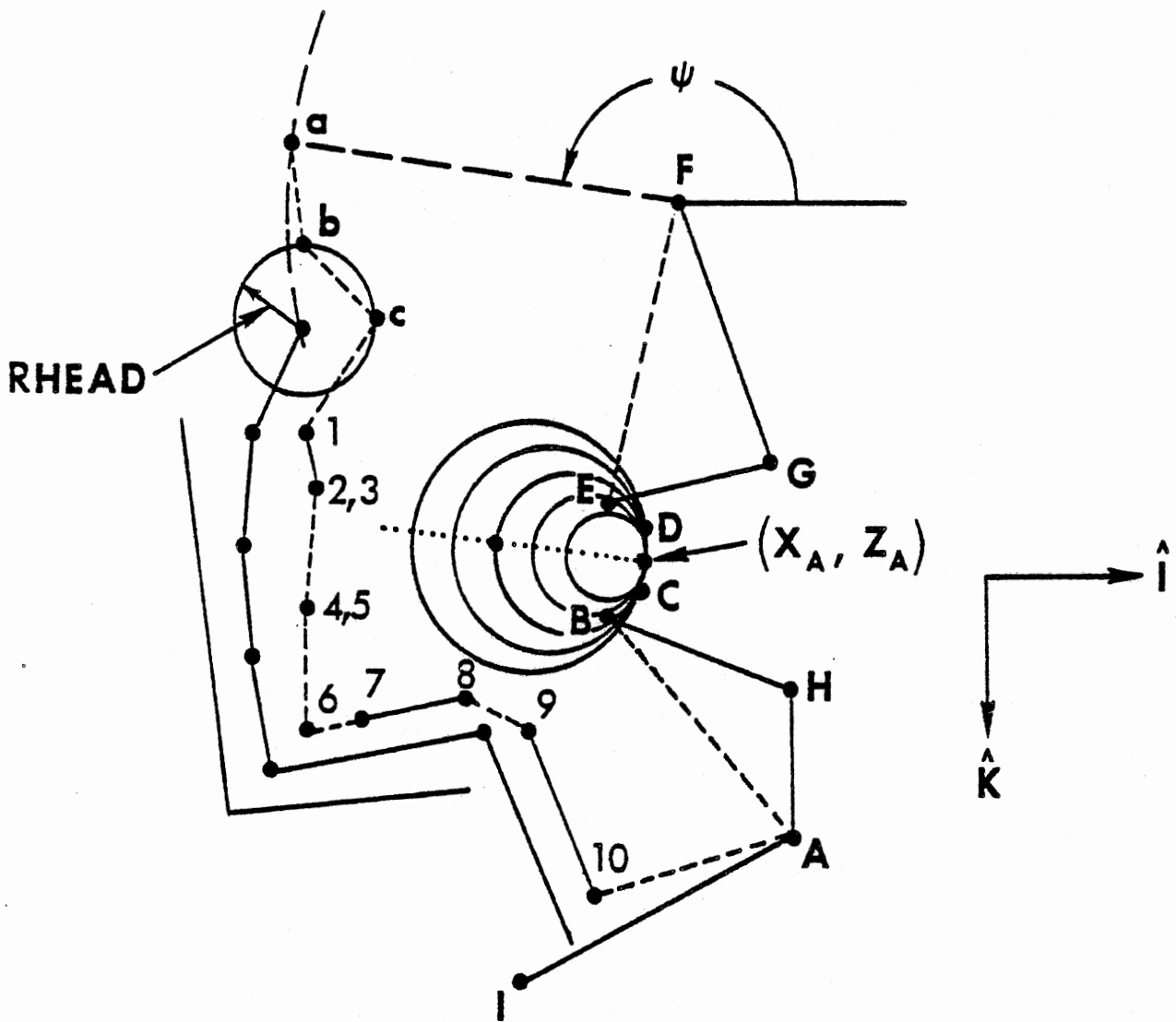


FIGURE 10-1 MVMA 2-D Airbag Model

SLIDE 10-3

### SLIDE 3

The airbag expands within a closed area illustrated in the figure. The area is defined by: a) five user-prescribed straight-line segments, 1-2, 2-4, 4-6, 7-8, and 9-10, attached, respectively, to the upper torso, middle torso, lower torso, upper legs, and lower legs; b) calculated straight-line segments joining the endpoints of the five primary line segments; c) two calculated straight-line segments approximating the front of the head; d) from one to five user-prescribed frontal-interior line segments; 3) a roof line extending to above and behind the head; and f) two calculated line segments, a-b and 10-A, which close the area. The dimension labeled "RHEAD" is a user-prescribed value for average head radius. It is used for determining the line segments bc and cl which approximate the front of the head.

The bag source may be arbitrarily positioned within the passenger compartment; for example, on the instrument panel. This point is shown as  $(X_A, Z_A)$  in the figure, and it is fixed in the vehicle. It cannot move either with the steering assembly system or with any part of the vehicle interior. The airbag will, however, react against line segments which define a frontal interior profile. This profile is comprised of from one to five connected line segments generated from two to six points specified by the user. The profile for airbag contact is normally identical to the profile of instrument panel lines defined for interaction with the vehicle occupant. The figure, however, illustrates a bag-sensing profile which is less detailed than the occupant-sensing profile. Entries on data cards for the occupant-sensing profile define points A, B, C, D, E, F and thus the line segments AB, BC, CD, DE, and EF. These five segments, the maximum number allowed, can only approximate the occupant-sensing profile, shown by solid lines. Since this profile is a reaction surface for the airbag, the user should make the approximation to the true interior line most accurate near the bag source. All vehicle-interior line-segment endpoints can be prescribed as functions of time, and the airbag will sense any collapse of the lines AB, BC, CD, DE, and EF about it. These lines are sensitive only to airbag contact while the example vehicle-interior configuration defined by FGEDCBHAI is sensitive only to interaction with contact ellipses.

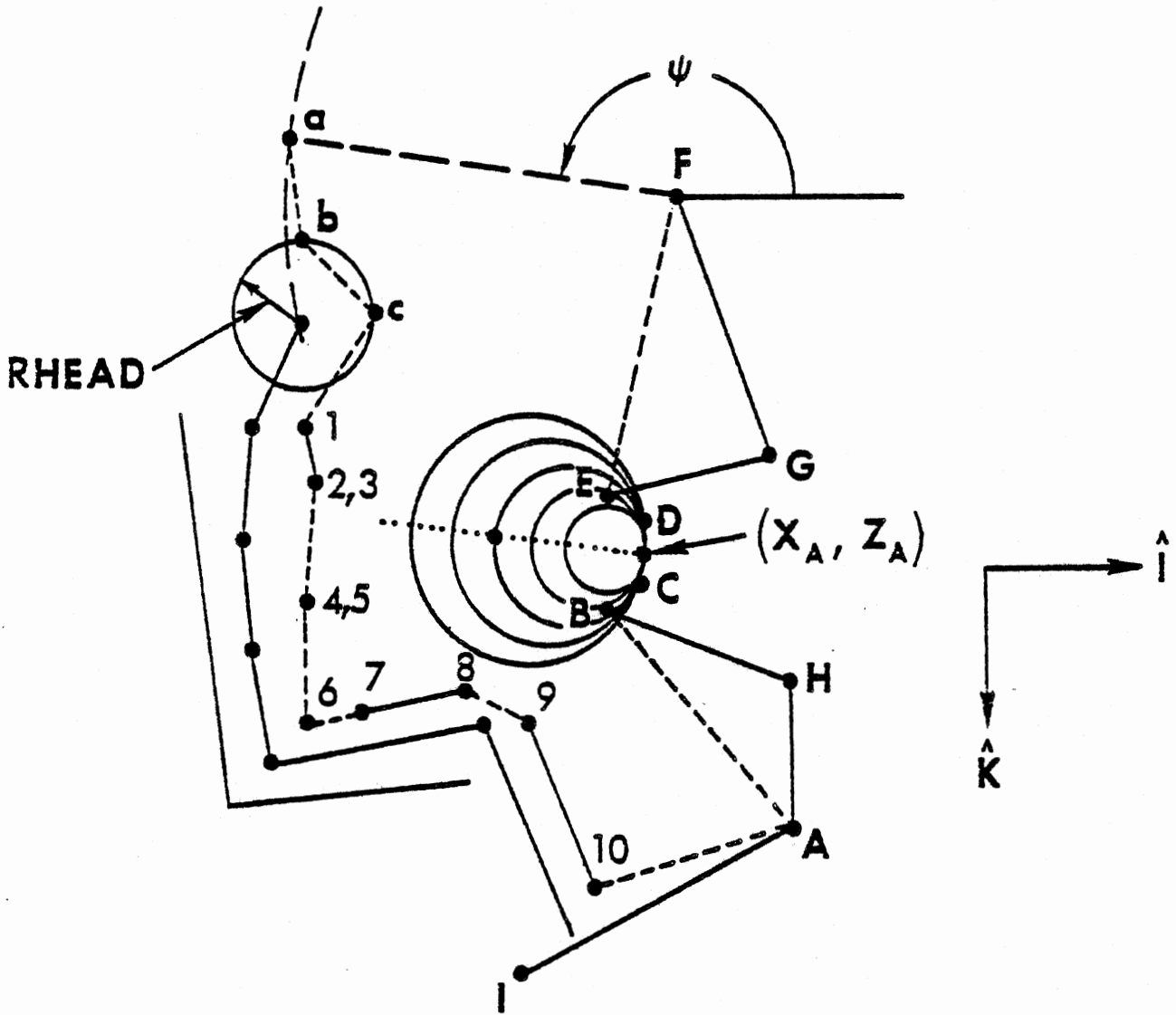


FIGURE 10-1 MVMA 2-D Airbag Model

SLIDE 10-3

Airbag forces and moments are applied to the occupant at segments C-1, 1-2, 3-4, 5-6, 7-8. These forces are the sum of elemental forces from elemental areas of contact between the bag and the occupant. Each elemental force is made up of two parts: one caused by pressure inside the bag and the other by tension in the bag skin. The first of these is calculated from the elemental length of bag contact, the width of the occupant at that point, and the pressure in the bag. The skin tension force results from the tendency of the bag to wrap around the sides of the occupant.

A vector heading must be specified to define an axis along which the bag center progresses as the bag becomes an ever-expanding circle. This axis is illustrated in the figure as the dotted line extending inward from line segment DC. The heading angle remains constant until contact occurs with bounding segments of the closed area in which the airbag expands. After such contact, the heading of the bag center motion is adjusted in order to balance z-direction forces on the bag.

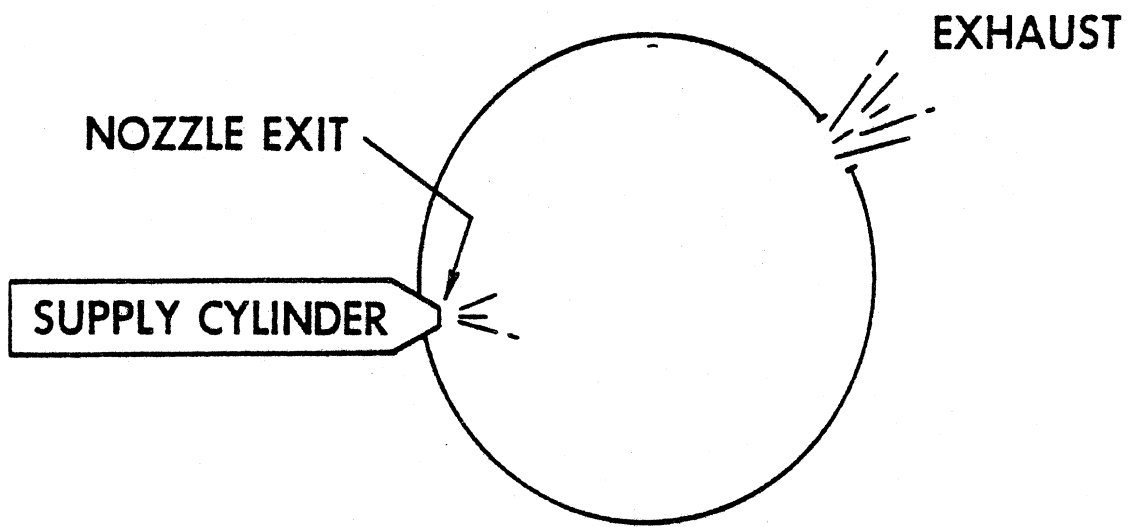


FIGURE 10-4 Supply Cylinder and Bag

SLIDE 10-4

#### SLIDE 4

The airbag is inflated at a time-dependent rate specified by the user; inlet mass flow rate is a tabular input to the simulation. Supply gas temperature is similarly specified in tabular form as a function of time. Energy absorption by the bag results by either or both of two means, controllable by the user. First, exhaust gas may be vented through user-defined orifices, as illustrated here. Second, the venting of gas over the surface of the bag may be simulated by defining the porosity of the bag fabric. For the first of these deflation mechanisms, the user specifies area of a deflation membrane and the pressure differential necessary to rupture it. Explicit assumptions made in the calculation of the exhaust mass flow rate are: 1) that unchoked flow through an orifice occurs with no losses, that is, with a value of 1 for the orifice discharge coefficient; and, 2) that the bag has two deflation orifices. Since the exhaust mass flow rate is directly proportional to the discharge coefficient and to the area of a deflation membrane, the user may effectively adjust the pre-assumed values for discharge coefficient and number of orifices by adjusting the value for deflation membrane area appropriately.

For the second optional method, venting gas through porous bag fabric, the user is required to specify bag porosity as a tabular function of pressure differential. The two deflation mechanisms may be combined in any crash simulation. But if it is desired to use only bag-porosity deflation, it is necessary to ensure against gas loss through the deflation orifices, which are an integral feature of the airbag model. This may be done by specifying an unrealistically large value for the pressure differential necessary to burst a deflation membrane or by setting the deflation membrane area equal to zero.

## OTHER USER-PRESCRIBED PARAMETERS

- Airbag "fire" time
- Bag perimeter when fully inflated
- Out-of-plane bag width
- Out-of-plane widths for occupant
- Gas constant, specific heat at constant pressure, and ratio of specific heats for source gas
- Exhaust pressure (one atmosphere)

SLIDE 10-5



SLIDE 5

Values for various quantities not mentioned so far, or mentioned only in passing, must be prescribed by the user. These include the bag fire time. Also, the perimeter of the bag when fully inflated and the bag width, that is, the out-of-plane dimension, must be specified. Other out-of-plane widths required are for the head, shoulders, torso, hip, and thighs. Quantities for which standard handbook values are normally specified are the gas constant for the source gas, and also the specific heat at constant pressure and the ratio of this value to the specific heat at constant volume. For real gases, the specific heats and also their ratio are dependent on temperature, but for the temperature range likely for airbag simulations, a mean ratio of 1.4 is accurate for either nitrogen or air. Finally, the exhaust pressure is specified. This is normally one atmosphere.



## SLIDE 6

Bag forces on the occupant result from interaction of the airbag with the occupant profile, mentioned previously as a section of the boundary of the closed area in which the airbag expands. This occupant profile is a series of straight-line segments. The user specifies the locations of eight points on the occupant frontal profile, each fixed with respect to some body link as illustrated. The coordinates  $\xi_i$  and  $\zeta_i$ , with "i" equal to 1, 2, 4, 6, 7, 8, 9, and 10, define these points. It is clear that as articulation occurs at body joints, any successive points of this group that are not defined with respect to the same body link will undergo relative motion. Solid line segments in the contact line profile are fixed in length and orientation by the input data. Dashed lines will vary in both length and orientation with respect to all body links; these are determined by the computer model from the input data so as to make the contact profile continuous.

## SUMMARY OF DATA REQUIREMENTS FOR AIRBAG SUBMODEL

- Bag "fire" time
- Bag source fixed in vehicle
- Vector heading for initial expansion of bag
- Inlet mass flow rate, function of time
- Supply gas temperature, function of time
- Thermodynamic constants for source gas
- Perimeter for fully-inflated bag
- Occupant profile for airbag contact
- Frontal-interior line segments for interaction with airbag
- Out-of-plane bag and occupant widths
- Deflation membrane parameters
- Bag fabric porosity, function of pressure differential

SLIDE 10-7

## SLIDE 7

Many quantities must be prescribed for simulations which use the airbag submodel. Most are included in this summary of data requirements. The bag fire time is specified by the user and the circular airbag issues from a source point, fixed in the vehicle, in a specified initial direction. Inlet mass flow rate and supply gas temperature are specified in tabular form as functions of time. Also, several thermodynamic constants are prescribed for the source gas, and the perimeter for the fully-inflated bag is required. Quantities directly pertinent to establishing airbag contacts and resulting forces include an occupant profile, a frontal-interior profile of the occupant compartment, and out-of-plane bag and occupant widths. Bag deflation may occur either through ruptured deflation membranes or over the surface of the bag through porous bag fabric.



**MVMA 2-D**  
**CRASH VICTIM SIMULATION**

**\* \* \***

**MODULE 13**

**EXAMPLE CRASH SIMULATIONS**

**MVMA 2-D  
CRASH VICTIM SIMULATION**

**\* \* \***

**MODULE 13**

**EXAMPLE CRASH SIMULATIONS**

**SLIDE 13-1**



## MODULE 13 -- EXAMPLE CRASH SIMULATIONS

### SLIDE 1

The purpose of this module is to give the user of the Tutorial System a "hands-on" feeling for input data sets required for exercising the MVMA 2-D Crash Victim Simulator and for the output which is generated. Data decks are described and assembled in this module for the following two simulations:

1. a 30-mph frontal barrier crash with vehicle interior deformation and a dummy passenger restrained only by a knee bar; and,
2. a crash with similar occupant and vehicle configurations except that the occupant is restrained additionally by a torso harness.

## Arbitrary Decomposition of MVMA 2-D Data Set Into Subsets

DATA SUBSET	CARD NUMBERS
Title Cards	100, 200, ..., 900
General Controls for IN and GO	101, 102, 103
Debugging Printout Controls	104, 105
Categories of Output Variables to be Stored	107 - 111
Vehicle Motion	601 - 604
Occupant Description	201 - 242
Occupant Position	217, 301-304
Vehicle Interior	401 - 411
Friction Characteristics	412
Allowed or Disallowed Contact Interactions	106
Belt Restraint System	218, 501, 701-723
Airbag Restraint System	901 - 909
End of Data Deck for INP	1000
Categories of Output Variables to be Printed	1001, 1002
HIC, Femur Loads, and Filtering	1003, 1004
Potential Injury Indicators	1100 - 1401
Printer-Plot Stick Figure Time Sequence	1500 - 1502
End of Data Deck for OUTP	1600

FIGURE 13-1 Arbitrary Decomposition of MVMA 2-D Data Set Into Subsets

SLIDE 13-2

## SLIDE 2

It is normally convenient to construct a data set card by card, beginning with Card 100 and proceeding through Card 1600. However, a complete data set also can be viewed as a collection of subsets which may be dealt with individually. In this module, discussion of the construction of data sets is in terms of eighteen largely independent subsets. These are identified in the slide. They include several which describe the occupant, the vehicle interior, restraint systems, and the crash acceleration or deceleration profiles. Others include controls for obtaining various types of printout, including those produced by post-processor functions of the model.

If various dependencies between some subsets are taken into account, subsets developed for different simulations can be assembled to yield complete data decks for new simulations. This approach often considerably simplifies the task of constructing a data deck. It also allows users to collect a library of possible data arrangements.

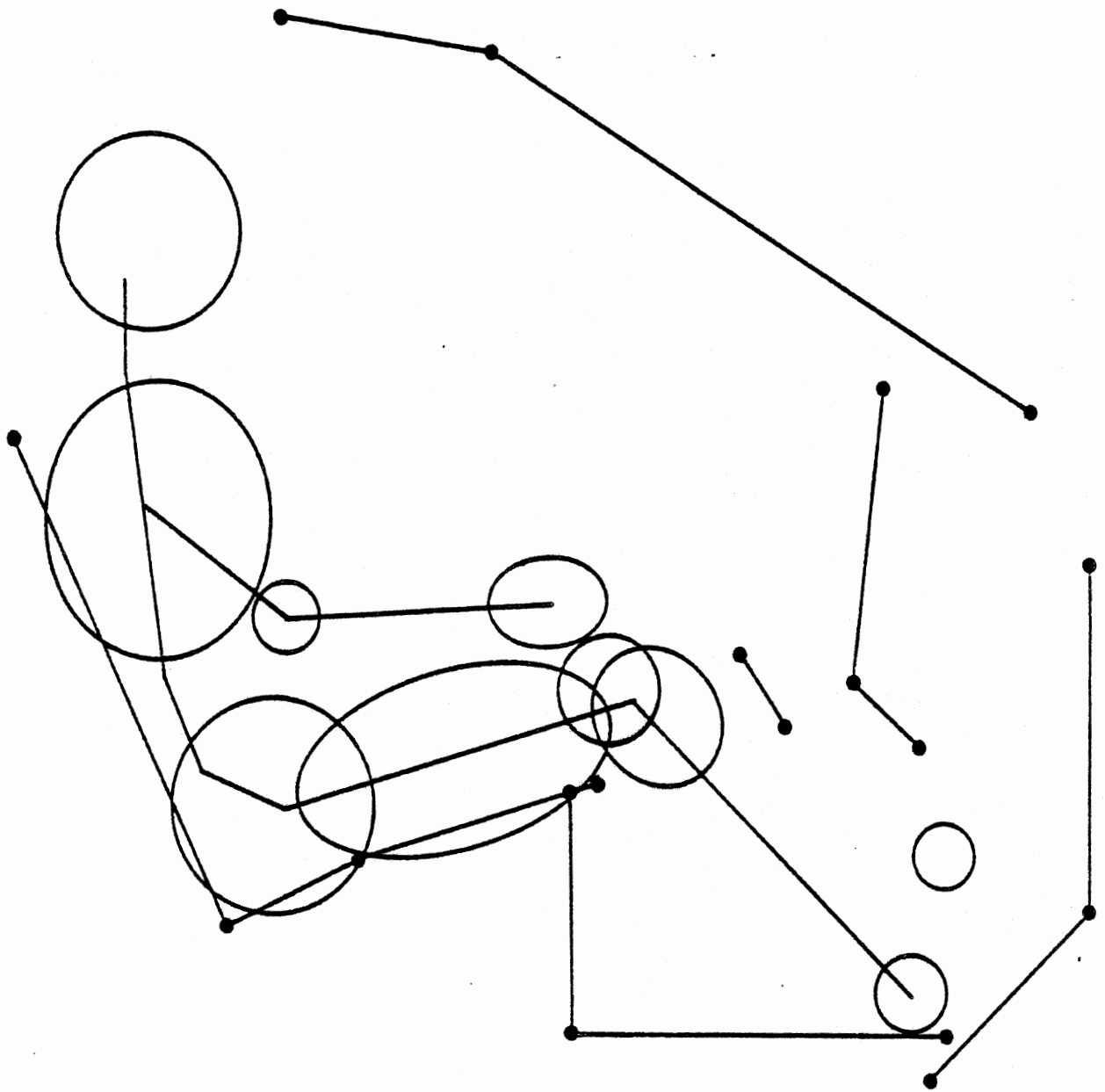


FIGURE 13-2 Occupant and Vehicle Interior Configuration for Example 1

SLIDE 13-3

### SLIDE 3

Construction of the data set for the first example simulation will now be discussed. Example 1 is a simulation of a 30-mph frontal barrier crash with a dummy passenger restrained only by a knee bar. The frontal portion of the vehicle interior displaces toward the occupant during the event, simulating intrusion. The occupant and vehicle interior configuration at crash onset are shown in the schematic.

	MVMA 2-D TUTORIAL EXAMPLE #1	
KNEE BAR		100
JCC. COMP. DISPL.		400
30MPH FRONT BARRIER		500
NO BELTS		500
		700

FIGURE 13-3 Title Cards for Example 1

1.	1.	32.174	0.	0.	200.	1.	5.	13.	101
0.	0.	0.	0.	0.	0.	10.	.000001	5.	102
.2	.05	100000.	15000.	10.	.05	10.	1.	1.	103

FIGURE 13-4 General Controls for IN and GO for Example 1

SLIDE 13-4

#### SLIDE 4

Title cards for this simulation are shown in the upper portion of this slide. Each page of output for a simulation is headed by such titles, supplied on Cards 100, 200, etc. - through 900. The 100-Card is for a "run title," which should be centered in the first 72 columns and which will appear on the first line of each page of print-out. The second line of page heading consists of the concatenated content of Cards 200 through 900. Each of these cards is normally used for description of a specific simulation characteristic. For example, the 700-Card normally describes the type of belt restraint system used. However, there are no restrictions on the content of these cards. The 19-column sub-title fields of Cards 200 through 700 plus the 17-column field of either Card 800 or Card 900 can be used together for any 131-character description of the simulation.

The title cards for Example I have been grouped together at the beginning of the data set except for the 200- and 300-cards, which have both been used for occupant description and are placed in the occupant data subset to be discussed later. Cards in data subsets which follow the title card subset in this example will, of course, have card identification numbers both higher and lower than those cards in the title card subset. Data cards can be positioned within the data deck in any order, without attention to card identification number. Exceptions to this are the 1000- and 1600-cards, which serve as "end-of-data-deck" markers and must be the last cards of the data decks for the Input and Output Pre-Processors, respectively.

A number of general controls are required for the operation of the Input and Execution Processors. These are on Cards 101, 102, and 103 and are illustrated in the lower portion of the slide. Some of the most important of these controls specify: 1) the system of units, either metric or English, for the simulation; 2) crash duration, integration time step, and time increment for printing of output; 3) use or non-use of the various restraint system options; 4) interpretation of "inhibition cards" for allowed or disallowed contact interactions; and 5) limits for the algorithm which determines shared-deflection force balance. The two examples used with this module are for 200 msec duration, one msec integration time step, and five msec printout interval. The simulations are made with English system data.

The cards shown here illustrate clearly the standard format of input cards for the MVMA 2-D Crash Victim Simulator -- nine fields of eight columns each and a card identification number in columns 73 through 80.

0.	44.	0.	0.	0.	0.	0.	0.	501
23.	1.	1.						502
0.	-1.7	1.	-1.4	7.	-33.9	12.	2.8	
13.5	3.9	18.	-21.2	21.5	-12.4	28.	-9.2	
32.	-24.0	33.	-24.0	36.	-9.9	37.	-9.9	
42.	-24.9	47.	-31.8	50.	-25.9	54.	-27.2	
58.	-32.2	61.	-29.0	76.	-5.9	90.	-1.4	
100.	-1.4	120.	0.	300.	0.			
2.	1.	1.						503
0.	0.	300.	0.					
2.	1.							504
0.	0.	300.	0.					

FIGURE 13-5 Vehicle Motion Cards for Example 1

SLIDE 13-5



## SLIDE 5

The vehicle motion, or more precisely, occupant compartment motion, is described with Cards 601 through 604. Cards for the 30-mph frontal barrier crash of Example 1 are shown. Initial position and velocity values for vehicle horizontal, vertical and pitch coordinates are on Card 601, together with two coordinates for an accelerometer location. The remaining cards specify acceleration histories for the three vehicle degrees of freedom.

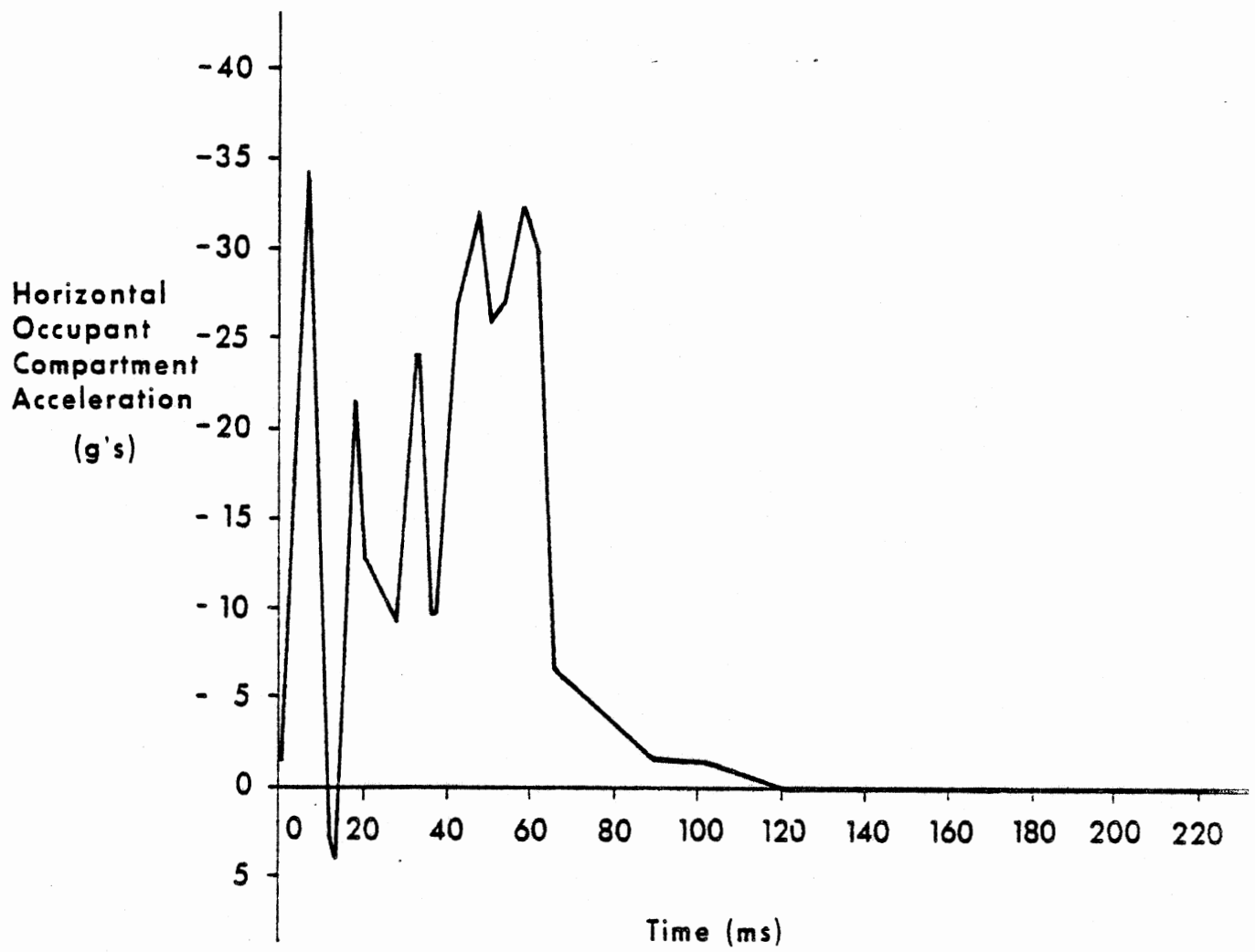


FIGURE 13-6 Horizontal Component of Vehicle Acceleration for Example 1

SLIDE 13-6

## SLIDE 6

Change in the horizontal component of vehicle velocity for this example results from the acceleration profile shown, which is defined by twenty-three time-acceleration points on cards following the 602-card. The crash simulated is for an impact velocity of 30 mph, a  $\Delta V$  of 32.8 mph, 33.9 g's peak acceleration, and a stopping distance (or "crush") of 21.8 inches.

GM HYBRID II DUMMY (PRELIMINARY DATA)									200
1.1	17.44	3.4	5.	15.8		10.3	3.25	-.88	201
2.75	7.	1.7	4.2	8.2	9.3	5.	5.8	.5	202
.0250	.0051	.0052	.0092	.0932	.0518	.022	.0256	.007	203
.108	1.07	.04	1.53	1.38	2.82	.18	.62		204
12.8	.58	0.	.52	17.4	1.		-25.	.35	205
12.8	.58	0.	.52	17.4	1.		-22.	.35	206
72.	15.	0.	.66	1000.	1.	-8.	-25.5	.35	207
102.5	-7.624	.1944	.66	1000.	1.	-33.099	-34.001	.35	208
84.44	-4.810	.1053	0.	850.	1.	-49.999	-50.001	.5	209
0.	29.8	0.	0.	204.	1.	135.	0.	.5	210
0.	10.	0.	0.	222.	1.	28.	-197.	.5	211
0.	10.	0.	0.	64.	1.	0.	-165.	.5	212
751.	0.	757.	1.98						213
20.	230.	0.	0.			2.		.5	214
38.	.58	0.	.52	0.	1.	-1.		.16	215
38.	.58	0.	.52	0.	1.	2.		.16	216
751.	0.	757.	1.98						242
HEAD				1.	3.				219
THORAX		CHESTMATL		2.	1.				219
HIP		HIPMATL		4.	1.				219
THIGH				5.	1.				219
KNEE				5.	1.				219
SHANK				6.	1.				219
HEEL				6.	2.				219
TOE				6.	2.				219
ELBOW				7.	1.				219
HAND				8.	3.				219
HEAD		0.	.5	4.	4.				220
THORAX		-.5	-.68	5.52	4.44				220
HIP		-.12	0.	4.5	4.5				220
THIGH		-.5	-.1	7.	3.				220
KNEE		7.	-.4	2.25	2.25				220
SHANK		-7.54	0.	3.	2.4				220
HEEL		8.57	0.	1.2	1.2				220
TOE		5.61	-5.16	1.2	1.2				220
ELBOW		5.3	0.	1.5	1.5				270
HAND		5.6	-.4	2.72	1.52				220
CHESTMATL		0.	0.	0.	100.	101.	0.	0.	??1
CHESTMATL		5.				CSTAT	IZERO	CGR	222
CGR		-1.	.1						223
CGR		0.	1.						224
CGR		.01	.64						224
CGR		.3	.5						224
CGR		1.35	.45						224
CSTAT		0.	0.						225
CSTAT		.01	1125.						225
CSTAT		.05	1460.						225
CSTAT		.3	1350.						225
CSTAT		.4	1260.						225
CSTAT		1.1	1260.						225
CSTAT		4.25	12600.						225
IZERO		-1.	0.						226
HIPMATL		0.	0.	0.	100.	101.	0.	0.	221
HIPMATL		5.				CSTAT	IZERO	CGR	222

FIGURE 13-7 Occupant Parameter Cards for Example 1

## SLIDE 7

The occupant description subset is shown in this slide. The data are preliminary data compiled by HSRI from several sources for a GM Hybrid II dummy. Cards 201 through 216 plus 227 through 242 describe mass and moment of inertia properties for the body links, link lengths, and joint properties. The contents of these cards are discussed in detail in Module 2. Cards 219 and 220 define ellipses which serve as the contact-sensing profile of the body. We see a total of 10 body ellipses representing head, thorax, hip, thigh, knee, shank, heel, toe, elbow, and hand. Next to two of these identifiers on the 219-Cards are CHESTMATL and HIPMATL. These indicate that material properties are to be specified for THORAX and HIP ellipses -- they are not rigid. Next to the identifiers on the 220-Cards are two columns defining ellipse location on the crash victim and two more columns defining semi-major axes. Loading and unloading characteristics of body materials are prescribed on Cards 221 through 226. You see the identifiers, CHESTMATL and HIPMATL, on Cards 221. The CGR cards (223 and 224) define the unloading characteristics of the force-deformation profiles while CSTAT, on Cards 225, defines the force-deflection relation itself.

-11.	-8.	-18.	-34.	-50.	0.	0.	0.		217
78.5	97.5	115.5	140.5	19.5	-45.	-41.	3.	89.5	301
0.	0.	0.	0.	0.	0.	0.	0.	0.	302
12.2	0.	-21.4	0.	3.28	0.				303
0.	0.	0.	0.						304

FIGURE 13-8 Occupant Position Cards for Example 1

SLIDE 13-8

## SLIDE 8

The seated occupant at "time zero" was shown in an earlier slide. Data required for positioning of the occupant are shown here. Among the data on these cards are initial position values for the fourteen occupant degrees of freedom, which include the initial link angles, neck length, shoulder coordinates, and horizontal and vertical locations within the occupant compartment of the upper torso center of gravity. For the two example simulations, initial link angles and upper torso CG location were estimated from scale drawings of the "time zero" occupant and vehicle-interior configurations, so the values here produce only approximate initial occupant equilibrium. The resulting total initial upward force on the occupant, for example, is 207.1 lb, which does not equal the occupant weight, 163.7 lb. The initial imbalance is not great enough to significantly affect the simulation results.

Values on Card 217 are for the so-called "joint equilibrium angles," and other data are the initial velocities for the fourteen occupant degrees of freedom. These velocities, on Cards 302 through 304, are 0. for the example simulations of this module since the occupant is to be initially at rest within the occupant compartment.

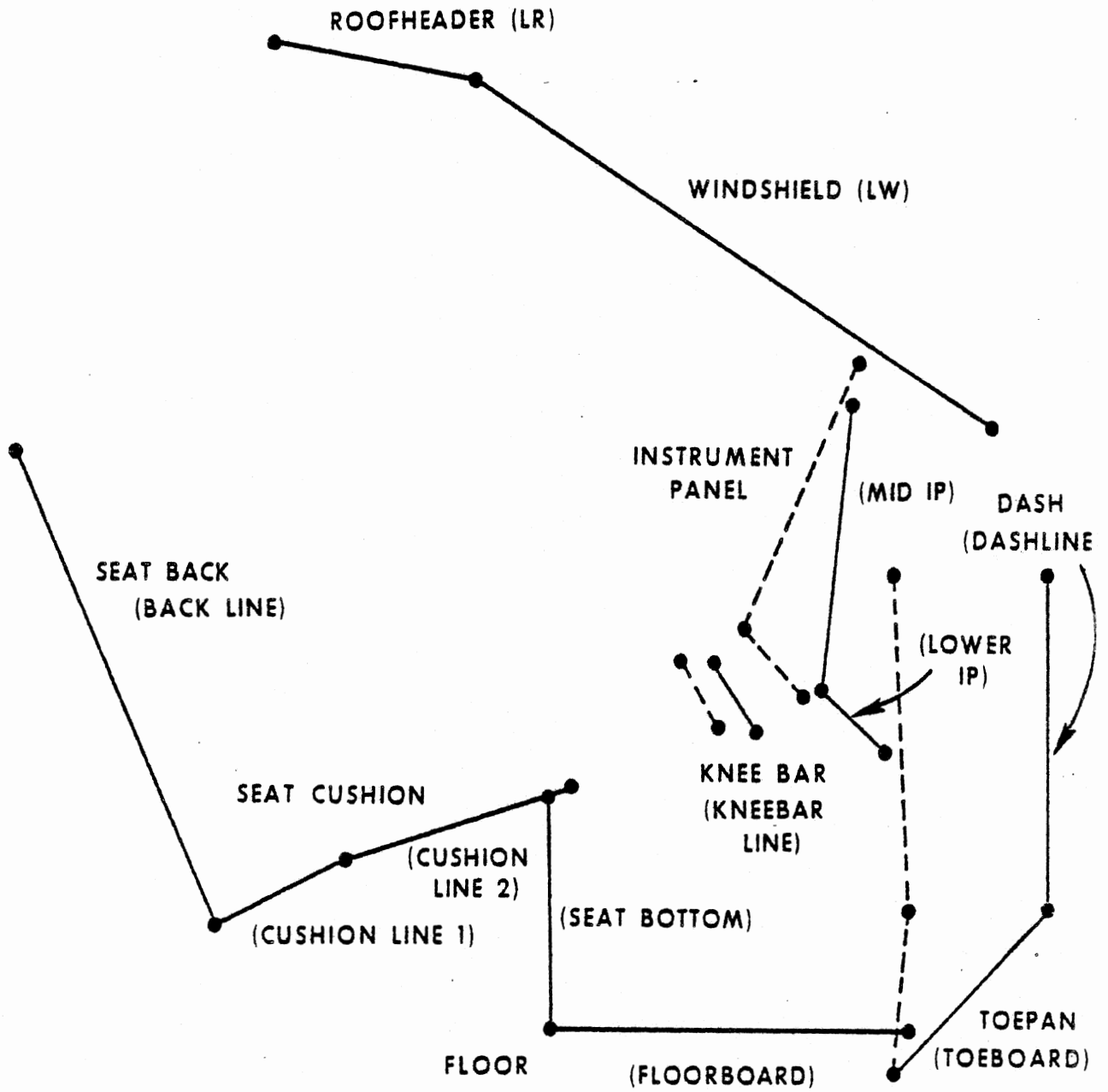


FIGURE 13-9 Vehicle Interior Profile for Example 1



## SLIDE 9

A vehicle interior with which the occupant is to interact must be prescribed by the user. Two types of data are required. The first of these describes the geometrical profile of the interior in the plane of occupant motion. The primary elements of this description are the endpoint coordinates of line segments which comprise so-called vehicle-interior "regions," a "region" being a set of connected straight-line segments having the same material properties. The slide shows the vehicle interior profile defined for Example 1. Region and segment names are indicated, segment names in parentheses. Solid lines indicate positions of line segments before frontal interior penetration into the occupant compartment, which begins at 40 ms. All penetration occurs between 40 and 80 ms, and the dashed lines represent the deformed vehicle interior. Note that the toeboard segment decreases considerably in length. There is no restriction that segment lengths be held constant while undergoing motion.

INSTRUMENT PANEL	IPMAT	0.	1.	1.	1.	401
INSTRUMENT PANEL 2	4.	1.	0.	0.	0.	402
MID IP	INSTRUMENT PANELS	0.	1.	1.		409
MID IP	4.					410
MID IP	0.	44.9	-27.3	43.7	-15.9	411
MID IP	40.	44.9	-27.3	43.7	-15.9	411
MID IP	80.	45.6	-29.3	40.6	-18.9	411
MID IP	300.	45.6	-29.3	40.6	-18.9	411
LOWER IP	INSTRUMENT PANELS	.5	1.	2.		409
LOWER IP	4.					410
LOWER IP	0.	43.7	-15.9	46.8	-12.8	411
LOWER IP	40.	43.7	-15.9	46.8	-12.8	411
LOWER IP	80.	40.6	-18.9	42.6	-14.9	411
LOWER IP	300.	40.6	-18.9	42.6	-14.9	411

IPMAT	0.	0.	0.	100.	101.	0.	0.	403
IPMAT	5.	0.	0.	0.	IPSTAT	IZERO	IPGR	404
IPGR	0.	0.						405
IPGR	2.	.75						405
IPGR	40.	.75						405
IPGR	0.	1.						406
IPGR	1.	.25						406
IPGR	2.	.1						406
IPGR	8.	.1						406
IPGR	8.4	.15						406
IPSTAT	0.	0.						407
IPSTAT	.165	80.						407
IPSTAT	.375	480.						407
IPSTAT	.665	750.						407
IPSTAT	.790	760.						407
IPSTAT	1.25	500.						407
IPSTAT	1.75	580.						407
IPSTAT	2.54	225.						407
IPSTAT	2.87	255.						407
IPSTAT	3.44	300.						407
IPSTAT	4.54	380.						407
IPSTAT	4.63	250.						407
IPSTAT	8.	250.						407
IPSTAT	12.	3850.						407

FIGURE 13-10 Data Cards for Definition of Geometrical Profile and Material Properties for a Typical Region

SLIDE 13-10

SLIDE 10

Data for one of the penetrating regions of the vehicle interior, the INSTRUMENT PANEL region, are illustrated here. The INSTRUMENT PANEL profile is defined entirely by Cards 401, 402, 409, 410, and 411.

The second type of data required for the vehicle interior describes material characteristics, that is, loading and unloading properties of regions of the defined profile. Data are on Cards 403 through 408.

An entry on the 402-Card for each vehicle interior region assigns the region to a "friction class." A "friction class" is similarly specified for each body ellipse on its 219-Card. The similarity between the data format for body ellipses and vehicle contact surfaces should be noted both with respect to geometric quantities and material properties.

1.	1.	.25	.125	.125	412
1.	2.	.5			412
1.	3.	.5			412
1.	4.	.4			412
2.	2.	.8			412
3.	1.	.4			412
3.	2.	.5			412
3.	4.	.4			412
3.	5.	.67			412
3.	6.	.9			412

FIGURE 13-11 Data Cards for Coefficients of Friction for Example 1

SLIDE 13-11

## SLIDE 11

Coefficients of friction are then specified, as the next data subset, on 412-Cards for combinations of ellipse and region classes. This slide shows one card for each pairing of friction classes represented in the set of contact interactions which can occur in simulation Example 1. For any simulation, coefficients of friction will default to 0. for any pairing not represented by a 412-Card. Frictional forces between the occupant and elements of the vehicle interior can be large enough to have a considerable effect on the magnitude and direction of the resultant force vector at the interaction interface. It is therefore important in simulations to account for frictional forces accurately.

HEAD	POORHEADER	106
HEAD	WINDSHIELD	106
HEAD	INSTRUMENT PANEL	106
THORAX	SEAT BACK	106
THORAX	SEAT CUSHION	106
THORAX	INSTRUMENT PANEL	106
HIP	SEAT BACK	106
HIP	SEAT CUSHION	106
HIP	FLOOR	106
THIGH	SEAT CUSHION	106
KNEE	INSTRUMENT PANEL	106
KNEE	KNEE BAR	106
SHANK	INSTRUMENT PANEL	106
SHANK	KNEE BAR	106
HEEL	FLOOR	106
HEEL	DASH	106
TOE	DASH	106
HEEL	TOEPAN	106
TOE	TOEPAN	106
HAND	SEAT CUSHION	106
HAND	INSTRUMENT PANEL	106
THIGH	THORAX	106

FIGURE 13-12 Interaction "Inhibition" Cards for Example 1

SLIDE 13-12

## SLIDE 12

Modules 4 and 5 discuss the use of 106-Cards for specification of allowed or disallowed combinations of potentially-interacting body ellipses and vehicle interior regions. "Allowed" combinations are normally specified when the number of probable interactions is less than the number of improbable interactions. This is judged to be the case for the first simulation example, so twenty-one allowed interactions have been specified between the ten body ellipses and nine vehicle-interior regions. One card, the last one on the slide, has been included for an allowed interaction between body ellipses THIGH and THORAX.

0, 1, 46-48, 10-14, 21, 22, 37, 38, 49, 50, 15, 23-26, 2-5, 18-20, 33-36, 30-32, 16,										1001
27-29, 39, 17, 40, 6-9, 45										1002
0.	0.	0.	11.55	.025						1003
40.	500.	560.	0.	.85	201.	5.	5.			1004
0.	0.	-3.	62.	5.	-44.	10.	0.			1500
21.	0.	0.	1.	1.	0.	1.	0.	10.		1501
										1600

FIGURE 13-13 Output Processor Data Deck for Example 1

SLIDE 13-13



## SLIDE 13

The last card in the data deck for the Input Pre-Processor must be the 1000-Card. It is blank except for the card identification number in columns 77 through 80. Cards 1001 through 1600 constitute a separate data deck from Cards 100 through 1000, which have been illustrated in the preceding slides and which are read separately by the Output Pre-Processor. These cards control post-processing and printout of data calculated and stored by the Execution Processor. These data and data generated by the Input Processor are stored in four external files; as long as the files are maintained intact, they can be processed by the Output Processor any number of times, using different control Cards 1001 through 1600.

The entire Output Pre-Processor data deck for Example 1 consists of seven cards. The first two cards, 1001 and 1002, are used for specification of categories of calculated data for which printout is desired and the order of printout for these categories. The fifty-one categories of results which may be printed are identified by Category Number in Modules 1 and 12. The ordering for printout shown in the slide is identical to the default ordering which would result if the 1001- and 1002-Cards were omitted from the data deck.

Various data are required on Cards 1003 and 1004 for the post-processor functions of filtering of occupant accelerations and determination of HIC and femur loads. In addition to HIC and femur loads, other potential injury indicators can be determined and printed by the Output Processor. They are requested by using Cards 1100 through 1401, none of which are included in the data deck for Example 1.

A time sequence of printer-plot pages can be produced which depict the occupant and all lines of the vehicle interior. Controls for producing the printout are read from Cards 1500 through 1502. The most important data on these cards are margin coordinates which frame the printer-plot image within the vehicle coordinate system and the simulation times to be included in the time sequence of printouts.

As for the Input Pre-Processor data deck, a single card is required to mark the end of the Output Pre-Processor data deck. It is Card 1600, which is blank except for the card identification number.

This slide and the preceding slides have illustrated the data subsets which together constitute the complete data deck for Example 1. They are shown assembled together in Module 13 of the Self-Study Guide. The following eight slides show selected pages of MVMA 2-0 printout for simulation Example 1.

```

1 100 * * * * * MVH*A 2-D TU*TORIAL E*EXAMPLE #*1 * * *
2 400 * KNEE *BAR * * * * * * * * *
3 500 *OCC. COM*P. DISPL* * * * * * * * *
4 600 *30MPH FR*ONT BARR*IER * * * * * * * * *
5 700 * NO B*ELTS * * * * * * * * *
6 101 *1. *1. *32.174 *0. *0. *200. *1. *5. *10. *
7 102 *0. *0. *0. *0. *0. *0. *10. *0.000001 *5. *
8 103 *.2 *.05 *100000. *15000. *10. *.05 *10. *1. *1. *
9 601 *0. *44. *0. *0. *0. *0. *0. *0. *0. *
10 602 *23. *1. *1. * * * * * * * * *
11 * 0.0 * -1.70* 1.00* -1.40* 7.00* -33.90* 12.00* 2.80* 0.0 *
12 * 13.50* 3.90* 18.00* -21.20* 21.50* -12.40* 28.00* -9.20* 0.0 *
13 * 32.00* -24.00* 33.00* -24.00* 36.00* -9.90* 37.00* -9.90* 0.0 *
14 * 42.00* -26.90* 47.00* -31.80* 50.00* -25.90* 54.00* -27.20* 0.0 *
15 * 58.00* -32.20* 61.00* -29.00* 76.00* -6.90* 90.00* -1.40* 0.0 *
16 * 100.00* -1.40* 120.00* 0.0 * 300.00* 0.0 * 0.0 * 0.0 * 0.0 *
17 603 *2. *1. *1. * * * * * * * * *
18 * 0.0 * 0.0 * 300.00* 0.0 * 0.0 * 0.0 * 0.0 * 0.0 * 0.0 *
19 604 *2. *1. * * * * * * * * *
20 * 0.0 * 0.0 * 300.00* 0.0 * 0.0 * 0.0 * 0.0 * 0.0 * 0.0 *
21 200 *GM HYBRID II DUM*MY * * * * * * * * *
22 300 *(PRELIMI*NARY DAT*A) * * * * * * * * *
23 201 *1.1 *13.44 *3.4 *5. *15.8 * * *10.3 *3.25 *-0.88 *
24 202 *2.75 *7. *1.7 *4.2 *8.2 *9.3 *5. *5.8 *.5 *
25 203 *.0254 *.0951 *.0052 *.0982 *.0932 *.0518 *.022 *.0256 *.007 *
26 204 *.194 *1.97 *.04 *1.53 *1.38 *2.82 *.18 *.62 *
27 205 *12.8 *.58 *0. *.52 *17.4 *1. * *-25. *.35 *
28 206 *12.8 *.58 *0. *.52 *17.4 *1. * *-22. *.35 *
29 207 *72. *15. *0. *.66 *1000. *1. *-8. *-25.5 *.35 *
30 208 *102.5 *-7.624 *.1944 *.06 *1000. *1. *-33.999 *-34.001 *.35 *
31 209 *94.44 *-4.810 *.1053 *0. *850. *1. *-49.999 *-50.001 *.5 *
32 210 *0. *29.8 *0. *0. *204. *1. *135. *0. *.5 *
33 211 *0. *10. *0. *0. *222. *1. *28. *-197. *.5 *
34 212 *0. *10. *0. *0. *64. *1. *0. *-165. *.5 *
35 213 *751. *0. *757. *1.98 * * * * * * * *
36 214 *20. *230. *0. *0. * * * * * * * *
37 215 *38. *0. *.52 *0. *1. *-1. * * *.16 *
38 216 *38. *.58 *0. *.52 *0. *1. *2. * * *.16 *
39 242 *751. *0. *757. *1.98 * * * * * * * *
40 219 *HEAD * * * * *1. *3. * * * * *
41 219 *THORAX * *CHESTMAT*L *2. *1. * * * * *
42 219 *HIP * *HIPMATL * *4. *1. * * * * *
43 219 *THIGH * * * * *5. *1. * * * * *
44 219 *KNEE * * * * *5. *1. * * * * *
45 219 *SHANK * * * * *6. *1. * * * * *
46 219 *HEEL * * * * *6. *2. * * * * *
47 219 *TOE * * * * *6. *2. * * * * *
48 219 *ELBOW * * * * *7. *1. * * * * *
49 219 *HAND * * * * *8. *3. * * * * *
50 220 *HEAD * *0. *.5 *4. *4. * * * * *
51 220 *THORAX * *-0.5 *-0.68 *5.52 *4.44 * * * * *
52 220 *HIP * *-0.12 *0. *4.5 *4.5 * * * * *
53 220 *THIGH * *-0.5 *-0.1 *7. *3. * * * * *
54 220 *KNEE * *7. *-0.4 *2.25 *2.25 * * * * *
55 220 *SHANK * *-7.54 *0. *3. *2.4 * * * * *
56 220 *HEEL * *8.57 *0. *1.2 *1.2 * * * * *
57 220 *TOE * *5.61 *-5.16 *1.2 *1.2 * * * * *
58 220 *ELBOW * *5.3 *0. *1.5 *1.5 * * * * *
59 220 *HAND * *0.6 *-0.4 *2.72 *1.52 * * * * *

```

FIGURE 13-15 Input Processor Data Deck Echo for Example 1 (example page)

## SLIDE 14

Both the Input and Output Pre-Processors always produce "echoes" of their data decks. An example page from the Input Pre-Processor "echo" for Example 1 is shown here. The eight-column data fields are separated by asterisks. You will recognize some of the items which have already been discussed such as vehicle deceleration, body linkage data and ellipses. (pause).

BODY PARAMETERS

HEAD LENGTH=	1.10	END OF LINK TO CENTER-OF-MASS LENGTHS (IN)	MASS OF BODY SEGMENTS (LBS SEC**2 IN)
UPPER TORSO LENGTH=	13.44	HEAD/NECK JOINT-HEAD CM LENGTH=	HEAD MASS=
MIDDLE TORSO LENGTH=	3.40	NECK-CHEST CM LENGTH=	CHEST MASS=
LOWER TORSO LENGTH=	5.00	UPPER TORSO JOINT-MIDDLE TORSO CM LENGTH=	MIDDLE TORSO MASS=
HIP-KNEE LENGTH=	15.00	LOWER TORSO JOINT-LOWER TORSO CM LENGTH=	LOWER TORSO MASS=
UPPER TORSO-SHOULDER=	0.0	HIP-UPPER LEG CM LENGTH=	UPPER LEG (BOTH LEGS)=
SHOULDER-ELBOW LENGTH=	10.10	KNEE-LOWER LEG CM LENGTH=	LOWER LEG (BOTH LEGS)=
X REST POINT OF SHOULDER=	3.25	SHOULDER-UPPER ARM CM LENGTH=	UPPER ARM (BOTH ARMS)=
Z REST POINT OF SHOULDER=	-0.49	ELBOW-LOWER ARM CM LENGTH=	LOWER ARM (BOTH ARMS)=
			HEAD-NECK MASS=
			UPPER TORSO-NECK MASS=

MOMENTS OF INERTIA

HEAD	0.20	"NATURAL" LINK ANGLES (FOR ZERO TORQUE) (DEG)	INITIAL BODY LINK ANGLES (RELATIVE TO VEHICLE) (DEG)	INITIAL ANGULAR VELOCITIES (RELATIVE TO VEHICLE) (DEG/SEC)
UPPER TORSO	1.97	-11.00	78.50	0.0
MIDDLE TORSO	0.04	-8.00	97.50	0.0
LOWER TORSO	1.53	-18.00	115.50	0.0
UPPER LEG	1.30	-34.00	149.50	0.0
LOWER LEG	2.02	-50.00	19.50	0.0
UPPER ARM	0.18	0.0	-45.00	0.0
LOWER ARM	0.62	0.0	-41.00	0.0
NECK	0.0	0.0	3.00	0.0
			89.50	0.0

OCCUPANT JOINT PARAMETERS

HEAD-NECK FORWARD	12.80	LINEAR ANGULAR DEFLECTION COEF. (IN-LBS/DEG**2)	QUADRATIC ANGULAR DEFLECTION COEF. (IN-LBS/DEG**2)	CUBIC ANGULAR DEFLECTION COEF. (IN-LBS/DEG**3)	CONSERVED-ABSORBED ENERGY RATIO
NECK-UPPER TORSO FORWARD	12.00	0.58	0.58	0.0	0.35
UPPER SPINE	72.00	72.00	15.00	0.0	0.35
LOWER SPINE	102.50	102.50	-7.62	0.19	0.35
HIP	84.44	84.44	-4.81	0.11	0.50
KNEE	0.0	0.0	29.80	0.0	0.50
UPPER ARM-UPPER TORSO	0.0	0.0	10.00	0.0	0.50
ELBOW	0.0	0.0	10.00	0.0	0.50
HEAD-NECK BEAR	38.00	38.00	0.58	0.0	0.50
NECK-UPPER TORSO BEAR	38.00	38.00	0.58	0.0	0.16
NECK (EXTENSIBLE) **	751.00	751.00	0.0	0.0	0.16
SHOULDER (EXTENSIBLE) **	20.00	20.00	270.00	757.00	NA
NECK (COMPRESSIBLE) **	751.00	751.00	0.0	757.00	0.50

\*\* UNITS FOR THE NECK (EXTENSIBLE), (COMPRESSIBLE) AND SHOULDER (EXTENSIBLE) PARAMETERS ARE GIVEN IN THE ROW BELOW (LB/IN\*\*2) (LB/IN\*\*3)

FIGURE 13-16 Summary of Input Data (example page)

## SLIDE 15

This slide shows an example page of printout from the summary of the input data. The entire input data summary for Example 1 is 63 pages. This printout is produced whenever category 0 is requested on the 1001-Card. The fact that this summary is 63 pages in length reflects the awesome amount of information required to define the crash victim and his environment. But, it should be remembered that each of the parameters may be changed by entering a new number in a line file, an activity requiring only a few moments of time. This task is considerably easier than building a new experiment to reflect the change in the parameter.

JUN 24, 197702:00:20

GM HYBRID II DUNNY (PRELIMINARY DATA)

KNEE BAB

MVNA 2-D TUTORIAL EXAMPLE 61

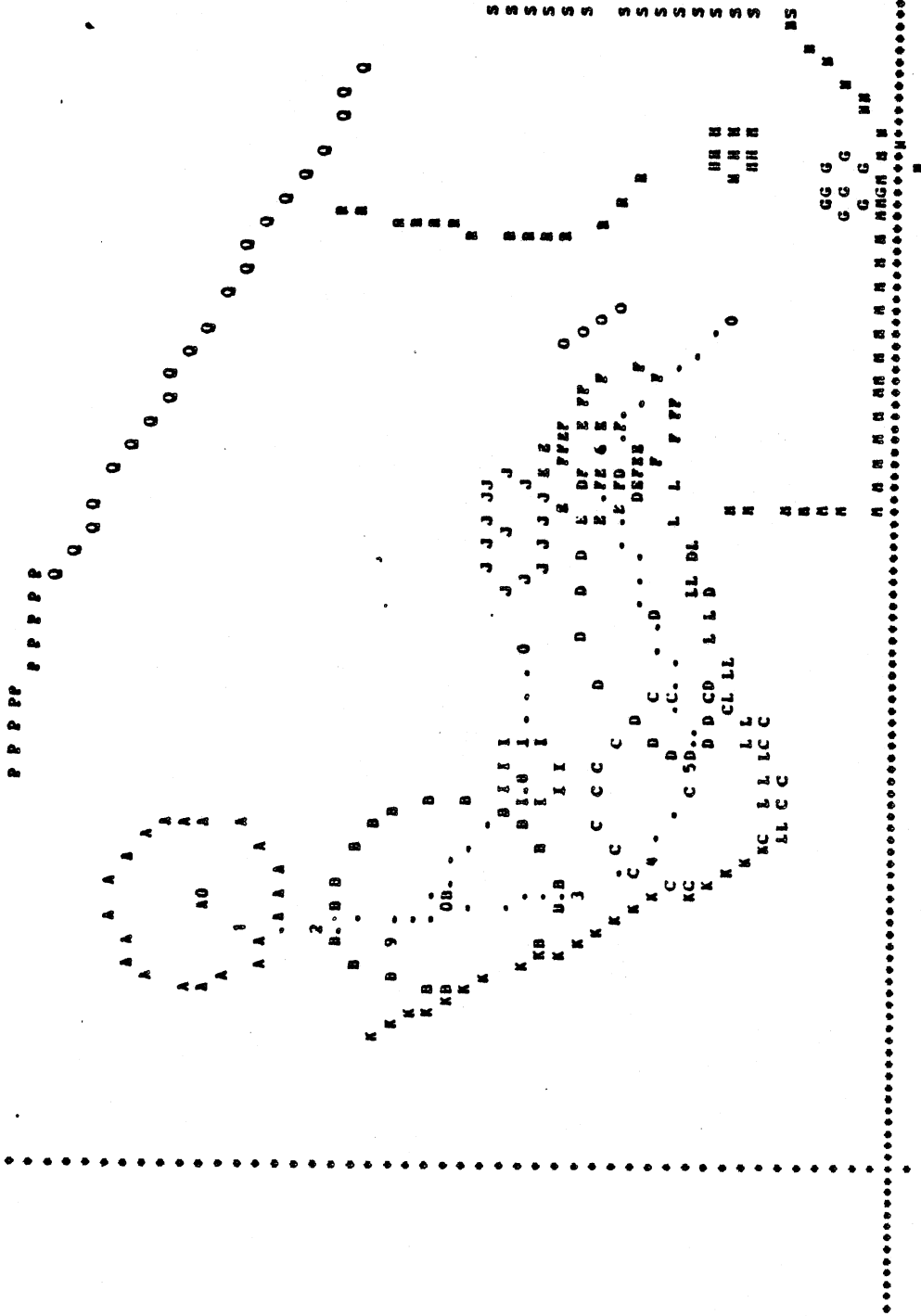
OCC. COMP. DISPL.

JUMP FRONT BARRIER

NO BELTS

PAGE 130-65  
MVNA 2-D, VER. 3

STICK FIGURE PRINTER PLOT FRAME FOR TIME= 0.0 MSEC.

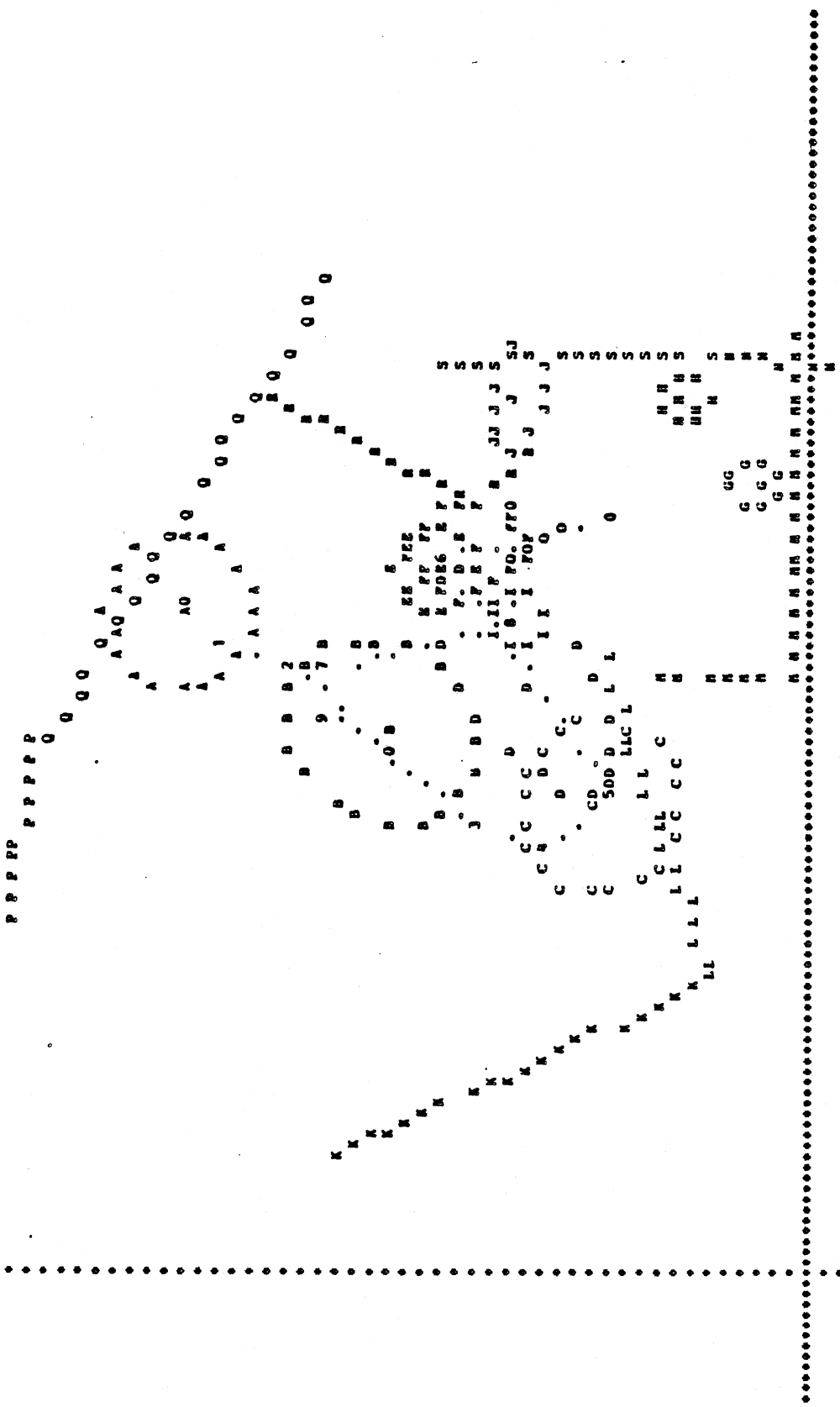


COORDINATE RANGES FOR PLOT ARE X= -6.56 (AT LEFT) TO 65.56 (AT RIGHT) AND Z= 5.00 (AT TOP) TO -44.00 (AT BOTTOM)  
 SCALE FACTOR IS (IN) = 5.547 (IN) , X AND Z POINT RESOLUTION ERRORS EQUAL RESPECTIVELY 0.277 AND 0.462 (IN) IN SCALE.

FIGURE 13-17a Printer-Plot Time Sequence for Example 1 (0 ms)

SLIDE 16

The data decks for Example 1 cause printer-plot stick figure output to be generated for each 10 ms of simulation time. Selected "frames" of the time sequence are shown for the knee-bar restrained passenger, here for time "zero" and on the next three slides without comment.



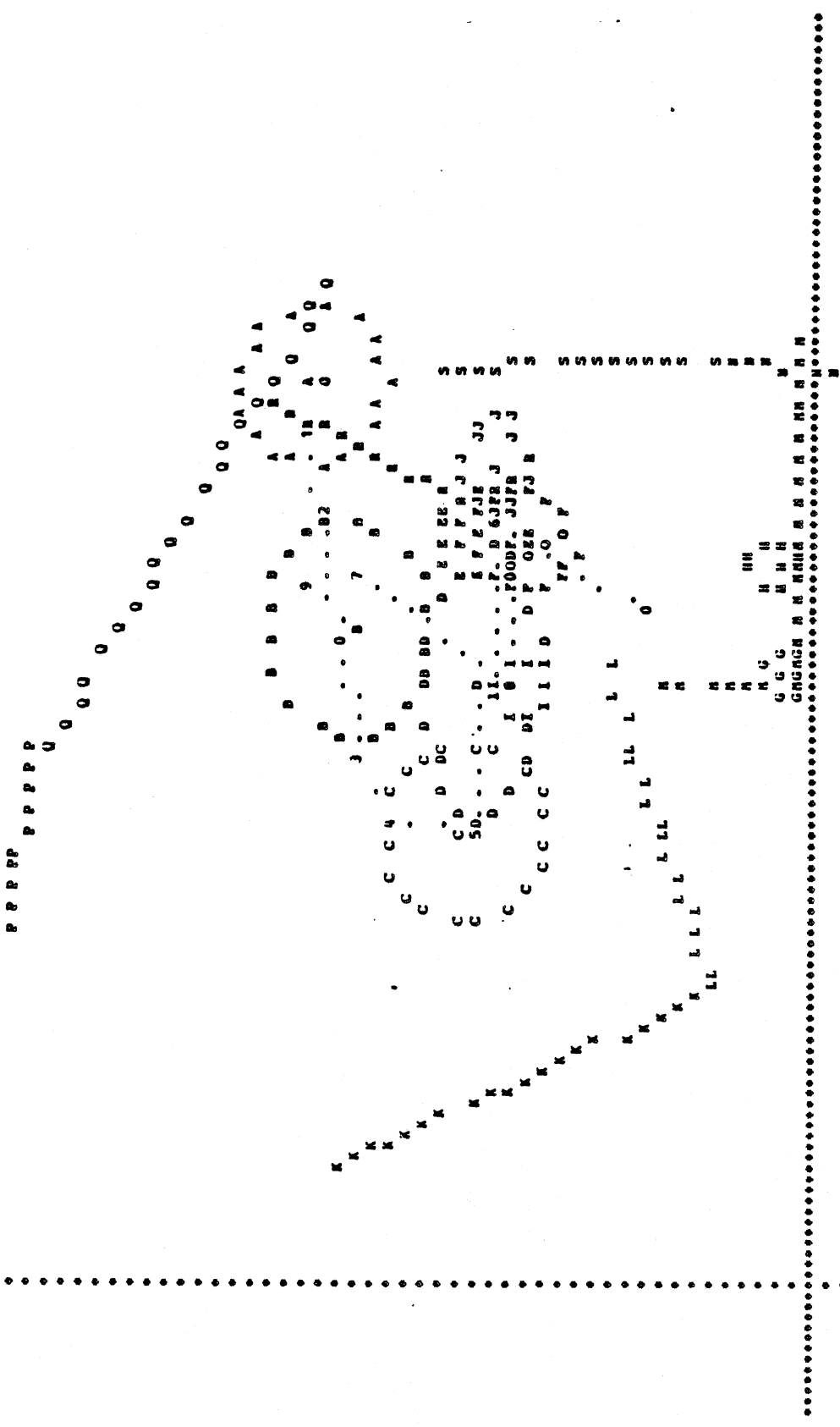
COORDINATE RANGES FOR PLOT ARE X = -6.56 (AT LEFT) TO 65.56 (AT RIGHT) AND Z = 5.00 (AT BOTTOM) TO -44.00 (AT TOP)  
SCALE FACTOR IS (IN) = 5.547 (IN) , X AND Z POINT RESOLUTION ERRORS EQUAL RESPECTIVELY 0.277 AND 0.462 (IN) IN SCALE.

FIGURE 13-17d Printer-Plot Time Sequence for Example 1 (80 ms)



SLIDE 17  
(pause) (10 sec)

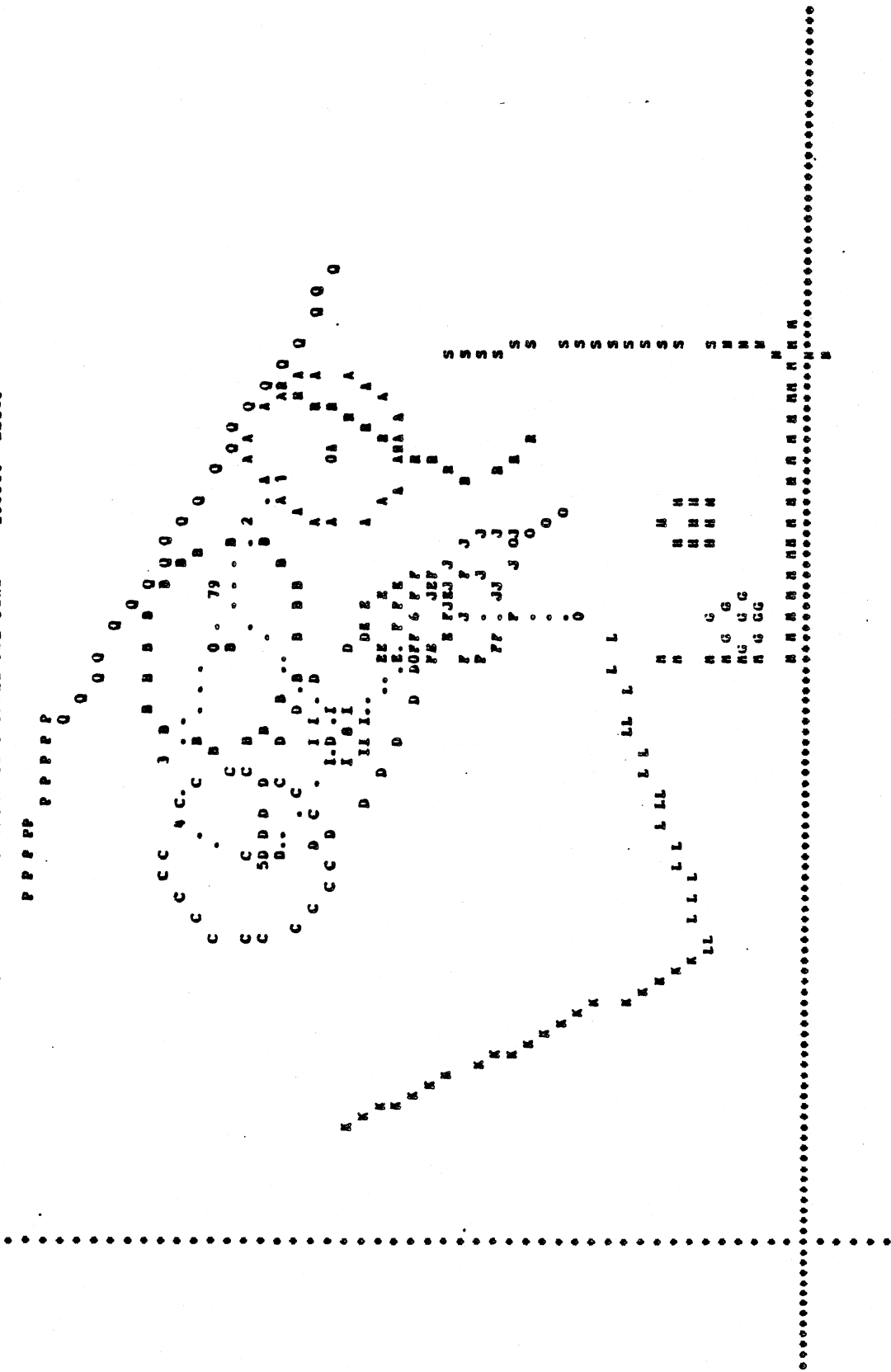
JUN 24, 1977 02:00:20  
 GR HYBRID II DUNNY (PRELIMINARY DATA) KNEE BAR OCC. COMP. DISPL. JONPH FRONT BARRIER NO BELTS PAGE 142-45  
 MVNA 2-D TUTORIAL EXAMPLE 01 MVNA 2-D, VER. 3  
 STICK FIGURE PRINTER PLOT FRAME FOR TIME= 120.00 MSEC.



COORDINATE RANGES FOR PLOT ARE X= -6.56 (AT LEFT) TO 65.56 (AT RIGHT) AND Z= 5.00 (AT BOTTOM) TO -44.00 (AT TOP)  
 SCALE FACTOR IS (IN) = 5.547 (IN) , X AND Z POINT RESOLUTION ERRORS EQUAL RESPECTIVELY 0.277 AND 0.462 (IN) IN -ALP.

FIGURE 13-17f Printer-Plot Time Sequence for Example 1 (120 ms)

SLIDE 18  
(pause) (10 sec)



COORDINATE RANGES FOR PLOT ARE X = -6.56 (AT LEFT) TO 65.56 (AT RIGHT) AND Z = 5.00 (AT BOTTOM) TO -44.00 (AT TOP)  
SCALE FACTOR IS (1M) = 5.547 (1M) , 1 AND 2 POINT RESOLUTION ERRORS EQUAL RESPECTIVELY 0.277 AND 0.462 (1M) IN SCALE.

FIGURE 13-17h Printer-Plot Time Sequence for Example 1 (200 ms)

SLIDE 19  
(pause) (10 sec)

VEHICLE RESPONSE

TIME (MSEC)	DISPL. (INCHES)	HORIZONTAL VELOCITY (MPH)	ACCEL. (G'S)	DISPL. (INCHES)	VERTICAL VELOCITY (FT/SEC)	ACCEL. (G'S)	ANGLE (DEGREES)	PITCH VELOCITY (RAD/SEC)	ACCEL. (RAD/SEC**2)
0.0	0.0	30.00	-1.70	0.0	0.0	0.0	0.0	0.0	0.0
5.00	2.61	28.09	-23.07	0.0	0.0	0.0	0.0	0.0	0.0
10.00	5.02	26.14	-11.80	0.0	0.0	0.0	0.0	0.0	0.0
15.00	7.31	26.04	-4.47	0.0	0.0	0.0	0.0	0.0	0.0
20.00	9.54	24.38	-16.17	0.0	0.0	0.0	0.0	0.0	0.0
25.00	11.62	23.02	-10.68	0.0	0.0	0.0	0.0	0.0	0.0
30.00	13.60	21.00	-16.60	0.0	0.0	0.0	0.0	0.0	0.0
35.00	15.42	19.54	-14.60	0.0	0.0	0.0	0.0	0.0	0.0
40.00	17.08	18.07	-20.10	0.0	0.0	0.0	0.0	0.0	0.0
45.00	18.55	15.17	-29.04	0.0	0.0	0.0	0.0	0.0	0.0
50.00	19.73	11.92	-25.90	0.0	0.0	0.0	0.0	0.0	0.0
55.00	20.66	8.98	-28.45	0.0	0.0	0.0	0.0	0.0	0.0
60.00	21.30	5.62	-30.07	0.0	0.0	0.0	0.0	0.0	0.0
65.00	21.66	2.68	-23.11	0.0	0.0	0.0	0.0	0.0	0.0
70.00	21.79	0.55	-15.74	0.0	0.0	0.0	0.0	0.0	0.0
75.00	21.78	-0.77	-8.37	0.0	0.0	0.0	0.0	0.0	0.0
80.00	21.68	-1.47	-5.33	0.0	0.0	0.0	0.0	0.0	0.0
85.00	21.52	-1.95	-3.16	0.0	0.0	0.0	0.0	0.0	0.0
90.00	21.34	-2.21	-1.40	0.0	0.0	0.0	0.0	0.0	0.0
95.00	21.14	-2.37	-1.40	0.0	0.0	0.0	0.0	0.0	0.0
100.00	20.92	-2.52	-1.40	0.0	0.0	0.0	0.0	0.0	0.0
105.00	20.70	-2.65	-1.05	0.0	0.0	0.0	0.0	0.0	0.0
110.00	20.46	-2.75	-0.70	0.0	0.0	0.0	0.0	0.0	0.0
115.00	20.21	-2.81	-0.35	0.0	0.0	0.0	0.0	0.0	0.0
120.00	19.96	-2.83	-0.00	0.0	0.0	0.0	0.0	0.0	0.0
125.00	19.71	-2.83	0.0	0.0	0.0	0.0	0.0	0.0	0.0
130.00	19.47	-2.83	0.0	0.0	0.0	0.0	0.0	0.0	0.0
135.00	19.22	-2.83	0.0	0.0	0.0	0.0	0.0	0.0	0.0
140.00	18.97	-2.83	0.0	0.0	0.0	0.0	0.0	0.0	0.0
145.00	18.72	-2.83	0.0	0.0	0.0	0.0	0.0	0.0	0.0
150.00	18.47	-2.83	0.0	0.0	0.0	0.0	0.0	0.0	0.0
155.00	18.22	-2.83	0.0	0.0	0.0	0.0	0.0	0.0	0.0
160.00	17.97	-2.83	0.0	0.0	0.0	0.0	0.0	0.0	0.0
165.00	17.72	-2.83	0.0	0.0	0.0	0.0	0.0	0.0	0.0
170.00	17.47	-2.83	0.0	0.0	0.0	0.0	0.0	0.0	0.0
175.00	17.23	-2.83	0.0	0.0	0.0	0.0	0.0	0.0	0.0
180.00	16.98	-2.83	0.0	0.0	0.0	0.0	0.0	0.0	0.0
185.00	16.73	-2.83	0.0	0.0	0.0	0.0	0.0	0.0	0.0
190.00	16.48	-2.83	0.0	0.0	0.0	0.0	0.0	0.0	0.0
195.00	16.23	-2.83	0.0	0.0	0.0	0.0	0.0	0.0	0.0
200.00	15.98	-2.83	0.0	0.0	0.0	0.0	0.0	0.0	0.0

FIGURE 13-18 Vehicle Motion for Example 1

## SLIDE 20

Nine example pages of printout of numerical results for Example 1 are shown in Module 13 of the Self-Study Guide. Two are shown here on slides for the purpose of illustrating output format for response variables. This slide shows displacements, velocities, and accelerations for the horizontal, vertical, and pitching components of occupant compartment motion. Time in milliseconds is in the first column. Units are indicated for each variable. The first two lines of printout result from the title cards 100, 200, etc. - through 900, and are used for describing the simulation.

ELLIPSE HIP MADE OF HIPKATL

AND

LINE CUSHION LINE 1 WHICH IS AN ELEMENT OF REGION SEAT CUSHION MADE OF SEAT MATERIAL

INITIAL LINE LENGTH = 13.50(IN) EDGE CONSTANT = 0.164

TIME (MSEC)	DEFLECTION		DEFL. RATE (IN/SEC)	ELLIPSE RATE (IN/SEC)	NORMAL (LB)	TANGTL. (LB)	POSITION (HORIZIN.) (IN/SEC)	CONTACT LOCATION ON LINE		CONTACT LOCATION IN SPACE		CONTACT LOCATION ON BODY SEG.	
	LINE (IN)	ELLIPSE (IN)						X (IN)	Z (IN)	X (IN)	Z (IN)	X (IN)	Z (IN)
0.0	0.87	0.00	0.	0.	174.4	0.0	0.311	19.67	-5.69	3.43	2.77	3.43	2.77
5.00	0.88	0.00	5.	0.	176.2	80.6	0.313	22.31	-5.69	3.43	2.77	3.43	2.77
10.00	0.95	0.00	21.	0.	198.0	95.5	0.328	24.94	-5.70	3.43	2.77	3.43	2.77
15.00	1.06	0.00	20.	0.	231.4	123.9	0.351	27.54	-5.72	3.42	2.77	3.42	2.77
20.00	1.10	0.00	29.	0.	268.6	153.2	0.376	30.13	-5.73	3.42	2.78	3.42	2.78
25.00	1.33	0.00	34.	0.	310.4	214.1	0.410	32.70	-5.75	3.42	2.77	3.42	2.77
30.00	1.51	0.00	38.	0.	374.6	272.7	0.449	35.23	-5.77	3.43	2.77	3.43	2.77
35.00	1.73	0.00	46.	0.	544.8	458.3	0.496	37.72	-5.81	3.43	2.77	3.43	2.77
40.00	1.95	0.01	45.	0.	802.4	702.1	0.549	40.13	-5.86	3.43	2.76	3.43	2.76
45.00	2.19	0.01	50.	1.	1071.1	1208.0	0.604	42.38	-5.91	3.45	2.74	3.45	2.74
50.00	2.42	0.03	44.	6.	1332.8	1747.8	0.659	44.35	-5.94	3.48	2.70	3.48	2.70
55.00	2.51	0.15	-5.	36.	1415.1	2075.7	0.705	45.92	-5.98	3.54	2.62	3.54	2.62
60.00	2.49	0.29	-3.	18.	1356.4	2114.3	0.737	47.02	-6.04	3.64	2.48	3.64	2.48
65.00	2.48	0.33	-3.	-2.	1318.3	2091.5	0.759	47.66	-6.11	3.79	2.22	3.79	2.22
70.00	2.42	0.27	-22.	-21.	1146.5	1712.6	0.773	47.93	-6.29	3.98	1.85	3.98	1.85
75.00	2.24	0.14	-50.	-32.	579.2	724.2	0.782	47.91	-6.63	4.18	1.34	4.18	1.34
80.00	1.82	0.07	-104.	-2.	209.5	196.5	0.793	47.78	-7.13	4.32	0.74	4.32	0.74
85.00	1.26	0.06	-127.	-3.	133.5	84.2	0.809	47.61	-7.75	4.38	0.15	4.38	0.15
90.00	0.57	0.04	-151.	-3.	41.3	15.4	0.832	47.45	-8.52	4.37	-0.32	4.37	-0.32
95.00	0.0	0.0	0.	0.	0.0	0.0	0.0	0.0	0.0	0.0	0.0	0.0	0.0
100.00	0.0	0.0	0.	0.	0.0	0.0	0.0	0.0	0.0	0.0	0.0	0.0	0.0
105.00	0.0	0.0	0.	0.	0.0	0.0	0.0	0.0	0.0	0.0	0.0	0.0	0.0
110.00	0.0	0.0	0.	0.	0.0	0.0	0.0	0.0	0.0	0.0	0.0	0.0	0.0
115.00	0.0	0.0	0.	0.	0.0	0.0	0.0	0.0	0.0	0.0	0.0	0.0	0.0
120.00	0.0	0.0	0.	0.	0.0	0.0	0.0	0.0	0.0	0.0	0.0	0.0	0.0
125.00	0.0	0.0	0.	0.	0.0	0.0	0.0	0.0	0.0	0.0	0.0	0.0	0.0
130.00	0.0	0.0	0.	0.	0.0	0.0	0.0	0.0	0.0	0.0	0.0	0.0	0.0
135.00	0.0	0.0	0.	0.	0.0	0.0	0.0	0.0	0.0	0.0	0.0	0.0	0.0
140.00	0.0	0.0	0.	0.	0.0	0.0	0.0	0.0	0.0	0.0	0.0	0.0	0.0
145.00	0.0	0.0	0.	0.	0.0	0.0	0.0	0.0	0.0	0.0	0.0	0.0	0.0
150.00	0.0	0.0	0.	0.	0.0	0.0	0.0	0.0	0.0	0.0	0.0	0.0	0.0
155.00	0.0	0.0	0.	0.	0.0	0.0	0.0	0.0	0.0	0.0	0.0	0.0	0.0
160.00	0.0	0.0	0.	0.	0.0	0.0	0.0	0.0	0.0	0.0	0.0	0.0	0.0
165.00	0.0	0.0	0.	0.	0.0	0.0	0.0	0.0	0.0	0.0	0.0	0.0	0.0
170.00	0.0	0.0	0.	0.	0.0	0.0	0.0	0.0	0.0	0.0	0.0	0.0	0.0
175.00	0.0	0.0	0.	0.	0.0	0.0	0.0	0.0	0.0	0.0	0.0	0.0	0.0
180.00	0.0	0.0	0.	0.	0.0	0.0	0.0	0.0	0.0	0.0	0.0	0.0	0.0

FIGURE 13-22 Example (A) Ellipse-Line Contact Interaction from Example 1

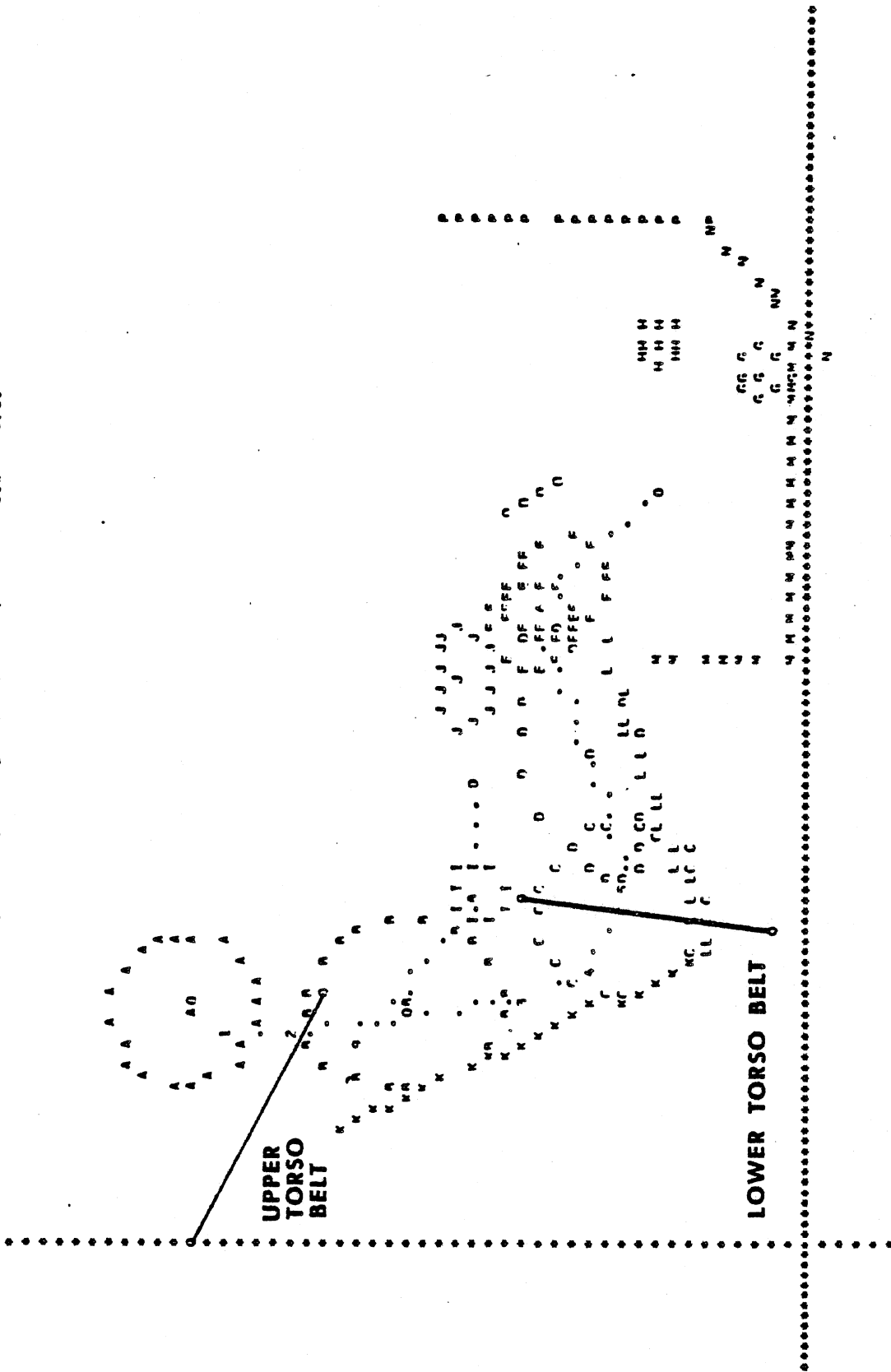
SLIDE 13-21



SLIDE 21

This slide illustrates the printout describing the contact interaction between the HIP ellipse and CUSHION LINE 1 of the SEAT CUSHION region. Deflection, normal force, friction force, and other variables are printed out.

(pause 5 sec.)



COORDINATE RANGES END PLOT ARE X= -6.96 (AT LEFT) TO 65.56 (AT RIGHT) AND Z= 5.00 (AT BOTTOM) TO -44.00 (AT TOP)  
 SCALE FACTOR IS (IN) = 5.567 (IN) ; X AND Z POINT RESOLUTION ERRORS EQUAL RESPECTIVELY 0.277 AND 0.462 (IN) IN SCALE.

FIGURE 13-31a Printer-Plot Time Sequence for Example 2 (0 ms)

## SLIDE 22

The second example data set discussed in this module includes the same 30-mph frontal barrier crash acceleration profile as used for Example 1. Simulation Example 2 is similar to Example 1 in other ways also. It uses the same occupant description data subset and the occupant is positioned within the vehicle in an identical manner. The vehicle interior used is basically the same. The primary difference between Examples 1 and 2 is that while both occupants are restrained by a knee bar, the occupant in Example 2 is additionally restrained by a torso harness. There are a number of other differences in the data sets. None of these affect the crash dynamics; they have been included to illustrate various program options.

This slide shows the seated occupant at time zero, restrained by upper and lower segments of a torso harness. The three-belt submodel described in Module 9 is used for this simulation.

2.75	7.	0.	0.	0.	1.8	-1.96	14.12	-5.07	218
0.	0.	0.	0.	0.	-33.52	17.	-1.2		501
100.	0.	15.13	-.00178	6600.	6600.	10.			701
NO STRENGTH				14.04	-.00172	2.	1.		702
6% WEARING #1				6% WEBBING #2					703
6% WEARING #1	0.	0.	0.	0.16	14.36	15.04	0.	0.	704
6% WEARING #1	5.					SBELT1	IZERO	G3ELT1	705
GAELT1	0.	0.							706
GAELT1	.16	0.							706
GBELT1	1.37	.56							706
GBELT1	6.15	.95							706
GBELT1	40.	.95							706
GBELT1	0.	1.							707
GAELT1	1.37	.33							707
GAELT1	2.06	.19							707
GAELT1	6.15	.05							707
GBELT1	40.	.05							707
SAELT1	0.	0.							708
SAELT1	.533	1500.							708
SAELT1	9.91	2000.							708
SAELT1	11.28	5300.							708
SAELT1	14.36	6600.							708
SAELT1	15.04	0.							708
6% WEARING #2	0.	0.	0.	.155	13.85	14.51	0.	0.	704
6% WEARING #2	5.					SBELT2	IZERO	G3ELT1	705
SAELT2	0.	0.							708
SAELT2	.396	1150.							708
SAELT2	9.56	1650.							708
SAELT2	10.9	5300.							708
SAELT2	13.85	6600.							708
SBELT2	14.51	0.							708
NO STRENGTH	0.	0.	0.	0.	10.	11.	0.	0.	704
NO STRENGTH	5.					SNOSTR	IZERO	GNOSTR	705
GNOSTR	-1.	0.							706
GNOSTR	-1.	1.							707
SNOSTR	-1.	0.							708

FIGURE 13-27 Belt Restraint System Cards for Example 2

SLIDE 13-23

## SLIDE 23

Since it is desired for this simulation to have only the torso harness and the knee bar as restraints, and not a lap belt, the belt system data subset shown here includes some specifications worthy of note.

While any of the seven belt segments of the Advanced Belt-Restraint Submodel may be included or omitted from a belt system design, the Three-Belt Submodel is not as flexible. It must include either both lap belt and torso harness or the lap belt alone. Therefore, in the data subset shown, in order to effectively eliminate the lap belt, a belt material named NO STRENGTH is defined by 704- and 705-Cards and is prescribed a zero stiffness with a 708-Card. This belt material is assigned to the lap belt on Card 702. Again, similarity of material property cards with ellipse and contact surface specifications should be noted.

The torso belts are each pre-tensioned to 5 lb. This is done by assigning negative values for initial slack on Cards 701 and 702. Belt anchor locations and attachment points on the occupant are prescribed on Cards 501 and 218.

0. C004F9021.1 C000F9003.1 00000000198. 555555551. 104

FIGURE 13-28 Debugging Printout Specifications for Example 2

0.	1.	1.	0.	0.	0.	1.	0.	1.	107
0.	0.	0.	0.	0.	0.	1.	1.	1.	108
1.	1.	0.	0.	0.	0.	0.	0.	1.	109
1.	1.	0.	0.	0.	1.	1.	1.	1.	110
0.	1.	1.	0.	0.	0.	0.	0.	0.	111

FIGURE 13-29 Specifications for Storage of Output Categories for Example 2

SLIDE 13-24

## SLIDE 24

Module 12 explains the use of 104- and 105-Cards for obtaining "debugging" printout of intermediate results from the Execution Processor. Time-dependent, multi-level switches may be set for sixteen divisions of program variables. The upper portion of the slide illustrates specifications for debugging printout for Example 2 from 0 to 3 ms and from 198 ms to the end of the simulation.

Field 9 of Card 104 is set to 1. in order to limit debugging printout to each final evaluation for the four-step Runge-Kutta integration. A "packing dictionary," which is often useful in interpreting debugging printout, is requested by defaulting the ninth field of Card 105 to 0. by omission of the card from the data deck.

There has been earlier mention of the use of Cards 1001 and 1002 for specifying categories of calculated data for which printout is desired. It should be kept in mind that in order for the Output Processor to print out variables in response to specifications on Cards 1001 and 1002, those variables must first be stored in an external file. Specification of categories which are to be stored during execution of the Execution Processor for possible later printout is made separately through use of Cards 107 through 111. For Example 1, these cards were omitted from the data deck and thus, by default, all categories were stored for printout. However, the data deck for Example 2 includes the cards shown in the lower portion of this slide. Only variables for categories for which a "0." is specified will be written to the external file for possible printout. Use of Cards 107 through 111 is explained in Module 12.

Additional differences between simulation Examples 1 and 2 are discussed in Module 13 of the Self-Study Guide, which includes complete data sets for both.





## SLIDE 25

Several example pages of output from simulation Example 2 are shown in the Self-Study Guide. One is the debugging printout illustrated here, which can be interpreted only by referencing Volume 3 of the MVMA 2-D report. Printout of this nature, while not ordinarily required, is useful to look inside the computational loops of the program to locate possible programming errors and to study anomalous behavior.

JUN 24 1977 02:07:15 MVMA 2-D TUTORIAL EXAMPLE #2  
GM HARJO 11 DUMMY (PRELIMINARY DATA) KNIFE BAR OCC. COMP. DISPL. 30MPH FRONT BARRIER FORCE-LIM. HARNESS

CONTACT FORCE FOR UPPER TOPSD BELT MADE OF 6X WERRING #1 VS. UPPER TOPSD LINK MADE OF

TIME (MSEC)	DEFLECTION (IN)	DEFLECTION RATE (IN/SEC)	RING EQUIL. TENSION (LB)	UNADJUSTED TENSION (LB)	TENSION ADJUSTMENT (LB)	RESULTANT FORCE (LB)	RESULTANT HEADING (DEGREES)	ARCORDED ENERGY (FT-LBS)
0.0	0.002	-0.0	9.0	5.009	0.0	5.009	-26.485	0.0
5.00	0.027	13.419	0.0	74.543	0.0	74.543	-26.436	0.0
10.00	0.184	38.526	0.0	523.284	0.0	523.284	-26.087	0.0
15.00	0.302	8.115	0.0	869.567	0.0	869.567	-25.743	0.0
20.00	0.340	12.848	0.0	857.781	0.0	857.781	-25.671	0.0
25.00	0.411	15.907	0.0	1157.509	0.0	1157.507	-25.816	0.0
30.00	0.447	11.172	0.0	1315.537	0.0	1315.537	-26.313	0.0
35.00	0.522	12.541	0.0	1459.591	0.0	1460.600	-27.084	0.0
40.00	0.547	2.651	0.0	1500.764	0.0	1500.763	-29.119	0.0
45.00	0.638	40.872	0.0	1505.412	0.0	1505.411	-29.259	0.0
50.00	0.854	91.305	0.0	1522.442	0.0	1522.442	-30.136	0.0
55.00	1.407	99.302	0.0	1546.586	0.0	1546.586	-30.713	0.0
60.00	1.947	116.605	0.0	1575.383	0.0	1575.383	-30.916	0.0
65.00	2.472	97.409	0.0	1603.780	0.0	1603.779	-30.774	0.0
70.00	2.810	40.054	0.0	1621.412	0.0	1621.411	-30.419	0.0
75.00	2.891	-5.704	0.0	1619.988	0.0	1619.987	-29.749	3428.47
80.00	2.947	-10.385	0.0	1519.299	0.0	1519.299	-28.483	0.0
85.00	2.751	-27.643	0.0	1300.570	0.0	1300.570	-27.187	0.0
90.00	2.599	-34.075	0.0	941.904	0.0	941.903	-26.268	0.0
95.00	2.400	-45.534	0.0	613.058	0.0	613.058	-25.720	0.0
100.00	2.182	-63.019	0.0	291.315	0.0	291.315	-25.470	0.0
105.00	1.950	-63.019	0.0	0.0	0.0	0.0	0.0	0.0
110.00	1.743	-34.056	0.0	0.0	0.0	0.0	0.0	0.0
115.00	1.502	-34.579	0.0	0.0	0.0	0.0	0.0	0.0
120.00	1.304	-47.984	0.0	0.0	0.0	0.0	0.0	0.0
125.00	1.149	-50.707	0.0	0.0	0.0	0.0	0.0	0.0
130.00	0.987	-55.345	0.0	0.0	0.0	0.0	0.0	0.0
135.00	0.621	-53.877	0.0	0.0	0.0	0.0	0.0	0.0
140.00	0.352	-55.047	0.0	0.0	0.0	0.0	0.0	0.0
145.00	0.085	-53.925	0.0	0.0	0.0	0.0	0.0	0.0
150.00	0.0	0.0	0.0	0.0	0.0	0.0	0.0	0.0
155.00	0.0	0.0	0.0	0.0	0.0	0.0	0.0	0.0
160.00	0.0	0.0	0.0	0.0	0.0	0.0	0.0	0.0
165.00	0.0	0.0	0.0	0.0	0.0	0.0	0.0	0.0
170.00	0.0	0.0	0.0	0.0	0.0	0.0	0.0	0.0
175.00	0.0	0.0	0.0	0.0	0.0	0.0	0.0	0.0
180.00	0.0	0.0	0.0	0.0	0.0	0.0	0.0	0.0
185.00	0.0	0.0	0.0	0.0	0.0	0.0	0.0	0.0
190.00	0.0	0.0	0.0	0.0	0.0	0.0	0.0	0.0
195.00	0.0	0.0	0.0	0.0	0.0	0.0	0.0	0.0
200.00	0.0	0.0	0.0	0.0	0.0	0.0	0.0	0.0

FIGURE 13-33 Belt System Response for Example 2

SLIDE 26

The printout on this slide is for response of the upper torso belt for Example No. 2. Included are belt elongation, rate of elongation, belt angle, and belt load.

## SUMMARY

- Example 1— a 30 mph frontal barrier crash with vehicle interior deformation and a dummy passenger restrained only by a knee bar
- Example 2— a crash with similar occupant and vehicle configurations except that the occupant is restrained additionally by a torso harness
- Input and Output Processor data sets constructed as collections of subsets
  - Occupant data
  - Vehicle interior data
  - Restraint system data
  - Vehicle motion
  - Various computer model controls

SLIDE 13-27

## SLIDE 27

In this module, data decks have been described for two example simulations and selected pages of printout have been illustrated. The simulations were for: first, a 30 mph frontal barrier crash with vehicle interior deformation and a dummy passenger restrained only by a knee bar; and second, a crash with similar occupant and vehicle configurations except that the occupant is restrained additionally by a torso harness. Discussion of the construction of data sets for the Input and Output Pre-Processors was in terms of subsets. They include several which describe the occupant, the vehicle interior, restraint systems, and the crash acceleration profile. Others include various computer model controls, including those for obtaining many different types of printout.





